UiT The Arctic University of Norway

Faculty of Biosciences, Fisheries and Economics
Department of Arctic and Marine Biology

Impacts of Vegetation and Temperature Changes on Carbon Cycling Microbial Communities in Arctic Wetlands

Kathrin Marina Bender

A dissertation for the degree of Philosophiae Doctor

September 2023

Impacts of Vegetation and Temperature Changes on Carbon Cycling Microbial Communities in Arctic Wetlands

KATHRIN MARINA BENDER

A dissertation for the degree of Philosophiae Doctor

September 2023

UiT The Arctic University of Norway

Faculty of Bioscience, Fisheries and Economics

Department of Arctic and Marine Biology

Microorganisms and Plants Research Group

Cells in the Cold Laboratory

The cover image was created with an open art generating Ai (openart.ai) using the prompt: “Arctic Peatlands Microbes Geese Drawing”.

Table of Contents

Acknowledgements

Alex, thank you so much for guiding me through this PhD. Your professional support and help was indispensable for the completion of my PhD. You taught me how to tackle every part of a project, from the very first stages of planning the fieldwork, through almost endless data analysis, to finalizing a manuscript. However, a PhD does not always go as smoothly as just described. Therefore, it was equally important that, no matter my problems or frustrations, you always provided a safe environment to discuss anything, and that we could find solutions together. Knowing you were also available for the more intense talks was very reassuring and much appreciated.

Andrea, I thank you for taking the time to teach me the depths of bioinformatics and for your very valuable help with my manuscripts. I know having the desk next to mine came with frequent interruptions. Thank you so much for dealing so well with that and calmly answering all my questions.

Sophie, even though corona prevented us from working together as planned, you were still an important part of my PhD and I thank you for the good meetings we had.

Mette, you have guided me from the very start of my time here in Tromsø. Even if you were not my official supervisor, your thoughtful input and support with my manuscripts and during fieldwork was very appreciated. Thank you.

I want to thank all my co-authors for their important contributions to my papers. Especially Yngvild and Vicky, without your hard work and effort I would not have the papers I have now.

For your support in the lab, but also in general for checking in on how I was doing, I want to thank our great technicians Bente, Anne-Grethe, Alena, Liabo, and Eva-Marie.

I also want to thank all my colleagues in the Microorganisms and Plants group for providing me with a pleasant work environment, for cakes and wine lottery (which I won 3 times in 5 years) on Fridays, and the retreats.

To all my friends in Tromsø and beyond, but especially Lena, Jørn, Vincent, Yin, Christophe, Edda, and Paul. Thank you for being my therapists in stressful times, my tour-guides on skies, on foot, and in kayaks, my chefs when I was too tired to cook, and for always being good company.

Mama and Papa, your unconditional support was pivotal in even attempting to start a PhD and much more so to finish it. Even though we were separated by, at times, three very stressful flights, you were always just a phone call away when I needed you.

To my sister Emma, thank you for turning Tromsø into a home away from home. I will always cherish the time we spend here together, with you I have always a friend by my side.

Håvar, thank you for motivating me to continue when I was exhausted and reminding me to take breaks when I needed them, which usually came with a lot of much needed snacks. I could not have done it without you. Now I am excited for what comes next in our lives.

And lastly to my grandmother, who since I never left university kept asking me if I am still learning. Oma Paula, thank you for checking in on me and the good times we have together. From this point forward I will learn no more.

Summary

Climate change causes disturbances to soil environments. Such disturbances include shifts in vegetation composition and rising temperatures, which can impact the microbial communities involved in soil carbon cycling. In this thesis, my emphasis was centered on two main aspects: the effects of vegetation changes, caused by herbivory, and the effects of temperature changes on soil organic matter decomposition and greenhouse gas emissions in Arctic wetland soils. We applied a broad range of methods, including detailed vegetation and soil physiochemical descriptions, metagenomics and metatranscriptomics, microbial growth and biomass estimates, and greenhouse gas measurements, to investigate changes in the soils and responses of the microbial communities. By combining these methods, we were able to uncover how vegetation changes can alter the activity of the soil organic matter decomposing microbial community, the soil microbial food web, and the speed of the microbial loop. We were further able describe how microbial physiological adjustments to temperature change can lead to higher methane emissions during autumn cooling compared to spring and summer warming.

This thesis therefore provides valuable new insights into the dynamics of carbon cycling and greenhouse gas emissions in Arctic wetlands, based on the response of the soil microbial communities to vegetation and temperature changes.

List of Papers

Paper 1:

Kathrin M. Bender, Mette M. Svenning, Yuntao Hu, Andreas Richter, Julia Schückel, Bodil Jørgensen, Susanne Liebner, Alexander T. Tveit

Microbial responses to herbivory-induced vegetation changes in a high-Arctic peatland

Polar Biology, DOI: 10.1007/s00300-021-02846-z

Paper 2:

Kathrin M. Bender, Victoria S. Martin, Yngvild Bjørdal, Andreas Richter, Maarten J.J.E. Loonen, Mette M. Svenning, Andrea Söllinger, Alexander T. Tveit

Tundra vegetation changes, in absence of herbivory, are coupled with an altered soil microbial food web and a faster microbial loop

Manuscript research article prepared for submission to Global Change Biology

Paper 3:

Yngvild Bjørdal, Kathrin M. Bender, Victoria S. Martin, Liabo Motleleng, Alena Didriksen, Oliver Schmidt, Torben R. Christensen, Maria Scheel, Tilman Schmider, Andreas Richter, Andrea Söllinger, Alexander T. Tveit

Physiological temperature responses in methanogenic communities control the timing and rates of methanogenesis

Manuscript research article prepared for submission to The ISME Journal

List of Figures

List of Tables

List of Abbreviations

C	Carbon
CH_4	Methane
CO	Carbon monoxide
CO_2	Carbon dioxide
ER	Ecosystem respiration
GEP	Gross ecosystem photosynthesis
GHG	Greenhouse gas(es)
O_2	Oxygen
OM	Organic matter
N	Nitrogen
NEE	Net ecosystem exchange
NH_3	Ammonia
NO	Nitric oxide
NO_2^-	Nitrite
NO_3^-	Nitrate
N_2O	Nitrous oxide
P	Phosphorus
SIC	Soil inorganic carbon
SO_4^{2-}	Sulfate
SOC	Soil organic carbon
SOM	Soil organic matter

Part I

Thesis

1 Introduction

1.1 Climate change

1.1.1 Facts in 2023

The United Nations defines "Climate change" as long-term shifts in temperature and weather patterns caused primarily by increasing emissions of greenhouse gases (GHG), such as carbon dioxide (CO_2), methane (CH_4) and nitrous oxide (N_2O), which are attributed to anthropogenic activities (IPCC, 2023; United Nations, 2023). The concentration of CO_2 in the atmosphere has increased by approximately 50 % since the pre-industrial era (~1750) and is currently at its highest concentration over the past two million years (Fahey et al., 2017; IPCC, 2023). CH_4 emissions have increased by 156 %, and N_2O emissions by 23 %, leading to concentrations higher than in the past 800,000 years (Fahey et al., 2017; IPCC, 2023). Approximately half of this increase has occurred in the past 40 years and was linked to anthropogenic activities. In 2019, the main contributors to anthropogenic GHG emissions were the energy sector (34 %), industry (24 %), agriculture, forestry, and other land use (AFOLU) (22 %), transport (15 %), and buildings (6 %) (IPCC, 2023). While GHG emissions are still increasing, land and ocean sinks have been consistently absorbing around 56 % of the global CO_2 emission per year over the past 60 years (IPCC, 2023).

The accumulation of GHG in the atmosphere has resulted in a wide range of consequences. The most prominent consequence is the increase in global surface temperatures, which has been 1.1 °C higher in 2011 – 2020 compared to 1850 – 1900. This increase in temperature has occurred faster since 1970 than in any other 50-year period over the past 2000 years, with larger temperature increases observed over land (1.59 °C) compared to over oceans (0.88 °C) (IPCC, 2023). Global surface warming has therefore large implications for soil carbon (C) cycling and the microbial communities involved in it.

A more detailed description of terrestrial C cycling and the effect temperature has on the involved microbial communities are provided in chapter **1.2.3** and **1.4.3**, respectively. However, before having a closer look into terrestrial C and soil microorganisms, the more general effects climate change has in the Arctic and its ecological consequences will be introduced.

1.1.2 Climate change in the Arctic

Between 1979 and 2021, the Arctic has experienced a warming rate nearly four times higher than any other region on Earth, a phenomenon known as Arctic amplification (Rantanen et al., 2022). By the end of the 21st century, temperatures in the Arctic are predicted to rise between 3.3 °C to 10 °C, depending on the model (AMAP, 2021). This accelerated warming has profound implications on Arctic environments, including the loss of Arctic sea ice at an annual rate of 3.5 % to 4.1 % since 1979 (AMAP, 2021), the reduction of snow cover in June by 65 % between 1967 and 2012, progressing at a rate of decline of 17.2 % per decade since 1979, the mass losses of ice sheets and glaciers, and the thawing of permafrost (Taylor et al., 2017). The thawing of permafrost and the subsequent release of previously frozen organic matter (OM) has the potential to trigger additional C emissions from soils (Schuur et al., 2015). By 2100, these emissions could range from 2 % to 11 %, resulting in a potential temperature increase of +0.29 (± 0.21 °C) (Taylor et al., 2017). However, through CO_2 uptake, the expected increase in plant growth and primary production in Arctic environments is anticipated to partially counterbalance the increased C emissions induced by permafrost thaw (Taylor et al., 2017).

1.1.3 Examples of ecological consequences of climate change

Climate change has had profound and increasingly irreversible effects on various ecosystems, spanning terrestrial, freshwater, cryosphere, coastal, and open ocean environments (McCarty, 2001; Turner et al., 2020; IPCC, 2023). Animals are directly influenced by climate change in their migration, reproduction (such as changes in breeding dates and accessibility to partners), changes of their habitats, and geographic range and distribution (McCarty, 2001). For instance, the warming of sub-Arctic regions has led to the expansion of the red fox (*Vulpes vulpes*) population, suppressing the Arctic fox (*Vulpes lagopus*) (McCarty, 2001). One of the major concerns arising from climate change is the loss of biodiversity and the unprecedented extinction of animals and plant species due to the loss of habitats (Hallmann et al., 2017; Cavicchioli et al., 2019). The risk of extinction depends on a species' ability to adapt to changes. However, with the increasing frequency and severity of extreme climate changes, this adaptive response becomes increasingly difficult (McCarty, 2001).

Rising temperatures have, further contribute to greater species richness of terrestrial plants in colder regions originally characterized by low species diversity, including Antarctica, the Arctic, and alpine areas. Additionally, elevated spring temperatures have led to longer

growing seasons in the Arctic, resulting in increased vascular plant growth and primary production (Elmendorf et al., 2012; Berner et al., 2015; Keenan and Riley, 2018). However, the trend of Arctic greening may be partly reversed by extreme weather events, that inhibit vegetation growth (Phoenix and Bjerke, 2016; Treharne et al., 2019).

1.2 Terrestrial carbon and climate change

The high soil C content, especially in northern, Arctic, and permafrost regions, makes them particularly important in the context of climate change, as rising temperatures directly affect the C store capacity of soils and thus can lead to substantial C emissions to the atmosphere (Tarnocai et al., 2009).

1.2.1 Terrestrial carbon storage

Soils are important C sinks, storing up to up 2500 gigatons (Gt; 1 Gt = 1 billion metric tons) in the upper 3 m of the soil horizon (Jansson et al., 2021), one quarter of which originates from anthropogenic sources (Cavicchioli et al., 2019). The total soil C pool is comprised of approximately 1550 Gt of soil organic C (SOC) and 950 Gt of soil inorganic C (SIC). This is more than plant biomass (560 Gt), microbial biomass in soil (110 Gt) and atmospheric C (760 Gt) combined (Figure 1) (Jansson et al., 2021).

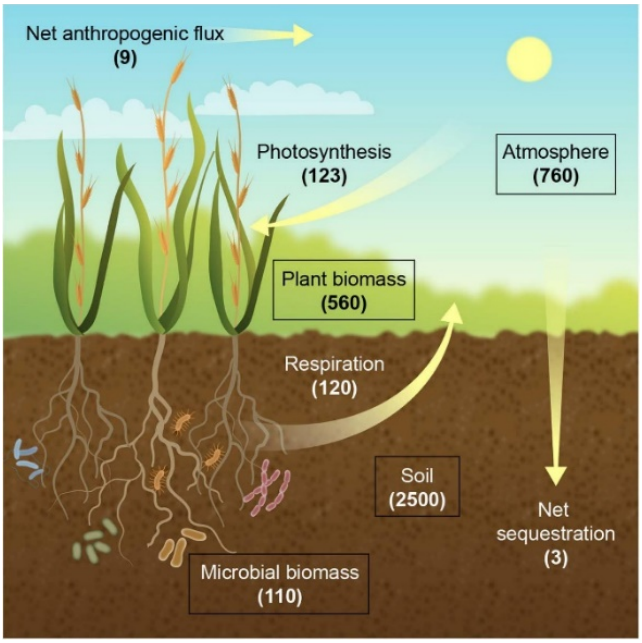

Figure 1: The figure illustrates the different terrestrial (including plant biomass, soil, and microbial biomass) and atmospheric C pools and their fluxes (mainly photosynthesis and respiration). The values of the C pools are given in gigaton (Gt), and the C fluxes in Gt per year (From: Jansson et al., 2021).

Soil C is differently distributed among different soil and vegetation types. Especially important C sinks, however, are Arctic wetland ecosystems, such as peatlands (Table 1).

Table 1: Estimated soil C storage comparing different vegetation and soil types and their respective land surface coverage. The overlap of between the vegetation and soil types causes the estimations to exceed 100%. Emphasis is the low land surface coverage to high C storage ratio of peat soils compared to the other vegetation and soil types.

Vegetation or soil type	Estimated soil C storage	Land surface coverage	References
Grasslands	~ 20 – 34 %	~ 26 – 45 %	Cavicchioli et al., 2019 Jansson and Hofmockel, 2020 Bai and Cotrufo., 2022
Forests	~ 45 %	~ 30 %	Cavicchioli et al., 2019 Poulter et al., 2014
Desert soils	~ 10 %	~ 31 %	Wang et al., 2021 Tchakerian and Pease, 2015
Peat soils	~ 30 – 40 %	~ 3%	Tarnocai et al., 2009 Xu, et al., 2018 Hugelius et al. 2020
Permafrost soils	~ 50 – 68 %	~ 11 %	Tarnocai et al., 2009 Schuur et al., 2015 Obu, 2021

1.2.2 The importance of Arctic peatlands and their role in a changing climate

Peatlands are located mostly in the northern hemisphere, and although covering only ~3 % of (Xu, et al., 2018, Hugelius et al., 2020), they contain 30 – 40 % of the global soil C (Table 1), making them the biggest terrestrial C sinks in surface to C ratio (Tarnocai et al., 2009; Cavicchioli et al., 2019). Arctic peatlands are forming where the underlying permafrost impedes drainage, establishing waterlogged, anoxic conditions (Gorham, 1991). In peatlands, the decomposability of plant litter is restricted by the structure and chemical composition of the plant input material, which is typically decomposition-inhibiting phenolics and recalcitrant polysaccharides of mosses (Ping et al., 2015; Hodgkins et al., 2018). More details about plant litter decomposability are described in chapter **1.3.3**. Additionally, the low oxygen (O_2) availability, low temperatures and often low pH decelerate rates of plant litter decomposition in permafrost affected soils (Limpens et al., 2008; Fenner and Freeman, 2011). Thus, the plant-derived C becomes locked up in the form of peat (Gorham, 1991), leading to the accumulation of enormous amounts of organic C (Limpens et al., 2008; Ping et al., 2015).

During the growing season, the upper peat (0 – 40 cm) is not always saturated with water, supporting a mix of aerobic and anaerobic biological processes. The deeper layers are usually waterlogged and anoxic (Limpens et al., 2008). The major C-fluxes that occur in the active layer of peatlands are: (1) assimilation of CO_2 (primarily through photosynthesis); (2) decomposition of plant material to CO_2 (aerobic) or CH_4 and CO_2 (anaerobic); and (3) oxidation of CH_4 to CO_2 (primarily aerobic) (Gorham, 1991; Wartiainen et al., 2003; Ping et al., 2015). A detailed description the terrestrial C cycle follows in the next chapter.

Peatlands and permafrost affected soils that have acted as C sinks for millennia are now at risk of becoming sources. This transition is driven by the thawing of permafrost (liberating previously stored C available for microbial decomposition), prolonged summer seasons (allowing for longer periods of microbial activity), and increased microbial decomposition rates, induced by higher temperatures (Strack et al., 2008; Jia et al., 2019).

1.2.3 Terrestrial carbon cycle

The terrestrial C cycle describes the balance between atmospheric C fixation and C emissions. Atmospheric C is fixed in the form of OM by autotrophic organisms through photosynthesis, and by photo- and chemoautotrophic microorganisms. Through photosynthesis 123 Gt CO_2 per year are fixed by plants and around the same amount (120 Gt CO_2) is released per year through respiration processes (Figure 1) (Jansson et al., 2021). Heterotrophic respiration by microorganisms and autotrophic respiration by plants are contributing equally to this flux with 60 Gt CO_2 per year each (Jansson et al., 2010; Cavicchioli et al., 2019; Jansson et al., 2021). On a globally scale most soils are oxic and unsaturated, and therefore the majority of C emission from soils occurs in the form of CO_2 (Gougoulias et al., 2014).

Following the fixation of CO_2 through photosynthesis, C becomes accessible to the soil environment via root exudation and through decomposition of plant litter and roots (Jansson et al., 2021). Polysaccharide hydrolysis, the depolymerization of polysaccharides from plant litter into oligo- and monosaccharides, occurs both under oxic and anoxic conditions (Warren, 1996; Tveit et al., 2013). This process is catalyzed by a wide variety of soil microorganisms from many lineages, including fungi and several bacterial phyla, such as *Actinobacteria*, *Verrucomicrobia*, and *Bacteroidetes* (van den Brink and de Vries, 2011; Tveit et al., 2013; Rai et al., 2015). The resulting oligo- and monosaccharides can be further oxidized to CO_2 through aerobic and anaerobic respiration. In aerobic respiration, O_2 acts as the

electron acceptor, while in anaerobic respiration alternative terminal electron acceptors, such as nitrate (NO_3^-) or sulfate (SO_4^{2-}), are used instead of O_2. In the absence of alternative terminal electron acceptors, fermentation of the depolymerized C takes over as the major energy harvesting metabolic process (Kelly et al., 2001; Tveit et al, 2013). Fermentation in soils is attributed to a wide range of microbial lineages, including *Firmicutes*, *Actinobacteria*, and *Bacteroidetes* (Philippot and Hallin, 2005; Wagner et al., 2005; Tveit et al., 2013). Fermentation products (e.g., ethanol, propionate, and butyrate) are degraded by secondary fermentative bacteria to intermediate fermentation products (e.g., hydrogen (H_2), acetate, and formate). Sometimes secondary fermenters and methanogenic archaea (methanogens) establish syntrophic relationships that prove mutually beneficial. This synergy arises when the fermenter benefits from the more favorable thermodynamic conditions created by low product concentrations, owing to the efficient uptake facilitated by the methanogenic partner, while the methanogen benefits from a consistent supply of substrate (Schink, 1997).
Methanogenesis is the final step in the anaerobic degradation of C and is carried out by strictly anaerobic methanogenic archaea (Schink, 1997), ultimately culminating in the production and emission of CH_4 and CO_2 through the utilization of the intermediate fermentation products (Liu and Whitman, 2008; Tveit et al., 2013; Schmidt et al., 2016). The production of CH_4 occurs via three main pathways: aceticlasitic, hydrogenotrophic, and methylotrophic methanogenesis. In aceticlastic methanogenesis, acetate is utilized for CH_4 production. In hydrogenotrophic methanogenesis, CO_2 is reduced using H_2 as electron donors. Additionally, formate, alcohols (e.g. ethanol), or C monoxide (CO) can be used as substrates for CO_2 reduction and methanogenesis (Ferry, 2011; Tveit et al., 2013; Enzmann et al., 2018; Conrad, 2020). The third main pathway of CH_4 production is methylotrophic methanogenesis, which is based on the utilization of methanol or other methylated compounds (Enzmann et al., 2018; Conrad, 2020). In most anoxic environments (e.g., water-saturated soils such as peat, lake sediments, or landfills), CH_4 is mainly produced via either aceticlastic or hydrogenotrophic methanogenesis (Conrad, 2020). Methylotrophic methanogenesis is common in saline environments (Conrad, 2020), but has also been detected in Arctic and temperate peatland soils (Söllinger et al., 2015; Tveit et al., 2015; Söllinger and Urich, 2019).

The net flux of CH_4 depends on the balance between methanogenesis and CH_4 oxidation. In the absence of O_2 in the water-saturated layers of the soils, CH_4 is oxidized by bacteria through nitrite (NO_2^-) reduction and intracellular O_2 production by nitric oxide (NO)

dismutation (Gougoulias et al., 2014, Lyu et al., 2018; Kalyuzhnaya et al., 2019; Rainer et al., 2020). In marine environments, anaerobic CH_4 oxidation by archaea (ANME) is an important process, driven by high concentrations of CH_4 and electron acceptors such as NO_3^- or SO_4^{2-}. However, so far archaeal CH_4 oxidation was not found to be important in freshwater environments or anaerobic soils (Kurth et al., 2019). CH_4 can further be oxidized aerobically in the upper oxic layers of wetland soils or freshwater environments (Rainer et al., 2020).

Terrestrial C cycling is influenced by a variety of factors, including temperature and vegetation changes. How, for example, herbivory and plant litter composition impact substrate quality and availability in soils and how this affect C cycling and C emissions from soils will be introduced in the next chapter.

1.3 Impact of herbivory on vegetation, soil organic matter composition, and carbon emissions

1.3.1 Herbivory in the Arctic

Due to climate warming, snow melt starts earlier in the Arctic, extending and enhancing plant productivity (van der Wal and Stien, 2014; Bjorkman et al., 2015). Changes in food resource availability (bottom-up effects) have the potential to improve reproduction, survival, and ultimately, population sizes of Arctic resident and migratory herbivores (Layton-Matthews et al., 2020). While some Arctic herbivore populations, like the Svalbard reindeer (*Rangifer tarandus platyrhynchus*) or the Barnacle goose (*Branta leucopsis*), have shown positive population trends associated with climate change (Albon et al., 2017; Layton-Matthews et al., 2020), there is no general increasing trend of all Arctic herbivore populations (Post et al., 2009). This can be attributed to top-down controls, for example fluctuations of predator populations like the Arctic fox (*Vulpes lagopus*), which influence the population sizes of small herbivores like lemmings (Angerbjorn et al., 1999) and voles (Ehrich et al., 2017), and the reproductive success of migratory geese (Layton-Matthews et al., 2020).

1.3.2 Arctic breeding geese

Arctic breeding geese are important herbivores (Bazely and Jefferies, 1989; Kuijper et al., 2006; Sjögersten et al., 2011) and contribute to the eutrophication of Arctic ecosystems (Hessen et al., 2017). Flyway geese are migrating to the Arctic in early spring for breeding and moulting. Since the 1950s, population sizes of European Arctic breeding geese have steadily increased, due to changes in agriculture (Fox and Abraham, 2017) and the

implementation of hunting bans (Fox and Madsen, 2017). However, the population sizes of Arctic breeding geese at their breeding grounds vary between species (Goosemap, 2023), but also between different flyway populations of the same species (AEWA, 2021). The European Goose Management International Working Group, has listed three different populations of Barnacle geese in Europe, all of which experienced huge increases in their populations; (1) the Svalbard/South-West Scotland population (Figure 2) increased from 1 350 individuals in 1950 to over 40 000 individuals in 2018, (2) the Greenland/Scotland and Ireland population had 8 277 individuals in 1950 and 72 162 individuals in 2018, and (3) the Russia/Germany and Netherlands population increased from 10 000 individuals in 1950 to 1 200 000 individuals in 2018 (AEWA, 2021). Besides Barnacle geese, the Pink-footed goose (*Anser brachyrhynchus*) also migrates to Svalbard in spring for breeding, coming from their wintering habitats in Belgium and the Netherlands (Figure 2). In 2017, the population of the Pink-footed goose was around 90 000 individuals (Madsen et al., 2017). A third, and less abundant, goose species breeding on Svalbard is the Light-bellied brent goose (*Branta bernicla hrota*), with a population size around 6 000 – 7 300 individuals in 2012 (Goosemap, 2023).

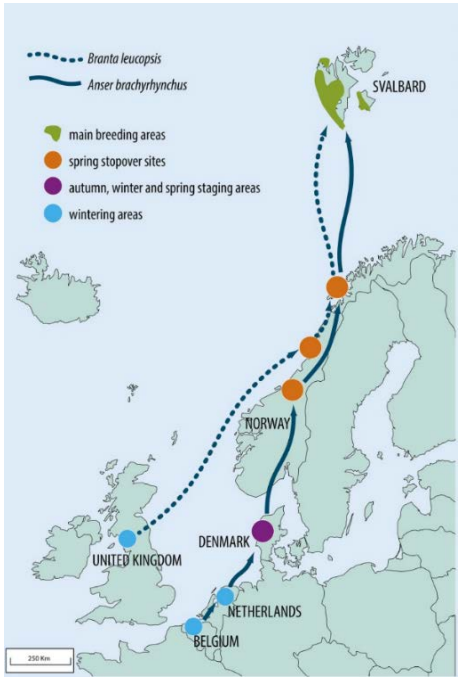

Figure 2. Migration routes of the Svalbard/South-West Scotland Barnacle goose population (*Branta leucopsis*) (blue dotted line) and the Pink-footed geese (*Anser brachyrhynchus*) (blue continuous line). Barnacle geese are wintering in the United Kingdom and South-West Scotland, while the Pink-footed geese stay in Belgium and the Netherlands over winter. Both geese species migrate in spring via Norway to their breeding grounds on Svalbard (From: Hessen et al., 2017).

1.3.3 Vegetation and carbon emissions

The effect of herbivory on tundra vegetation can range from depriving soil C stocks through disturbance and consumption of the plant cover (Sjögersten et al., 2011) to positive effects on the net C stocks through fertilization (Anderson et al., 2018) and removal of easily flammable shrubs, thereby mitigating vegetation destruction by wildfire (Kristensen et al., 2021). Furthermore, herbivory can directly alter the composition of plant communities (Zacheis et al., 2001; Maron and Crone, 2006). For example, herbivory can lead to higher plant productivity through preservation of the dominant plant species while excluding less productive ones (Bardgett et al., 1998; Bardgett and Wardle, 2003, Wardle et al., 2004) or to decreased plant and root biomass due to the depletion of the soil seed bank, by grazing on early plant shoots before they reach the flowering stage (Kuijper et al., 2006; Sjögersten et al., 2011). In Arctic tundra wetlands, herbivory by geese has been shown to negatively affect the moss layer thickness, reducing the insulating effect of mosses and their capacity to retain water (van der Wal et al., 2001; Gornall et al., 2009). Additionally, herbivory can lead to an overall decrease of litter quality by lowering the abundance and biomass of high-quality food plants, such as grasses (Kuijper et al., 2009; Sjögersten et al., 2011). Geese break down plant litter, leaving behind nutrient-rich feces pellets. These pellets contain soluble ammonia (NH_3), which supply N to the soil. This N input may enhance plant litter decomposition processes by alleviating N limitation and favoring more efficient but N-demanding decomposers (Bazely and Jefferies, 1985; Ågren et al., 2001). However, this stands in contrast to a study from 2010 which found that N from feces is mainly taken up by the moss layer, making it largely unavailable for microorganisms (Sjögersten et al., 2010).

The way in which herbivory in Arctic wetlands influences GHG emissions does not follow a clear trend. In a high-Arctic wetland, a herbivory-induced shift in vegetation composition, from vascular plant dominance to bryophyte-dominated vegetation, resulted in the transition from net CO_2 uptake to net emissions of both CO_2 and CH_4 (Sjögersten et al., 2011; Rainer et al., 2020; Foley et al., 2022). However, alterations in vegetation do not consistently result in changes in net C emissions when comparing Arctic wetland soils exposed to herbivory to those protected from it (Petit Bon et al., 2023). Hence, while herbivory by geese influences the vegetation structure and litter quality (as described in the following chapter **1.3.4**), it does not necessarily lead to shifts in GHG emissions. Potential reasons leading to this observation are discussed in chapter **4.3**.

1.3.4 Characterization of soil organic matter

The quality of plant litter can be determined by the number of enzymatic steps required to release a C atom from an organic substance. Consequently, substrates that require more steps are considered more complex and of lower quality (Bosatta and Ågren, 1999). The complexity of plant litter varies between different plant lineages, since the organization and composition of polymeric compounds is distinctive for different types of plant cell walls (Sarkar et al., 2009). Plant cell walls are composed of polysaccharide fibers like cellulose, hemicelluloses (e.g. xylan, xyloglucan, and mannan), and pectins (e.g. homogalacturonan and rhamnogalacturonan), as well as phenolic polymers like lignin, and structural proteins (Sarkar et al., 2009). In Arctic wetlands, the two predominant plant lineages, bryophytes, and vascular plants, are distinctly different in the molecular composition of their cell walls. Bryophyte cell walls are richer in mannans and galacturonans compared to vascular plants, which have higher contents of lignin and xylans (Popper and Fry, 2003; Sarkar et al., 2009). Bryophytes are typically described as decomposition-inhibiting and recalcitrant (Ping et al., 2015; Hodgkins et al., 2018). This is attributed to their high content of polyphenolics (such as lignan), structurally sturdy polysaccharides (including mannan-containing hemicelluloses), and pectins with acidic functional groups (such as rhamnogalacturonan) (Hájek et al., 2011; Roberts et al., 2012). Additionally, the breakdown of bryophyte cell wall components has been shown to release humic acids and lower the pH, further inhibiting microbial decomposition (Hájek et al., 2011; Pipes and Yavitt, 2022). Importantly, although decomposition of bryophyte cell walls may be slower compared to that of vascular plants, decomposition of bryophytes still takes place (Lang et al., 2009).

1.4 Soil microbial responses to environmental and climate changes

In terrestrial environments, microorganisms regulate the turnover of soil organic matter (SOM), making them key players in climate feedback loops (Jansson and Hofmockel, 2020; Naylor et al., 2020; Tiedje et al., 2022). The following chapters will introduce soil microorganisms in the context of climate change (**1.4.1**). Subsequently, the following two chapters will focus on soil C cycling microorganisms in the context of vegetation changes (**1.4.2**), and in the context of temperature changes (**1.4.3**), as the two main investigated factors of change in this thesis.

1.4.1 Soil microorganisms in the context of climate change

Microorganisms play crucial roles in climate change both as producers and consumers of GHG, such as CH_4, CO_2, and N_2O (Singh et al., 2010; Jansson and Hofmockel, 2020; American Society for Microbiology, 2021; Tiedje et al., 2022).

During 3.8 billion years of evolution, microorganisms have adapted to constant changes and have developed resilience. However, the current pace of climate change poses a considerable threat to microorganisms (American Society for Microbiology, 2021; Tiedje et al., 2022). Microorganisms respond to changing conditions through physiological acclimation, adaptation, dormancy, or death, but the ability to adapt to changes depends on the time required for gene regulation, transcription, translation, and mutation (Jansson and Hofmockel, 2020; Naylor et al., 2020). Those climate changes include increased temperatures (**1.4.3**), changes in vegetation (**1.4.2**), soil moisture, elevated atmospheric CO_2 concentrations, increased N deposition, and changes in physiochemical soil properties such as porosity and pH. Each of these factors has the potential to alter microbial communities in their composition, size, diversity, and distribution, both in isolation as well as in combination (Sheik et al., 2011; Maestre et al., 2015; Cavicchioli et al., 2019; Hutchins et al., 2019). Consequently, alterations in microbial communities and the expected loss of microbial diversity have been associated with reduced ecosystem multifunctionality, changing the metabolic potential of an ecosystem (Delgado-Baquerizo et al., 2016; Delgado-Baquerizo et al., 2017; Hutchins et al., 2019; Jansson and Hofmockel, 2020; American Society for Microbiology, 2021). Adding to the complexity of microbial responses to climate change is the fact that different microbial species and strains can react differently to change (Jansson and Hofmockel, 2020; Tveit et al., 2023). The multitude of potentially changing factors associated with climate change and the individual responses of different microbial species, alongside their interactions with each other, highlights the challenges to predict and generalize microbial responses across soil ecosystems (Jansson and Hofmockel, 2020).

1.4.2 Influence of vegetation on carbon cycling microbial communities

Greater diversity of vascular plants can lead to the establishment of different types of microbial communities in microhabitats centered around the roots. This favors more specialized communities that rely on root exudation or specific litter types, that may be unique to the different vascular plant types (Chroňáková et al., 2019; Sokol et al., 2022).

Furthermore, it increases the overall spatial and functional diversity of the soils due to the establishment of more different microhabitats with a more diverse input of plant litter (Sayer et al., 2017; Chroňáková et al., 2019; Sokol et al., 2022). Thereby, shifts in microbial community composition driven by changes in vegetation have the potential to influence soil C cycling by altering the functional potential of the microbial community (Antala et al., 2022).

SOM quality and microbial C decomposition

As mentioned in chapter **1.3.4**, the presence of vascular plants distinctly changes the SOM chemistry towards higher concentrations of labile C compounds in soils, compared to bryophytes (Dieleman et al., 2017). Microorganisms are utilizing SOM as a key energy source (Allison et al., 2010; Blagodatsky et al., 2010), therefore changes in the composition of SOM have the potential to either enhance microbial decomposition through priming with labile C compounds (Blagodatsky et al., 2010; Bengston et al., 2012; Dieleman et al., 2017) or reduce microbial metabolic activity through higher input of recalcitrant C (Straková et al., 2010; Dieleman et al., 2017). Microorganisms require a constant supply of labile C to efficiently degrade the recalcitrant compounds (Fontaine et al., 2007). A more diverse vegetation, composed of vascular plants and bryophytes, can therefore enhance microbial activity, and increase the microbial metabolic potential for C decomposition (Dieleman et al., 2017). Particularly in peat soils, a broadening of microbial metabolic potential can enhance the decomposition of more complex C and is believed to contribute to the breakdown and release of "old" C (Hartley et al., 2012; Walker et al., 2016; Dieleman et al., 2017), thereby leading to increased GHG emissions from soils.

1.4.3 Temperature effects on soil microorganisms

A major concern associated with climate change is the warming-induced acceleration of soil C mineralization rates and the subsequent rise in GHG emissions (Jansson and Hofmockel, 2020). It has been shown that soil warming leads to faster C loss from soil ecosystems (Tveit et al., 2015; Xue et al., 2016; Walker et al., 2018). However, C emissions often decrease after long term soil warming compared to initial warming responses, due to the depletion of more easily degradable labile C compounds (Oechel et al., 2000; Luo et al., 2001; Melillo et al., 2002; Zhou et al., 2012; Frey et al., 2013).

Temperature as control of enzymatic activity

Temperature is an important control of enzyme activity (Wallenstein et al., 2011). Essentially, each enzyme has an optimal temperature range, with reduced activity beyond those limits. Importantly though, in environmental enzyme pools, such as soils, this relationship is more intricate (Daniel et al., 2008) and enzyme activity is controlled also by the physical and chemical conditions (Wallenstein et al., 2011). For instance, the temperature sensitivity of degrading enzymes is influenced by C structure. Labile C compounds exhibit lower temperature sensitivities for enzymatic degradation compared to more recalcitrant compounds. This means that labile compounds can be more easily degraded at lower temperatures compared to more complex C compounds (Bosatta and Ågren, 1999; Knorr et al., 2005; Davidson and Janssens, 2006). Furthermore, even enzymes within the same category can display varying temperature sensitivities across different soil types (Wallenstein et al., 2011). Consequently, static thermodynamic models, such as the Q10 model (which describes the rate change of enzymatic activity with a 10 °C temperature change), are likely over- or underestimating the release of C from soils to the atmosphere in response to warming (Tang and Riley, 2015). This becomes eminent considering that for example the Q10 for soil respiration varies between 1.3 – 3.3 depending on soil type, vegetation cover, and depth (Jiang et al., 2015; Oertel et al., 2016). Additionally, temperature can influence microbial investment into enzyme production (Mairet et al., 2021). This is important because the effect of temperature on the rate of specific process depends not only its impact on catalytic activity but also the number of enzymes involved in catalysis. Therefore, such physiological adjustments can have considerable impact on C cycling.

Temperature effects on C cyling microbial communities

Temperature can also instigate changes in the diversity of soil microbial communities and the abundances of its members (Newsham et al., 2016; Zhou et al., 2016; Guo et al., 2018). Such community alterations can affect soil C cycling (Newsham et al., 2016), as shown in the case of warming-induced increases in fungal abundance corresponding with higher decomposition rates in soils (Mayer et al., 2021). Importantly though, while most microorganisms are sensitive to changes in temperature, the direction of temperature response is not always predictable (Oliverio et al., 2017). Therefore, taxon identity alone is not sufficient to

anticipate microbial responses to temperature change and should be linked to the functional potential of the microbial community (Oliverio et al., 2017; Xue et al., 2016).

Examples of temperatures dependency of different C cycling steps with focus on methanogenesis

In soil C cycling, the different steps in C degradation, which were introduced in chapter **1.2.3**, have different temperature dependencies (Yvon-Durocher et al., 2014). Methanogenesis requires a higher activation Energy (E_a = 106 Kj mol^{-1}), compared to e.g. polysaccharide hydrolysis (E_a = 54 – 125 Kj mol^{-1}) or respiration (E_a = 49 Kj mol^{-1}) (Conrad, 2023). Consequently, methanogens are more rate-restricted relative to other microbial C cycling functional groups at lower temperatures. However, the relatively larger rate increase at higher temperature can allow faster energy harvest, depending on substrate availability (Conrad, 2023).

For example, in an experiment based on anoxic microcosms with Arctic peat soil, a temperature threshold of 7 °C was identified that marked a pathway shift in SOC decomposition, resulting in changes in CH_4 production. At temperatures below 7 °C, propionate and acetate accumulated to much higher concentrations than above 7 °C, suggesting a shift in the ability of the microbial community to convert fermentation intermediates to CH_4 (Tveit et al., 2015). The pathway shifts were linked to alterations in the microbial groups responsible for SOC decomposition leading to CH_4 production, highlighting the intricate nature and complexity of microbial responses to temperature change (Tveit et al., 2015; Xue et al., 2016). Other temperature dependent pathway shifts include which of two main methanogenesis pathways in anoxic soils are dominating. Aceticlastic methanogenesis occurs usually at lower temperatures, and hydrogenotrophic methanogenesis at higher temperatures (Tveit et al., 2015; Conrad, 2020; Conrad, 2023), thereby changing the dependency of methanogens on substrate supply from SOC decomposition.

The temperature dependency of methanogenesis can help explain recent observations of higher CH_4 emission rates from wetlands during autumn cooling (CH_4 hysteresis) relative to spring and summer warming (Chang et al, 2020; Chang et al., 2021). This hysteretic CH_4 emission pattern was suggested to be linked to the accumulation of substrates for methanogenesis and the higher biomass of methanogenic archaea that had increased during

spring and summer warming, leading to the higher rates of CH_4 emissions during autumn (Chang et al, 2020).

This highlights how changing temperatures can influence *in-situ* CH_4 emissions, via changes in substrate supply, microbial community composition, physiological responses, and pathway shifts (Yvon-Durocher et al., 2014; Tveit et al., 2015; Chang et al., 2020)

1.5 Soil microbial food webs

The previous chapters have explained the basis of soil C cycling (**1.2**) and how it may be impacted by climate change (**1.4.1**), vegetation changes (**1.4.2**), and temperature changes (**1.4.3**). This chapter will elaborate on C cycling in the context of microbial trophic interactions.

As reviewed by Fierer (2017) and Thakur and Geisen (2019), abiotic factors such as pH, soil moisture, and substrate availability have traditionally been considered as the primary drivers for soil ecosystem functioning (Fierer, 2017; Thakur and Geisen, 2019). Due to the complexity of soil ecosystems, only recent advances in sequencing (metagenomic and metatranscriptomic approaches) enabled the simultaneous study of bacteria, eukaryotes, archaea, and viruses. This allowed for the inclusion of biotic factors like microbial physiological adjustments (Söllinger et al., 2022) and soil microbial food webs (Thakur and Geisen, 2019; Petters et al., 2021) into comprehensive soil ecosystem studies. We are only starting to understand the impact of trophic interactions in soil C cycling, but there is already consensus that food web interactions play a major role in ecosystem functioning (Trap et al., 2015; Geisen et al., 2018; Thakur and Geisen, 2019; Lucas et al., 2020; Petters et al., 2021).

Keystone taxa of soil microbial food webs

In general, a food web structure describes several trophic interactions among members of an ecosystem in predator-prey relationships and are often used to explain changes in population densities (Berryman,1992). In the study of soil microbial food webs, much focus has been directed towards protists and other eukaryotic micro-predators, such as nematodes and micro-arthropods as keystone taxa (Figure 3) (Trap et al., 2015; Geisen et al., 2018; Thakur and Geisen, 2019; Erktan et al., 2020; Lucas et al., 2020). More recently, prokaryotic predators, such as *Myxococcota* and *Bdellovibrionota*, have gained attention as important participants in soil microbial food webs (Figure 3) (Hungate et al., 2021; Petters et al., 2021), even though

their predatory traits have been known for some time (Stolp and Starr, 1963; Sillman and Casida, 1986; Shimkets, 1990). Additionally, more studies are now published about the soil virome and it is assumed that viruses play an equally important role in soil food webs (Figure 3) and C cycling (Paez-Espino et al., 2016; Emerson et al., 2018; Trubl et al., 2018) as reported for the other keystone taxa.

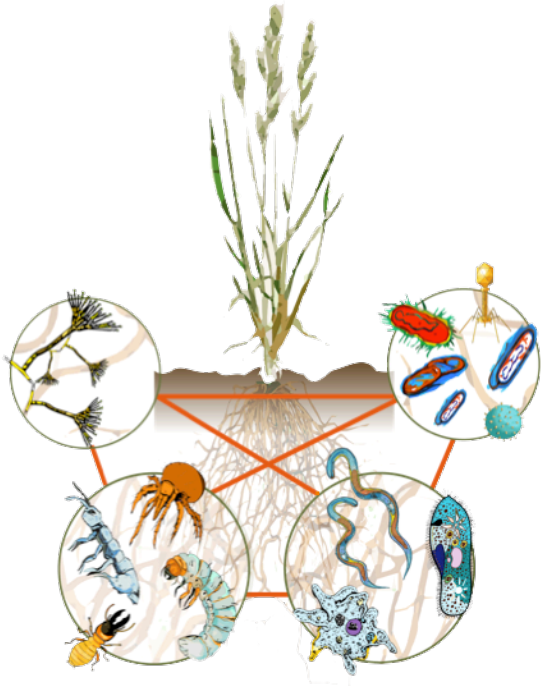

Figure 3: Illustration depicting a microbial food web structure within rhizosphere soil. The diagram comprises four groups: Bacteria and viruses (upper right); nematodes, amoeba, and other protists (lower right); micro-arthropods (lower left); and fungi, including saprophagous and mycorrhizal fungi (upper left). Predation occurs both within and between these groups, highlighting the complex interactions driving nutrient cycling and OM decomposition in the rhizosphere (From: Navarro Lab, 2023).

Ways of microbial predation and its influence on soil C composition

Soil predators exhibit diverse feeding strategies, including both selective or non-selective predation (Thakur and Geisen, 2019; Sokol et al., 2022). Different protist species, for instance, have been observed to act on several trophic levels, preying on other protists, nematodes, fungi, and bacteria (Geisen, 2016; Hünninghaus et al., 2017). Bacterivorous protists, in particular, preferentially feed on easily digestible Gram-negative bacteria (Thakur and Geisen, 2019). Soil nematodes, on the other hand, primarily feed on bacteria or fungi (Neher, 2010; Thakur and Geisen, 2019). Bacterivorous nematodes consume bacteria via

filter-feeding indiscriminately of their taxonomy, while fungi-feeding nematodes have been observed to penetrate fungal hyphae, thereby limiting hyphal growth (Neher, 2010; Thakur and Geisen, 2019). Micro-arthropods, such as collembola or mites, are known for their omnivorous lifestyle (Thakur and Geisen, 2019). While most collembola species primarily feed on fungi (Chahartaghi et al., 2005), some also consume bacteria (Ferlian et al., 2015) and plant material (Potapov et al., 2016). Viruses are commonly host specific (Sokol et al., 2022), but different lineages of viruses can infect a broad range of hosts (Emerson, 2019). Additionally, saprophagous soil animals such as earth worms and isopods as well as fungi are important consumers of decayed OM (Thakur and Geisen, 2019).

The different forms of predation can impact the composition of SOC, as the cause of microbial death can influence the input of microbial necromass into the soil (Sokol et al., 2022). This has important implications for soil C cycling, since microbial necromass is assumed to constitute more than half of the SOC (Liang et al., 2019). For instance, predation by larger protists or nematodes may result in the transfer of necromass to a higher trophic level, making the OM unavailable for other microbial groups, as it becomes sequestered within the predator (Sokol et al., 2022). Bacterial predators, on the other hand, primarily consume the cytoplasm after cell lysis (Pasternak et al., 2014), leading to necromass mainly composed of cell wall compounds and membranes (Sokol et al., 2022). In contrast, viral cell lysis additionally releases the cytoplasm to the environment, leading to a higher OM input, compared to bacterial cell lysis (Jover et al., 2014).

Implications for C cycling

Predation can influence the availability and composition of soil C. Due to the complexity of competitive and trophic microbial interactions, it however remains challenging to predict their response to climate changes (Crowther et al., 2015; Buchkowski et al., 2017), as the roles of microbial trophic interactions in C cycling remain uncertain (Jia et al., 2019).

1.6 Objectives

Arctic wetlands are exposed to numerous environmental changes, including variations in herbivory intensity, shifts in vegetation composition, and fluctuations in temperature. These wetlands store large amounts of organic C, making them highly susceptible to climate change. Whether they continue to act as C sinks or become C sources depends on how they respond to these environmental shifts.

The overall aim of the PhD thesis was to identify mechanisms that underlie microbial responses and therefore control microbial functioning in Arctic wetland soils exposed to changes in vegetation and temperature. Emphasize was laid on microbial community members involved in organic C degradation and CH_4 production.

The main objectives of the 3 papers were:

Paper 1: How does herbivory affect microbial decomposition of organic matter in Arctic peat soils?

Paper 2: How do herbivory-driven shifts in vegetation influence microbial trophic interactions and the microbial loop in Arctic wetlands?

Paper 3: What is the biological basis for CH_4 emission hysteresis (increased CH_4 emissions during autumn cooling) in Arctic wetland soils?

2 Materials and Methods

2.1 Field sites and sampling design (Paper 1 and Paper 2)

The fieldwork for **Paper 1** and **Paper 2** was carried out in the two high-Arctic wetlands Solvatn and Thiisbukta, situated close to the research settlement Ny-Ålesund, Svalbard (78°55´N, 11°56´E) (Figure 4). In the past decade (2013 – 2022) Ny-Ålesund had a mean annual temperature of -2.86 °C, a mean summer (June – August) temperature of 5.03 °C, and a mean annual total precipitation of 544.09 mm. Both wetlands are situated on top of continuous permafrost and are under the influence of herbivory by Barnacle geese (*Branta leucopsis*) and Svalbard reindeer (*Rangifer tarandus platyrhynchus*). Experimental exclosures (areas closed by 0.5 m tall fences) established at different timepoints have been used to study the effects of herbivore exclusion. Generally, herbivore exclusion has led to large changes in the vegetation in both wetlands, characterized by increased vascular plant coverage relative to bryophytes. Samples for **Paper 1** and **Paper 2** were collected inside and outside of the exclosures at the peak of the growing season in early August. In the following, details for both papers are given.

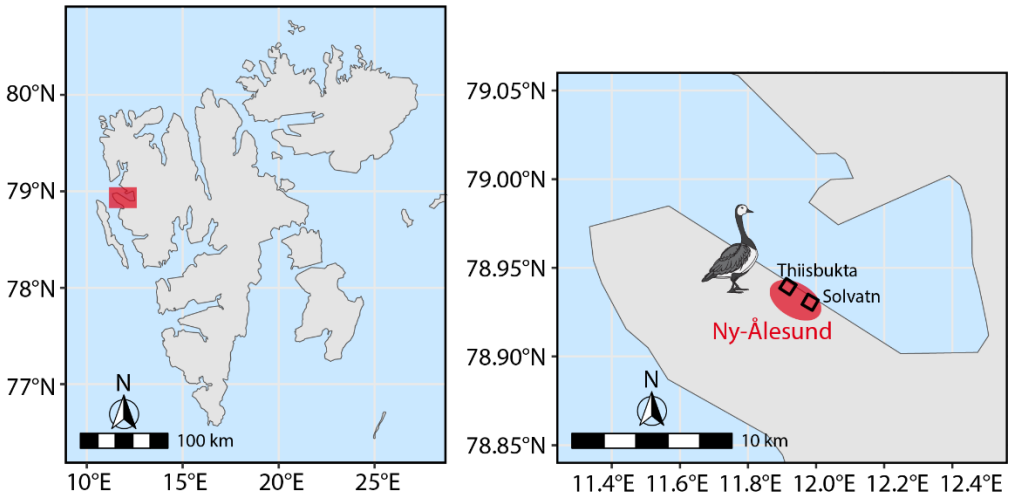

Figure 4: Sampling site location of Paper 1 and Paper 2. The map on the left depicts the Svalbard peninsula, with the Ny-Ålesund area highlighted in red. The map on the right shows the locations of Solvatn wetland (Paper 1) and Thiisbukta wetland (Paper 2) within Ny-Ålesund, where the effect of herbivory by Barnacle geese on the peat soil microbial communities was studied (Disclaimer: Barnacle goose not according to scale).

Paper 1: This study was based on samples from the Solvatn wetland (Figure 4). Experimental exclosures (0.7 x 0.7 m), adjacent to herbivory control plots, had been established in 1998, hence 18 years prior to the sampling campaign in 2016. During these 18 years a different

vegetation, mainly composed of grasses (*Poa arctica*), had formed inside the exclosures. The herbivory exposed vegetation in the control plots was dominated by brown mosses of the family *Amblystegiaceae*. Samples were taken from inside the exclosures and from the herbivory control plots at a depth of 1 – 2 cm after the removal of vegetation.

The following main methods were used to analyze the samples taken for this study (see **Paper 1:** Materials and methods for more details and references):

Vegetation description

We identified the main vascular plants and bryophytes based on their coverage to compare the effect of herbivory and herbivore exclusion on the vegetation composition.

Soil physicochemical parameters

Soil O_2 content, temperature [°C], pH, gravimetric water content [%], and total organic matter content were estimated for the characterization of the peat soils protected from and exposed to herbivory.

Plant polymer profiling

The polysaccharide composition of Arctic peat soils was measured using Comprehensive Microarray Polymer Profiling (CoMPP) and used as an indication for vegetation induced changes of SOM composition comparing the treatments.

Pore-water analysis: Amino acids and sugars

Pore-water amino acids were analyzed via mass spectrometry, and pore-water sugars via high pressure liquid chromatography (HPLC). Similar to the plant polymer profiling, the measurements of amino acids and sugars were used to characterize the soils nutrient contents comparing the treatments.

Enzyme assays

The rates of extracellular enzyme activity, focusing on polysaccharide degrading enzymes, were measured using the GlycoSpot™ technology. Those measurements were used as indications for alterations of degradation processes comparing herbivory to herbivore exclusion.

Total nucleic acids extractions and sequencing

Total DNA and RNA was isolated from the soils using a phenol-chloroform extraction protocol and used for the sequencing of DNA and mRNA. Metagenomes (DNA) and metatranscriptomes (mRNA) were used for the description of the microbial community composition and its functional activity in degradation processes.

Paper 2: This study was based on samples from the Thiisbukta wetland (Figure 4). Experimental exclosures had been established in 2006 and 2016, hence 14 and 4 years prior to the sampling campaign in 2020 (Figure 5). The herbivory control (Hr) and the 14 year exclosures (Ex-14) covered an area of 2 x 2 m. The 4 year exclosures (Ex-4) (1 x 1 m) were established 10 years after Ex-14 and set up within the Hr areas, reducing the size of Hr by the size of Ex-4 (Figure 5). Similarly to **Paper 1**, the exclusion of herbivores in Thiisbukta also led to the establishment of vascular plants dominated by *Poa arctica* and *Equisetium variegatum* within the exclosures. Samples were taken at 1 – 3 cm depth after removal of the vegetation.

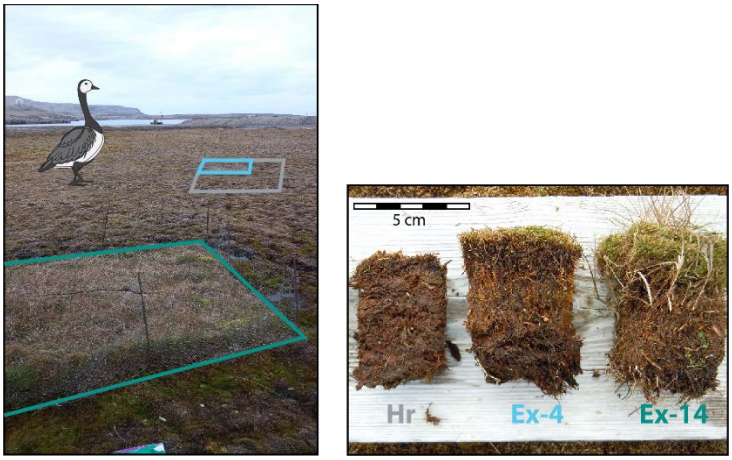

Figure 5: The picture on the left shows an example of the experimental exclosure set-up in Thiisbukta wetland. The area framed in grey depicts the herbivory plot (Hr) that allowed access of herbivores, framed in light blue is the 4-year-old herbivore exclusion plot (Ex-4), and framed in dark green is the 14-year-old herbivore exclusion plot (Ex-14). The picture on the right illustrates a comparison of the top layer peat soils and vegetation between Hr, Ex-4, and Ex-14. (Disclaimer: Barnacle goose not according to scale).

The following main methods were used to analyze the samples taken for this study (see **Paper 2:** Materials and methods for details and references):

Vegetation description

The vegetation composition was identified using the point-intercept method and used for the comparison of the effect of herbivore exclusion for 4 and 14 years compared to herbivory sites.

Root biomass

Root biomass was determined by separating and weighing roots from peat soils of the same volume, comparing the three treatments for the purpose of connecting changes in vegetation to changes in root biomass of the soils.

Soil physicochemical parameters

Soil O_2 content, temperature [°C], pH, and gravimetric water content [%] were measured for the characterization of the peat soils protected from and exposed to herbivory.

Soil carbon (C), nitrogen (N), and phosphorus (P)

Total soil C and N were measured using an elemental analyzer coupled to a continuous-flow isotopic ratio mass spectrometer. Total soil P was photometrically determined using the malachite-green method. Those measurements were used to compare the availability of substrates in the three treatments.

Fingerprinting of soil organic matter (SOM) chemical composition

Pyrolysis-gas chromatography/mass spectrometry was used for characterizing the chemical composition of SOM and to compare the effect of herbivory and exclusion of herbivores on potential alterations in the SOM composition.

Ecosystem respiration (ER)

ER, reflecting the total microbial and root CO_2 production, was measured using gas chromatography (GC). We measured ER to compare the effects of changes in vegetation and microbial community composition between the treatments.

Microbial growth rates

The effect herbivory and herbivore exclusion on microbial growth rates was estimated via $H_2{}^{18}O$ incorporation into DNA.

Microbial biomass

Soil microbial C and N were obtained by the chloroform fumigation extraction method and used as estimates for intact cells comparing herbivory to herbivore exclusion.

Total nucleic acids extractions and sequencing

Total DNA and RNA was isolated from the soils using a phenol-chloroform extraction protocol and used for the sequencing of total RNA. Metatranscriptomes (total RNA) were used for the description of the active microbial community composition and food web structure.

2.2 Experimental design (Paper 3)

Paper 3 was based on temperature incubation experiments of anoxic peat soil microcosms. The samples for the experiments were coming from five different wetlands located around the northern hemisphere focusing on the Arctic; (1) Svalbard - Knudsenheia (78°55´N, 11°56´E), (2) Greenland - Zackenberg (74°28´N, 20°35´W), (3) Norway - Håkøybotn (69°37´N, 18°47´E), (4) Canada - Komakuk beach (69°35´N, 140°11´W), and (5) Germany - Schlöppnerbrunnen (50°07´N, 11°52´E) (Figure 6). The mean annual temperature at the five locations ranged from -8.48 (Greenland) to 9.97 °C (Germany), and the mean annual total precipitation was between 302 (Canada) – 942.47 mm (Norway) in the past decade.

Figure 6: Location of the five wetlands investigated in Paper 3, listed from northernmost to southernmost: (1) Svalbard (78°55´N, 11°56´E), (2) Greenland (74°28´N, 20°35´W), (3) Norway (69°37´N, 18°47´E), (4) Canada (69°35´N, 140°11´W), and (5) Germany (50°07´N, 11°52´E). The samples from the five wetlands were used for anoxic temperature experiments with a focus on CH_4 producing microbial communities.

The samples were taken at -20 – 40 cm depth from the water saturated layer of the peat at all five locations and homogenized with peat water to a slurry in a 1:1 peat to water ratio. Following a two month long pre-incubation phase at 2 °C, the main temperature experiment was carried out (Figure 7). Over a period of 5 weeks the anaerobic peat soil slurry microcosms were incubated at weekly increasing temperatures starting at 2 °C, over 4 °C, 6 °C and 8 °C to a maximum of 10 °C, followed by a temperature decrease back to 2°C over the next 4 weeks (Figure 7).

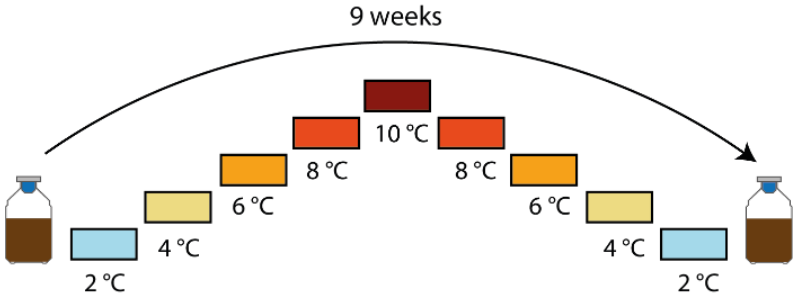

Figure 7: Experimental design of the main temperature incubation experiment. The peat soil samples were incubated under anoxic conditions over the course of 9 weeks. Starting at 2 °C, each temperature was maintained for one week, with weekly increments of 2 °C up to 10 °C, followed by a cooling period back to 2 °C.

The following main methods were used to analyze the samples of this study (see **Paper 3:** Materials and methods for details and references):

Physicochemical parameters: Gravimetric water content [%] and pH were measured to characterize the soils (i.e., the peat soil slurries) from the different locations.

Pore-water analysis: Fermentation intermediates (acetate and propionate)

Acetate and propionate are important intermediates of anaerobic C decomposition to CH_4 and were measured by high pressure liquid chromatography (HPLC). We measured these fermentation intermediates to investigate temperature-induced changes in their concentration and the potential relationship with changes in methanogenesis rates.

CH_4 and CO_2 production rates

CH_4 and CO_2, the end products of anaerobic decomposition of organic C, were measured using gas chromatography (GC) to investigate to effect of temperature on GHG production.

Microbial growth rates

The effect temperature on microbial growth rates was estimated via $H_2{}^{18}O$ incorporation into DNA.

Total nucleic acids extractions Total DNA and RNA was isolated from the soils using a phenol-chloroform extraction protocol. The ratios of RNA to DNA were used for the estimation of changes in cellular content of ribosomes.

3 Summary of Papers

3.1 Paper 1: Microbial responses to herbivory-induced vegetation changes in a high-Arctic peatland

Kathrin M. Bender, Mette M. Svenning, Yuntao Hu, Andreas Richter, Julia Schückel, Bodil Jørgensen, Susanne Liebner, Alexander T. Tveit

Research article published in Polar Biology 2021 (DOI: 10.1007/s00300-021-02846-z)

Herbivory by barnacle geese (*Branta leucopsis*) alters the vegetation composition and reduces ecosystem productivity in high-Arctic wetland, limiting the C sink strength of these ecosystems. Here we investigate how herbivory-induced vegetation changes affect the activities of peat soil microbiota using metagenomics, metatranscriptomics, and targeted metabolomics in a comparison of fenced exclosures and nearby herbivory sites. Our results show that a different vegetation with a high proportion of vascular plants developed due to reduced herbivory, resulting in a larger and more diverse input of polysaccharides to the soil at exclosed study sites. This coincided with higher sugar and amino acid concentrations in the soil at this site as well as the establishment of a more abundant and active microbiota, including saprotrophic fungi with broad substrate ranges, like *Helotiales* (Ascomycota) and *Agaricales* (Basidiomycota). A detailed description of fungal transcriptional profiles revealed higher gene expression for cellulose, hemicellulose, pectin, lignin and chitin degradation at herbivory-exclosed sites. Furthermore, we observed an increase in the number of genes and transcripts for omnivorous eukaryotes such as *Entomobryomorpha* (Arthropoda). In connection to the higher concentrations of polysaccharides, we observed increased potential rates of extracellular hydrolytic enzymes that target plant polysaccharides and transcripts for genes encoding such enzymes, implying that the changes in vegetation led to overall higher decomposition rates. We conclude that in the absence of herbivory, the development of a vascular vegetation alters the soil polysaccharide composition and supports larger and more active populations of fungi and omnivorous eukaryotes, co-occurring with higher potential rates of polymer degradation. This study establishes a fundament for targeting molecular and microbial mechanisms that are key to the interactions between above and below ground biology in high-Arctic wetlands.

3.2 Paper 2: Tundra vegetation changes, in absence of herbivory, are coupled with an altered soil microbial food web and a faster microbial loop

Kathrin M. Bender, Victoria S. Martin, Yngvild Bjørdal, Andreas Richter, Maarten J.J.E. Loonen, Mette M. Svenning, Andrea Söllinger, Alexander T. Tveit

Manuscript research article prepared for submission to Global Change Biology

Increases in geese populations and changes in their migratory routes have large consequences for Arctic tundra soil ecosystems, influencing the vegetation composition and thereby affecting the SOM input from plants. We have investigated the influence of herbivory by barnacle geese on vegetation, SOM quality, microbial activities, and microbial food web composition in a high-Arctic wet tundra. Tundra vegetation was exposed to three treatments: (1) Herbivory (natural state), (2) 4-year exclusion of herbivores, (3) 14-year exclusion of herbivores. These treatments resulted in (1) bryophyte-dominated vegetation, (2) a mix of higher vascular plants and bryophytes, (3) and vascular-plant-dominated vegetation. After 4 and 14 years of herbivore exclusion, we observed increased root biomass, decreased soil pH and moisture, and increased dissolved and total P contents. While dissolved and total soil C did not change with exclusion of herbivores, SOM composition had shifted towards a higher content of N containing compounds and lignin derivates in the 14-year-old exclosures. Microbial growth and ecosystem respiration rates were also higher in the exclosures while the total microbial biomass remained constant, indicating faster microbial turnover and higher activity of SOM decomposition processes. Based on 55 total RNA libraries, the overall relative abundances of prokaryotes, eukaryotes and viruses were similar in the three treatments. However, herbivore exclusion resulted in higher relative abundances of saprotrophic and mycorrhizal fungi and a shift and overall reduction in the relative abundances of multiple bacterial and eukaryotic micro-predators, reflecting a re-structured food web.

We conclude that more than a decade after the changes in aboveground herbivory, the ecosystem has altered into a different state, characterized by changes in vegetation, SOM composition, the soil microbial food web, and a faster microbial biomass turnover. Our results demonstrate the major effect that altered above-ground ecosystem dynamics have on the below-ground microbial interactions that control C cycling in Arctic tundra ecosystems.

3.3 Paper 3: Physiological temperature responses in methanogenic communities control the timing and rates of methanogenesis

Yngvild Bjørdal, Kathrin M. Bender, Victoria S. Martin, Liabo Motleleng, Alena Didriksen, Oliver Schmidt, Torben R. Christensen, Maria Scheel, Tilman Schmider, Andreas Richter, Andrea Söllinger, Alexander T. Tveit

Manuscript research article prepared for submission to The ISME Journal

Observations of higher wetland CH_4 emissions during autumn cooling relative to spring warming (CH_4 emission hysteresis) have been reported in recent years, potentially conflicting with the idea that CH_4 emissions are largely controlled by the temperature dependency of methanogenesis. We have investigated the temporal temperature responses of microorganisms involved in CH_4 production, by simulating an Arctic growing season in temperature-ramp time-series laboratory experiments (2 °C – 10 °C – 2 °C), with 2 °C increments per week for nine weeks. Using anoxic wetland soils from high-Arctic Svalbard, we showed that net CH_4 production rates are significantly higher in the second half of the temperature experiment, during cooling. This cooling-induced elevation of net production of CH_4 corresponded with a drop in the concentrations of propionate and acetate. At the same time, the ratio of soil RNA to DNA increased, indicative of larger microbial investment into ribosomes for protein biosynthesis. The highest microbial growth rates were reached after the initiation of cooling, based on ^{18}O-H_2O incorporation into DNA, which corresponded with increasing abundances of methanogenic archaea. We propose that the observed CH4 emission hysteresis resulted from a combination of factors, including the warming-induced increases in methanogenesis, the thermodynamic favorability of aceticlastic methanogenesis, and increased ribosome synthesis in response to cooling to compensate for reduced catalytic activity. . We repeated the experiment with wetland soils from high-Arctic Svalbard, Northern Norway, Greenland, Arctic Canada, and Germany, resulting in three out of five tested soils demonstrating sustained net CH_4 production during cooling. Our study highlights how CH_4 emissions depend both directly on the temperature dependency of enzymatic reactions during warming and indirectly on physiological adjustments to temperature change during cooling. This demonstrated that microbial physiology must be accounted for in predictions of climate change effects on natural GHG emissions.

4 Results and Discussion

The overall goal of this thesis was to examine how Arctic peat soil microbial communities respond to environmental changes, in particular alterations in vegetation and temperature. Climate change is driving shifts in animal populations, vegetation composition and temperature dynamics in Arctic environments. These changes, in turn, can have large effects on microbial communities and their functions, as observed in **Papers 1**, **2**, and **3**.

The papers presented in this thesis are time-series studies, comparing long-term (years to decades) effects of herbivory-induced vegetation changes on microbial community composition and interactions with implications for SOM decomposition (**Paper 1** and **Paper 2**), and short-term (weekly to seasonal) effects of temperature changes on microbial communities and GHG emissions (**Paper 3**).

Paper 1 and **Paper 2** demonstrated how herbivory affects the vegetation in Arctic wetlands. Those changes were leading to the establishment of a different and more active polysaccharide degrading microbial community (**Paper 1**) and to alterations in the microbial food web and the rate of the microbial loop (rates of growth and death) in the peat soils (**Paper 2**). This thesis further illustrates the underlying mechanisms behind the effect of temperature on CH_4 producing microbial communities in Arctic wetlands (**Paper 3)**.

The combination of papers illustrates microbial community and functional responses to changes in vegetation and temperature in Arctic wetlands, providing detailed descriptions of soil ecosystem processes, with a focus on C cycling and GHG emissions.

4.1 Methods for a holistic study approach

In order to obtain a complete picture of C cycling dynamics in Arctic wetlands both the topsoil (**Paper 1** and **Paper 2**) and subsoil (**Paper 3**) layers were investigated. The combination of methods describing vegetation composition, soil physiochemical composition, microbial biomass, growth and activity, and the microbial community composition in **Paper 1** and **Paper 2**, allowed for the simultaneous investigation of multiple aspects of ecosystem functioning in the Arctic wetlands. In **Paper 3**, we combined methods for the description of microbial growth, cellular content of ribosomes, fermentation intermediates, and CH_4 production rates to gain new insights into temperatures dependencies of microbial physiology

and how it affects ecosystem CH_4 emissions. This approach enhanced our comprehension of seasonal patterns in CH_4 emissions from wetlands.

Through the combination of a wide range of methodologies, this work extends our current understanding of microbial C cycling dynamics in Arctic wetlands. The focus on one or a few methods only may prevent new insights and the connection of observations to established theory, because of the complexity of soil ecosystems. Therefore, comprehensive, and interdisciplinary microbe-centric approaches, combining soil and plant science, environmental genomics, and ecosystem modelling, are necessary to fill important gaps in the understanding of microbial ecology and gain deeper insights into the effects of climate change (Singh et al., 2010; Tiedje et al., 2022).

4.2 Herbivory alters the vegetation and peat soil characteristics

4.2.1 Vegetation composition

Herbivory by geese can lead to a reduction in vegetation diversity and the depletion of the soil seed bank (Zacheis et al., 2001; Kuijper et al., 2006), which we also observed in **Paper 1** and **Paper 2**. The two studied wetlands, Solvatn (**Paper 1**) and Thiisbukta (**Paper 2**), were both under the influence of herbivory, mainly by Barnacle geese and occasionally by Svalbard reindeer. Herbivory on both field sites has led to the suppression of vascular plant growth and created a vegetation cover mainly composed of different brown mosses belonging to the family *Amblystegiaceae* with a coverage of 98 – 100 %. Within the experimental exclosures, preventing herbivory, we observed the establishment of vascular plants, dominated by *Poa* grasses and *Equisetum variegatum* (horsetail). After 4 years of herbivore exclusion vascular plants covered 72 % of the ground, and after 14 years of herbivore exclusion the vascular plant coverage had increased to 92 % (**Paper 2**). In the neighboring Solvatn wetland (**Paper 1**), the two dominating vascular plant types after 18 years of herbivore exclusion, were *Poa* grasses and flowering plant *Cardamine pratensis*. These observations align with previous studies by Sjögersten et al. (2011) for the Solvatn wetland and Petit Bon et al. (2023) for the Thiisbukta wetland.

4.2.2 Root biomass

Concurrent with the higher coverage of vascular plants was the higher root biomass content of the peat soils. After 4 years of herbivore exclusion, we observed a 6-fold increase in the root content of the soil, after 14 years the root content was 24-fold higher compared to peat soils exposed to herbivory (**Paper 2**). Our findings align with earlier measurements of root biomass in Thiisbukta wetland, where root biomass was found to be higher after just 4 years of herbivore exclusion compared to the herbivory exposed peat (Sjögersten et al., 2011). We did not quantify root biomass after 18 years of herbivore exclusion (**Paper 1**), however, Sjögersten et al. (2011) found a 12 times higher root content 9 years after establishment of the Solvatn exclosures, indicating a similar trend for this wetland.

4.2.3 Soil chemistry

We measured comparable O_2 levels and temperatures [°C] in the studied peat layers (at 1 – 3 cm depth) in areas protected from and exposed to herbivory in both Solvatn and Thiisbukta wetlands (**Paper 1** and **Paper 2**). The peat soil pH at Thiisbukta wetland significantly decreased from a pH of 7.3 in herbivory controls to a pH of 6.3 after 14 years of herbivore exclusion, while the pH after 4 years of herbivore exclusion was similar to the herbivory control (**Paper 2**). This stands contrary to our observations of the same pH of 7.1 after 18 years of herbivore exclusion and herbivory at the Solvatn wetland (**Paper 1**). Although pH decreased after 14 years of herbivore exclusion in **Paper 2**, the pH in both wetlands was relatively neutral, compared to more acidic *Sphagnum* dominated peat which can have a pH down to 4 (Shotyk, 1988). Therefore, pH is likely not one of the driving factors for alterations of microbial responses in **Paper 1** and **Paper 2.** The gravimetric water content of the peat soils was highest in the herbivory controls compared to the exclosures in both wetlands (**Paper 1** and **Paper 2**), likely due to the high water-holding capacity of bryophytes (Oishi, 2018). The peat soil of the Thiisbukta field site (**Paper 2**) was in general dryer compared to Solvatn (**Paper 1**), at the time of sampling, with a water content of 86.1 H_2O [%] at Thiisbukta and 92.4 H_2O [%] at Solvatn (the two measurements display the water content of the herbivory treatment; i.e., the current natural state).

4.2.4 Soil organic matter composition and concentration

The observed shifts in vegetation composition corresponded with changes in the SOM composition. We found overall higher SOM contents in peat soils from herbivore exclosures compared to herbivory controls in the Solvatn wetland. This difference was attributed to

higher concentrations of monosaccharides, polysaccharides, and amino acids, which reflected the changes in vegetation towards higher abundance of vascular plants (**Paper 1**). We further found higher contents of lignin derivates within the exclosures in Thiisbukta wetland (**Paper 2**). Lignin and some of the measured polysaccharides found in higher concentrations, do not occur in mosses and are likely originating from the altered plant litter input (Sarkar et al., 2009) reflecting the changes in vegetation.

Despite the observed changes in SOM composition, total soil C content was comparable in herbivore exclosures and herbivory controls (**Paper 2**). In the herbivore exclosures, we found slightly higher, yet not significantly different, total N and total P contents (**Paper 2**). This observation corresponds to previous descriptions of the same wetland (Petit Bon et al., 2023). Considering the slightly elevated N concentrations in the herbivore exclosures, it appears that the observed input of feces in herbivory controls did not lead to increases in N concentrations. A possible explanation is that additive N from feces is mainly taken up by mosses (Sjögersten et al., 2010), where it remains locked due to the rather slow decomposition rates of mosses (Hájek et al., 2011). Additionally, geese are likely removing more N from the system through grazing on vascular plants than the input of N through feces could compensate for, resulting in the lower N contents at herbivory sites. The elevated concentrations of P as observed in herbivore exclosures may be attributed to the presence of a deeper-reaching root systems, which can access lower P pools and transport them to the upper soil layers.

4.3 Herbivory alters peat soil microorganisms and processes

4.3.1 Microbial growth and biomass turnover

In connection with the increases of vascular plant biomass in herbivore exclosures, we observed trends (p-value: < 0.1) of elevated mass-specific microbial growth rates after 14 years of herbivore exclusion leading to significantly (p-value: < 0.05) shorter DNA turnover times. This faster DNA turnover reflects a combination of faster growth and death, the difference to the mass-specific microbial growth rates being whether the ^{18}O isotope incorporation from H_2O into DNA is normalized by the microbial biomass estimates or by DNA content (**Paper 2**). As such, the different p-values are due to the variation in the dataset used to normalize the data and not the rate of isotope incorporation. The higher growth rates were likely driven by the observed system change after 14 years of herbivore exclusion, including the shift in vegetation, higher root exudation, and an altered SOM composition.

Concurrently, microbial biomass, based on the measurement of microbial C and N from intact cells, remained unchanged when comparing herbivory to herbivore exclusion (**Paper 2**). A similar observation was previously reported for the Thiisbukta and Solvatn wetlands (Sjögersten et al., 2011). The combination of accelerated growth rates and stable biomass in the 14-year-old herbivore exclosures therefore suggests a faster microbial loop, where the microbial community despite growing faster, does not increase in size.

We further found significantly lower DNA and RNA concentrations in peat soils after 14 years of herbivore exclusion in Thiisbukta wetland (**Paper 2**). The lower DNA concentrations might result from the observed shift in the microbial community towards higher relative abundances of fungi (based on total RNA). In general, bacteria have a higher DNA to C ratio compared to fungi (Neidhardt et al., 1990; Yamada and Sgarbieri, 2005; Feijó Delgado et al., 2013). A shift towards higher abundances of fungi could therefore lead to lower amounts of DNA relative to microbial C. Alternatively, given that we detected shorter DNA turnover times, indicated by a combination of faster isotope incorporation into DNA and a smaller DNA pool, the lower DNA concentration in herbivore exclosures may be attributed to a more rapid consumption of extracellular DNA, compared to herbivory. Additionally, there might be fewer microbial cells in the peat soils from herbivore exclosures, resulting in the lower DNA concentrations.

In **Paper 1,** we detected higher concentrations of DNA after 18 years of herbivore exclusion compared to herbivory, while RNA concentrations were similar under both treatments. These observations therefore imply somewhat different effects of herbivore exclusion and altered vegetation between the two study sites. However, the different number of replicates analyzed, and the time of sampling could have contributed to those variations.

4.3.2 Ecosystem respiration

In **Paper 2,** ecosystem respiration (ER), which is the net CO_2 production rate [µmol CO_2 g^{-1} DW soil $day(d)^{-1}$], was determined. We found significantly higher ER in peat soils after 14 years of herbivore exclusion compared to both the 4-year-old exclosures (1.2 times higher) and the herbivory control plots (1.4 times higher). Petit Bon et al. (2023) described a similar relationship between ER and the length of herbivore exclusion at Thiisbukta wetland. Their study further reported a 3 times greater gross ecosystem photosynthesis (GEP) after 15 years of herbivore exclusion compared to herbivory exposure. Importantly though, while both ER

and GEP were higher under a vegetation dominated by vascular plants (herbivore exclosures) compared to bryophytes (herbivory controls), neither condition resulted in the release of CO_2 into the atmosphere (Petit Bon et al., 2023). ER was not measured in **Paper 1**, but Sjögersten et al. (2011) reported similar trends of ER and GEP from Solvatn wetland comparing herbivory controls to herbivore exclosures of 4 years. However, the net ecosystem exchange (NEE) of CO_2 was slightly positive in herbivory controls in Solvatn wetland, and negative following herbivore exclusion (Sjögersten et al., 2011). These observations suggest slightly varying responses to herbivory and changes in vegetation at the two neighboring wetlands, highlighting that even seemingly similar vegetation changes can result in slightly different ecosystem responses. It is possible that the more easily degradable plant litter and root exudates originating from vascular plants is causing the increase of ER in herbivore exclosures at both field sites, through priming effects on the microbial community that accelerate the mineralization of organic C (Blagodatsky et al., 2010; Bengston et al., 2012; Dieleman et al., 2017). This illustrates that the inclusion of below-ground microbial responses can help explain differences in ecosystem processes that cannot be understood based on vegetation changes alone.

4.3.3 Microbial decomposition of soil organic matter

Consistent with the alterations in SOM composition attributed to the changes in vegetation, we observed higher potential enzymatic activities and higher relative abundances of transcripts for the decomposition of the most common plant polymers in the peat soils of herbivore exclosures (**Paper 1**). Higher availabilities of C substrates in rhizosphere soils have been suggested to fuel microbial investments into production of extracellular polymer degrading enzymes (Zak and Kling, 2006; Wallenstein and Weintraub, 2008; Nuccio et al., 2020), supporting our observation in **Paper 1**.

Microbial transcription and enzymatic activities for polymer decomposition were found to be highest for cellulose degradation, followed by hemicellulose, pectin, and lignin, and were always higher inside the herbivore exclosures compared to herbivory exposure (**Paper 1**). The higher transcriptional activities for polysaccharide degradation were assigned primarily to *Actinobacteriota* and *Proteobacteria,* accounting for 42.20 % of all transcripts for polysaccharide degradation in herbivore exclosures and for 34.65 % when exposed to herbivory. Additionally, *Ascomycota* and *Basidiomycota* contributed to polysaccharide degradation, accounting for 16.88 % of the transcripts for polysaccharide degradation in

herbivore exclosures and for 1.08 % when exposed to herbivory. Therefore, we observed a shift in the polysaccharide degrading microbial community towards higher involvement of fungi and slightly higher bacterial activities in herbivore exclosures. This increase might be linked to the combination of higher concentrations of polysaccharides, presumably stemming from root exudates and plant litter, but also from the change towards a more complex mix of polymers (Edgecombe, 1938; Thormann, 2006; Broeckling et al., 2008; Koranda et al., 2014). Lignin degradation was mainly assigned to *Proteobacteria* in both herbivore exclosures and herbivory controls, accounting for 28.15 % and 33.03 % of transcripts for lignin degradation, respectively, while fungi were seemingly not involved in the degradation of lignin compounds (**Paper 1**). Hence, even though total lignin degradation was higher (based on the total number of transcripts) in herbivore exclosures, the same core community was responsible for the degradation of lignin in the peat soils in herbivore exclosures and herbivory controls (**Paper 1**).

The observed higher decomposition rates in the peat soils in herbivore exclosures in Solvatn wetland (**Paper 1**) are likely contributing to the observed higher ER under the same treatment in Thiisbukta wetland (**Paper 2**), as the first steps in SOM degradation, polysaccharide hydrolysis and the subsequent oxidation of monosaccharides, can result in the release of CO_2 (Tveit et al., 2013). Given the similar changes in vegetation and soil chemistry comparing Solvatn and Thiisbukta wetlands, combined with the higher ER in Thiisbukta wetland, we therefore assume, that similar decomposition processes might also be present in Thiisbukta wetland.

Additionally, we noted an increase in the relative abundances of omnivores, specifically the springtail collembola. The investigation of the degradation profile of one family within collembola, *Entomobryomorpha*, revealed its capability to depolymerize bacterial cell walls as well as plant and fungal polymers (**Paper 1**). While microbial omnivores, such as collembola, are well known for their involvement in SOM decomposition (Thakur and Geisen, 2019), our study adds more in-depth insights about their range of substrate usage and participation in decomposition processes.

4.3.4 Microbial food webs and the microbial loop

After 14 years of herbivore exclusion, we observed faster microbial growth rates while the microbial biomass remained stable in peat soils exposed to and protected from herbivory. This suggested the establishment of a faster microbial loop, with accelerated microbial death and turnover rates, resulting in a new ecosystem state, as discussed in chapter **4.3.1** (**Paper 2**). Although microbial mortality can have various causes, such as stress events (Camenzind et al., 2023) or exposure to antibiotics (Kohanski et al., 2010), in **Paper 2**, we focused on alterations in microbial predation patters and viral lysis as a potential cause for the faster microbial death and turnover rates.

The relative abundances of prokaryotes and eukaryotes, based on DNA sequences (16s rRNA gene and 18s rRNA gene) in **Paper 1** and RNA sequences (16s rRNA and 18s rRNA) in **Paper 2**, were similar comparing herbivory to herbivore exclusion, with about 80 % of all reads assigned to prokaryotes and ~ 20 % assigned to eukaryotes.

Following the 14 years of herbivore exclusion, we observed a decrease in the relative abundance of predatory prokaryotic and eukaryotic phyla and families. This decline was attributed to potentially predatory families belonging to the two bacterial phyla, *Bdellovibrionota* and *Myxococcota*, as well as several potential predatory eukaryotic families, belonging to the phyla *Choanoflagellida, Cercozoa, Ciliophora, Euglenida,* and *Lobosa*. Despite the general decrease in relative abundance of potential predatory microorganisms, we found that a few predatory families were increasing in relative abundance (**Paper 2**). This and the faster DNA turnover rate suggested a change in the food web dynamic towards a smaller, but more potent, and possibly more specialized predatory community. Additionally, we observed higher relative abundances of viruses within herbivore exclosures. This increase was mainly attributed to an increase in fungi infecting viruses, suggesting that the overall increase of the fungi kingdom was responsible for the increase of viruses. We therefore concluded that viruses may be contributors to the increasing rate of the microbial loop, but not the main driving factor.

Consequently, even with fewer members, the microbial predatory community, and viruses in herbivore exclosures appeared more potent by maintaining the microbial biomass and DNA concentrations at the same or lower levels, respectively, despite strong indications for increasing microbial growth and DNA turnover (**Paper 2**).

The higher root biomass observed in the soils within herbivore exclosures (**Paper 2**), could potentially create rhizosphere hotspots of microbial growth and biomass turnover, due to the higher localized input of easily degradable nutrients (Kuzyakov, 2010). Therefore, predatory microorganisms and viruses may have easier access to higher concentrations of their prey within these hotspots. This could further explain, how a select group of microbial predators come to dominate and lead to a faster microbial loop within the herbivore exclosures.

Broader relevance

Trophic interactions play major roles in ecosystem functioning (Trap et al., 2016; Geisen et al., 2018; Thakur and Geisen, 2019; Lucas et al., 2020; Petters et al., 2021). Changes in the vegetation have been identified as a driver of alterations in trophic interactions, leading to faster biomass cycling and higher rates of organic C flow (Sokol et al., 2022, Wang et al., 2022), as also observed in **Paper 1** and **Paper 2**. However, the exact mechanisms by which microbial food webs shape and impact soil C cycling remain uncertain (Jia et al., 2019).

Currently, global scale C models often overlook microbial dynamics in their predictions, relying on the comparison of the flow of C from one large pool (like SOM) to another (like GHG emissions) (Sokol et al., 2022). The complexity of microbial ecology and soil ecosystems is challenging for the incorporation of those fine-scale processes into large-scale global C models (Crowther et al., 2015; Buchkowski et al., 2017). Nevertheless, the inclusion of microbial ecology into global scale C models is essential for enhancing our understanding of SOM cycling and predicting future GHG emissions.

Therefore, in order to fully comprehend the role of microbial food webs for soil C cycling, more comprehensive studies are needed. Through the combination of a broad range of methods, we were able to connect different levels of ecosystem functioning, by identifying the underlying microbial drivers (**Paper 1** and **Paper 2**). The large shifts in vegetation, microbial decomposition, growth and biomass, and food web interactions, resulted in two very different ecosystems states, with however seemingly very similar ER. The findings presented in **Paper 1** and **Paper 2** represent valuable contributions to advancing our understanding of this complex field.

4.4 Seasonal temperature changes influences greenhouse gas fluxes in Arctic wetlands

4.4.1 Mechanisms behind seasonal methane hysteresis

We wanted to investigate the impact of seasonal temperature changes (specifically, spring warming compared to autumn cooling) on GHG production in Arctic wetlands (**Paper 3**). For this purpose, we conducted several anoxic temperature ramp experiments, incubating peat soils from 2 °C to 10 °C, in weekly increments of 2 °C (thereby simulating an Arctic spring), followed by a cooling period from to highest temperature at 10 °C back to 2 °C (simulating an Arctic autumn).

In the first experiment, using high-Arctic peat soils from Svalbard, we observed significantly higher net CH_4 production rates during cooling, compared to the same temperatures during warming. Similar hysteretic patterns of seasonal CH_4 emissions have been documented in previous *in-situ* studies from sub-Arctic wetlands (Chang et al., 2020; Chang et al., 2021). This suggested that our experimental observations were consistent with patterns observed in natural settings. In their studies from 2020 and 2021, Chang et al. suggested that the basis for the CH_4 emission hysteresis was an accumulation of methanogenic archaea and methanogenic substrates, such as acetate, during spring and summer, leading to the higher rates of net CH_4 production during autumn (Chang et al., 2020; Chang et al., 2021). Contrarily, in our experiment, the concentrations of acetate remained stable during warming, and started depleting during cooling after reaching the temperature maximum of 10 °C. This suggested two things: (1) during warming the upstream processes leading to production of acetate were still able to balance the consumption of acetate during methanogenesis, but this balance shifted after reaching 10 °C; (2) reaching 10 °C triggered a response of the aceticlastic methanogens, enabling them to use the available acetate faster.

Different temperature dependencies

In comparison to upstream C degradation processes, such as hydrolysis and respiration, aceticlastic methanogenesis has a higher temperature dependence, requiring an activation energy (Ea) of 106 Kj mol $^{-1}$, while hydrolysis requires an Ea between 54 – 125 Kj mol $^{-1}$ and respiration an Ea of 49 Kj mol $^{-1}$ (Conrad, 2023). This could explain the higher rates of methanogenesis after reaching 10 °C, as methanogens were able to gain more energy at this maximum temperature in the experiment relative to the other processes.

Further, Yvon-Durocher et al. (2014) showed that the temperature dependence of methanogenesis is similar in natural settings compared to methanogens in pure cultures. We therefore assume that the methanogens in our anoxic incubations follow similar temperature dependencies.

Increasing microbial growth rates

Shortly before the onset of acetate depletion, we observed increasing microbial growth rates at 8 °C during warming, with the highest rates at the start of the cooling period at 8 °C. This coincided with an increase of the *mcrA* gene (marker gene for anaerobic CH_4 cycling, commonly used as a biomarker for methanogenic archaea), suggesting that methanogenic archaea were among the actively growing microorganisms. We therefore assumed that methanogenic archaea were more abundant at the start of the cooling compared to warming. This suggested that the hysteretic CH_4 emissions during cooling were likely triggered by the increased consumption of acetate by the more abundant methanogenic archaea. This finding aligns with the observations of higher *in-situ* methanogenic biomass at the beginning of autumn, which has been identified as one of the main factors leading to higher autumn CH_4 emissions (Chang et al., 2020; Chang et al., 2021).

Increases of cellular content of ribosomes

We further observed increasing ratios of RNA to DNA at the onset of cooling, indicating an accumulation of ribosomes in microbial cells during this phase. Temperature changes have previously been related to alterations in the investment of microorganisms into ribosomes for protein biosynthesis, resulting in different rRNA contents of the cells (Söllinger et al., 2022; Tveit et al., 2023), suggesting that similar mechanisms might be occurring in our study.
We hypothesize that the larger methanogenic population, coupled with their capacity to extract more energy from acetate at higher temperatures compared to other processes, allowed for an increased investment into ribosomes during subsequent cooling. As a result, the presumed increase in ribosome content within methanogenic cells could drive the depletion of acetate by compensating for lower protein synthesis rates during cooling.

Potential feedback loop leading to CH_4 hysteresis

The observed CH_4 hysteresis pattern in our experiment appears to be the result of a potential feedback loop. At higher temperatures of 10 °C, aceticlastic methanogenesis gains more energy from one acetate molecule compared to the lower temperatures (Conrad, 2023). This may have allowed for increased investments by methanogens into growth and protein production, leading to the depletion of acetate, and thereby to the higher net CH_4 production during cooling.

Remaining questions

The energy yield gained from methanogenesis decreases relatively faster during cooling compared to other C degrading processes. Therefore, while we are able to explain the basis to CH_4 hysteresis in our experiment, it does not provide an explanation as to why the upstream processes could not balance the consumption of acetate during cooling. However, we hypothesize that the accumulation of methanogen biomass and ribosomes leads to a relatively faster rate during the cooling phase. Over time, as the acetate pool depletes, the energy limitation of the methanogens results in reduced cellular ribosome concentrations, ultimately restoring the balance between upstream decomposition and methanogenesis. To test this hypothesis, methanogens and methanogen ribosomes need to be quantified throughout the time series experiments.

4.4.2 Broader relevance

To investigate the relevance of the mechanisms described above in wetlands from different locations, we repeated the temperature experiment using wetland soils from Svalbard, Norway, Greenland, Canada, and Germany. These experiments revealed varying patterns of CH_4 production rates during cooling compared to the initial experiment, as described in the previous chapter. Wetlands soils from Svalbard, Norway, and Greenland, consistently exhibited higher net CH_4 production rates during cooling, with some variations in the strength of the hysteretic pattern. In the wetland soils from Canada and Germany we did not observe higher net CH_4 production rates during cooling compared to warming. The relatively warmer in-situ temperatures of the wetland soils from Germany compared to our experiment temperatures, which were designed to simulate an Arctic growing season, might explain why we did not observe CH_4 emission hysteresis in the German wetland soils.

The variations in the strength of hysteretic patterns observed across different locations underscore the complexity of CH_4 emissions in response to changing temperatures and substrate availability. The question arises, whether similar mechanisms underlie hysteresis when it occurs, and whether the absence of hysteresis is due to different temperature thresholds that trigger it.

The findings of **Paper 3** therefore highlight how CH_4 emissions from Arctic wetlands, are influenced both directly by the temperature dependence of enzymatic reactions and indirectly by physiological adaptations of microorganisms to changing temperatures. This emphasizes the importance in understanding these nuances to accurately account for wetland microbial processes and their implications for GHG emissions in a changing climate.

5 Conclusion and Outlook

Herbivory has led to the suppression of vascular plant growth in two high-Arctic wetlands. The comparison of soils exposed to herbivory and soils protected from herbivory revealed subsequent changes in the soils SOM composition, decomposition rates of SOM, microbial growth, and the microbial food web. Although microbial growth rates were higher in herbivore excluded soils, microbial biomass remained stable in both conditions, suggesting an acceleration of the microbial loop and microbial turnover times. The acceleration of the microbial loop was driven by changes in microbial predation, as indicated by the alterations of the microbial food web. The overall higher rates of soil C flow in herbivory excluded soils, as indicated by the faster SOM decomposition rates and microbial turnover times, were leading to higher ER rates. Despite those observed large scale responses to herbivory, other studies of the same sites have shown that no net CO_2 emissions were detected under both treatments, likely due to the higher CO_2 uptake through photosynthesis in herbivore exclosures. In conclusion, both herbivory-exposed and herbivory-protected wetlands maintained their C stability, albeit through different underlying mechanisms as reflected in two very different ecosystem states. The microbial food web appeared to act as a stabilizing system, capable of balancing increased growth rates and C emissions when SOM input changed.
This dynamic raises questions regarding the stabilizing capability of microbial food webs amidst additional climate change stressors, such as higher temperatures or droughts. It is possible that one of the treatments, either herbivory or herbivore exclusion, may have a stronger capacity to mitigate the effect of such stressors, while the other could prove more vulnerable, transitioning into a CO_2 source. Future work should investigate how both treatments respond to additional environmental stressors to gain better understanding of how C cycling microorganisms might react.

Based on the insights gained from **Paper 3**, we further conclude that the hysteretic CH_4 emission pattern, as observed in the anoxic incubations of high-Arctic wetland soils during the simulated autumn cooling from 10 °C to 2 °C, was facilitated by the increased consumption of acetate. This increase was driven by the combination of kinetic and thermodynamic favorability of methanogenesis at higher temperatures relative to other C degrading processes, and the increase in abundances of methanogenic archaea and higher cellular content of ribosomes.

The intensity of the hysteretic response showed variation among wetland soils from different locations and was absent in some cases, indicating that location-specific factors are influencing the microbial physiological response to temperature. Despite this variability, this study provides valuable new insights into the fundamental mechanisms behind CH_4 hysteresis and the importance of temporal acclimation of microbial physiology to temperature change generally. Consequently, our findings enhance our ability to make more accurate predictions regarding future wetland CH_4 emissions.

6 References

AEWA (2021). Defining favourable reference values for the populations of the Barnacle goose (Branta leucopsis). *6th Meeting of the AEWA European goose management international working group* (*EGM IWG 6*). Online conference format. In press.

Albon, S. D., Irvine, R. J., Halvorsen, O., Langvatn, R., Loe, L. E., Ropstad, E., Veiberg, V., van der Wal, R., Bjorkvoll, E. M., Duff, E. I., Hansen, B. B., Lee, A. M., Tveraa, T., & Stien, A. (2017). Contrasting effects of summer and winter warming on body mass explain population dynamics in a food-limited Arctic herbivore. *Global Change Biology, 23*(4), 1374-1389. https://doi.org/10.1111/gcb.13435

Allison, S. D., Wallenstein, M. D., & Bradford, M. A. (2010). Soil-carbon response to warming dependent on microbial physiology. *Nature Geoscience, 3*(5), 336-340. https://doi.org/10.1038/Ngeo846

AMAP (2021). AMAP Arctic Climate Change Update 2021: Key Trends and Impacts. Summary for Policy-makers. *Arctic Monitoring and Assessment Programme (AMAP), Tromsø, Norway 2021*, 16.

American Society for Microbiology (2021). Microbes and Climate Change -- *Science, People & Impacts: Report on an American Academy of Microbiology Virtual Colloquium Held on November 5, 2021* /. American Society for Microbiology.

Anderson, T. M., Griffith, D. M., Grace, J. B., Lind, E. M., Adler, P. B., Biederman, L. A., Blumenthal, D. M., Daleo, P., Firn, J., Hagenah, N., Harpole, W. S., MacDougall, A. S., McCulley, R. L., Prober, S. M., Risch, A. C., Sankaran, M., Schütz, M., Seabloom, E. W., Stevens, C. J., . . . Borer, E. T. (2018). Herbivory and eutrophication mediate grassland plant nutrient responses across a global climatic gradient. *Ecology, 99*(4), 822-831. https://doi.org/10.1002/ecy.2175

Angerbjorn, A., Tannerfeldt, M., & Erlinge, S. (1999). Predator-prey relationships: Arctic foxes and lemmings. *Journal of Animal Ecology, 68*(1), 34-49. https://doi.org/10.1046/j.1365-2656.1999.00258.x

Antala, M., Juszczak, R., van der Tol, C., & Rastogi, A. (2022). Impact of climate change-induced alterations in peatland vegetation phenology and composition on carbon balance. *Science of The Total Environment, 827,* 154294. https://doi.org/10.1016/j.scitotenv.2022.154294

Bai, Y., & Cotrufo, M. F. (2022). Grassland soil carbon sequestration: Current understanding, challenges, and solutions. *Science, 377*(6606), 603-608. https://doi.org/10.1126/science.abo2380

Bardgett, R. D., Wardle, D. A., & Yeates, G. W. (1998). Linking above-ground and below-ground interactions: how plant responses to foliar herbivory influence soil organisms. *Soil Biology and Biochemistry, 30*(14), 1867-1878. https://doi.org/10.1016/S0038-0717(98)00069-8

Bardgett, R. D., & Wardle, D. A. (2003). Herbivore-Mediated Linkages between Aboveground and Belowground Communities. *Ecology, 84*(9), 2258-2268. http://www.jstor.org/stable/3450132

Bazely, D. R., & Jefferies, R. L. (1985). Goose Faeces: A Source of Nitrogen for Plant Growth in a Grazed Salt Marsh. *Journal of Applied Ecology, 22*(3), 693-703 https://doi.org/10.2307/2403222

Bazely, D. R., & Jefferies, R. L. (1989). Leaf and Shoot Demography of an Arctic Stoloniferous Grass, Puccinellia-Phryganodes, in Response to Grazing. *Journal of Ecology, 77*(3), 811-822. https://doi.org/10.2307/2260987

Bengtson, P., Barker, J., & Grayston, S. J. (2012). Evidence of a strong coupling between root exudation, C and N availability, and stimulated SOM decomposition caused by rhizosphere priming effects. *Ecology and Evolution, 2*(8), 1843-1852. https://doi.org/10.1002/ece3.311

Berner, L. T., Massey, R., Jantz, P., Forbes, B. C., Macias-Fauria, M., Myers-Smith, I., Kumpula, T., Gauthier, G., Andreu-Hayles, L., Gaglioti, B. V., Burns, P., Zetterberg, P., D'Arrigo, R., & Goetz, S. J. (2020). Summer warming explains widespread but not uniform greening in the Arctic tundra biome. *Nature Communications, 11*(1), 4621. https://doi.org/10.1038/s41467-020-18479-5

Berryman, A. A. (1992). The Origins and Evolution of Predator Prey Theory. *Ecology, 73*(5), 1530-1535. https://doi.org/10.2307/1940005

Bjorkman, A. D., Elmendorf, S. C., Beamish, A. L., Vellend, M., & Henry, G. H. (2015). Contrasting effects of warming and increased snowfall on Arctic tundra plant phenology over the past two decades. *Global Change Biology, 21*(12), 4651-4661. https://doi.org/10.1111/gcb.13051

Blagodatsky, S., Blagodatskaya, E., Yuyukina, T., & Kuzyakov, Y. (2010). Model of apparent and real priming effects: Linking microbial activity with soil organic matter decomposition. *Soil Biology and Biochemistry, 42*(8), 1275-1283. https://doi.org/10.1016/j.soilbio.2010.04.005

Bosatta, E., & Ågren, G. I. (1999). Soil organic matter quality interpreted thermodynamically. *Soil Biology and Biochemistry, 31*(13), 1889-1891. https://doi.org/10.1016/S0038-0717(99)00105-4

Broeckling, C. D., Broz, A. K., Bergelson, J., Manter, D. K., & Vivanco, J. M. (2008). Root Exudates Regulate Soil Fungal Community Composition and Diversity. *Applied and Environmental Microbiology, 74*(3), 738-744. https://doi.org/10.1128/AEM.02188-07

Buchkowski, R. W., Bradford, M. A., Grandy, A. S., Schmitz, O. J., & Wieder, W. R. (2017). Applying population and community ecology theory to advance understanding of belowground biogeochemistry. *Ecology Letters, 20*(2), 231-245. https://doi.org/10.1111/ele.12712

Camenzind, T., Mason-Jones, K., Mansour, I., Rillig, M. C., & Lehmann, J. (2023). Formation of necromass-derived soil organic carbon determined by microbial death pathways. *Nature Geoscience, 16*(2), 115-122. https://doi.org/10.1038/s41561-022-01100-3

Cavicchioli, R., Ripple, W. J., Timmis, K. N., Azam, F., Bakken, L. R., Baylis, M., Behrenfeld, M. J., Boetius, A., Boyd, P. W., Classen, A. T., Crowther, T. W., Danovaro, R., Foreman, C. M., Huisman, J., Hutchins, D. A., Jansson, J. K., Karl, D. M., Koskella, B., Mark Welch, D. B., . . . Webster, N. S. (201 9). Scientists' warning to humanity: microorganisms and climate change. *Nature Reviews Microbiology, 17*(9), 569-586. https://doi.org/10.1038/s41579-019-0222-5

Chahartaghi, M., Langel, R., Scheu, S., & Ruess, L. (2005). Feeding guilds in Collembola based on nitrogen stable isotope ratios. *Soil Biology and Biochemistry, 37*(9), 1718-1725. https://doi.org/10.1016/j.soilbio.2005.02.006

Chang, K.-Y., Riley, W. J., Crill, P. M., Grant, R. F., & Saleska, S. R. (2020). Hysteretic temperature sensitivity of wetland CH4 fluxes explained by substrate availability and microbial activity. *Biogeosciences, 17*(22), 5849-5860. https://doi.org/10.5194/bg-17-5849-2020

Chang, K.-Y., Riley, W. J., Knox, S. H., Jackson, R. B., McNicol, G., Poulter, B., Aurela, M., Baldocchi, D., Bansal, S., Bohrer, G., Campbell, D. I., Cescatti, A., Chu, H., Delwiche, K. B., Desai, A. R., Euskirchen, E., Friborg, T., Goeckede, M., Helbig, M., . . . Zona, D. (2021). Substantial hysteresis in emergent temperature sensitivity of global wetland CH_4 emissions. *Nature Communications, 12*(1), 2266. https://doi.org/10.1038/s41467-021-22452-1

Chroňáková, A., Bárta, J., Kaštovská, E., Urbanová, Z., & Picek, T. (2019). Spatial heterogeneity of belowground microbial communities linked to peatland microhabitats with different plant dominants. *FEMS Microbiology Ecology, 95*(9). https://doi.org/10.1093/femsec/fiz130

Conrad, R. (2020). Importance of hydrogenotrophic, aceticlastic and methylotrophic methanogenesis for methane production in terrestrial, aquatic and other anoxic environments: A mini review. *Pedosphere, 30*(1), 25-39. https://doi.org/10.1016/S1002-0160(18)60052-9

Conrad, R. (2023). Complexity of temperature dependence in methanogenic microbial environments. *Frontiers in Microbiology, 14*, 1232946. https://doi.org/10.3389/fmicb.2023.1232946

Crowther, T. W., Thomas, S. M., Maynard, D. S., Baldrian, P., Covey, K., Frey, S. D., van Diepen, L. T., & Bradford, M. A. (2015). Biotic interactions mediate soil microbial feedbacks to climate change. *Proceedings of the National Academy of Sciences, 112*(22), 7033-7038. https://doi.org/10.1073/pnas.1502956112

Daniel, R. M., Danson, M. J., Eisenthal, R., Lee, C. K., & Peterson, M. E. (2008). The effect of temperature on enzyme activity: new insights and their implications. *Extremophiles, 12*(1), 51-59. https://doi.org/10.1007/s00792-007-0089-7

Davidson, E. A., & Janssens, I. A. (2006). Temperature sensitivity of soil carbon decomposition and feedbacks to climate change. *Nature, 440*(7081), 165-173. https://doi.org/10.1038/nature04514

Delgado-Baquerizo, M., Maestre, F. T., Reich, P. B., Jeffries, T. C., Gaitan, J. J., Encinar, D., Berdugo, M., Campbell, C. D., & Singh, B. K. (2016). Microbial diversity drives multifunctionality in terrestrial ecosystems. *Nature Communications, 7*(1), 10541. https://doi.org/10.1038/ncomms10541

Delgado-Baquerizo, M., Eldridge, D. J., Ochoa, V., Gozalo, B., Singh, B. K., & Maestre, F. T. (2017). Soil microbial communities drive the resistance of ecosystem multifunctionality to global change in drylands across the globe. *Ecology Letters, 20*(10), 1295-1305. https://doi.org/https://doi.org/10.1111/ele.12826

Dieleman, C. M., Branfireun, B. A., & Lindo, Z. (2017). Northern peatland carbon dynamics driven by plant growth form - the role of graminoids. *Plant and Soil, 415*(1-2), 25-35. https://doi.org/10.1007/s11104-016-3099-3

Edgecombe, A. E. (1938). The Effect of Galactose on the Growth of Certain Fungi. *Mycologia, 30*(6), 601-624. https://doi.org/10.1080/00275514.1938.12017303

Ehrich, D., Cerezo, M., Rodnikova, A. Y., Sokolova, N. A., Fuglei, E., Shtro, V. G., & Sokolov, A. A. (2017). Vole abundance and reindeer carcasses determine breeding activity of Arctic foxes in low Arctic Yamal, Russia. *BMC Ecology, 17*(1), 32. https://doi.org/10.1186/s12898-017-0142-z

Elmendorf, S. C., Henry, G. H. R., Hollister, R. D., Björk, R. G., Boulanger-Lapointe, N., Cooper, E. J., Cornelissen, J. H. C., Day, T. A., Dorrepaal, E., Elumeeva, T. G., Gill, M., Gould, W. A., Harte, J., Hik, D. S., Hofgaard, A., Johnson, D. R., Johnstone, J. F., Jónsdóttir, I. S., Jorgenson, J. C., . . . Wipf, S. (2012). Plot-scale evidence of tundra vegetation change and links to recent summer warming. *Nature Climate Change, 2*(6), 453-457. https://doi.org/10.1038/nclimate1465

Emerson, J. B., Roux, S., Brum, J. R., Bolduc, B., Woodcroft, B. J., Jang, H. B., Singleton, C. M., Solden, L. M., Naas, A. E., Boyd, J. A., Hodgkins, S. B., Wilson, R. M., Trubl, G., Li, C., Frolking, S., Pope, P. B., Wrighton, K. C., Crill, P. M., Chanton, J. P., . . . Sullivan, M. B. (2018). Host-linked soil viral ecology along a permafrost thaw gradient. *Nature Microbiology, 3*(8), 870-880. https://doi.org/10.1038/s41564-018-0190-y

Emerson, J. B. (2019). Soil Viruses: A New Hope. *mSystems, 4*(3), 10.1128/msystems.00120-00119. https://doi.org/10.1128/msystems.00120-19

Enzmann, F., Mayer, F., Rother, M., & Holtmann, D. (2018). Methanogens: biochemical background and biotechnological applications. *AMB Express, 8*(1), 1. https://doi.org/10.1186/s13568-017-0531-x

Erktan, A., Or, D., & Scheu, S. (2020). The physical structure of soil: Determinant and consequence of trophic interactions. *Soil Biology and Biochemistry, 148*, 107876. https://doi.org/10.1016/j.soilbio.2020.107876

Fahey, D. W., Doherty, S. J., Hibbard, K. A., Romanou, A., & Taylor, P. C. (2017). Physical drivers of climate change. In D. J. Wuebbles, D. W. Fahey, K. A. Hibbard, D. J. Dokken, B. C. Stewart, & T. K. Maycock (Eds.), *Climate Science Special Report: Fourth National Climate Assessment, Volume I* (pp. 73-113). https://doi.org/10.7930/J0513WCR

Feijó Delgado, F., Cermak, N., Hecht, V. C., Son, S., Li, Y., Knudsen, S. M., Olcum, S., Higgins, J. M., Chen, J., Grover, W. H., & Manalis, S. R. (2013). Intracellular Water Exchange for Measuring the Dry Mass, Water Mass and Changes in Chemical Composition of Living Cells. *Plos One, 8*(7), e67590. https://doi.org/10.1371/journal.pone.0067590

Fenner, N., & Freeman, C. (2011). Drought-induced carbon loss in peatlands. *Nature Geoscience, 4*(12), 895-900. https://doi.org/10.1038/ngeo1323

Ferlian, O., Klarner, B., Langeneckert, A. E., & Scheu, S. (2015). Trophic niche differentiation and utilisation of food resources in collembolans based on complementary analyses of fatty acids and stable isotopes. *Soil Biology and Biochemistry, 82*, 28-35. https://doi.org/10.1016/j.soilbio.2014.12.012

Ferry, J. G. (2011). Fundamentals of methanogenic pathways that are key to the biomethanation of complex biomass. *Current Opinion in Biotechnology, 22*(3), 351-357. https://doi.org/10.1016/j.copbio.2011.04.011

Fierer, N. (2017). Embracing the unknown: disentangling the complexities of the soil microbiome. *Nature Reviews Microbiology, 15*(10), 579-590. https://doi.org/10.1038/nrmicro.2017.87

Foley, K. M., Beard, K. H., Atwood, T. B., & Waring, B. G. (2022). Herbivory changes soil microbial communities and greenhouse gas fluxes in a high-latitude wetland. *Microbial Ecology, 83*(1), 127-136. https://doi.org/10.1007/s00248-021-01733-8

Fontaine, S., Barot, S., Barre, P., Bdioui, N., Mary, B., & Rumpel, C. (2007). Stability of organic carbon in deep soil layers controlled by fresh carbon supply. *Nature, 450*(7167), 277-280. https://doi.org/10.1038/nature06275

Fox, A. D., & Abraham, K. F. (2017). Why geese benefit from the transition from natural vegetation to agriculture. *Ambio, 46*(Suppl 2), 188-197. https://doi.org/10.1007/s13280-016-0879-1

Fox, A. D., & Madsen, J. (2017). Threatened species to super-abundance: The unexpected international implications of successful goose conservation. *Ambio, 46*(Suppl 2), 179-187. https://doi.org/10.1007/s13280-016-0878-2

Frey, S. D., Lee, J., Melillo, J. M., & Six, J. (2013). The temperature response of soil microbial efficiency and its feedback to climate. *Nature Climate Change, 3*(4), 395-398. https://doi.org/10.1038/nclimate1796

Geisen, S. (2016). The bacterial-fungal energy channel concept challenged by enormous functional versatility of soil protists. *Soil Biology and Biochemistry, 102*, 22-25. https://doi.org/10.1016/j.soilbio.2016.06.013

Geisen, S., Mitchell, E. A. D., Adl, S., Bonkowski, M., Dunthorn, M., Ekelund, F., Fernandez, L. D., Jousset, A., Krashevska, V., Singer, D., Spiegel, F. W., Walochnik, J., & Lara, E. (2018). Soil protists: a fertile frontier in soil biology research. *FEMS Microbiology Reviews, 42*(3), 293-323. https://doi.org/10.1093/femsre/fuy006

Goosemap (2023). Retrieved 11.08.2023 from https://goosemap.nina.no/goosemap_eng/Information-about-the-geese

Gorham, E. (1991). Northern Peatlands: Role in the Carbon Cycle and Probable Responses to Climatic Warming. *Ecological Applications, 1*(2), 182-195. https://doi.org/10.2307/1941811

Gornall, J. L., Woodin, S. J., Jonsdottir, I. S., & Van der Wal, R. (2009). Herbivore impacts to the moss layer determine tundra ecosystem response to grazing and warming. *Oecologia, 161*(4), 747-758. https://doi.org/10.1007/s00442-009-1427-5

Gougoulias, C., Clark, J. M., & Shaw, L. J. (2014). The role of soil microbes in the global carbon cycle: tracking the below-ground microbial processing of plant-derived carbon for manipulating carbon dynamics in agricultural systems. *Journal of the Science of Food and Agriculture, 94*(12), 2362-2371. https://doi.org/10.1002/jsfa.6577

Guo, X., Feng, J., Shi, Z., Zhou, X., Yuan, M., Tao, X., Hale, L., Yuan, T., Wang, J., Qin, Y., Zhou, A., Fu, Y., Wu, L., He, Z., Van Nostrand, J. D., Ning, D., Liu, X., Luo, Y., Tiedje, J. M., . . . Zhou, J. (2018). Climate warming leads to divergent succession of grassland microbial communities. *Nature Climate Change, 8*(9), 813-818. https://doi.org/10.1038/s41558-018-0254-2

Hájek, T., Ballance, S., Limpens, J., Zijlstra, M., & Verhoeven, J. T. A. (2011). Cell-wall polysaccharides play an important role in decay resistance of Sphagnum and actively depressed decomposition in vitro. *Biogeochemistry, 103*(1), 45-57. https://doi.org/10.1007/s10533-010-9444-3

Hallmann, C. A., Sorg, M., Jongejans, E., Siepel, H., Hofland, N., Schwan, H., Stenmans, W., Muller, A., Sumser, H., Horren, T., Goulson, D., & de Kroon, H. (2017). More than 75 percent decline over 27 years in total flying insect biomass in protected areas. *Plos One, 12*(10). https://doi.org/10.1371/journal.pone.0185809

Hartley, I. P., Garnett, M. H., Sommerkorn, M., Hopkins, D. W., Fletcher, B. J., Sloan, V. L., Phoenix, G. K., & Wookey, P. A. (2012). A potential loss of carbon associated with greater plant growth in the European Arctic. *Nature Climate Change, 2*(12), 875-879. https://doi.org/10.1038/Nclimate1575

Hessen, D. O., Tombre, I. M., van Geest, G., & Alfsnes, K. (2017). Global change and ecosystem connectivity: How geese link fields of central Europe to eutrophication of Arctic freshwaters. *Ambio, 46*(1), 40-47. https://doi.org/10.1007/s13280-016-0802-9

Hodgkins, S. B., Richardson, C. J., Dommain, R., Wang, H., Glaser, P. H., Verbeke, B., Winkler, B. R., Cobb, A. R., Rich, V. I., Missilmani, M., Flanagan, N., Ho, M., Hoyt, A. M., Harvey, C. F., Vining, S. R., Hough, M. A., Moore, T. R., Richard, P. J. H., De La Cruz, F. B., . . . Chanton, J. P. (2018). Tropical peatland carbon storage linked to global latitudinal trends in peat recalcitrance. *Nature Communications, 9*(1), 3640. https://doi.org/10.1038/s41467-018-06050-2

Hugelius, G., Loisel, J., Chadburn, S., Jackson, R. B., Jones, M., MacDonald, G., Marushchak, M., Olefeldt, D., Packalen, M., Siewert, M. B., Treat, C., Turetsky, M., Voigt, C., & Yu, Z. (2020). Large stocks of peatland carbon and nitrogen are vulnerable to permafrost thaw. *Proceedings of the National Academy of Sciences, 117*(34), 20438-20446. https://doi.org/pnas.1916387117

Hungate, B. A., Marks, J. C., Power, M. E., Schwartz, E., Groenigen, K. J. v., Blazewicz, S. J., Chuckran, P., Dijkstra, P., Finley, B. K., Firestone, M. K., Foley, M., Greenlon, A., Hayer, M., Hofmockel, K. S., Koch, B. J., Mack, M. C., Mau, R. L., Miller, S. N., Morrissey, E. M., . . . Pett-Ridge, J. (2021). The Functional Significance of Bacterial Predators. *Mbio, 12*(2), 10.1128/mbio.00466-00421. https://doi.org/10.1128/mbio.00466-21

Hünninghaus, M., Koller, R., Kramer, S., Marhan, S., Kandeler, E., & Bonkowski, M. (2017). Changes in bacterial community composition and soil respiration indicate rapid successions of protist grazers during mineralization of maize crop residues. *Pedobiologia, 62*, 1-8. https://doi.org/10.1016/j.pedobi.2017.03.002

Hutchins, D. A., Jansson, J. K., Remais, J. V., Rich, V. I., Singh, B. K., & Trivedi, P. (2019). Climate change microbiology — problems and perspectives. *Nature Reviews Microbiology, 17*(6), 391-396. https://doi.org/10.1038/s41579-019-0178-5

IPCC (2023). In H. Lee and J. Romero (Eds.), *Climate Change 2023: Synthesis Report.* A Report of the Intergovernmental Panel on Climate Change. Contribution of Working Groups I, II and III to the Sixth Assessment Report of the Intergovernmental Panel on Climate Change IPCC, Geneva, Switzerland. In press.

Jansson, C., Wullschleger, S. D., Kalluri, U. C., & Tuskan, G. A. (2010). Phytosequestration: Carbon Biosequestration by Plants and the Prospects of Genetic Engineering. *BioScience, 60*(9), 685-696. https://doi.org/10.1525/bio.2010.60.9.6

Jansson, J. K., & Hofmockel, K. S. (2020). Soil microbiomes and climate change. *Nature Reviews Microbiology, 18*(1), 35-46. https://doi.org/10.1038/s41579-019-0265-7

Jansson, C., Faiola, C., Wingler, A., Zhu, X. G., Kravchenko, A., de Graaff, M. A., Ogden, A. J., Handakumbura, P. P., Werner, C., & Beckles, D. M. (2021). Crops for Carbon Farming. *Frontiers Plant Science, 12*, 636709. https://doi.org/10.3389/fpls.2021.636709

Jia, G., Shevliakova, E., Artaxo, P., De Noblet-Ducoudré, N., Houghton, R., House, J., Kitajima, K., …, Verchot, L. (2019). Land–climate interactions. In P.R. Shukla, J. Skea, E. Calvo Buendia, V. Masson-Delmotte, H.-O. Pörtner, D.C. Roberts,…, J. Malley (Eds.), *Climate Change and Land: an IPCC special report on climate change, desertification, land degradation, sustainable land management, food security, and greenhouse gas fluxes in terrestrial ecosystems.* In press.

Jiang, J., Guo, S., Zhang, Y., Liu, Q., Wang, R., Wang, Z., Li, N., & Li, R. (2015). Changes in temperature sensitivity of soil respiration in the phases of a three-year crop rotation system. *Soil and Tillage Research, 150*, 139-146. https://doi.org/10.1016/j.still.2015.02.002

Jover, L. F., Effler, T. C., Buchan, A., Wilhelm, S. W., & Weitz, J. S. (2014). The elemental composition of virus particles: implications for marine biogeochemical cycles. *Nature Reviews Microbiology, 12*(7), 519-528. https://doi.org/10.1038/nrmicro3289

Kalyuzhnaya, M. G., Gomez, O. A., & Murrell, J. C. (2019). The Methane-Oxidizing Bacteria (Methanotrophs). In T. J. McGenity (Ed.), T*axonomy, Genomics and Ecophysiology of Hydrocarbon-Degrading Microbes* (pp. 1-34). Springer International Publishing. https://doi.org/10.1007/978-3-319-60053-6_10-1

Keenan, T. F., & Riley, W. J. (2018). Greening of the land surface in the world's cold regions consistent with recent warming. *Nature Climate Change, 8*, 825-828. https://doi.org/10.1038/s41558-018-0258-y

Kelly, D. J., Hughes, N. J., & Poole, R. K. (2001). Microaerobic Physiology: Aerobic Respiration, Anaerobic Respiration, and Carbon Dioxide Metabolism. In H.L.T. Mobley, G.L. Mendz and S.L. Hazell (Eds.), *Helicobacter pylori* (pp. 111-124). https://doi.org/10.1128/9781555818005.ch10

Knorr, W., Prentice, I. C., House, J. I., & Holland, E. A. (2005). Long-term sensitivity of soil carbon turnover to warming. *Nature, 433*(7023), 298-301. https://doi.org/10.1038/nature03226

Kohanski, M. A., Dwyer, D. J., & Collins, J. J. (2010). How antibiotics kill bacteria: from targets to networks. *Nature Reviews Microbiology, 8*(6), 423-435. https://doi.org/10.1038/nrmicro2333

Koranda, M., Kaiser, C., Fuchslueger, L., Kitzler, B., Sessitsch, A., Zechmeister-Boltenstern, S., & Richter, A. (2014). Fungal and bacterial utilization of organic substrates depends on substrate complexity and N availability. *FEMS Microbiology Ecology, 87*(1), 142-152. https://doi.org/10.1111/1574-6941.12214

Kristensen, J. A., Svenning, J.-C., Georgiou, K., & Malhi, Y. (2022). Can large herbivores enhance ecosystem carbon persistence? *Trends in Ecology & Evolution, 37*(2), 117-128. https://doi.org/10.1016/j.tree.2021.09.006

Kuijper, D. P. J., Bakker, J. P., Cooper, E. J., Ubels, R., Jónsdóttir, I. S., & Loonen, M. J. J. E. (2006). Intensive grazing by Barnacle geese depletes High Arctic seed bank. *Canadian Journal of Botany, 84*(6), 995-1004. https://doi.org/10.1139/b06-052

Kuijper, D. P. J., Ubels, R., & Loonen, M. J. J. E. (2009). Density-dependent switches in diet: a likely mechanism for negative feedbacks on goose population increase? *Polar Biology, 32*, 1789–1803. https://doi.org/10.1007/s00300-009-0678-2

Kurth, J. M., Smit, N. T., Berger, S., Schouten, S., Jetten, M. S. M., & Welte, C. U. (2019). Anaerobic methanotrophic archaea of the ANME-2d clade feature lipid composition that differs from other ANME archaea. *FEMS Microbiology Ecology, 95*(7). https://doi.org/10.1093/femsec/fiz082

Kuzyakov, Y. (2010). Priming effects: Interactions between living and dead organic matter. *Soil Biology and Biochemistry, 42*(9), 1363-1371. https://doi.org/10.1016/j.soilbio.2010.04.003

Lang, S. I., Cornelissen, J. H. C., Klahn, T., Van Logtestijn, R. S. P., Broekman, R., Schweikert, W., & Aerts, R. (2009). An experimental comparison of chemical traits and litter decomposition rates in a diverse range of subarctic bryophyte, lichen and vascular plant species. *Journal of Ecology, 97*(5), 886-900. https://doi.org/10.1111/j.1365-2745.2009.01538.x

Layton-Matthews, K., Hansen, B. B., Grotan, V., Fuglei, E., & Loonen, M. (2020). Contrasting consequences of climate change for migratory geese: Predation, density dependence and carryover effects offset benefits of high-arctic warming. *Global Change Biology, 26*(2), 642-657. https://doi.org/10.1111/gcb.14773

Liang, C., Amelung, W., Lehmann, J., & Kastner, M. (2019). Quantitative assessment of microbial necromass contribution to soil organic matter. *Global Change Biology, 25*(11), 3578-3590. https://doi.org/10.1111/gcb.14781

Limpens, J., Berendse, F., Blodau, C., Canadell, J. G., Freeman, C., Holden, J., Roulet, N., Rydin, H., & Schaepman-Strub, G. (2008). Peatlands and the carbon cycle: from local processes to global implications – a synthesis. *Biogeosciences, 5*(5), 1475-1491. https://doi.org/10.5194/bg-5-1475-2008

Liu, Y., & Whitman, W. B. (2008). Metabolic, phylogenetic, and ecological diversity of the methanogenic archaea. *Annals of the New York Academy of Science, 1125*, 171-189. https://doi.org/10.1196/annals.1419.019

Lucas, J. M., McBride, S. G., & Strickland, M. S. (2020). Trophic level mediates soil microbial community composition and function. *Soil Biology & Biochemistry, 143*. https://doi.org/10.1016/j.soilbio.2020.107756

Luo, Y., Wan, S., Hui, D., & Wallace, L. L. (2001). Acclimatization of soil respiration to warming in a tall grass prairie. *Nature, 413*(6856), 622-625. https://doi.org/10.1038/35098065

Lyu, Z., Shao, N., Akinyemi, T., & Whitman, W. B. (2018). Methanogenesis. *Current Biology, 28*(13), R727-R732. https://doi.org/10.1016/j.cub.2018.05.021

Madsen, J., Jensen, G. H., Cottaar, F., Amstrup, O., Bak, M., Bakken, J., Balsby, T. T. J., Christensen, T. K., Clausen, K. K., Frikke, J., Gundersen, O. M., Kjeldse, J. P., Koffijberg, K., Kuijken, E., Månsson, J., Nicolaisen, P. I., Nielsen, H. H., Nilsson, L., Reinsborg, T., . . . Verscheure, C. (2017). Svalbard Pink-footed goose. Population status report 2017-2018, AEWA EGM IWG 3.8. In press.

Maestre, F. T., Delgado-Baquerizo, M., Jeffries, T. C., Eldridge, D. J., Ochoa, V., Gozalo, B., Quero, J. L., García-Gómez, M., Gallardo, A., Ulrich, W., Bowker, M. A., Arredondo, T., Barraza-Zepeda, C., Bran, D., Florentino, A., Gaitán, J., Gutiérrez, J. R., Huber-Sannwald, E., Jankju, M., . . . Singh, B. K. (2015). Increasing aridity reduces soil microbial diversity and abundance in global drylands. *Proceedings of the National Academy of Sciences, 112*(51), 15684-15689. https://doi.org/doi:10.1073/pnas.1516684112

Mairet, F., Gouzé, J.-L., & de Jong, H. (2021). Optimal proteome allocation and the temperature dependence of microbial growth laws. *npj Systems Biology and Applications, 7*(1), 14. https://doi.org/10.1038/s41540-021-00172-y

Maron, J. L., & Crone, E. (2006). Herbivory: effects on plant abundance, distribution and population growth. *Proceedings of the Royal Society B: Biological Sciences, 273*(1601), 2575-2584. https://doi.org/10.1098/rspb.2006.3587

Mayer, M., Rewald, B., Matthews, B., Sanden, H., Rosinger, C., Katzensteiner, K., Gorfer, M., Berger, H., Tallian, C., Berger, T. W., & Godbold, D. L. (2021). Soil fertility relates to fungal-mediated decomposition and organic matter turnover in a temperate mountain forest. *New Phytologist, 231*(2), 777-790. https://doi.org/10.1111/nph.17421

McCarty, J. P. (2001). Ecological consequences of recent climate change. *Conservation Biology, 15*(2), 320-331. https://doi.org/10.1046/j.1523-1739.2001.015002320.x

Melillo, J. M., Steudler, P. A., Aber, J. D., Newkirk, K., Lux, H., Bowles, F. P., Catricala, C., Magill, A., Ahrens, T., & Morrisseau, S. (2002). Soil Warming and Carbon-Cycle Feedbacks to the Climate System. *Science, 298*(5601), 2173-2176. https://doi.org/doi:10.1126/science.1074153

Navarro Lab (2023). *Microbial trophic interactions in soil*. Retrieved 25.09.2023 from https://hostmicrobiome.info/soil-microbiome/

Naylor, D., Sadler, N., Bhattacharjee, A., Graham, E. B., Anderton, C. R., McClure, R., Lipton, M., Hofmockel, K. S., & Jansson, J. K. (2020). Soil Microbiomes Under Climate Change and Implications for Carbon Cycling. *Annual Review of Environment and Resources, 45*(1), 29-59. https://doi.org/10.1146/annurev-environ-012320-082720

Neher, D. A. (2010). Ecology of Plant and Free-Living Nematodes in Natural and Agricultural Soil. *Annual Review of Phytopathology, 48*(1), 371-394. https://doi.org/10.1146/annurev-phyto-073009-114439

Neidhardt, F. C., Ingraham, J. L., & Schaechter, M. (1990). Physiology of the Bacterial Cell. A Molecular Approach:. In C. A. Smith (Ed.), *Biochemical Education* (Vol. 20, pp. 124-125). https://doi.org/10.1016/0307-4412(92)90139-D

Newsham, K. K., Hopkins, D. W., Carvalhais, L. C., Fretwell, P. T., Rushton, S. P., O'Donnell, A. G., & Dennis, P. G. (2016). Relationship between soil fungal diversity and temperature in the maritime Antarctic. *Nature Climate Change, 6*(2), 182-186. https://doi.org/10.1038/nclimate2806

Nuccio, E. E., Starr, E., Karaoz, U., Brodie, E. L., Zhou, J., Tringe, S. G., Malmstrom, R. R., Woyke, T., Banfield, J. F., Firestone, M. K., & Pett-Ridge, J. (2020). Niche differentiation is spatially and temporally regulated in the rhizosphere. *The ISME Journal, 14*(4), 999-1014. https://doi.org/10.1038/s41396-019-0582-x

Obu, J. (2021). How Much of the Earth's Surface is Underlain by Permafrost*? Journal of Geophysical Research: Earth Surface, 126*(5). https://doi.org/10.1029/2021jf006123

Oechel, W. C., Vourlitis, G. L., Hastings, S. J., Zulueta, R. C., Hinzman, L., & Kane, D. (2000). Acclimation of ecosystem CO2 exchange in the Alaskan Arctic in response to decadal climate warming. *Nature, 406*(6799), 978-981. https://doi.org/10.1038/35023137

Oertel, C., Matschullat, J., Zurba, K., Zimmermann, F., & Erasmi, S. (2016). Greenhouse gas emissions from soils—A review. *Geochemistry, 76*(3), 327-352. https://doi.org/10.1016/j.chemer.2016.04.002

Oishi, Y. (2018). Evaluation of the Water-Storage Capacity of Bryophytes along an Altitudinal Gradient from Temperate Forests to the Alpine Zone. *Forests, 9*(7), 433. https://www.mdpi.com/1999-4907/9/7/433

Oliverio, A. M., Bradford, M. A., & Fierer, N. (2017). Identifying the microbial taxa that consistently respond to soil warming across time and space. *Global Change Biology, 23*(5), 2117-2129. https://doi.org/https://doi.org/10.1111/gcb.13557

Paez-Espino, D., Eloe-Fadrosh, E. A., Pavlopoulos, G. A., Thomas, A. D., Huntemann, M., Mikhailova, N., Rubin, E., Ivanova, N. N., & Kyrpides, N. C. (2016). Uncovering Earth's virome. *Nature, 536*(7617), 425-430. https://doi.org/10.1038/nature19094

Pasternak, Z., Njagi, M., Shani, Y., Chanyi, R., Rotem, O., Lurie-Weinberger, M. N., Koval, S., Pietrokovski, S., Gophna, U., & Jurkevitch, E. (2014). In and out: an analysis of epibiotic vs periplasmic bacterial predators. *The ISME Journal, 8*(3), 625-635. https://doi.org/10.1038/ismej.2013.164

Petit Bon, M., Hansen, B. B., Loonen, M. J. J. E., Petraglia, A., Bråthen, K. A., Böhner, H., Layton-Matthews, K., Beard, K. H., Moullec, M. L., Jónsdóttir, I. S., & Wal, R. v. d. (2023). Long-term herbivore removal experiments reveal different impacts of geese and reindeer on vegetation and ecosystem CO_2-fluxes in high-Arctic tundra. *bioRxiv*, 2023.2001.2027.525821. https://doi.org/10.1101/2023.01.27.525821

Petters, S., Groß, V., Söllinger, A., Pichler, M., Reinhard, A., Bengtsson, M. M., & Urich, T. (2021). The soil microbial food web revisited: Predatory myxobacteria as keystone taxa? *The ISME Journal, 15*(9), 2665-2675. https://doi.org/10.1038/s41396-021-00958-2

Philippot, L., & Hallin, S. (2005). Finding the missing link between diversity and activity using denitrifying bacteria as a model functional community. *Current Opinion in Microbiology, 8*(3), 234-239. https://doi.org/10.1016/j.mib.2005.04.003

Phoenix, G. K., & Bjerke, J. W. (2016). Arctic browning: extreme events and trends reversing arctic greening. *Global Change Biology, 22*(9), 2960-2962. https://doi.org/10.1111/gcb.13261

Ping, C. L., Jastrow, J. D., Jorgenson, M. T., Michaelson, G. J., & Shur, Y. L. (2015). Permafrost soils and carbon cycling. *SOIL, 1*(1), 147-171. https://doi.org/10.5194/soil-1-147-2015

Pipes, G. T., & Yavitt, J. B. (2022). Biochemical components of Sphagnum and persistence in peat soil. *Canadian Journal of Soil Science, 102*(3), 785-795. https://doi.org/10.1139/cjss-2021-0137

Popper, Z. A., & Fry, S. C. (2003). Primary cell wall composition of bryophytes and charophytes. *Annals of Botany, 91*(1), 1-12. https://doi.org/10.1093/aob/mcg013

Post, E., Forchhammer, M. C., Bret-Harte, M. S., Callaghan, T. V., Christensen, T. R., Elberling, B., Fox, A. D., Gilg, O., Hik, D. S., Hoye, T. T., Ims, R. A., Jeppesen, E., Klein, D. R., Madsen, J., McGuire, A. D., Rysgaard, S., Schindler, D. E., Stirling, I., Tamstorf, M. P., . . . Aastrup, P. (2009). Ecological dynamics across the Arctic associated with recent climate change. *Science, 325*(5946), 1355-1358. https://doi.org/10.1126/science.1173113

Potapov, A. A., Semenina, E. E., Korotkevich, A. Y., Kuznetsova, N. A., & Tiunov, A. V. (2016). Connecting taxonomy and ecology: Trophic niches of collembolans as related to taxonomic identity and life forms. *Soil Biology and Biochemistry, 101*, 20-31. https://doi.org/10.1016/j.soilbio.2016.07.002

Poulter, B., Frank, D., Ciais, P., Myneni, R. B., Andela, N., Bi, J., Broquet, G., Canadell, J. G., Chevallier, F., Liu, Y. Y., Running, S. W., Sitch, S., & van der Werf, G. R. (2014). Contribution of semi-arid ecosystems to interannual variability of the global carbon cycle. *Nature, 509*(7502), 600-603. https://doi.org/10.1038/nature13376

Rai, K. M., Balasubramanian, V. K., Welker, C. M., Pang, M., Hii, M. M., & Mendu, V. (2015). Genome wide comprehensive analysis and web resource development on cell wall degrading enzymes from phyto-parasitic nematodes. *BMC Plant Biology, 15*(1), 187. https://doi.org/10.1186/s12870-015-0576-4

Rainer, E. M., Seppey, C. V. W., Tveit, A. T., & Svenning, M. M. (2020). Methanotroph populations and CH_4 oxidation potentials in high-Arctic peat are altered by herbivory induced vegetation change. *FEMS Microbiology Ecology, 96*(10). https://doi.org/10.1093/femsec/fiaa140

Rantanen, M., Karpechko, A. Y., Lipponen, A., Nordling, K., Hyvarinen, O., Ruosteenoja, K., Vihma, T., & Laaksonen, A. (2022). The Arctic has warmed nearly four times faster than the globe since 1979. *Communications Earth and Environment, 3*(1). https://doi.org/10.1038/s43247-022-00498-3

Roberts, A. W., Roberts, E. M., & Haigler, C. H. (2012). Moss cell walls: structure and biosynthesis. *Frontiers in Plant Science, 3*, 166. https://doi.org/10.3389/fpls.2012.00166

Sarkar, P., Bosneaga, E., & Auer, M. (2009). Plant cell walls throughout evolution: towards a molecular understanding of their design principles. *Journal of Experimental Botany, 60*(13), 3615-3635. https://doi.org/10.1093/jxb/erp245

Sayer, E. J., Oliver, A. E., Fridley, J. D., Askew, A. P., Mills, R. T., & Grime, J. P. (2017). Links between soil microbial communities and plant traits in a species-rich grassland under long-term climate change. *Ecology and Evolution, 7*(3), 855-862. https://doi.org/10.1002/ece3.2700

Schink, B. (1997). Energetics of syntrophic cooperation in methanogenic degradation. *Microbiology and Molecular Biology Reviews, 61*(2), 262-280. https://doi.org/10.1128/mmbr.61.2.262-280.1997

Schmidt, O., Hink, L., Horn, M. A., & Drake, H. L. (2016). Peat: home to novel syntrophic species that feed acetate- and hydrogen-scavenging methanogens. *The ISME Journal, 10*(8), 1954-1966. https://doi.org/10.1038/ismej.2015.256

Schuur, E. A., McGuire, A. D., Schadel, C., Grosse, G., Harden, J. W., Hayes, D. J., Hugelius, G., Koven, C. D., Kuhry, P., Lawrence, D. M., Natali, S. M., Olefeldt, D., Romanovsky, V. E., Schaefer, K., Turetsky, M. R., Treat, C. C., & Vonk, J. E. (2015). Climate change and the permafrost carbon feedback. *Nature, 520*(7546), 171-179. https://doi.org/10.1038/nature14338

Sheik, C. S., Beasley, W. H., Elshahed, M. S., Zhou, X., Luo, Y., & Krumholz, L. R. (2011). Effect of warming and drought on grassland microbial communities. *The ISME Journal, 5*(10), 1692-1700. https://doi.org/10.1038/ismej.2011.32

Shimkets, L. J. (1990). Social and developmental biology of the myxobacteria. *Microbiological Reviews, 54*(4), 473-501. https://doi.org/10.1128/mr.54.4.473-501.1990

Shotyk, W. (1988). Review of the inorganic geochemistry of peats and peatland waters. *Earth-Science Reviews, 25*(2), 95-176. https://doi.org/10.1016/0012-8252(88)90067-0

Sillman, C. E., & Casida Jr., L. E. (1986). Isolation of nonobligate bacterial predators of bacteria from soil. *Canadian Journal of Microbiology, 32*(9), 760-762. https://doi.org/10.1139/m86-139

Singh, B. K., Bardgett, R. D., Smith, P., & Reay, D. S. (2010). Microorganisms and climate change: terrestrial feedbacks and mitigation options. *Nature Reviews Microbiology, 8*(11), 779-790. https://doi.org/10.1038/nrmicro2439

Sjögersten, S., Kuijper, D. P. J., van der Wal, R., Loonen, M. J. J. E., Huiskes, A. H. L., & Woodin, S. J. (2010). Nitrogen transfer between herbivores and their forage species. *Polar Biology, 33*(9), 1195-1203. https://doi.org/10.1007/s00300-010-0809-9

Sjögersten, S., van der Wal, R., Loonen, M. J., & Woodin, S. J. (2011). Recovery of ecosystem carbon fluxes and storage from herbivory. *Biogeochemistry, 106*(3), 357-370. https://doi.org/10.1007/s10533-010-9516-4

Sokol, N. W., Slessarev, E., Marschmann, G. L., Nicolas, A., Blazewicz, S. J., Brodie, E. L., Firestone, M. K., Foley, M. M., Hestrin, R., Hungate, B. A., Koch, B. J., Stone, B. W., Sullivan, M. B., Zablocki, O., Trubl, G., McFarlane, K., Stuart, R., Nuccio, E., Weber, P., . . . Consortium, L. S. M. (2022). Life and death in the soil microbiome: how ecological processes influence biogeochemistry. *Nature Reviews Microbiology, 20*(7), 415-430. https://doi.org/10.1038/s41579-022-00695-z

Stolp, H., & Starr, M. P. (1963). Bdellovibrio bacteriovorus gen. et sp. n., a predatory, ectoparasitic, and bacteriolytic microorganism. *Antonie van Leeuwenhoek, 29*(1), 217-248. https://doi.org/10.1007/BF02046064

Strack, M., Waddington, J., Turetsky, M., Roulet, N., and Byrne, K.: Northern Peatlands, Greenhouse Gas Exchange and Climate Change. In M. Strack (Ed.), *Peatlands and Climate Change* (pp. 44–69). ISBN 978-952-99401-1-0, International Peatland Society, 2008.

Strakova, P., Anttila, J., Spetz, P., Kitunen, V., Tapanila, T., & Laiho, R. (2010). Litter quality and its response to water level drawdown in boreal peatlands at plant species and community level. *Plant and Soil, 335*(1-2), 501-520. https://doi.org/10.1007/s11104-010-0447-6

Söllinger, A., Schwab, C., Weinmaier, T., Loy, A., Tveit, A. T., Schleper, C., & Urich, T. (2015). Phylogenetic and genomic analysis of Methanomassiliicoccales in wetlands and animal intestinal tracts reveals clade-specific habitat preferences. *FEMS Microbiology Ecology, 92*(1). https://doi.org/10.1093/femsec/fiv149

Söllinger, A., & Urich, T. (2019). Methylotrophic methanogens everywhere - physiology and ecology of novel players in global methane cycling. *Biochemical Society Transactions, 47*(6), 1895-1907. https://doi.org/10.1042/BST20180565

Söllinger, A., Seneca, J., Borg Dahl, M., Motleleng, L. L., Prommer, J., Verbruggen, E., Sigurdsson, B. D., Janssens, I., Penuelas, J., Urich, T., Richter, A., & Tveit, A. T. (2022). Down-regulation of the bacterial protein biosynthesis machinery in response to weeks, years, and decades of soil warming. *Science Advances, 8*(12), eabm3230. https://doi.org/10.1126/sciadv.abm3230

Tang, J., & Riley, W. J. (2015). Weaker soil carbon–climate feedbacks resulting from microbial and abiotic interactions. *Nature Climate Change, 5*(1), 56-60. https://doi.org/10.1038/nclimate2438

Tarnocai, C., Canadell, J. G., Schuur, E. A. G., Kuhry, P., Mazhitova, G., & Zimov, S. (2009). Soil organic carbon pools in the northern circumpolar permafrost region. *Global Biogeochemical Cycles, 23*(2) https://doi.org/10.1029/2008GB003327

Taylor, P. C., Maslowski, W., Perlwitz, J., & Wuebbles, D. J. (2017). Arctic changes and their effects on Alaska and the rest of the United States. In D. J. Wuebbles, D. W. Fahey, K. A. Hibbard, D. J. Dokken, B. C. Stewart, & T. K. Maycock (Eds.), *Climate Science Special Report: Fourth National Climate Assessment, Volume I* (pp. 303-332). https://doi.org/10.7930/J00863GK

Tchakerian, V., & Pease, P. (2015). The Critical Zone in Desert Environments. In J. R. Giardino & C. Houser (Eds.), *Developments in Earth Surface Processes* (Vol. 19, pp. 449-472). Elsevier. https://doi.org/10.1016/B978-0-444-63369-9.00014-8

Thakur, M. P., & Geisen, S. (2019). Trophic Regulations of the Soil Microbiome. *Trends in Microbiology, 27*(9), 771-780. https://doi.org/10.1016/j.tim.2019.04.008

Thormann, M. N. (2006). Diversity and function of fungi in peatlands: A carbon cycling perspective. *Canadian Journal of Soil Science, 86*(Special Issue), 281-293. https://doi.org/10.4141/s05-082

Tiedje, J. M., Bruns, M. A., Casadevall, A., Criddle, C. S., Eloe-Fadrosh, E., Karl, D. M., Nguyen, N. K., & Zhou, J. Z. (2022). Microbes and Climate Change: a Research Prospectus for the Future. *Mbio, 13*(3). https://doi.org/10.1128/mbio.00800-22

Trap, J., Bonkowski, M., Plassard, C., Villenave, C., & Blanchart, E. (2016). Ecological importance of soil bacterivores for ecosystem functions. *Plant and Soil, 398*(1-2), 1-24. https://doi.org/10.1007/s11104-015-2671-6

Treharne, R., Bjerke, J. W., Tommervik, H., Stendardi, L., & Phoenix, G. K. (2019). Arctic browning: Impacts of extreme climatic events on heathland ecosystem CO_2 fluxes. *Global Change Biology, 25*(2), 489-503. https://doi.org/10.1111/gcb.14500

Trubl, G., Jang, H. B., Roux, S., Emerson, J. B., Solonenko, N., Vik, D. R., Solden, L., Ellenbogen, J., Runyon, A. T., Bolduc, B., Woodcroft, B. J., Saleska, S. R., Tyson, G. W., Wrighton, K. C., Sullivan, M. B., & Rich, V. I. (2018). Soil Viruses Are Underexplored Players in Ecosystem Carbon Processing. *mSystems, 3*(5). https://doi.org/10.1128/mSystems.00076-18

Turner, M. G., Calder, W. J., Cumming, G. S., Hughes, T. P., Jentsch, A., LaDeau, S. L., Lenton, T. M., Shuman, B. N., Turetsky, M. R., Ratajczak, Z., Williams, J. W., Williams, A. P., & Carpenter, S. R. (2020). Climate change, ecosystems and abrupt change: science priorities. *Philosophical Transactions of the Royal Society B-Biological Sciences, 375*(1794). https://doi.org/10.1098/rstb.2019.0105

Tveit, A., Schwacke, R., Svenning, M. M., & Urich, T. (2013). Organic carbon transformations in high-Arctic peat soils: key functions and microorganisms. *The ISME Journal, 7*(2), 299-311. https://doi.org/10.1038/ismej.2012.99

Tveit, A. T., Urich, T., Frenzel, P., & Svenning, M. M. (2015). Metabolic and trophic interactions modulate methane production by Arctic peat microbiota in response to warming. *Proceedings of the National Academy of Sciences*, *112*(19), E2507-2516. https://doi.org/10.1073/pnas.1420797112

Tveit, A. T., Söllinger, A., Rainer, E. M., Didriksen, A., Hestnes, A. G., Motleleng, L., Hellinger, H.-J., Rattei, T., & Svenning, M. M. (2023). Thermal acclimation of methanotrophs from the genus Methylobacter. *The ISME Journal, 17*(4), 502-513. https://doi.org/10.1038/s41396-023-01363-7

United Nations (2023). What Is Climate Change? Retrieved 01.08.2023 from: https://www.un.org/en/climatechange/what-is-climate-change

van den Brink, J., & de Vries, R. P. (2011). Fungal enzyme sets for plant polysaccharide degradation. *Applied Microbiology and Biotechnology, 91*(6), 1477-1492. https://doi.org/10.1007/s00253-011-3473-2

van der Wal, R., van Lieshout, S. M. J., & Loonen, M. J. J. E. (2001). Herbivore impact on moss depth, soil temperature and arctic plant growth. *Polar Biology, 24*(1), 29-32. https://doi.org/10.1007/s003000000170

van der Wal, R., & Stien, A. (2014). High-arctic plants like it hot: a long-term investigation of between-year variability in plant biomass. *Ecology, 95*(12), 3414-3427. https://doi.org/10.1890/14-0533.1

Wagner, N., Tran, Q. H., Richter, H., Selzer, P. M., & Unden, G. (2005). Pyruvate Fermentation by Oenococcus oeni and Leuconostoc mesenteroides and Role of Pyruvate Dehydrogenase in Anaerobic Fermentation. *Applied and Environmental Microbiology, 71*(9), 4966-4971. https://doi.org/10.1128/AEM.71.9.4966-4971.2005

Walker, T. N., Garnett, M. H., Ward, S. E., Oakley, S., Bardgett, R. D., & Ostle, N. J. (2016). Vascular plants promote ancient peatland carbon loss with climate warming. *Global Change Biology, 22*(5), 1880-1889. https://doi.org/10.1111/gcb.13213

Walker, T. W. N., Kaiser, C., Strasser, F., Herbold, C. W., Leblans, N. I. W., Woebken, D., Janssens, I. A., Sigurdsson, B. D., & Richter, A. (2018). Microbial temperature sensitivity and biomass change explain soil carbon loss with warming. *Nature Climate Change, 8*(10), 885-889. https://doi.org/10.1038/s41558-018-0259-x

Wallenstein, M. D., & Weintraub, M. N. (2008). Emerging tools for measuring and modeling the in situ activity of soil extracellular enzymes. *Soil Biology and Biochemistry, 40*(9), 2098-2106. https://doi.org/10.1016/j.soilbio.2008.01.024

Wallenstein, M., Allison, S. D., Ernakovich, J., Steinweg, J. M., & Sinsabaugh, R. (2011). Controls on the Temperature Sensitivity of Soil Enzymes: A Key Driver of In Situ Enzyme Activity Rates. In G. Shukla & A. Varma (Eds.), *Soil Enzymology* (pp. 245-258). Springer Berlin Heidelberg. https://doi.org/10.1007/978-3-642-14225-3_13

Wang, B., Liu, J., Zhang, X., & Wang, C. (2021). Changes in soil carbon sequestration and emission in different succession stages of biological soil crusts in a sand-binding area. *Carbon Balance and Management, 16(1)*, 27. https://doi.org/10.1186/s13021-021-00190-7

Wang, B., Zhu, Y., Chen, X., Chen, D., Wu, Y., Wu, L., Liu, S., Yue, L., Wang, Y., & Bai, Y. (2022). Even short-term revegetation complicates soil food webs and strengthens their links with ecosystem functions. *Journal of Applied Ecology, 59*(7), 1721-1733. https://doi.org/10.1111/1365-2664.14180

Wardle, D. A., Bardgett, R. D., Klironomos, J. N., Setälä, H., van der Putten, W. H., & Wall, D. H. (2004). Ecological Linkages Between Aboveground and Belowground Biota. *Science, 304*(5677), 1629-1633. https://doi.org/10.1126/science.1094875

Warren, R. A. J. (1996). Microbial hydrolysis of polysaccharides *Annual Review of Microbiology, 50*(1), 183-212. https://doi.org/10.1146/annurev.micro.50.1.183

Wartiainen, I., Hestnes, A. G., & Svenning, M. M. (2003). Methanotrophic diversity in high arctic wetlands on the islands of Svalbard (Norway)--denaturing gradient gel electrophoresis analysis of soil DNA and enrichment cultures. *Canadian Journal of Microbiology, 49*(10), 602-612. https://doi.org/10.1139/w03-080

Xu, J., Morris, P. J., Liu, J., & Holden, J. (2018). PEATMAP: Refining estimates of global peatland distribution based on a meta-analysis. *CATENA, 160*, 134-140. https://doi.org/10.1016/j.catena.2017.09.010

Xue, K., M. Yuan, M., J. Shi, Z., Qin, Y., Deng, Y., Cheng, L., Wu, L., He, Z., Van Nostrand, J. D., Bracho, R., Natali, S., Schuur, E. A. G., Luo, C., Konstantinidis, K. T., Wang, Q., Cole, James R., Tiedje, James M., Luo, Y., & Zhou, J. (2016). Tundra soil carbon is vulnerable to rapid microbial decomposition under climate warming. *Nature Climate Change, 6*(6), 595-600. https://doi.org/10.1038/nclimate2940

Yamada, E. A., & Sgarbieri, V. C. (2005). Yeast (Saccharomyces cerevisiae) Protein Concentrate: Preparation, Chemical Composition, and Nutritional and Functional Properties. *Journal of Agricultural and Food Chemistry, 53*(10), 3931-3936. https://doi.org/10.1021/jf0400821

Yvon-Durocher, G., Allen, A. P., Bastviken, D., Conrad, R., Gudasz, C., St-Pierre, A., Thanh-Duc, N., & del Giorgio, P. A. (2014). Methane fluxes show consistent temperature dependence across microbial to ecosystem scales. *Nature, 507*(7493), 488-491. https://doi.org/10.1038/nature13164

Zacheis, A., Hupp, J. W., & Ruess, R. W. (2001). Effects of migratory geese on plant communities of an Alaskan salt marsh. *Journal of Ecology, 89*(1), 57-71. https://doi.org/10.1046/j.1365-2745.2001.00515.x

Zak, D. R., & Kling, G. W. (2006). Microbial community composition and function across an arctic tundra landscape. *Ecology, 87*(7), 1659-1670. https://doi.org/10.1890/0012-9658(2006)87[1659:mccafa]2.0.co;2

Zhou, J., Xue, K., Xie, J., Deng, Y., Wu, L., Cheng, X., Fei, S., Deng, S., He, Z., Van Nostrand, J. D., & Luo, Y. (2012). Microbial mediation of carbon-cycle feedbacks to climate warming. *Nature Climate Change, 2*(2), 106-110. https://doi.org/10.1038/nclimate1331

Zhou, J., Deng, Y., Shen, L., Wen, C., Yan, Q., Ning, D., Qin, Y., Xue, K., Wu, L., He, Z., Voordeckers, J. W., Nostrand, J. D. V., Buzzard, V., Michaletz, S. T., Enquist, B. J., Weiser, M. D., Kaspari, M., Waide, R., Yang, Y., & Brown, J. H. (2016). Temperature mediates continental-scale diversity of microbes in forest soils. *Nature Communications, 7*(1), 12083. https://doi.org/10.1038/ncomms12083

Ågren, G. I., Bosatta, E., & Magill, A. H. (2001). Combining theory and experiment to understand effects of inorganic nitrogen on litter decomposition. *Oecologia, 128*(1), 94-98. https://doi.org/10.1007/s004420100646

Part II

Publications

Paper 1

Polar Biology
https://doi.org/10.1007/s00300-021-02846-z

ORIGINAL PAPER

Microbial responses to herbivory-induced vegetation changes in a high-Arctic peatland

Kathrin M. Bender[1] · Mette M. Svenning[1] · Yuntao Hu[2] · Andreas Richter[2] · Julia Schückel[3] · Bodil Jørgensen[3] · Susanne Liebner[4,5] · Alexander T. Tveit[1]

Received: 23 September 2020 / Revised: 5 March 2021 / Accepted: 9 March 2021

Abstract

Herbivory by barnacle geese (*Branta leucopsis*) alters the vegetation cover and reduces ecosystem productivity in high-Arctic peatlands, limiting the carbon sink strength of these ecosystems. Here we investigate how herbivory-induced vegetation changes affect the activities of peat soil microbiota using metagenomics, metatranscriptomics and targeted metabolomics in a comparison of fenced exclosures and nearby grazed sites. Our results show that a different vegetation with a high proportion of vascular plants developed due to reduced herbivory, resulting in a larger and more diverse input of polysaccharides to the soil at exclosed study sites. This coincided with higher sugar and amino acid concentrations in the soil at this site as well as the establishment of a more abundant and active microbiota, including saprotrophic fungi with broad substrate ranges, like *Helotiales* (*Ascomycota*) and *Agaricales* (*Basidiomycota*). A detailed description of fungal transcriptional profiles revealed higher gene expression for cellulose, hemicellulose, pectin, lignin and chitin degradation at herbivory-exclosed sites. Furthermore, we observed an increase in the number of genes and transcripts for predatory eukaryotes such as Entomobryomorpha (Arthropoda). We conclude that in the absence of herbivory, the development of a vascular vegetation alters the soil polysaccharide composition and supports larger and more active populations of fungi and predatory eukaryotes.

Keywords Arctic peat soils · Predation · Saprotrophic fungi · Metagenomics · Metatranscriptomics · Vascular plants · Herbivory

Introduction

Arctic terrestrial peatlands store 30–40% of the world`s soil organic carbon (SOC) (Tarnocai et al. 2009), the fate of which is determined by the balance between plant growth, herbivory and microbial decomposition (Ping et al. 2015). Herbivory has a large impact on the composition of plant communities (Zacheis et al. 2001; Maron and Crone 2006), which in turn affects the quality of litter input to the soil (Bardgett and Wardle 2003; Wardle et al. 2004; Van der Heijden et al. 2008; Fivez et al. 2014). Plant cell wall polymers, such as cellulose, hemicelluloses, pectins and lignin, are the major constituents of photosynthetically fixed organic carbon in peatlands (Chesworth et al. 2008; Gilbert 2010) and the cell walls of different plant lineages have characteristic macromolecular organization and polymer composition (Sarkar et al. 2009). Thus, the vegetation is assumed to determine the SOC composition and its decomposability (Davidson and Janssens 2006; Ping et al. 2015).

Our knowledge of soil ecosystem functioning is largely based on studies that focus on one or a few components of these complex ecosystems, but in order to thoroughly understand processes like decomposition it is important to study the microbial food web structures and linkages (Crotty et al. 2014). Fungi degrade detritus organic matter, consisting of a variety of plant polysaccharides and lignin (Thormann 2006). Bacterial communities in soils are known to be involved in

✉ Alexander T. Tveit
alexander.t.tveit@uit.no

[1] Department of Arctic and Marine Biology, UiT The Arctic University of Norway, Tromsø, Norway

[2] Centre for Microbiology and Environmental Systems Science, University of Vienna, Vienna, Austria

[3] Department of Plant and Environmental Sciences, University of Copenhagen, Copenhagen, Denmark

[4] Section Geomicrobiology, GFZ German Research Center for Geosciences, Potsdam, Germany

[5] University of Potsdam, Institute of Biogeochemistry and Biology, Potsdam, Germany

Published online: 30 March 2021

numerous activities including degradation of detritus polymers (Tveit et al. 2013), microbial necromass (Müller et al. 2018) and active predation (Davidov et al. 2006; Morgan et al. 2010). Groups of non-fungal eukaryotes are involved in both predation and degradation of microbial and plant polymers (Crotty et al. 2011). The numbers of omnivorous eukaryotes such as Collembola (orders: Entomobryomorpha, Poduromorpha, Symphypleona) have been shown to positively and negatively correlate with microbial biomasses (Sabais et al. 2011; Thakur et al. 2015), making it difficult to reconstruct the linkages of microbial food webs based on abundances of taxa alone. Geisen et al. (2016) described different groups of protists and arthropods, so far believed to be bacteriovorous, as facultative mycophagous, refining our understanding of protists and arthropods as key players that control the biomass of both bacteria and fungi in soil food webs.

In a productive ecosystem, herbivory can lead to higher productivity by maintaining the dominant plant species while excluding less productive species (Bardgett et al. 1998; Bardgett and Wardle 2003). In less productive ecosystems, herbivory can lead to decreased plant and root biomass like shown for a high-Arctic peatland, Svalbard (Sjögersten et al. 2011) or in the coastal marshes of Hudson Bay, Canada (Jefferies et al. 2006). The effect of increased plant species richness and productivity resulted in larger microbial biomasses and rates of respiration (Zak et al. 2003; Zak and Kling 2006), and an overall increase in the density and diversity of microorganisms (Eisenhauer et al. 2013). In western Svalbard, increased peatland herbivory by barnacle geese (*Branta leucopsis*) has led to a suppression of vascular plant growth and dominance of mosses within the family Amblystegiaceae (brown mosses) (Kuijper et al. 2006), possibly changing these peatlands from carbon sources into carbon sinks (Sjögersten et al. 2011).

Here we compared peat protected from grazing for 18 years (exclosure; experimental condition) with grazed peat (grazed sites; natural condition), studying the differences in soil, soil polysaccharide composition, microbial community composition and microbial activities directed at polysaccharide decomposition, targeting all three domains of life. For this, we have sequenced eight metagenomes and eight metatranscriptomes, and performed targeted metabolomics, antibody staining of polysaccharides and extracellular enzyme assays in addition to describing the peat soil and the vegetation.

Materials and methods

Study site and sampling

The fieldwork was carried out in the high-Arctic peatland Solvatn, situated close to the research settlement Ny-Ålesund, Svalbard (78° 55′ N, 11° 56′ E), in August 2016. In the Solvatn peatland, experimental exclosures had been maintained since 1998 by 0.5-m tall fences prohibiting Barnacle geese grazing from areas of 0.7 × 0.7 m (Sjögersten et al. 2011) (Fig. 1). A total of four replicates from the grazed areas and four replicates for the exclosed areas were collected for DNA and RNA extractions, enzyme assays and plant polymer profiling while 12 replicates from each condition were collected for pore water amino acid and sugar measurements. Samples were collected at 1–2 cm depth and immediately frozen in liquid nitrogen or processed for pore water extraction and filtration; 400 µl of pore water was filtered with Whatman™ Mini-UniPrep™ G2 Syringeless Filters (GE Healthcare, Buckinghamshire, UK). The O_2 [%] and temperature T [°C] of the sites were measured at four different depths using an optical O_2 sensor and thermometer (Fibox 4, PreSens Precision Sensing GmbH, Regensburg, Germany) (Table S1—online resource 2). The water [%] and total organic matter (TOM) contents were estimated as described in Tveit et al. (2013) (Table S2—online resource

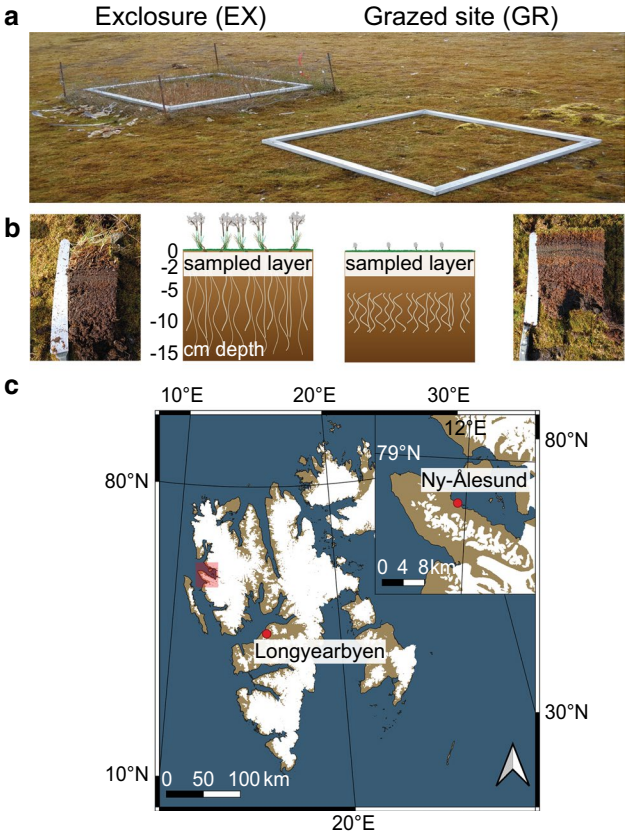

Fig. 1 Sampling sites and sample collection. **a** In the picture one of the exclosures, EX1, and grazed sites, GR1, are shown, displaying the different vegetation. **b** The top peat layer at 1–2 cm below the living vegetation was sampled as indicated by the boxes across the peat profile figures. **c** Location of the Solvatn peatland, within the settlement Ny-Ålesund, Svalbard

2). The pH was measured in pore water using a portable field pH meter (Multi 350i, WTW, Weilheim, Germany). Plant material was collected for plant species characterizations.

Analysis of pore water amino acids and sugars

Free amino acids in the pore water samples were analyzed using a Thermo UPLC system consisting of an Accucore HILIC column (150 mm × 2.1 mm, 2.6 µm particle size) coupled to an Orbitrap Exactive mass spectrometer. The separation was carried out using a gradient from 95% eluent B (acetonitrile, 0.1% v/v formic acid) to 40% eluent A (water, 0.1% v/v formic acid) (Hu et al. 2017). The mass resolution was set to 50.000 and the injection volume was 25 µL. Sugar concentrations in pore water were measured with an HPLC (Dionex ICS-5000) using a Thermo CarboPac column (0.4 mm × 150 mm; pre-column 0.4 mm × 35 mm) and an electrochemical detector. The eluent was 3 mM KOH and samples were processed at 30 °C at a flow rate of 9 µl min^{-1}, with an injection volume of 40 µL. All of the peaks were integrated by Xcalibur 2.2.

Comprehensive microarray polymer profiling (CoMPP)

The polysaccharide composition of Arctic peat soils and of three different plant types were measured using Comprehensive Microarray Polymer Profiling (CoMPP) at the University of Copenhagen as described in Moller et al. (2008). For further details, see supplementary materials and methods section 1 (online resource 1).

Enzyme assays

Polysaccharide degradation enzyme assays were carried out using the GlycoSpot™ technology (Copenhagen/Denmark). The substrates used were xylan (beechwood), arabinoxylan (wheat), 2HE-cellulose (synthetic), arabinan (sugar beet), pectic galactan (lupin), galactomannan (carob), xyloglucan (tamarind) and rhamnogalacturonan (soy bean). For further details, see supplementary materials and methods section 2 (online resource 1).

Nucleic acids extraction and rRNA depletion

Nucleic acids were extracted and quantified as described previously (Urich et al. 2008; Tveit et al. 2013). Total RNA samples were processed with the Ribo-Zero Magnetic Kit for Bacteria from Illumina (San Diego, CA/USA) to remove 16 and 23S rRNA molecules and enrich the mRNA fraction of the metatranscriptome. For further details, see supplementary materials and methods section 3 (online resource 1).

Sequencing and sequence preprocessing

Sequencing was performed at the "Norwegian High Throughput Sequencing Centre" NSC Oslo, Norway (http://www.sequencing.uio.no). DNA samples were prepared for sequencing with the TruSeq Nano DNA Library Prep Kit (Illumina, San Diego, CA/USA), with an input mass of 100 ng DNA. RNA samples were prepared with the TruSeq Stranded mRNA Library Prep Kit (Illumina, San Diego, CA/USA) with random primers and an input mass of 10 ng RNA. Single reads were sequenced using the HiSeq 4000 with a read length of 150 bp, resulting in approximately 38–55 Mio reads per library. Trimmomatic (Bolger et al. 2014) was used for an initial quality filtering of the sequences to remove low quality reads. Sequences were further processed with SortMeRNA v. 2.0 to separate reads into SSU rRNA, LSU rRNA and non-rRNA (Kopylova et al. 2012).

Analysis of SSU rRNA coding reads

Blastn searches against the SILVA SSU reference database (v. 128) were performed to taxonomically classify the SSU rRNA gene reads (-evalue 10^{-1}—num_alignments 50—num_descriptions 50). The Blast outputs were analyzed using MEGAN (Huson et al. 2011) v. 6.13.1 (parameters: min bit score 100.0; top percent 2.0; min support percent 0.01, 25 best hits) as described previously (Söllinger et al. 2018).

Taxonomic and functional annotation of mRNA and mRNA coding genes

Randomly selected subsamples of 5 million nucleotide reads from the non-RNA datasets were taxonomically and functionally classified using NCBI nr (as of March 2017) and KEGG (v. 81.0) databases, respectively. NCBI nr was used for taxonomic annotation with DIAMOND v. 0.9.17 (Buchfink et al. 2015) applying an e-value threshold of 10^{-3}. The output was uploaded in MEGAN v. 6.13.1 (parameters: min score 50.0; top percent 2.0; min support percent 0.01, 25 best hits), as described previously (Söllinger et al. 2018). Reads that had been taxonomically classified using the NCBI nr database were used as queries in a blastx search against the KEGG database with e-value threshold 10^{-10} as described previously (Tveit et al. 2015).

Functional and taxonomic annotation of CAZyme encoding genes and transcripts

Randomly selected subsamples of 5 million nucleotide reads from each of the DNA and non-rRNA datasets (for non-rRNA the same subsets were used as above) were translated into open reading frames (ORFs) of 30 amino acids or longer

by the program Open Reading Frame (ORF) finder (Wheeler et al. 2003). The ORFs were screened for Protein families using the Pfam (protein family) database (v. 31) (Finn et al. 2014) and HMMsearch, a tool within the hidden markov models (HMMs) package (v 3.1b2) (Finn et al. 2015). All database hits with e-values below a threshold of 10^{-4} were counted. The resulting Pfam annotations were screened for CAZymes using Pfam models of previously identified CAZymes (Tveit et al. 2015; Söllinger et al. 2018) including starch, cellulose, hemicellulose, pectin and lignin degrading enzymes. Translated reads assigned to the selected CAZymes were extracted, followed by blastp against the NCBI nr database with an e-value threshold of 10^{-1} to obtain taxonomic information (as of March 2017) and analyzed using MEGAN (parameters: min score 50; top percent 2.0; min support percent 0.01; 25 best hits). In order to provide more depth in the analysis of the eukaryotic taxa, the full datasets were taxonomically annotated and reads assigned to *Helotiales*, *Agaricales* and Entomobryomorpha were extracted and functionally annotated as described above.

Statistical analyses and data visualization

Significance testing was performed with the Wilcoxon rank sum test using the R package (R Core Team 2014). The results from statistical tests are summarized in Table S3 (online resource 2). Correspondence analyses (Greenacre 2017) were performed as described previously (Tveit et al. 2015). The R packages ggplot2 and heatmap3 were used for plotting. Spearman correlation analysis was performed, using the function cor() in R. The geographical map of Svalbard was created using QGIS (v. 3.18.0), the base map was provided by the Norwegian Polar Institute (https://geodata.npolar.no).

Results

The effects of herbivore grazing on peat vegetation and soil O_2 availability

The exclosures (EX) were established 18 years prior to sampling, preventing the access of herbivores to the vegetation (Fig. 1a). During this time, a vascular plant community dominated by *Poa arctica* (up to 90% coverage) and *Cardamine pratensis* (up to 20% coverage) had developed. The vascular plants *Ranunculus hyperborus, Saxifraga cernua* and *Saxifraga cespitosa* were also present. Eight moss species within the brown moss family Amblystegiaceae were identified, making up the entire moss community within the exclosures (Table 1). At the grazed sites (GR), a total of seven moss species dominated the vegetation (up to 100% coverage), while two vascular plant species were detected (*P. arctica* and *R. hyperborus*) (Table 1).

Due to the higher coverage of vascular plants in the exclosures, these sites contained much higher root densities, previously quantified by Sjögersten et al. (2011) to be 12 times higher. The O_2 [%] within the first two centimeters of peat was ~ 20% in both the exclosures and grazed sites. The O_2 concentration decreased with depth, being ~ 19–20% at 5 cm depth within the exclosures and 13–16% in the grazed sites (Table S1—online resource 2). We observed surface temperatures in the range of 10.4–10.8 °C (EX) and 8.3–14 °C (GR), while at 10 cm soil depth the temperature was approximately 5–6 °C in both sites (Table S1—online resource 2). The water content of the peat soils was lower in the exclosures (mean: 84.5%) compared to the grazed sites (mean: 92.4%) (Table S2—online resource 2). The total soil organic matter percentage of the fresh weight was higher in the exclosures (mean EX: 13.0%; mean GR: 6.5%) (Table S2—online resource 2). The pH of the upper soil layer in both the exclosures and grazed sites was between 7.0 and 7.1.

Soil polysaccharide, sugar and amino acid content vary between exclosures and grazed sites

To identify the relationship between vegetation and soil polysaccharide composition we mapped the polysaccharide content in three different plant types—*P. arctica*, *S. cespitosa* and a mixture of Amblystegiaceae mosses. The same polysaccharide identification was done for the peat soil from the exclosures and grazed sites. A correspondence analysis confirmed that all three plant polysaccharide profiles were distinctly different from one another (Figures S1a and S1b—online resource 3). *Saxifraga cespitosa* was richer in the pectins homogalacturonan, rhamnogalacturonan and arabinan as well as cellulose and the hemicelluloses xyloglucan, mixed linkage glucans (MLG) and xylan. *Poa arctica* was richer in glucan, arabinoxylan and the glycoprotein AGP (arabinogalactan protein), while the mosses were richer in mannan-containing hemicelluloses, homogalacturonan (HG) with an intermediate degree of methyl esterification (DE) and galactan (Table S4—online resource 2).

Correspondingly we found that cellulose, glucan, xyloglucan, arabinoxylan and rhamnogalacturonan were more abundant in the soils from the exclosures while homogalacturonan was equally abundant at both sites. For arabinan and mannan-containing hemicelluloses, only some tested antibodies had significantly higher abundances in the exclosures (Table 2 and Figure S1c and S1d—online resource 3).

The pore water concentrations of sugars, including glucose, fructose, mannose, xylose and galactose, were significantly higher in the peat soils from the exclosures (Fig. 2a). Glucose was the most abundant sugar in the pore water of

Table 1 Vegetation description of the Solvatn peatland

	Exclosure 1	Exclosure 2	Grazed 1	Grazed 2
Vascular plants				
Poa arctica	90	15	15	< 1
Cardamine pratensis	< 1	20		
Ranunculus hyperboreus	< 5	1		< 1
Saxifraga cernua		5		
Saxifraga cespitosa		1		
Mosses				
Sanonia type	30	50	40	40
Plagiomnium type	5	10	1	
Polytrichum type	1			
Pohlia/Bryum type	3	4	5	5
Mnium type	10	5	2	
Aulacomnium palustre	1	1		1
Calliergon richardsonii	40	25	50	40
Paludella squarrosa	10	5	2	
Lichens				
Cetraria islandica	1	3		
Stereocaulon				< 1
Mushroom	< 1			
Bare ground/dead mosses				14

Comparison of the coverage (%) of vascular plants, mosses and lichens at exclosed and grazed sites. The coverage is estimated at different heights. Thus, the vascular plants that are growing above the mosses can have a 100% coverage while the mosses growing below the vascular plants in the same site can simultaneously reach a 100% coverage

the exclosures (mean: 40.3 µM) and the grazed sites (mean: 9.9 µM), followed by fructose (EX mean: 18.3 µM and grazed site mean: 5.4 µM). There was less mannose, xylose and galactose in the peat, but the concentrations were always higher in the exclosures (mean EX: mannose 5.8 µM, xylose 2.2 µM, galactose 0.4 µM) than the grazed sites (mean GR: mannose 0.8 µM, xylose b.d., galactose 0.02 µM).

We also observed significantly higher concentrations of a broad range of amino acids in the exclosures (Fig. 2b and Table S3—online resource 2). Aspartic acid and alanine had the highest concentrations with mean values of 10.5 and 13.2 µM, respectively, in the exclosures, while the concentrations in the grazed sites were much lower (0.9 and 2.3 µM). The amino acids glycine, leucine, proline, serine and threonine ranged from 4.0 to 6.8 µM in the exclosures and 0.6 to 1.3 µM in the grazed sites. Only glutamic acid was found at lower concentrations in the exclosures (mean EX: 0.9 µM) compared to the grazed sites (mean GR: 2.0 µM). The other amino acids were below 1.8 µM (mean values) but always at higher concentrations in the exclosures than the grazed sites.

Microbial activities in the peat soil

To study the link between the vegetation, soil chemistry and the composition and activity of the microbial community we extracted total nucleic acids for the analysis of DNA and RNA from four replicate samples of the upper 2 cm oxic layer of peat soil in the exclosures and four from the grazed sites. As depicted in Fig. 2c we observed higher DNA amounts in the exclosures than the grazed sites (mean: EX 92.5 µg DNA gDW peat^{-1}, GR 58.3 µg DNA gDW peat^{-1}), while the amount of RNA per gram dry weight was equally high at the two sites (mean: EX 71.2 µg RNA gDW peat^{-1}, GR 69.6 µg RNA gDW peat^{-1}) (Fig. 2c and Table S5—online resource 2). Next, we investigated the potential enzyme activities for decomposition of some of the most common plant polysaccharides—cellulose, mannan, xyloglucan, xylan, arabinoxylan, galactan, arabinan and rhamnogalacturonan (Sarkar et al. 2009). This confirmed that the potential for polysaccharide degradation was significantly higher in the exclosures than the grazed sites (Fig. 2d and Table S3—online resource 2).

In order to study the microbial communities and their patterns of gene transcription, we removed ribosomes from the total RNA by ribodepletion and sequenced the remaining RNA as well as the total DNA from four replicates collected in the exclosures, and four in the grazed sites, giving eight metatranscriptomic and eight metagenomic libraries in total. Each of the 16 libraries contained ~ 38–55 million sequence reads with a length of ~ 150 bp. The ribodepleted RNA libraries contained 48–83% non-rRNA sequences, ~ 30%

Table 2 Polysaccharide composition of the peat soils

Polysaccharide (antibody ID)	Exclosure Mean value ± sd ($n = 4$)	Grazing Mean value ± sd ($n = 4$)
Cellulose (mAb CBM3a)	1.50E−03 ± 1.63E−04	5.70E−04 ± 1.58E−04*
(1 → 3)-β-D-glucan (mAb BS-400–2)	2.58E−04 ± 3.12E−05	1.15E−04 ± 3.72E−05*
(1 → 3)(1 → 4)-β-D-glucan (mAb BS-400–3)	5.61E−03 ± 2.12E−03	8.20E−04 ± 4.19E−04*
Xyloglucan (mAb LM15)	2.60E−03 ± 7.33E−04	1.38E−04 ± 9.97E−05*
Xyloglucan (mAb LM24)	2.40E−04 ± 2.09E−05	7.89E−05 ± 1.89E−05*
Xyloglucan (mAb LM25)	2.58E−03 ± 2.48E−04	5.29E−04 ± 2.63E−04*
(1 → 4)-β-D-xylan (mAb LM10)	1.09E−03 ± 3.02E−04	4.50E−04 ± 2.06E−04*
(1 → 4)-β-D-xylan/arabinoxylan (mAb LM11)	2.45E−03 ± 1.18E−03	3.25E−04 ± 2.16E−04*
(1 → 4)-β-D-(galacto)mannan (mAb BS-400–4)	3.40E−03 ± 9.71E−04	1.15E−04 ± 5.08E−04
(1 → 4)-β-D-(galacto)(gluco)mannan (mAb LM21)	2.96E−03 ± 6.60E−04	1.18E−03 ± 2.78E−04*
(1 → 4)-β-D-(gluco)mannan (mAb LM22)	7.80E−04 ± 1.44E−04	4.22E−04 ± 1.88E−04
Non-acetylated xylosyl residues (mAb LM23)	1.27E−03 ± 4.54E−04	3.74E−04 ± 7.14E−05*
Anti callose/MLG like binding (mAb JIM6)	4.90E−04 ± 1.24E−04	2.61E−04 ± 2.28E−04
Arabinogalactan protein (mAb LM2)	1.49E−03 ± 8.74E−04	1.08E−04 ± 4.54E−05*
Homogalacturonan (Low DE) (mAb JIM5)	2.11E−04 ± 1.48E−04	2.46E−04 ± 9.68E−05
Homogalacturonan (Intermediate DE) (mAb LM7)	1.86E−04 ± 1.17E−04	4.36E−05 ± 1.39E−05
Homogalacturonan (High DE) (mAb JIM7)	8.48E−04 ± 6.13E−04	2.42E−04 ± 8.83E−05
Homogalacturonan (mAb LM18 MUC2)	3.94E−04 ± 4.41E−04	3.53E−04 ± 1.21E−04
Homogalacturonan (mAb LM19 XGA2)	4.73E−04 ± 6.01E−04	3.49E−04 ± 1.35E−04
Xylogalacturan (mAb LM8)	6.08E−05 ± 1.60E−05	2.69E−05 ± 7.94E−06
(1 → 4)-β-D-galactan (mAb LM5)	2.16E−03 ± 1.02E−03	5.37E−04 ± 3.65E−04
(1 → 5)-α-L-arabinan (mAb LM6)	1.07E−03 ± 2.58E−04	3.00E−04 ± 7.65E−05
(1 → 5)-α-L-arabinan (mAb LM13)	1.66E−05 ± 6.75E−06	3.52E−06 ± 1.95E−06*
(1 → 5)-α-L-arabinan (mAb LM16)	4.88E−05 ± 2.69E−05	2.11E−05 ± 1.01E−05
Rhamnogalacturonan (mAb INRA-RU1)	2.26E−03 ± 3.82E−04	5.94E−04 ± 2.53E−04*
Rhamnogalacturonan (mAb INRA-RU2)	8.94E−04 ± 3.74E−04	1.13E−04 ± 6.08E−05*

The table lists the mean values (±—the standard deviations) of binding signals (for dry weight soil; gDW) for polysaccharides in the peat soils. The mean values are derived from four replicates from the exclosures and four replicates from the grazed sites. The polysaccharide composition of the soil matrix was determined using Comprehensive Microarray Polymer Profiling (CoMPP). In cases where there are several antibodies for the same polysaccharide, these are antibodies with different binding properties, e.g., for different numbers of backbone repeats. All polysaccharides marked with an '*' show a significant difference of the grazed and the exclosed. For statistical testing the Wilcoxon rank sum test was used with R (v3.6.1), values can be found in Table S3

mAb monoclonal antibody, *MLG* mixed linkage glycan, *DE* degree of methyl esterification

of which could be taxonomically classified and 10–15% of which could be functionally classified (Table S6—online resource 2). The microbial community composition based on taxonomic annotation of mRNA was overall similar in the exclosures and grazed sites, but notable differences were also observed (Figs. 3 and S2—online resource 3). Bacterial genes and transcripts comprised approximately 90% of total mRNA and 92% of total rRNA genes at exclosed sites, compared to approximately 96% of total mRNA and 95% of total rRNA genes at grazed sites. Correspondingly, the abundances of reads assigned to eukaryotic kingdoms (fungi, Protista and Metazoa) were particularly high in the exclosures relative to the grazed sites (Figs. 3 and S3—online resource 3). However, the 16S rRNA gene abundance and transcriptional activity were dominated by *Actinobacteria*, followed by *Alpha-*, *Beta-*, *Delta-* and *Gamma-proteobacteria*, *Chloroflexi*, *Acidobacteria*, *Verrucomicrobia* and *Bacteriodetes* in both grazed sites and exclosures. There were also considerable numbers of reads assigned to Ciliophora, fungi and Nematoda (Figs. 3 and S2—online resource 3). Overall, the most abundant taxa (SSU rRNA gene abundance) were the transcriptionally (mRNA abundance) most active ($r = 0.86$–0.94; only the taxa displayed in the boxes considered: Fig. 3a and b).

To identify which microbial taxa were responsible for polymer degradation we extracted from the metagenomes and metatranscriptomes genes and transcripts encoding enzymes for polysaccharide and lignin degradation (Table S7—online

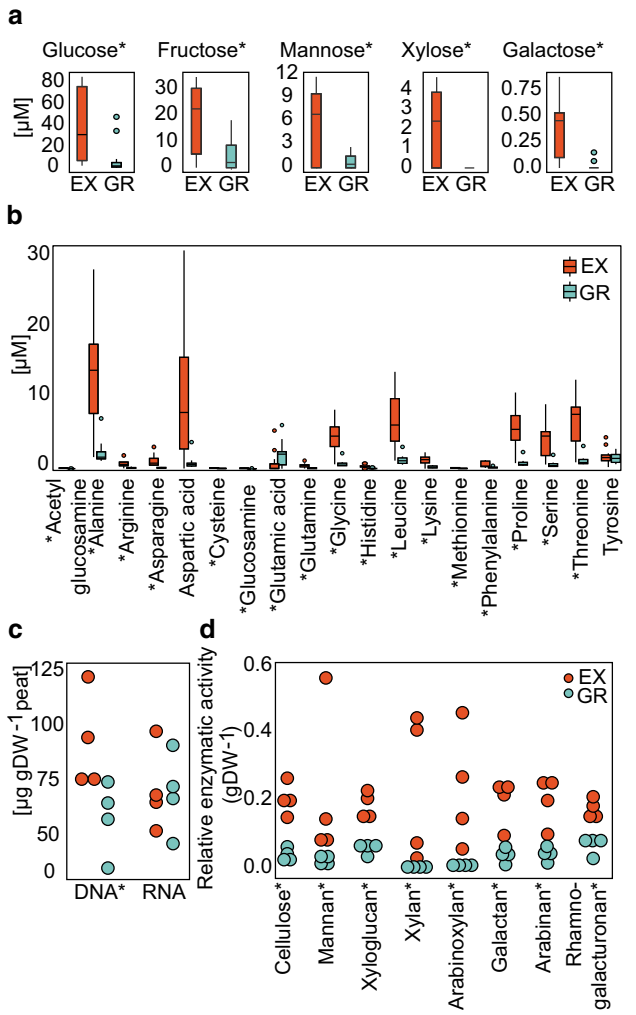

Fig. 2 Sugar and amino acid concentrations, masses of nucleic acids and polysaccharide degrading enzyme rates in peat soil samples exclosures (red) and grazed sites (blue). **a** Pore water concentrations [µM] of the sugars glucose, fructose, mannose, xylose and galactose. **b** Pore water concentrations [µM] of amino acids. **c** Masses of DNA and RNA in micrograms per gram of dry peat soil [µg gDW^{-1} peat]. **d** Enzymatic potential for polysaccharide degradation on eight polysaccharide substrates. Individual dots show the signal strength relative to the sum of measured signal strength for each substrate. The values thus indicate the potential enzyme activity in the eight samples relative to each other. The rates were normalized by dry weights (DW). All compounds marked with an '*' show a significant difference of the grazed and the exclosed. For statistical testing the Wilcoxon rank sum test was used with R (v3.6.1), values can be found in Table S3

resource 2). In the exclosures, the microbial transcription for cellulose degradation was highest (0.40%), followed by hemicellulose (0.36%), pectin (0.24%) and lignin (0.16%) (Fig. 4a). In the grazed sites, the transcription for hemicellulose degradation was highest (0.31%), followed by cellulose (0.21%), pectin (0.07%) and lignin (0.04%). Corresponding to the higher abundance of fungi (Figs. 3 and S3—online resource 3), a larger fraction of the genes and transcripts for polymer decomposition were assigned to fungi in the exclosures (18.95%) than the grazed sites (1.38%) (Fig. 4a). The majority of these transcripts were assigned to the fungal phyla *Basidiomycota* (6.32% EX & 0.60% GR) and *Ascomycota* (10.56% EX & 0.48% GR). *Actinobacteria* (30.92% EX & 20.14% GR), *Proteobacteria* (11.28% EX & 14.51% GR) and *Bacteriodetes* (8.46% EX & 13.82% GR) were the most transcriptionally active bacterial polysaccharide degraders, while the majority of transcripts for lignin degradation were assigned to *Proteobacteria* (28.15% EX & 33.03% GR) (Fig. 4b). The taxonomic distribution of genes for polymer degradation was similar at exclosed and grazed sites, with the exception that the transcript to gene ratio was much higher for fungal than bacterial taxa (Fig. 4b).

Taxa that had different transcriptional activities in the exclosures and grazed sites were identified by correspondence analysis (Figure S4a—online resource 3). The transcriptional profiles from the exclosures were separated from the grazed sites along the first axis, explaining 42.7% of the inertia. By their contribution to the first axis inertia we identified the major eukaryotic and prokaryotic orders with different transcriptional activities in the exclosures and grazed sites. Out of the 20 taxa contributing most to inertia in each direction (Figure S4b—online resource 3; and Table S8—online resource 2), 15 taxa had higher numbers of transcripts in either the exclosures or the grazed sites, and an average relative abundance of mRNA transcripts above 0.5%. Among these, three eukaryotic (*Agaricales*, *Helotiales* and Entomobryomorpha) and seven bacterial orders (*Lactobacillales, Chitinophagales, Burkholderiales, Sphingobacteriales, Nakamurellales, Corynebacteriales, Micrococcales*) were more active in the exclosures, whereas five bacterial orders (*Methylococcales*, *Anaerolineales*, *Solibacterales*, *Thiotrichales*, *Desulfobacterales*) were more active in the grazed sites. These 15 orders accounted for 7 to 18% of the total number of microbial mRNA transcripts. We then compared the transcriptional activity and relative abundance of SSU rRNA genes for these 15 taxa (Figure S4b—online resource 3), finding similar patterns in the SSU rRNA genes and the mRNA for some of the taxa. Particularly interesting were the much higher relative abundances of the three eukaryotic orders in the exclosures: *Agaricales* was on average 7.7-fold (SSU rRNA genes) and 71.4-fold (mRNA) higher, *Helotiales* was 29.8-fold (SSU rRNA genes) and 46.9-fold (mRNA) higher, while Entomobryomorpha was 20.4-fold (SSU rRNA genes) and 11.8-fold (mRNA) more abundant and transcriptionally active (Fig. 5).

The number of polymer degradation transcripts assigned to *Helotiales* (of fungal transcripts: 21.5% EX, 4.0% GR) and *Agaricales* (of fungal transcripts: 37.6% EX, 4.3% GR) show that these are the major fungal polysaccharide degraders in the exclosures. Their profiles

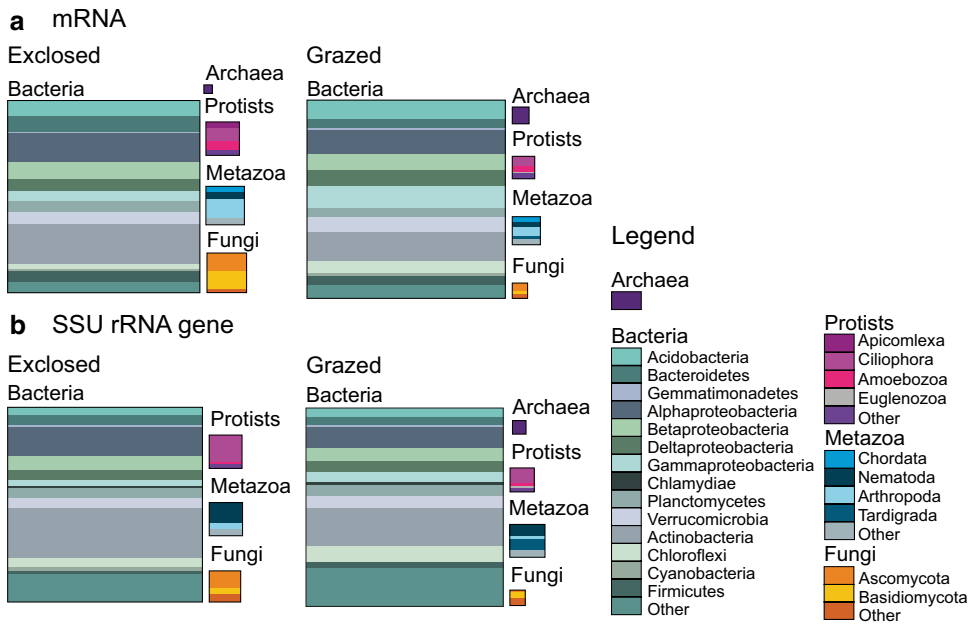

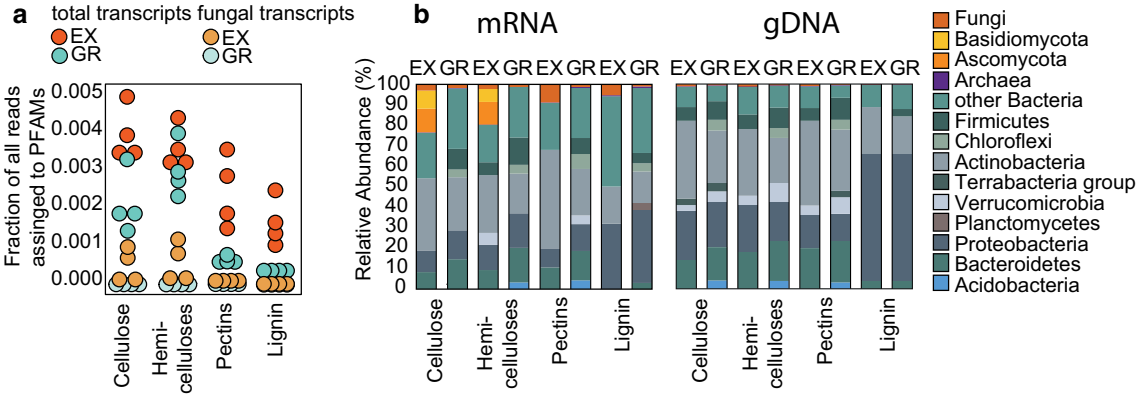

Fig. 3 Microbial community composition **a** based on mRNA sequences and therefore representing the transcriptionally active microbial community. **b** Based on SSU rRNA gene sequences reflecting the potential microbial community in peat soil from exclosures and grazed sites. The size of the boxes reflect the relative abundances of taxa. Taxonomy profiles are displayed at phylum-level (class-level for *Proteobacteria*) and are generated by averaging data sets from four replicates

Fig. 4 Genes and transcripts for polysaccharide and lignin degradation in prokaryotes and eukaryotes. **a** Number of transcripts for cellulose, hemicellulose, pectins and lignin degradation relative to the total number of reads assigned to a function for all microorganisms (left) and fungi (right). **b** Taxonomic assignment of metatranscriptomic (mRNA) and metagenomic (gDNA) sequences encoding enzymes involved in polysaccharide and lignin degradation. The functional annotation is at phylum-level, comparing exclosures (EX) and grazed (GR) sites

included transcripts for cellulose, xylans, glucans, mannans, pectins, lignin, chitin and bacterial cell walls (Fig. 5a and Table S9—online resource 2). *Helotiales* expressed genes for a broader range of substrates than *Agaricales* (Table S9—online resource 2), but for both fungal orders the relative abundance of transcripts for most polymers were higher in the exclosures (Fig. 5a). Similarly, the transcriptional activity of the arthropod order Entomobryomorpha was much higher in the exclosures (Fig. 5b). It had a narrower substrate range than the fungi, lacking transcripts for xylan, pectin and lignin decomposition (Table S9—online resource 2). However, Entomobryomorpha transcripts for bacterial cell wall, chitin, cellulose and oligosaccharide degradation were present, and consistently more abundant in the exclosures than the grazed sites (Fig. 5b). Finally we assessed whether the above patterns of transcription for polymer degradation were reflected in the transcription for central metabolisms in these three orders. We functionally annotated the *Agaricales*, *Helotiales* and Entomobryomorpha transcripts using KEGG (Kyoto encyclopedia of genes and genomes). This revealed that the transcript abundances for central metabolisms were highest in the exclosures for all three taxa (Figure S5—online resource 3), but with considerable variation between samples, especially for the fungi.

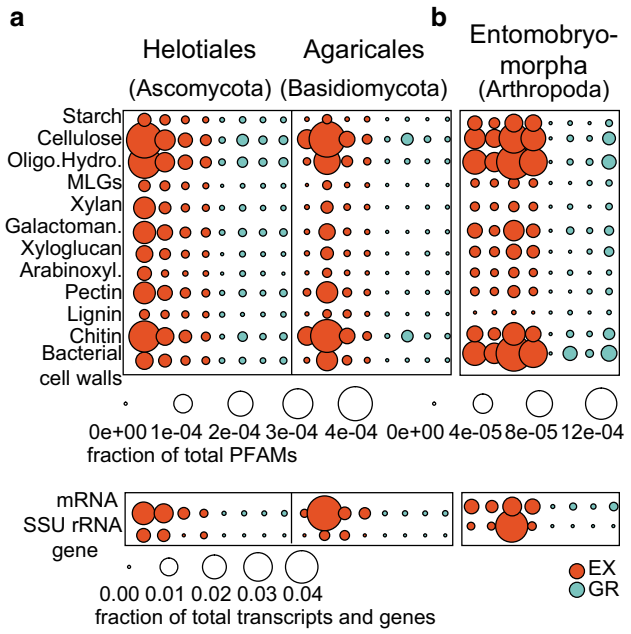

Fig. 5 Transcriptional profiles for polymer degradation by *Helotiales, Agaricales* and Entomobryomorpha. **a** Functional profile of the two fungal orders *Helotiales* and *Agaricales* displaying relative abundances of transcripts in exclosures (red) and grazed sites (blue) for enzymes involved in polymer degradation as described in Table S9. The fraction of total transcripts (mRNA) and rRNA genes assigned to these two fungal orders are shown in the lower box. **b** Functional profile of the order Entomobryomorpha showing its transcription for polymer degradation in the replicates of peat soils from the exclosures (red) and grazed sites (blue). In the lower square, the fraction of total transcripts (mRNA) and rRNA genes assigned to Entomobryomorpha is displayed. Oligo.Hydro—oligosaccharide hydrolysis; MLGs—mixed linkage glycans; Galactoman.—galactomannan; Arabinoxyl.—arabinoxylan

Discussion

In this study we have compared the microbial communities in soils below high-Arctic peat vegetation exposed to grazing and soils below peat vegetation protected from grazing for 18 years. The investigation of both the above- and belowground biology has allowed us to study the relationship between the vegetation and the soil microorganisms. Our comparison of the two soil treatments demonstrated that the removal of herbivores and altered vegetation leads to a different soil polysaccharide composition, lower potential extracellular enzymatic activities and a different microbial community with lower abundances and activities of fungi and putative predatory eukaryotes.

Reduced herbivore grazing alters the vegetation, soil structure and soil composition

We observed that a different vegetation with an 8 times larger coverage of vascular plants had established after 18 years of protection inside the exclosures. This shift, primarily caused by increased abundance of *P. arctica*, was already observed some years earlier as evidenced by a 12 times larger root biomass and 28 times larger vascular plant biomass in the exclosures than the grazed sites (Sjögersten et al. 2011). The vascular vegetation was associated with reduced soil water contents and higher oxygen levels in deeper layers, presumably due to the increased root formation. Similar observations were made in a study of a temperate peatland, where lower water table heights were observed in areas with greater vascular plant biomass (Murphy et al. 2009). The lowering of the water table and the diffusion of gases through the roots of vascular plants might be the reasons for the higher oxygen availabilities (Colmer 2003). However, at the surface (top ~ 0–2 cm) sampled for our molecular and chemical analyses, the oxygen levels were the same in exclosures and grazed sites, suggesting that oxygen limitation is mostly relevant in deeper layers.

The increased input of organic matter from *P. arctica* and other vascular plants to the soil inside the exclosures can explain the higher organic matter content and abundance of polysaccharides compared to the grazed sites. Previously, geese grazing and grubbing were found to reduce carbon stocks in Arctic wetlands from Svalbard and Canada (Van der Wal 2006; Speed et al. 2010; Sjögersten et al. 2011). In particular, we identified higher soil content of xyloglucan, arabinoxylan and pectins in the exclosures, matching the higher concentrations of monosaccharides. However, determining the exact origin of the monosaccharides in soils is challenging, as they might be root exudates (Bertin et al. 2003; Bais et al. 2006), polysaccharide hydrolysis products (Tveit et al. 2013) or both. The release of low-molecular weight compounds like sugars through root exudation varies e.g. with the plant type, its age and environment (Uren 2000; Bertin et al. 2003; Bais et al. 2006; McNear 2013). Monosaccharide stocks also depend on the kinetics of their usage, for which we do not have estimates. Nevertheless, the occurrence of more roots, more polysaccharides and higher potential rates of extracellular polysaccharide degrading enzymes suggests a combination of root exudation and polysaccharide hydrolysis as sources for the monosaccharides.

Increased input from vascular plants supports a more abundant and active microbiota

The higher availability of carbohydrates fueled a more abundant and active microbiota in the exclosures, judging by the amount of DNA per gram of dry soil. Although not a direct measure of total microbial biomass or the number of cells, nucleic acids provide good estimates for relative differences in the size of the microbiota between samples with similar properties for nucleic acids extraction (Tveit et al. 2015; Söllinger et al. 2018). Considering the higher

organic matter content in the exclosures, the more abundant microbiota might be the result of higher substrate availability. This could explain the higher rates for extracellular polysaccharide degradation in the exclosures as more organisms generally would produce more enzymes. We also observed a considerably higher relative abundance of transcripts for extracellular polymer degrading enzymes in the exclosures, supporting the view that increased substrate availabilities leads not only to increased number of microorganisms but also to larger investments into extracellular polymer decomposing enzymes by microorganisms (Zak and Kling 2006; Wallenstein and Weintraub 2008). The altered organic matter quality may also be the reason for the increased relative abundance of fungi as they are believed to be specialists for the decomposition of, e.g., lignocellulose (Baldrian 2008). The effect of substrate quality on microbial activities was also seen in the higher potential enzyme rates for degradation of multiple different polysaccharides, in the exclosures, matching the higher abundances of these polysaccharides in the exclosures.

Altered structure and activity of the microbial communities

In line with the considerable changes in vegetation and soil chemistry we observed two-fold higher eukaryote to prokaryote gene ratios and five-fold higher transcript ratios in the exclosures than the grazed sites. A handful of taxa were instrumental to this shift; saprotrophic fungi of the orders *Helotiales* (*Ascomycota*) and *Agaricales* (*Basidiomycota*), and microbial predators and plant litter consumers of the order Entomobryomorpha (Arthropoda). In previous studies, fungal abundances were shown to be positively correlating with root exudation (Broeckling et al. 2008) and more generally the availabilities of easily degradable compounds like sugars (Edgecombe 1938; Thormann 2006) or increased nitrogen availability (Koranda et al. 2014). Increased monosaccharide concentrations could also be products of fungal degradation of polysaccharides. Thus, in our case, it is not possible to conclude on the causality between monosaccharide concentrations and fungal abundances. Nevertheless, *Helotiales* and *Agaricales* have very broad substrate ranges that includes cellulose and all major hemicelluloses and might thus have benefitted from the altered substrate quality and contributed to a variety of carbon decomposition activities once established in the exclosures.

Geisen et al. (2016) found that many protists and arthropods are facultative mycophagous, making them key players in soil microbial food webs. Hence, the higher fungal abundances in the exclosures might have supported the increase in protists and metazoan taxa abundances.

Overall, the vascular vegetation seems to sustain a more complex food web of prokaryotic and fungal detritivores that are food sources for predatory eukaryotes. Whether this is what sustains the larger amino acid pools observed in the exclosures is unclear, but if the transcriptional activity and relative abundance of putative predators reflects predation rates, it may, as bacterial and fungal cells consist of 10–70% protein (Ritala et al. 2017). Our results suggest that Entomobryomorpha are able to degrade bacterial cell walls but also plant and fungal polymers. By regulating microbial turnover, Entomobryomorpha have previously been shown to enhance nutrient mineralization rates and increase nitrogen availability in soils (Cragg and Bardgett 2001; Thakur et al. 2015). Additionally, amino acids may be released through root exudations (Canarini et al. 2019), offering an alternative explanation for the amino acid pools. The origin of the nitrogen needed to support a larger microbial biomass and amino acid pool cannot be directly identified with our data. However, Solheim et al. (1996) showed that nitrogen fixation in Svalbard soils protected from grazing is limited compared to grazed soils where it was supported by epiphytic cyanobacteria. This indicates that nitrogen is lost from grazed systems and regained through fixation, while in the absence of herbivores the microbiota are able to recycle the nitrogen in decaying plants, supporting larger plant and microbial biomasses, and pools of free amino acids.

Low molecular weight nitrogen sources, like amino acids, are important for several microbial processes, hence fueling the microbial community in soils (Schimel and Weintraub 2003; Jones et al. 2004), but also the vegetation (Jones et al. 2004, 2005; Sauheitl et al. 2009). Thus, in the absence of herbivory, feedback effects between an increasingly active microbial community and vegetation might have accelerated the establishment of a new ecosystem state. An important future task will be to identify the fluxes of amino acids, sugars and other metabolites between plants and microorganisms during this ecosystem transition from a grazed to non-grazed state.

Conclusion

The establishment of a larger vascular plant biomass in the absence of herbivores led to higher soil concentrations of polysaccharides, monosaccharides and amino acids. We found that this corresponded with larger and more active populations of saprotrophic fungi and putative predatory eukaryotes. This study establishes a fundament for targeting molecular and microbial mechanisms that control the interactions between above and below ground biology in high-Arctic peatlands.

Supplementary Information The online version contains supplementary material available at https://doi.org/10.1007/s00300-021-02846-z.

Acknowledgements We thank Maarten Loonen for access to the field sites. ArcBiont project Helmholtz Foundation-UiT for financial support and Edda Marie Rainer for help with the fieldwork. Sequencing was performed at The Norwegian Sequencing Centre. We thank Thomas Rattei for bioinformatics support. The computations were performed on resources provided by UNINETT Sigma2—the National Infrastructure for High Performance Computing and Data Storage in Norway, account nos. NN9639K and NS9593K. We would like to thank the two reviewers Josef Elster and Elie Verleyen for helpful comments.

Author contributions ATT, KMB and MMS conceived the study. KMB and ATT performed fieldwork. KMB, YH, JS and BJ performed experiments. AR contributed pore water analyses. KMB and ATT analyzed the data. KMB and ATT wrote the manuscript with input from all authors.

Funding Open access funding provided by UiT The Arctic University of Norway (incl University Hospital of North Norway).. A.T.T. was supported by the Research Council of Norway FRIPRO Mobility Grant Project Time and Energy 251027/RU, co-funded by ERC under Marie Curie Grant 608695, and Tromsø Research Foundation starting grant project Cells in the Cold 17_SG_ATT. K.M.B was supported by Tromsø Research Foundation starting grant project Cells in the Cold 17_SG_ATT.

Data availability Metagenomes and metatranscriptomes have been deposited in the Sequence Read Archive (SRA) database (BioProject Accession: PRJNA170725, https://www.ncbi.nlm.nih.gov/sra/PRJNA170725). For details about run accession numbers, see supplementary data availability (online resource 1).

Compliance with ethical standards

Conflict of interest The authors declare that they have no conflicts of interest.

Research involving human and animal participants The research was performed without involving human participants or animals subjects. We declare informed consent.

References

Bais HP, Weir TL, Perry LG, Gilroy S, Vivanco JM (2006) The role of root exudates in rhizosphere interactions with plants and other organisms. Annu Rev Plant Biol 57:233–266. https://doi.org/10.1146/annurev.arplant.57.032905.105159

Baldrian P (2008) Wood-inhabiting ligninolytic basidiomycetes in soils: ecology and constraints for applicability in bioremediation. Fungal Ecol 1:4–12. https://doi.org/10.1016/j.funeco.2008.02.001

Bardgett RD, Wardle DA (2003) Herbivore-mediated linkages between aboveground and belowground communities. Ecology 84:2258–2268. https://doi.org/10.1890/02-0274

Bardgett RD, Wardle DA, Yeates GW (1998) Linking above-ground and below-ground interactions: how plant responses to foliar herbivory influence soil organisms. Soil Biol Biochem 30:1867–1878. https://doi.org/10.1016/S0038-0717(98)00069-8

Bertin C, Yang X, Weston LA (2003) The role of root exudates and allelochemicals in the rhizosphere. Plant Soil 256:67–83. https://doi.org/10.1023/A:1026290508166

Bolger AM, Lohse M, Usadel B (2014) Trimmomatic: a flexible trimmer for illumina sequence data. Bioinformatics 30:2114–2120. https://doi.org/10.1093/bioinformatics/btu170

Broeckling CD, Broz AK, Bergelson J, Manter DK, Vivanco JM (2008) Root exudates regulate soil fungal community composition and diversity. Appl Environ Microbiol 74:738–744. https://doi.org/10.1128/AEM.02188-07

Buchfink B, Xie C, Huson DH (2015) Fast and sensitive protein alignment using DIAMOND. Nat Methods 12:59–60. https://doi.org/10.1038/nmeth.3176

Canarini A, Kaiser C, Merchant A, Richter A, Wanek W (2019) Root exudation of primary metabolites: mechanisms and their roles in plant responses to environmental stimuli. Front Plant Sci 10:157. https://doi.org/10.3389/fpls.2019.00157

Chesworth W, Camps Arbestain M, Macías F, Spaargaren O, Mualem Y, Morel-Seytoux HJ, Horwath WR (2008) Carbon cycling and formation of soil organic matter. In: Chesworth W (ed) Encyclopedia of soil science. Encyclopedia of earth sciences series. Springer, Dordrecht. https://doi.org/10.1007/978-1-4020-3995-9_88

Colmer TD (2003) Long-distance transport of gases in plants: a perspective on internal aeration and radial oxygen loss from roots. Plant Cell Environ 26:17–36. https://doi.org/10.1046/j.1365-3040.2003.00846.x

Cragg RG, Bardgett RD (2001) How changes in soil faunal diversity and composition within a trophic group influence decomposition processes. Soil Biol Biochem 33:2073–2081. https://doi.org/10.1016/S0038-0717(01)00138-9

Crotty FV, Blackshaw RP, Murray PJ (2011) Tracking the flow of bacterially derived ^{13}C and ^{15}N through soil faunal feeding channels. Rapid Commun Mass Spectrom 25:1503–1513. https://doi.org/10.1002/rcm.4945

Crotty FV, Blackshaw RP, Adl SM, Inger R, Murray PJ (2014) Divergence of feeding channels within the soil food web determined by ecosystem type. Ecol Evol 4:1–13. https://doi.org/10.1002/ece3.905

Davidov Y, Friedjung A, Jurkevitch E (2006) Structure analysis of a soil community of predatory bacteria using culture-dependent and culture-independent methods reveals a hitherto undetected diversity of *Bdellovibrio*-and-like organisms. Environ Microbiol 8:1667–1673. https://doi.org/10.1111/j.1462-2920.2006.01052.x

Davidson EA, Janssens IA (2006) Temperature sensitivity of soil carbon decomposition and feedbacks to climate change. Nature 440:165–173. https://doi.org/10.1038/nature04514

Edgecombe AE (1938) The effect of galactose on the growth of certain fungi. Mycologia 30:601–624. https://doi.org/10.2307/3754358

Eisenhauer N, Dobies T, Cesarz S, Hobbie SE, Meyer RJ, Worm K, Reich PB (2013) Plant diversity effects on soil food webs are stronger than those of elevated CO_2 and N deposition in

a long-term grassland experiment. Proc Natl Acad Sci USA 110:6889–6894. https://doi.org/10.1073/pnas.1217382110
Finn RD, Bateman A, Clements J, Coggill P, Eberhardt RY, Eddy SR et al (2014) Pfam: the protein families database. Nucleic Acids Res 42:D222–D230. https://doi.org/10.1093/nar/gkt1223
Finn RD, Clements J, Arndt W, Miller BL, Wheeler TJ, Schreiber F et al (2015) HMMER web server: 2015 update. Nucleic Acids Res 43:W30–W38. https://doi.org/10.1093/nar/gkv397
Fivez L, Vicca S, Janssens IA, Meire P (2014) Western Palaearctic breeding geese can alter carbon cycling in their winter habitat. Ecosphere 5:1–20. https://doi.org/10.1890/ES14-00012.1
Geisen S, Koller R, Hünninghaus M, Dumack K, Urich T, Bonkowski M (2016) The soil food web revisited: Diverse and widespread mycophagous soil protists. Soil Biol Biochem 94:10–18. https://doi.org/10.1016/j.soilbio.2015.11.010
Gilbert HJ (2010) The biochemistry and structural biology of plant cell wall deconstruction. Plant Physiol 153:444–455. https://doi.org/10.1104/pp.110.156646
Greenacre M (2017) Correspondence analysis in practice. Interdisciplinary statistics series, 3rd edn. Chapman and Hall/CRC, Boca Raton
Hu Y, Zheng Q, Wanek W (2017) Flux analysis of free amino sugars and amino acids in soils by isotope tracing with a novel liquid chromatography/high resolution mass spectrometry platform. Anal Chem 89:9192–9200. https://doi.org/10.1021/acs.analchem.7b01938
Huson DH, Mitra S, Ruscheweyh H-J, Weber N, Schuster SC (2011) Integrative analysis of environmental sequences using MEGAN4. Genome Res 21:1552–1560. https://doi.org/10.1101/gr.120618.111
Jefferies RL, Jano AP, Abraham KF (2006) A biotic agent promotes large-scale catastrophic change in the coastal marshes of Hudson Bay. J Ecol 94:234–242. https://doi.org/10.1111/j.1365-2745.2005.01086.x
Jones DL, Shannon D, Murphy DV, Farrar J (2004) Role of dissolved organic nitrogen (DON) in soil N cycling in grassland soils. Soil Biol Biochem 36:749–756. https://doi.org/10.1016/j.soilbio.2004.01.003
Jones DL, Healey JR, Willett VB, Farrar JF, Hodge A (2005) Dissolved organic nitrogen uptake by plants - an important N uptake pathway? Soil Biol Biochem 37:413–423. https://doi.org/10.1016/j.soilbio.2004.08.008
Kopylova E, Noé L, Touzet H (2012) SortMeRNA: fast and accurate filtering of ribosomal RNAs in metatranscriptomic data. Bioinformatics 28:3211–3217. https://doi.org/10.1093/bioinformatics/bts611
Koranda M, Kaiser C, Fuchslueger L, Kitzler B, Sessitsch A, Zechmeister-Boltenstern S, Richter A (2014) Fungal and bacterial utilization of organic substrates depends on substrate complexity and N availability. FEMS Microbiol Ecol 87:142–152. https://doi.org/10.1111/1574-6941.12214
Kuijper DPJ, Bakker JP, Cooper EJ, Ubels R, Jónsdóttir IS, Loonen MJJE (2006) Intensive grazing by Barnacle geese depletes High Arctic seed bank. Can J Bot 84:995–1004. https://doi.org/10.1139/b06-052
Maron JL, Crone E (2006) Herbivory: effects on plant abundance, distribution and population growth. Proc R Soc B 273:2575–2584. https://doi.org/10.1098/rspb.2006.3587
McNear DH Jr (2013) The rhizosphere—roots, soil and everything in between. Nat Educ Knowl 4:1
Moller I, Marcus SE, Haeger A, Verhertbruggen Y, Verhoef R, Schols H et al (2008) High-throughput screening of monoclonal antibodies against plant cell wall glycans by hierarchical clustering of their carbohydrate microarray binding profiles. Glycoconj J 25:37–48. https://doi.org/10.1007/s10719-007-9059-7
Morgan AD, Maclean RC, Hillesland KL, Velicer GJ (2010) Comparative analysis of *Myxococcus* predation on soil bacteria. Appl Environ Microbiol 76:6920–6927. https://doi.org/10.1128/AEM.00414-10
Murphy MT, McKinley A, Moore TR (2009) Variations in above- and below-ground vascular plant biomass and water table on a temperate ombrotrophic peatland. Botany 87:845–853. https://doi.org/10.1139/B09-052
Müller AL, Pelikan C, de Rezende JR, Wasmund K, Putz M, Glombitza C et al (2018) Bacterial interactions during sequential degradation of cyanobacterial necromass in a sulfidic arctic marine sediment. Environ Microbiol 20:2927–2940. https://doi.org/10.1111/1462-2920.14297
Ping CL, Jastrow JD, Jorgenson MT, Michaelson GJ, Shur YL (2015) Permafrost soils and carbon cycling. Soil 1:147–171. https://doi.org/10.5194/soil-1-147-2015
R Core Team (2014) R: a language and environment for statistical computing. R Foundation for Statistical Computing, Vienna, Austria. http://www.R-project.org/
Ritala A, Häkkinen ST, Toivari M, Wiebe MG (2017) Single cell protein—state-of-the-art, industrial landscape and patents 2001–2016. Front Microbiol 8:2009. https://doi.org/10.3389/fmicb.2017.02009
Sabais ACW, Scheu S, Eisenhauer N (2011) Plant species richness drives the density and diversity of Collembola in temperate grassland. Acta Oecol (Montrouge) 37:195–202. https://doi.org/10.1016/j.actao.2011.02.002
Sarkar P, Bosneaga E, Auer M (2009) Plant cell walls throughout evolution: towards a molecular understanding of their design principles. J Exp Bot 60:3615–3635. https://doi.org/10.1093/jxb/erp245
Sauheitl L, Glaser B, Weigelt A (2009) Uptake of intact amino acids by plants depends on soil amino acid concentrations. Environ Exp Bot 66:145–152. https://doi.org/10.1016/j.envexpbot.2009.03.009
Schimel JP, Weintraub MN (2003) The implications of exoenzyme activity on microbial carbon and nitrogen limitation in soil: a theoretical model. Soil Biol Biochem 35:549–563. https://doi.org/10.1016/S0038-0717(03)00015-4
Sjögersten S, van der Wal R, Loonen MJJE, Woodin SJ (2011) Recovery of ecosystem carbon fluxes and storage from herbivory. Biogeochemistry 106:357–370. https://doi.org/10.1007/s10533-010-9516-4
Solheim B, Endal A, Vigstad H (1996) Nitrogen fixation in Arctic vegetation and soils from Svalbard, Norway. Polar Biol 16:35–40. https://doi.org/10.1007/BF01876827
Speed JDM, Woodin SJ, Tømmervik H, van der Wal R (2010) Extrapolating herbivore-induced carbon loss across an arctic landscape. Polar Biol 33:789–797. https://doi.org/10.1007/s00300-009-0756-5
Söllinger A, Tveit AT, Poulsen M, Noel SJ, Bengtsson M, Bernhardt J et al (2018) Holistic assessment of rumen microbiome dynamics through quantitative metatranscriptomics reveals multifunctional redundancy during key steps of anaerobic feed degradation. mSystems 3:e00038-e118. https://doi.org/10.1128/mSystems.00038-18
Tarnocai C, Canadell JG, Schuur EAG, Kuhry P, Mazhitova G, Zimov S (2009) Soil organic carbon pools in the northern circumpolar permafrost region. Glob Biogeochem Cycles. https://doi.org/10.1029/2008GB003327
Thakur MP, Herrmann M, Steinauer K, Rennoch S, Cesarz S, Eisenhauer N (2015) Cascading effects of belowground predators on plant communities are density-dependent. Ecol Evol 5:4300–4314. https://doi.org/10.1002/ece3.1597
Thormann MN (2006) Diversity and function of fungi in peatlands: a carbon cycling perspective. Can J Soil Sci 86:281–293
Tveit AT, Schwacke R, Svenning MM, Urich T (2013) Organic carbon transformations in high-Arctic peat soils: key functions and

microorganisms. ISME J 7:299–311. https://doi.org/10.1038/ismej.2012.99

Tveit AT, Urich T, Frenzel P, Svenning MM (2015) Metabolic and trophic interactions modulate methane production by Arctic peat microbiota in response to warming. Proc Natl Acad Sci USA 112:E2507-2516. https://doi.org/10.1073/pnas.1420797112

Uren NC (2000) Types, amounts, and possible functions of compounds released into the rhizosphere by soil-grown plants. In: Willig S, Varanini Z, Nannipieri P (eds) The rhizosphere: biochemistry and organic substances at the soil-plant interface, 1st edn. CRC Press, Boca Raton, pp 19–40

Urich T, Lanzén A, Qi J, Huson DH, Schleper C, Schuster SC (2008) Simultaneous assessment of soil microbial community structure and function through analysis of the meta-transcriptome. PLoS ONE 3:e2527. https://doi.org/10.1371/journal.pone.0002527

Van der Heijden MGA, Bardgett RD, van Straalen NM (2008) The unseen majority: soil microbes as drivers of plant diversity and productivity in terrestrial ecosystems. Ecol Lett 11:296–310. https://doi.org/10.1111/j.1461-0248.2007.01139.x

Van der Wal R (2006) Do herbivores cause habitat degradation or vegetation state transition? Evidence from the tundra. Oikos 114:177–186. https://doi.org/10.1111/j.2006.0030-1299.14264.x

Wallenstein MD, Weintraub MN (2008) Emerging tools for measuring and modeling the in situ activity of soil extracellular enzymes. Soil Biol Biochem 40:2098–2106. https://doi.org/10.1016/j.soilbio.2008.01.024

Wardle DA, Bardgett RD, Klironomos JN, Setälä H, van der Putten WH, Wall DH (2004) Ecological linkages between aboveground and belowground biota. Science 304:1629–1633. https://doi.org/10.1126/science.1094875

Wheeler DL, Church DM, Federhen S, Lash AE, Madden TL, Pontius JU et al (2003) Database resources of the National Center for Biotechnology. Nucleic Acids Res 31:28–33. https://doi.org/10.1093/nar/gkg033

Zacheis A, Hupp JW, Ruess RW (2001) Effects of migratory geese on plant communities of an Alaskan salt marsh. J Ecol 89:57–71. https://doi.org/10.1046/j.1365-2745.2001.00515.x

Zak DR, Kling GW (2006) Microbial community composition and function across an arctic tundra landscape. Ecology 87:1659–1670. https://doi.org/10.1890/0012-9658(2006)87[1659:MCCAFA]2.0.CO;2

Zak DR, Holmes WE, White DC, Peacock AD, Tilman D (2003) Plant diversity, soil microbial communities, and ecosystem function: are there any links? Ecology 84:2042–2050. https://doi.org/10.1890/02-0433

Supplementary figures:

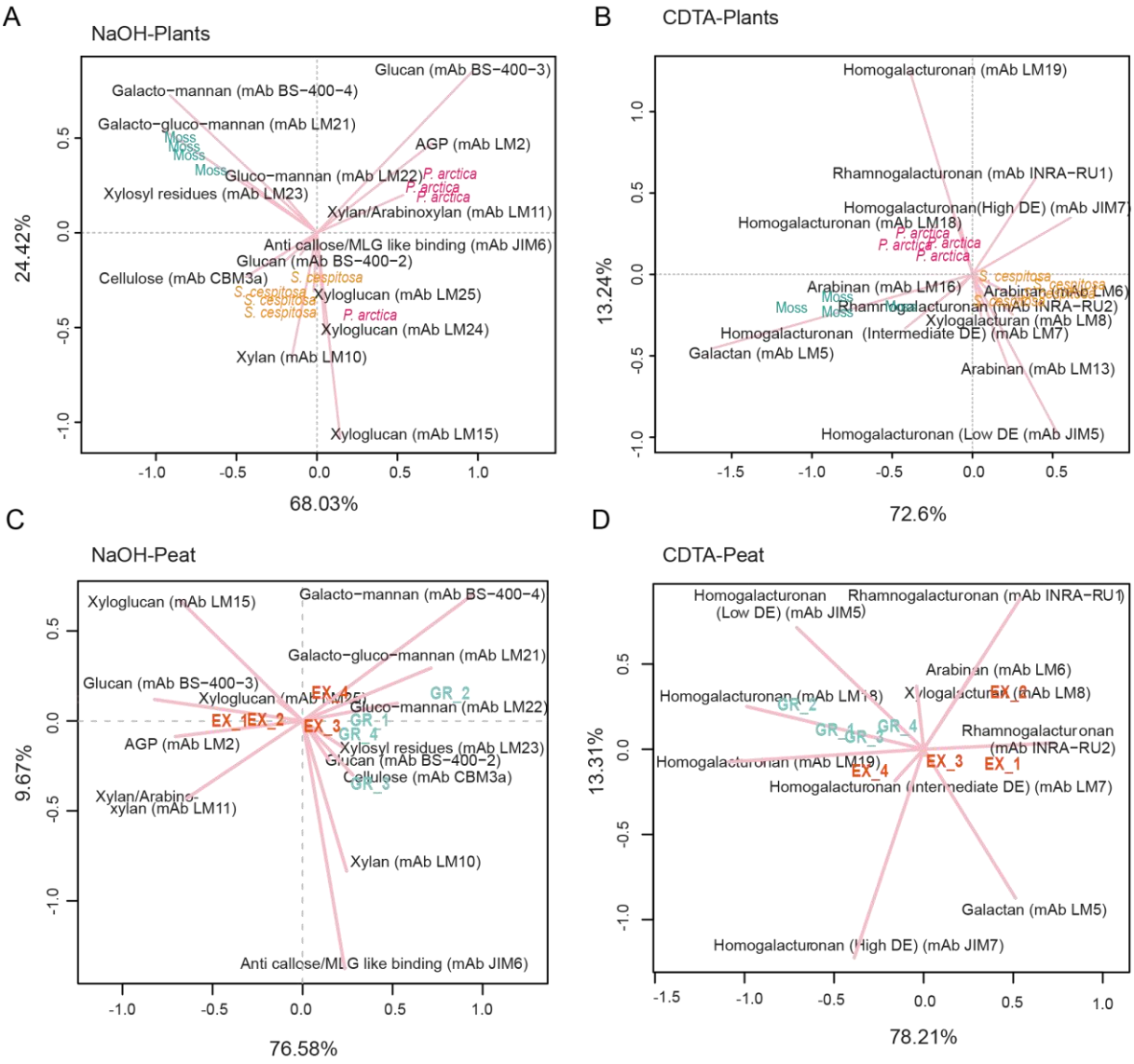

Figure S1: Correspondence Analysis of polysaccharide binding signals in *Poa arctica*, *Saxifraga cespitosa* and a moss mix. A) NaOH extraction (cellulose, hemicelluloses and glycoproteins) of the three plants. B) CDTA extraction (pectins) of the three plants. **Correspondence Analysis of polysaccharide binding signals in exclosed and grazed sites.** C) NaOH extraction (cellulose, hemicelluloses and glycoproteins) of the two sites. D) CDTA extraction (pectins) of the two sites.

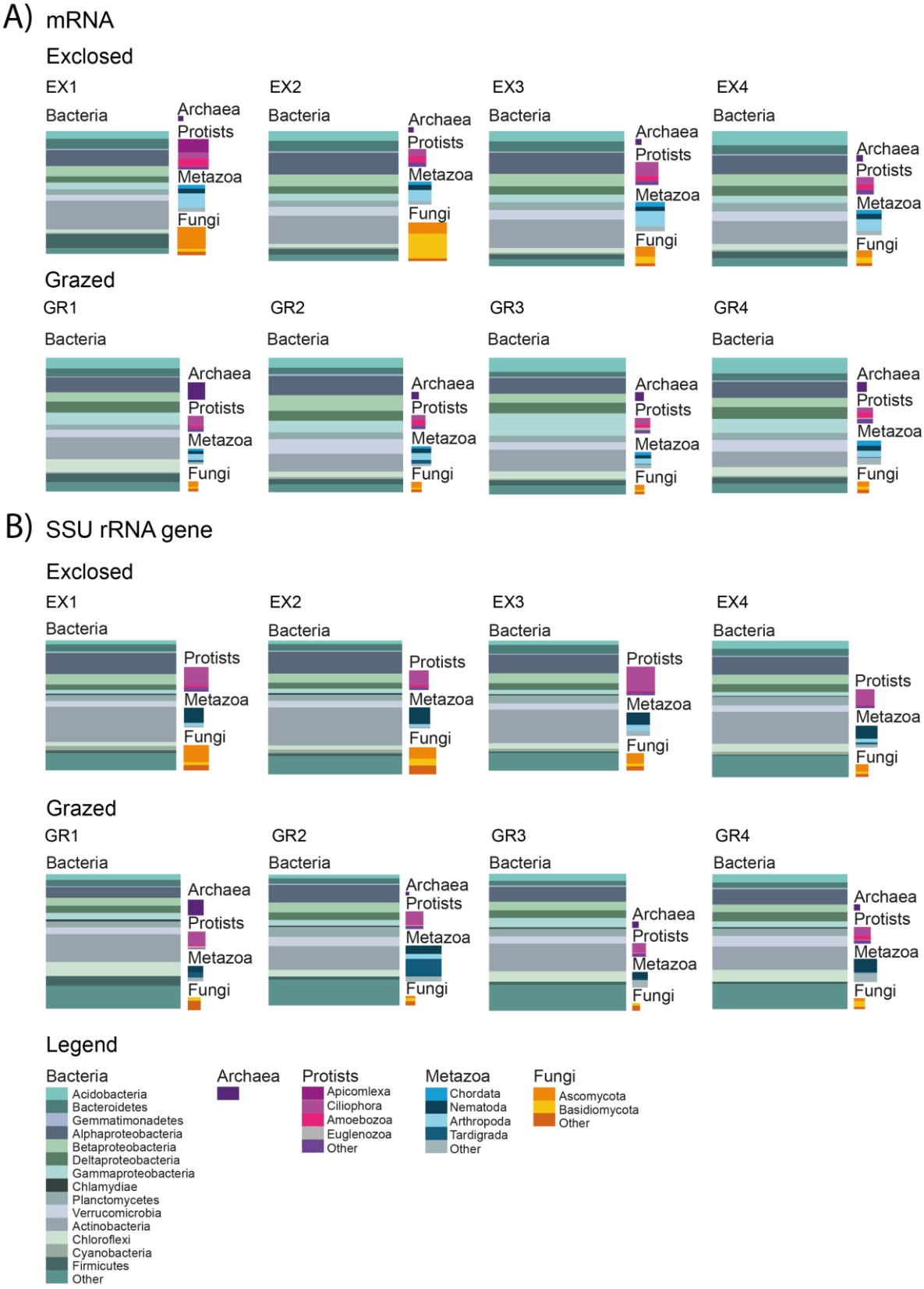

Figure S2: Microbial community composition A) based on mRNA sequences and therefore representing the transcriptionally active microbial community. B) based on SSU rRNA gene sequences reflecting the potential microbial community in peat soil from exclosures and grazed sites. The size of the boxes reflect the relative abundances of taxa. Taxonomy profiles are displayed at phylum-level (class-level for *Proteobacteria*) and show each replicate separately.

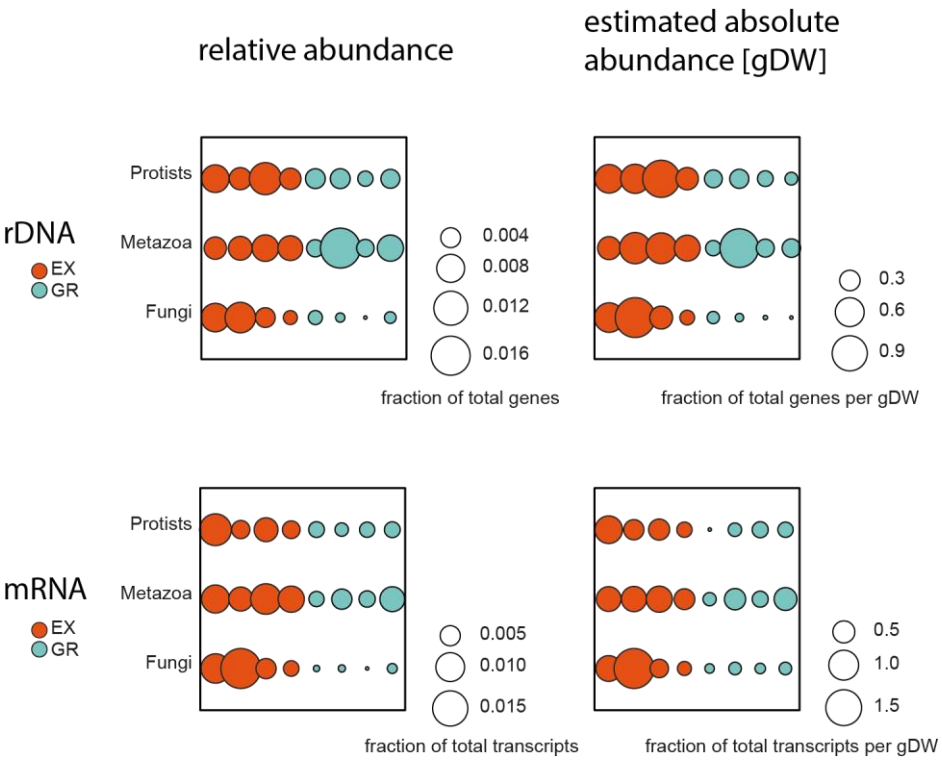

Figure S3: Abundances of eukaryotic kingdoms in the grazed sites and exclosures. Fraction of eukaryotic reads belonging to fungi, Protista and Metazoa for the mRNA and SSU rRNA gene datasets as relative abundances and relative abundances normalized by DNA and RNA masses per gram of dry soil (gDW). The size of each circle represents the fraction of reads in the total number of genes or transcripts.

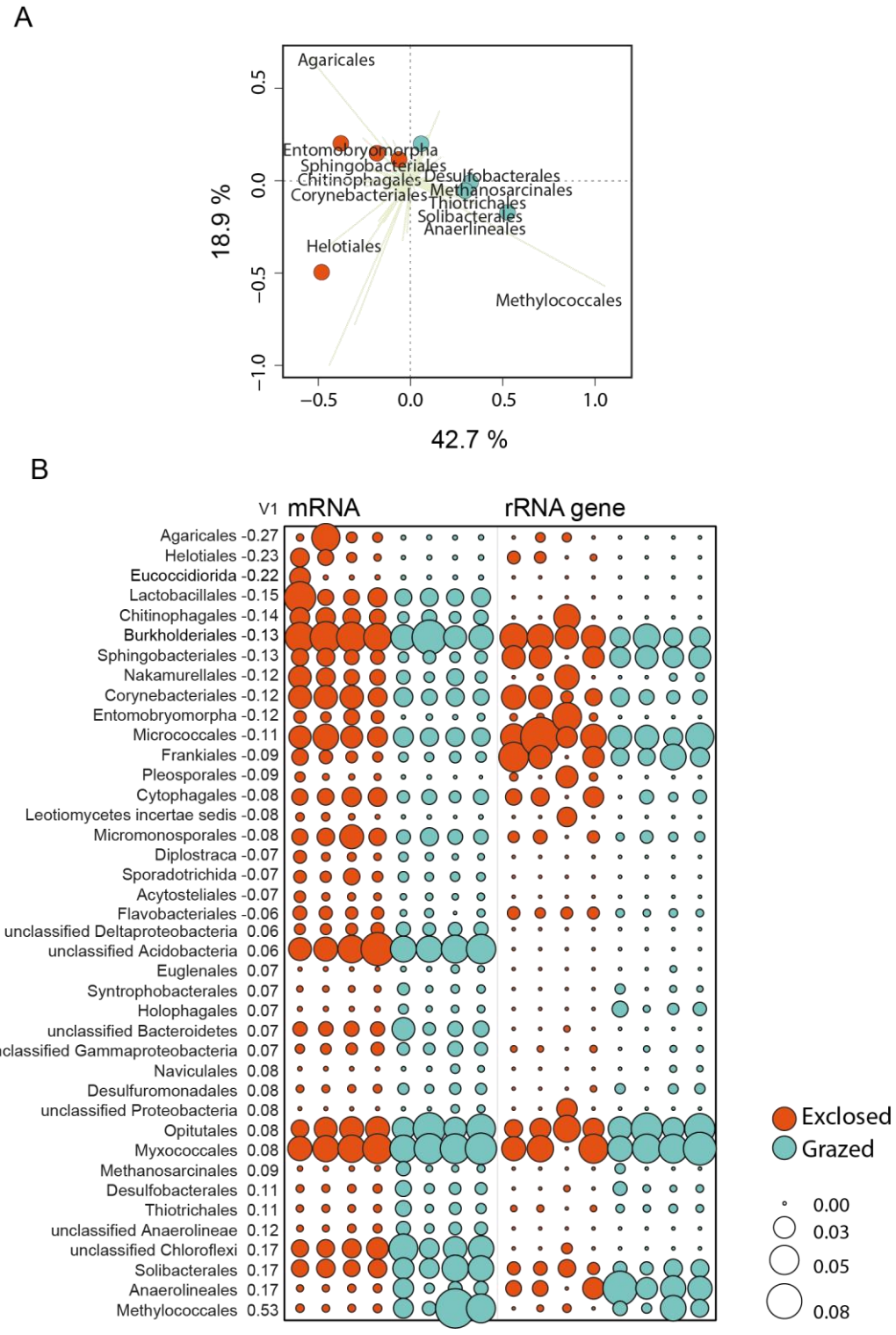

Figure S4: Extraction of the microbial orders that have the largest differences in transcriptional activity between the exclosures and grazed sites. A) Correspondence analysis based on mRNA counts at order level taxonomy. B) Number of mRNA transcripts and rRNA genes assigned to the 20 taxa with the largest differences in transcriptional activity between exclosures and grazed sites along the first axis in both directions from A).

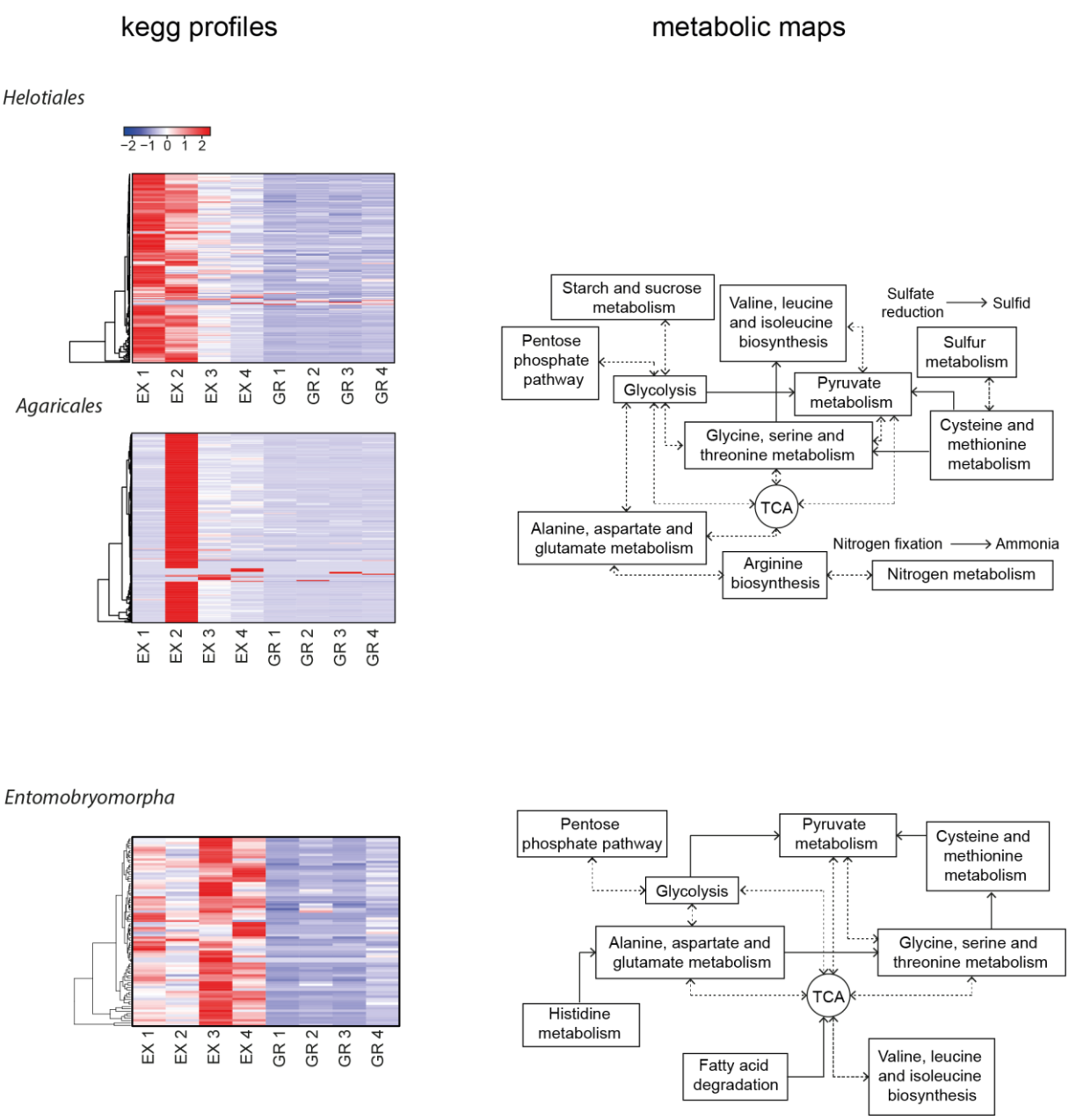

Figure S5: Kegg profiles of the central metabolism in the eukaryotic orders *Helotiales*, *Agaricales* and Entomobryomorpha. Each line in the heatmap corresponds to a k number, which represents one molecular function. The central metabolism map to the right of each heatmap show the categories of central metabolism functions included in the heatmap. Overall, the figure shows that the transcription of genes for the central metabolism enzymes is higher for all three taxa in the exclosures.

Supplementary tables:

Table S1: Comparison of air saturation [O2 %] and temperature [T °C] for the exclosed and grazed sites at four different depths.

	O_2 [%]				T [°C]				measured
	- 2 cm	-5 cm	-10 cm	-15 cm	0 cm	-5 cm	-10 cm	-15 cm	
Exclosure 1	20.0	18.9	13.2	6.9	10.4	6.5	4.9	3.6	01.08.2016
Exclosure 2	20.3	19.9	16.4	-	10.8	8.8	5.4	-	02.08.2016
Grazed 1	20.1	16.4	4.0	3.0	8.3	7.1	4.9	3.4	01.08.2016
Grazed 2	19.9	13.2	0.4	1.6	14	10	6.9	4.9	02.08.2016

Table S2: Water content and total organic matter (TOM) content of the peat soils from the exclosed and grazed sites.

Sample ID	Water content [%]	TOM [%]
EX1	83.5	14.2
EX2	85.3	12.4
EX3	85.9	11.3
EX4	83.2	14.0
GR1	94.7	4.7
GR2	92.8	6.5
GR3	90.5	7.7
GR4	91.6	7.2

Table S3: Statistical testing of results presented in figure 2 (sugars, amino acids, microbial biomass and enzymatic activity) and table 3 (polysaccharides), comparing the exclosed and grazed sites. The Wilcoxon rank sum test were used with R (v3.6.1).

		Wilcoxon rank sum test	
Sugars			
	Glucose	0.0023	*
	Mannose	0.047	*
	Xylose	0.0011	*
	Galactose	0.0006	*
	Fructose	0.0455	*
Amino acids			
	AcetylGlucosamine	0.01	*
	Phenylalanine	0.0145	*
	Tyrosine	0.8428	
	Leucine	0.0018	*
	Methionine	0.0173	*
	Cysteine	0.0173	*
	GlutamicAcid	0.0483	*
	Alanine	0.0023	*
	Threonine	0.0014	*
	Serine	0.0112	*
	AsparticAcid	0.0529	
	Glycine	0.0009	*
	Proline	0.0112	*
	Asparagine	0.0002	*
	Glutamine	0.0068	*
	Glucosamine	0.002	*
	Histidine	0.01	*
	Arginine	0.0145	*
	Lysine	0.0121	*
Microbial biomass			
	DNA [gDW]	0.0286	*
	RNA [gDW]	0.4857	
Enzymes			
	Cellulose	0.029	*
	Mannan	0.029	*
	Xyloglucan	0.029	*
	Xylan	0.029	*
	Arabinoxylan	0.029	*
	Galactan	0.029	*
	Arabinan	0.029	*
	Rhamnogalacturonan	0.029	*
Polysaccharides			
	mAb		
(1→3)-β-D-glucan	BS-400-2	0.02857	*

(1→3)(1→4)-β-D-glucan	BS-400-3	0.02857	*
(1→4)-β-D-(galacto)mannan	BS-400-4	0.05714	
Cellulose	CBM3a	0.02857	*
Rhamnogalacturonan_1	INRA-RU1	0.02857	*
Rhamnogalacturonan_2	INRA-RU2	0.02857	*
HG (Low DE)	JIM5	0.6857	
Anti callose/MLG like binding	JIM6	0.2	
HG (High DE)	JIM7	0.3429	
(1→4)-β-D-xylan	LM10	0.02857	*
(1→4)-β-D-xylan/arabinoxylan	LM11	0.02857	*
(1→5)-α-L-arabinan_2	LM13	0.02857	*
Xyloglucan_1	LM15	0.02857	*
(1→5)-α-L-arabinan_3	LM16	0.1143	
HG_1	LM18 (MUC2)	0.8857	
HG_2	LM19 (XGA2)	0.8857	
AGP	LM2	0.02857	*
(1→4)-β-D-(galacto)(gluco)mannan	LM21	0.02857	*
(1→4)-β-D-(gluco)mannan	LM22	0.05714	
Non-acetylated xylosyl residues	LM23	0.02857	*
Xyloglucan_2	LM24	0.02857	*
Xyloglucan_3	LM25	0.02857	*
(1→4)-β-D-galactan	LM5	0.05714	
(1→5)-α-L-arabinan_1	LM6	0.02857	*
HG (Intermediate DE)	LM7	0.02857	*
Xylogalacturan	LM8	0.02857	*

Table S4: Polysaccharide composition of two vascular plants and a mix of the mosses growing in the Solvatn peatland. The table list the mean values (+- the standard deviations) of binding signals for each tested polysaccharide in the plants from four replicates from the exclosures and four replicates from the grazed sites. The polysaccharide composition of the soil matrix was determined using Comprehensive Microarray Polymer Profiling (CoMPP) as described in the materials and methods.

	Polysaccharide	Antibody ID	*Poa arctica* mean value		sd	*Saxifraga cespitosa* mean value		sd	mosses mean value		sd
1	(1→3)-β-D-glucan	BS-400-2	0.0005	+-	0.0003	0.0023	+-	0.0003	0.0012	+-	0.0007
2	(1→3)(1→4)-β-D-glucan	BS-400-3	0.0382	+-	0.0186	0.013	+-	0.0037	0.0058	+-	0.0003
3	(1→4)-β-D-(galacto)mannan	BS-400-4	0.0004	+-	0.0003	0.0068	+-	0.0012	0.0123	+-	0.0017
4	Arabinogalactan protein	LM2	0.0123	+-	0.005	0.0011	+-	0.0008	0.0007	+-	0.0006
5	(1→4)-β-D-galactan	LM5	0.0112	+-	0.0013	0.0118	+-	0.0015	0.0126	+-	0.0004
6	(1→5)-α-L-arabinan_1	LM6	0.0014	+-	0.0006	0.0062	+-	0.0002	0.0004	+-	0.0002
7	Homogalacturonan (Intermediate DE)	LM7	0.0004	+-	0.0001	0.0005	+-	0.0002	0.0007	+-	0.0001
8	Xylogalacturan	LM8	0.0003	+-	0.0003	0.0013	+-	0.0002	0.0002	+-	0.0001
9	(1→4)-β-D-xylan	LM10	0.0037	+-	0.0015	0.0103	+-	0.0014	0.0024	+-	0.0004
10	(1→4)-β-D-xylan/arabinoxylan	LM11	0.0156	+-	0.0081	0.0096	+-	0.0018	0.002	+-	0.0004
11	(1→5)-α-L-arabinan_2	LM13	0.0004	+-	0.0003	0.0036	+-	0.0015	0.0003	+-	0.0001
12	Xyloglucan_1	LM15	0.0184	+-	0.0014	0.0325	+-	0.0043	0.0037	+-	0.001
13	(1→5)-α-L-arabinan_3	LM16	0.0001	+-	0	0.0003	+-	0.0001	0.0001	+-	0
14	Homogalacturonan_1	LM18 (MUC2)	0.0066	+-	0.0018	0.0131	+-	0.0018	0.0029	+-	0.0006
15	Homogalacturonan_2	LM19 (XGA2)	0.0104	+-	0.002	0.0117	+-	0.0019	0.0035	+-	0.0007
16	(1→4)-β-D-(galacto)(gluco)mannan	LM21	0.0018	+-	0.0012	0.0116	+-	0.0013	0.0159	+-	0.0007
17	(1→4)-β-D-(gluco)mannan	LM22	0	+-	0.0001	0.002	+-	0.0006	0.003	+-	0.0004
18	Non-acetylated xylosyl residues	LM23	0.0004	+-	0.0002	0.0007	+-	0.0002	0.0011	+-	0.0002
19	Xyloglucan_2	LM24	0.0038	+-	0.0017	0.0063	+-	0.0007	0.0008	+-	0.0002
20	Xyloglucan_3	LM25	0.0171	+-	0.0065	0.0261	+-	0.0022	0.009	+-	0.0001
21	Homogalacturonan (Low DE)	JIM5	0.0065	+-	0.0024	0.0338	+-	0.0015	0.0041	+-	0.0015
22	Anti callose/MLG like binding	JIM6	0.0002	+-	0.0002	0.0011	+-	0.0003	0.0004	+-	0.0002
23	Homogalacturonan (High DE)	JIM7	0.0152	+-	0.0027	0.0447	+-	0.0035	0.0033	+-	0.0008
24	Rhamnogalacturonan_1	INRA-RU1	0.0045	+-	0.0021	0.0106	+-	0.001	0.0002	+-	0.0001
25	Rhamnogalacturonan_2	INRA-RU2	0.004	+-	0.0017	0.0122	+-	0.0018	0.0021	+-	0.0034
26	Cellulose	CBM3a	0.0034	+-	0.0018	0.0151	+-	0.0044	0.0072	+-	0.0011

Table S5: DNA and RNA extractions. The table shows masses of DNA and RNA, the percentage of plant DNA and RNA in the samples and the masses of microbial DNA and RNA [µg/g soil].

	EX1	EX2	EX3	EX4	GR1	GR2	GR3	GR4
g soil/sample [dw]	0.11	0.08	0.09	0.09	0.04	0.06	0.07	0.08
ug DNA/g soil [dw]	82.53	132.23	109.17	84.14	58.05	66.31	74.82	35.72
%plant_DNA [dw]	8.88	7.14	13.06	8.46	0.58	1.49	0.39	0.49
ug microbial DNA/g soil [dw]	75.2	122.79	94.91	77.02	57.71	65.32	74.52	35.54
ug RNA/g soil [dw]	90.95	117.98	75.59	62.06	46.98	92.57	67.67	73.39
%plant_mRNA [dw]	24.3	16.91	13.34	15.37	0.56	1	0.53	0.9
ug microbial RNA/g soil [dw]	68.85	98.03	65.51	52.52	46.71	91.64	67.31	72.73

Table S6: Sequence read processing.

Sample	Label	Molecule	PE input read pairs	After trimmomatic	rRNA	non-rRNA	fraction non-rRNA	Assigned taxonomy Diamond NCBI nr	subsample	Assigned taxonomy Diamond NCBI nr	assigned pfam - HMMER
1	1-SV1EX1_S7	DNA	40110589	39549509	32907	39516602	0.999		5000000		857484
2	2-SV1EX2_S8	DNA	39211438	38786159	32549	38753610	0.999		5000000		908511
3	3-SV2EX1_S1	DNA	41387588	40887012	32234	40854778	0.999		5000000		922797
4	4-SV2EX2_S2	DNA	38868695	38444822	27553	38417269	0.999		5000000		902805
5	5-SV1GR1_S3	DNA	46640253	45177386	45941	45131445	0.999		5000000		928532
6	6-SV1GR2_S4	DNA	47843485	47324098	32082	47292016	0.999		5000000		933670
7	7-SV2GR1_S5	DNA	47539855	46909364	29765	46879599	0.999		5000000		932655
8	8-SV2GR1_S6	DNA	52234340	51672485	32981	51639504	0.999		5000000		928690
9	9-SV1EX1_S10	RNA	44840112	44556971	22720940	21836031	0.49	7756628	5000000	1706160	586026
10	10-SV1EX2_S11	RNA	45916642	45336765	23189787	22146979	0.488	8560199	5000000	1817805	674879
11	11-SV2EX1_S12	RNA	53742180	53371652	25019438	28352214	0.531	10374434	5000000	1685816	624831
12	12-SV2EX2_S13	RNA	54049261	53646056	18623860	35022196	0.653	10922592	5000000	1600519	582726
13	13-SV1GR1_S14	RNA	52320760	52016247	87954335	43220815	0.831	8483536	5000000	1264058	457988
14	14-SV1GR2_S15	RNA	39681563	39443065	11535736	27907330	0.708	7888546	5000000	1335876	501529
15	15-SV2GR1_S16	RNA	45171463	44848274	12397684	32450591	0.724	9342801	5000000	1358142	502498
16	16-SV2GR2_S9	RNA	54813817	54388451	22157802	32230650	0.593	9309721	5000000	1342685	500670

Table S7: Plant cell wall polymer degrading enzymes that were used for the functional annotation of the main figures 4 and 5 and the supplement figure S6. Adjusted from Rytioja *et al.*(1).

	Substrate	Enzyme Activity	CAZyme family	EC no
Hemicelluloses	Cellulose	exo-1,3-1,4-glucanase	GH_3	EC 3.2.1.-
		endo-β-1,4-glucanase	GH_5, _6, _7, _8, _9, _44, _45, _48	EC 3.2.1.4
		endo-β-1,3(4)-glucanase	GH_9, _16	EC 3.2.1.6
		α-glucan lyase	GH_31	EC 4.2.2.13
		endo-β-1,3-glucanase	GH_16, _81	EC 3.2.1.39
		exo-β-1,4-glucanase	GH_1, _5, _9	EC 3.2.1.74
		reducing end-acting cellobiohydrolase	GH_7, _48	EC 3.2.1.176
	Mixed-linkage glucan	endo-β-1,3-glucanase	GH_16, _81	EC 3.2.1.39
	Xylan	xylan endotransglycosylase	GH_10	EC 2.4.2.-
		endo-β-1,4-xylanase	GH_5, _8, _10, _11, _30, _43	EC 3.2.1.8
		endo-β-1,3-xylanase	GH_10, _11, _26	EC 3.2.1.32
		reducing-end-xylose releasing exo-oligoxylanase	GH_8	EC 3.2.1.156
	Galactomannan	mannan transglycosylase	GH_5	EC 2.4.1.-
		galactan galactosyltransferase	GH_27	EC 2.4.1.-
		β-1,3-mannanase	GH_5	EC 3.2.1.-
		mannobiose-producing exo-β-mannanase	GH_26	EC 3.2.1.-
		[inverting] exo-α-1,5-L-arabinanase	GH_43	EC 3.2.1.-
		endo-β-N-acetylglucosaminidase	GH_18	EC 3.2.1.96
		exo-β-1,4-mannobiohydrolase	GH_26	EC 3.2.1.100
		α-1,6-mannanase	GH_76	EC 3.2.1.101
		endo-β-1,6-galactanase	GH_5, _30	EC 3.2.1.164
		mannosylglycerate hydrolase	GH_38, _63	EC 3.2.1.170
	Xyloglucan	[inverting] exo-α-1,5-L-arabinanase	GH_43	EC 3.2.1.-
		isoprimeverose-producing oligoxyloglucan hydrolase	GH_3	EC 3.2.1.120
		xyloglucanase	GH_5, _9, _16, _44	EC 3.2.1.151
		xyloglucan:xyloglucosyltransferase	GH_16	EC 2.4.1.207
	Arabinoxylan	arabinoxylan-specific endo-β-1,4-xylanase	GH_5	EC 3.2.1.-
		[inverting] exo-α-1,5-L-arabinanase	GH_43	EC 3.2.1.-
		glucuronoarabinoxylan endo-β-1,4-xylanase	GH_30	EC 3.2.1.136
	Pectin	galactan galactosyltransferase	GH_27	EC 2.4.1.-
		endo-xylogalacturonan hydrolase	GH_28	EC 3.2.1.-
		[inverting] exo-α-1,5-L-arabinanase	GH_43	EC 3.2.1.-
		polygalacturonase	GH_28	EC 3.2.1.15

	invertase	GH_32	EC 3.2.1.26
	α-galacturonase	GH_4, _28	EC 3.2.1.67
	endo-β-1,3-galactanase	GH_53	EC 3.2.1.89
	3-O-α-glucopyranosyl-L-rhamnose phosphorylase	GH_43	EC 3.2.1.99
	rhamnogalacturonase	GH_28	EC 3.2.1.171
	rhamnogalacturonan α-1,2-galacturonohydrolase	GH_28	EC 3.2.1.173
	rhamnogalacturonan α-L-rhamnohydrolase	GH_78	EC 3.2.1.174
	β-porphyranase	GH_16	EC 3.2.1.178
	endo-β-1,3-galactanase	GH_16	EC 3.2.1.181
	3-O-α-glucopyranosyl-L-rhamnose phosphorylase	GH_65	EC 2.4.1.282
		Pfam accession no	
Lignin	Peroxidase	PF00141.18	
	Dioxygenase_C	PF00775.16	
	Cu-oxidase_4	PF02578.10	

Table S8: Microbial taxa for which the largest differences in transcription between exclosures and grazed sites were found. Shown are the twenty taxa (order level) that contribute the most to the inertia represented by the x-axis in figure S4. Negative values indicate that the highest numbers of transcripts were found in the libraries from the exclosures. Positive values indicate the opposite.

	V1
Agaricales	-0.27
Helotiales	-0.23
Eucoccidiorida	-0.22
Lactobacillales	-0.15
Chitinophagales	-0.14
Burkholderiales	-0.13
Sphingobacteriales	-0.13
Nakamurellales	-0.12
Corynebacteriales	-0.12
Entomobryomorpha	-0.12
Micrococcales	-0.11
Frankiales	-0.09
Pleosporales	-0.09
Cytophagales	-0.08
Leotiomycetes incertae sedis	-0.08
Micromonosporales	-0.08
Diplostraca	-0.07
Sporadotrichida	-0.07
Acytosteliales	-0.07
Flavobacteriales	-0.06
unclassified Deltaproteobacteria	0.06
unclassified Acidobacteria	0.06
Euglenales	0.07
Syntrophobacterales	0.07
Holophagales	0.07
unclassified Bacteroidetes	0.07
unclassified Gammaproteobacteria	0.07
Naviculales	0.08
Desulfuromonadales	0.08
unclassified Proteobacteria	0.08
Opitutales	0.08
Myxococcales	0.08
Methanosarcinales	0.09
Desulfobacterales	0.11
Thiotrichales	0.11
unclassified Anaerolineae	0.12
unclassified Chloroflexi	0.17
Solibacterales	0.17
Anaerolineales	0.17
Methylococcales	0.53

Table S9: Expression of genes for polymer degradation by the detritivorous fungi *Helotiales* and *Agaricales* and the predator and omnivore Entomorbyomorpha. Presence of a coloured circle indicate that transcripts for the respective pfam domain, represented by a Pfam accession number, is assigned to the corresponding taxon. Several circles per line indicate that the Pfam domain is known to be part of genes for decomposition of more than one polymer.

	Cellulose	Galacto-mannan	MLG	Xylo-glucan	Xylan	Arabino-xylan	Pectins	Lignin	Chitin	Bact. cell walls
PF01055										
PF01915										
PF00232										
PF04616										
PF00141										
PF01532										
PF00933										
PF00722										
PF02156										
PF03311										
PF00728										
PF01476										
PF00775										
PF07745										
PF02837										
PF06964										
PF01183										
PF00295										
PF03639										
PF02015										
PF00704										
PF00251										
PF00703										
PF00150										
PF02836										
PF01301										
PF09206										
PF03663										
PF01341										
PF00457										
PF00840										
PF12891										
PF00759										
PF03632										
PF07748										
PF01074										
PF02055										
sum	9-10-5	6-3-5	2-1-2	3-4-3	5-3-1	2-1-1	7-5-2	2-1-0	9-6-4	6-5-7
									Total sum PFAMs	120

References

1. Rytioja J, Hildén K, Yuzon J, Hatakka A, de Vries RP, Mäkelä MR. Plant-Polysaccharide-Degrading Enzymes from Basidiomycetes. Microbiol Mol Biol Rev. 2014;78(4):614–49.

Supplementary Data availability

Metagenomes and metatranscriptomes have been deposited in the Sequence Read Archive (SRA) database (Run Accession nos.: SRR13614422, SRR13614421, SRR13614414, SRR13614413, SRR13614412, SRR13614411, SRR13614410, SRR13614409, SRR13614408, SRR13614407, SRR13614420, SRR13614419, SRR13614418, SRR13614417, SRR13614416, SRR13614415).

Supplementary materials and methods

Section 1: **Comprehensive microarray polymer profiling (CoMPP)**

The polysaccharide composition of Arctic peat soils were measured using Comprehensive Microarray Polymer Profiling (CoMPP) at the University of Copenhagen as described in Moller *et al.* (1). To optimize the method for best possible signal strength for peat samples some adjustments were made to the development solution. The optimized recipe of the development solution is as follows: 10 mL of alkaline phosphatase buffer (100 mM NaCl, 5 mM $MgCl_2$, 100 mM diethanolamine, pH 9.5) with 82.5 µL of BCIP (20 mg/mL) (5-bromo-4-chloro-3-indolylphosphate) and 66 µL of NBT (50 mg/mL) (nitro blue tetrazolium). The strength of a binding signal was used as an indication for the amount of a polysaccharide in a sample. Since all samples were processed the same way, the differences in the binding signals indicate the differences in the amount of polysaccharides per gram of dry weight of the different samples. In theory, hemicelluloses should be in the NaOH extract and pectins in the CDTA extract. However, some of the pectins showed higher binding signals in the NaOH extract. This might be due to covalent attachments of pectin side chains with hemicelluloses (2). Whenever pectins were showing binding signals in both extractions, the strongest binding signal was used for the evaluation. Stronger binding signals of pectins in the NaOH extraction were found for the antibodies LM5, LM6, INRA-RU1 and INRA-RU2. The same method was used to investigate the polysaccharide composition of the three plant samples (*Poa arctica, Saxifraga cespitosa* and a moss mix). The reason for selecting

these two vascular species is that they are both among the most common vascular plants in the Arctic vegetation of Svalbard and that *P. arctica* was the by far most abundant vascular plant in the studied site. A moss mix was chosen since the moss vegetation consisted of an even mix of many different species. An overview of the antibodies used for polysaccharide detection is given in table 2 and table S4.

Section 2: **Enzyme Assays**

Polysaccharide degradation enzyme assays were carried out using the GlycoSpot™ technology (Copenhagen/Denmark). The ground peat samples were tested on eight different blue stained Chromogenic Polymer Hydrogel (CPH) substrates distributed in eight 96 well plates according to the kits instructions (3). The tested substrates were xylan (beechwood), arabinoxylan (wheat), 2HE-cellulose (synthetic), arabinan (sugar beet), pectic galactan (lupin), galactomannan (carob), xyloglucan (tamarind) and rhamnogalacturonan (soy bean). Each sample was diluted in a ratio of 0.2 g soil/ml reaction buffer (100 mM sodium phosphate buffer, pH 6.0). During pipetting the sample solutions were stirred in a glass beaker on a magnetic plate to gain best possible homogenization and equal distribution of the samples in the reaction buffer. Finally, 150 µL of each sample solution (in triplicates) was added to a well in a 96 well plate. The plates were sealed and shaken at 10 °C for 44.5 h to achieve a sufficient signal strength from the enzymes. After incubation, the plates were centrifuged for 10 min at 2700 x g and the absorbance of the supernatants was measured at 595 nm (blue CPH substrate) using a plate reader (SpectraMax M5, Molecular Devices, Sunnyvale, USA).

Section 3: **Nucleic acids extraction and rRNA depletion**

Nucleic acids were extracted from eight samples. Referring to table S5, we used four replicates from the fenced exclosures and four replicates from the grazed sites. Prior to extraction, 5

grams of soil from each replicate was ground in liquid nitrogen. From each of these ground samples, three nucleic acid extractions were performed as described previously (4,5). The three extracts were pooled prior to further processing.

To purify DNA from the total nucleic acids, the samples were treated with RNase A/T1 (Thermo Fisher Scientific, Waltham, MA/USA) for 30 min at 37°C to digest the RNA. The remaining DNA was recovered with a phenol:chloroform:isoamylalcohol and chloroform:isoamylalcohol extraction to remove the RNase enzyme. For the purification of RNA, DNA was digested using the Promega DNAase kit (Promega, Madison, WI/USA) and the remaining RNA purified with the Megaclear™ Kit (Thermo Fisher Scientific, Waltham, MA/USA) according to the manufacturers' protocol. The absence of DNA in the RNA preparations was verified by PCR assays targeting bacterial SSU rRNA genes. The total RNA samples were processed with the Ribo-Zero Magnetic Kit for Bacteria from Illumina (San Diego, CA/USA) to remove 16 and 23S rRNA molecules and enrich the mRNA fraction of the metatranscriptome. Nucleic acids were quantified (ng/µL) using a NanoDrop spectrophotometer (Thermo Fisher Scientific, Madison, WI/USA). The quality of DNA extracts were evaluated on a 1 % agarose gel. The quality of the RNA extracts were evaluated by automated gel electrophoresis using a standard sensitivity chip (Experion™, BioRad, Hercules, CA/USA).

In order to quantify the microbial DNA and RNA in the total DNA and RNA, we substracted the fraction of DNA and RNA corresponding to the proportion of plant sequences (as judged from the abundance of the 18s rRNA genes or plant mRNA transcripts) from the total DNA or RNA per gram of dry soil.

References

1. Moller I, Marcus SE, Haeger A, Verhertbruggen Y, Verhoef R, Schols H, et al. High-throughput screening of monoclonal antibodies against plant cell wall glycans by hierarchical clustering of their carbohydrate microarray binding profiles. Glycoconj J. 2008;25:37–48.

2. Moller I, Sørensen I, Bernal AJ, Blaukopf C, Lee K, Øbro J, et al. High-throughput mapping of cell-wall polymers within and between plants using novel microarrays. Plant J. 2007;50:1118–28.

3. Kračun SK, Schückel J, Westereng B, Thygesen LG, Monrad RN, Eijsink VGH, et al. A new generation of versatile chromogenic substrates for high-throughput analysis of biomass-degrading enzymes. Biotechnol Biofuels. 2015;8:70.

4. Tveit AT, Schwacke R, Svenning MM, Urich T. Organic carbon transformations in high-Arctic peat soils: key functions and microorganisms. ISME J. 2013 Feb;7:299–311.

5. Urich T, Lanzén A, Qi J, Huson DH, Schleper C, Schuster SC. Simultaneous Assessment of Soil Microbial Community Structure and Function through Analysis of the Meta-Transcriptome. PLoS One. 2008;3(6):e2527.

Paper 2

Tundra vegetation changes, in absence of herbivory, are coupled with an altered soil microbial food web and a faster microbial loop

Kathrin M. Bender[1], Victoria Martin[2], Yngvild Bjørdal[1], Andreas Richter[2], Maarten Loonen[3], Mette M. Svenning[1], Andrea Söllinger[1], Alexander T. Tveit[1]

[1]Department of Arctic and Marine Biology, UiT, The Arctic University of Norway, Tromsø, Norway.

[2]Department of Microbiology and Ecosystem Science, Division of Terrestrial Ecosystems research, University of Vienna, Austria.

[3]Arctic Centre, University of Groningen, Groningen, The Netherlands.

Abstract

Increases in geese populations and changes in their migratory routes have large consequences for Arctic tundra soil ecosystems, influencing the vegetation composition and thereby affecting the soil organic matter (SOM) input from plants. We have investigated the influence of herbivory by barnacle geese on vegetation, SOM quality, microbial activities, and microbial food web composition in a high-Arctic wet tundra. Tundra vegetation was exposed to three treatments: (1) Herbivory (natural state), (2) 4-year exclusion of herbivores, (3) 14-year exclusion of herbivores. These treatments resulted in (1) bryophyte-dominated vegetation, (2) a mix of higher vascular plants and bryophytes, (3) and vascular-plant-dominated vegetation. After 4 and 14 years of herbivore exclusion, we observed increased root biomass, decreased soil pH and moisture, and increased dissolved and total phosphorus (P) contents. While dissolved and total soil carbon (C), SOM composition had shifted towards a higher content of N containing compounds and lignin derivates in the 14-year-old exclosures. Microbial growth and cumulative soil respiration rates were also higher in the exclosures while the total microbial biomass remained constant, indicating faster turnover of microbial biomass and higher SOM decomposition rates. Based on 55 total RNA libraries, the overall relative abundances of prokaryotes, eukaryotes and viruses were similar in the three treatments. However, herbivore exclusion resulted in higher relative abundances of saprotrophic and mycorrhizal fungi and a shift and overall reduction in the relative abundances of multiple bacterial and eukaryotic micro-predators, reflecting a re-structured food web. We conclude that more than a decade after the changes in aboveground herbivory,

the ecosystem has altered into a different state, characterized by changes in vegetation and SOM composition. This has led to the establishment of an altered soil microbial food web and an overall faster microbial biomass turnover rate. Our results demonstrate the major effect that altered above-ground ecosystem dynamics have on the below-ground microbial interactions that control C cycling in Arctic tundra ecosystems.

Keywords

Barnacle geese, herbivory, exclosure, microbial biomass, predation, metatranscriptomics

Introduction

The Arctic is warming four times faster than the rest of the planet, an effect known as Arctic amplification (Rantanen et al. 2022). A major consequence of Arctic amplification is Arctic greening, driven by higher temperatures, primarily in areas with high moisture (Berner et al. 2020) and resulting in increased biomass of vascular plants (grasses, shrubs) over cryptogams (mosses, lichens) (Bao et al. 2022). Climate change also affects animal populations, including the common Arctic herbivores, reindeers (Rosqvist et al. 2022) and migratory geese (Layton-Matthews et al. 2020). The increasing population sizes of Arctic-breeding geese, such as the Barnacle goose (*Branta leucopsis*) and the Pink-footed goose (*Anser brachyrhynchus*) have intensified the grazing pressure in both European and Canadian Arctic wetlands, which serve as their feeding and resting habitats during breeding and moulting (Fox et al. 2005; Kuijper et al. 2006; Kuijper et al. 2009). Similarly, intensified grazing pressure has been reported from geese wintering grounds and migration routes, for example in northern Germany, as well as in Greenland, Scotland, Ireland and the Baltic regions, Russia, the Norwegian coastline, and other Scandinavian countries (Lameris et al. 2013; Bjerke et al. 2021; Heldbjerg et al. 2021; Düttmann et al. 2023; Madsen et al. 2023).

Herbivory has a substantial impact on the composition of plant communities (Zacheis et al. 2001; Maron and Crone 2006) and can lead to higher productivity by maintaining the dominant plant species, which are often characterized by high growth rates that allow withstanding the recurrent disturbance pressure, while less productive species are excluded (Bardgett et al. 1998; Bardgett and Wardle 2003). Nevertheless, herbivory was also shown to reduce productivity and decrease plant and root biomass (Jefferies et al. 2006; Sjögersten et

al. 2011). Yet, which mechanism prevails presumably depends on the type of vegetation, type of herbivores and location.

Vascular plants have been shown to be less resistant to decomposition than mosses (Bartsch and Moore 1985; Szumigalski and Bayley 1996), and among vascular plants the quality and quantity of root exudates differ (Bardgett et al. 2008; De Deyn et al. 2008). Thus, vegetation composition can influence SOM composition, its decomposability by soil microorganisms and thereby microbial-derived CO_2 production (Davidson and Janssens 2006). Yet, the C balance of the system is also impacted by plant biomass formation, plant and root respiration rates, and microbial CO_2 fixation. Together with the substantial effects of plant litter quality and quantity on microbial communities, differences in the composition and identity of prevailing vegetation are thought to drive the ecosystem's CO_2 sink strength (Bardgett et al. 2008; Kuiper et al. 2014; Antala et al. 2022). Therefore, systems dominated by vascular plants sometimes show higher respiration rates and lower CO_2 sink strength (Ward et al. 2013) and sometimes increased CO_2 sink strength (Sjögersten et al. 2011), relative to bryophyte dominated systems.

Substrate availability and quality are considered main drivers for microbial population size and activities, and thus act as bottom-up controls on microbial decomposition and the CO_2 flux (Lützow et al. 2006; Schmidt et al. 2011). However, from theoretical ecology and population ecology we know that populations across scales are also controlled by top-down mechanisms such as predation, viral infections or other trophic interactions that constitute food webs (Suttle 2007; Hatton et al. 2019). The establishment of soil microbial food webs often corresponds to the establishment of more complex microbial communities and interactions (Geisen et al. 2018; Thakur and Geisen 2019). So far, most of the attention was directed towards protists and other eukaryotic micro-predators, such as nematodes, micro-arthropods and saprophagous soil animals as keystone taxa in microbial food webs (Trap et al. 2016; Geisen et al. 2018; Thakur and Geisen 2019; Erktan et al. 2020). Additionally, the awareness of predatory bacteria (Petters et al. 2021; Dahl et al. 2023) and viruses (Ji et al. 2023) and their key roles in soil food webs have increased recently.

Changes in predation intensity have been linked to shifts in bacterial and fungal composition (Trap et al. 2016; Thakur and Geisen 2019; Erktan et al. 2020; Lucas et al. 2020). However, the connection between predation and microbial biomass has not been resolved. Observations have been made of a negative effect (Trap et al. 2016), no effect (Erktan et al. 2020), or even

a positive effect of predation on microbial biomass (Trap et al. 2016; Lucas et al. 2020). This suggests that although increased predation leads to higher microbial death rates, it can positively reinforce growth rates. Furthermore, it is known that soil trophic interactions can have a positive effect on plant communities via mobilization of soil nutrients (Trap et al. 2016; Geisen et al. 2018; Thakur and Geisen 2019).

Literature indicates the existence of strong links between herbivory, vegetation, SOM composition, the microbial food web, and greenhouse gas fluxes. An understanding of these connections is needed to identify the consequences of Arctic greening and altered animal populations and migratory routes. A recent study showed that the long-term (18 years) absence of herbivores in an Arctic wetland (Svalbard) led to altered plant polymer composition in the soils, higher activity of microbial extracellular enzymes for plant polymer decomposition and higher soil concentrations of monosaccharides and amino acids (Bender et al. 2021). Additionally, changes in the greenhouse gas fluxes and the microbial community structure have been observed as a result of herbivory exclusion (Foley et al. 2022). However, we are missing detailed insights into how microbial food webs change in response to herbivory, and how this links to changes in vegetation, soil chemistry and microbial activity over time.

The so far introduced aspects, collectively demonstrate the multifaceted influence of intensified herbivory and vegetation changes on soil C cycling and greenhouse gas emissions. An example of how vegetation change affects C cycling comes from western Svalbard, where increased herbivory by Barnacle geese in wet tundra led to a suppression of vascular plant growth and a dominance of mosses within the family *Amblystegiaceae* (brown mosses) (Kuijper et al. 2006), leading to a transition of these ecosystems from C sinks into C sources (Sjögersten et al. 2011). Here, we have studied three treatments of these high-Arctic wet tundra systems: Exposure to Herbivory (Hr), exclusion from herbivores for 4 years (Ex-4) and exclusion from herbivores for 14 years (Ex-14). We combined traditional ecology and state-of-the-art microbial ecology methods including vegetation mapping, physicochemical soil analyses, microbial growth estimation using ^{18}O-H_2O incorporation into DNA, targeted and non-targeted metabolomics, and metatranscriptomics.

Materials and Methods

(a) Study site and sampling design

The fieldwork was carried out in Thiisbukta, Ny-Ålesund, Svalbard (78.93°N, 11.92°E) in August 2020 (Figure 1A and B). Thiisbukta is a small bay dominated by an Arctic fen, also known as wet tundra (Olefeldt et al. 2021). Experimental field exclosures have been maintained in Thiisbukta since 2006, hence 14 years prior to sampling (Ex-14), and since 2016, hence 4 years prior to sampling (Ex-4). Herbivory by Barnacle geese and Svalbard reindeer (*Rangifer tarandus platyrhynchus*) has been prevented by 0.5-m tall fences and metal wires crossing on top of the exclosures (Figure 1C). The Ex-14 plots and the adjacent Herbivory control plots (Hr) covered an area of 2 × 2 m respectively, while Ex-4 plots were 1 × 1 m. The fences for the Ex-4 plots were set up within the 2 × 2 m Hr plot, 10 years after the initiation of the experiment, reducing the size of the Hr plots by the area of Ex-4 (Figure 1C and D). A total of five sampling sectors (i.e., biological replicates), each including all three treatments were used for this study (Figure 1A).

All five sectors were established on shallow peat (< 50 cm depth) dominated by moss vegetation. After 4 years of herbivore exclusion (Ex-4), higher abundances of vascular plants were observed, while after 14 years (Ex-14) vascular plants had become the dominating part of the vegetation (Figure 1F). From each Ex-14 and Ex-4 plot, four replicate soil samples were collected, while from each Hr plot, three soil samples were collected (Figure 1D), resulting in a total of 55 samples. The samples were taken from 1–3 cm depth, below the vegetation (Figure 1E), by cutting blocks of peat with a sharp knife. The knife was cleaned with alcohol and water between each sampling. For minimizing the processing time of samples and concurrent disturbing effects of soil manipulation prior to freezing the samples for microbiological assays, we decided against the homogenization of soil and the removal of root biomass. To account for the lack of homogenization of larger soil samples, within-sector replication was carried out. After removal of the vegetation cover, by cutting it off with the knife, the peat blocks were split into three sets of samples: (a) fresh (processed on the day of sampling), (b) cooled (stored at 4 °C until further processing), (c) flash frozen in liquid N (stored at -80 °C until further processing). Fresh samples (a) were used for measuring soil water contents, pH, and for the determination of microbial growth (^{18}O-H_2O incubations). Cooled

151 samples (b) were used for measuring microbial biomass and total CO_2 emission (cumulative
152 respiration). Flash frozen samples (c) were used for nucleic acid extraction and sequencing of
153 total RNA, and for measurements of soil C, N, and P.

154 **(b) Vegetation and roots**

155 The point-intercept method was used for the identification and description of the variation of
156 plant species coverage and height (Drezner and Drezner 2021). Root biomass [g m^{-3} peat] was
157 determined by cutting 10 × 10 × 10 cm blocks from the peat soil (one block per plot) and
158 manual separation and weighing.

159 **(c) Soil physicochemical parameters**

160 Soil oxygen content [µmol L^{-1}] and temperature [°C] were measured *in-situ* starting at 0 cm
161 (vegetation) down to 10 cm depth in 1 cm intervals, using an optical oxygen sensor (Otpo-
162 3000, Unisense, Aarhus, Denmark) and a temperature probe (Temp-UniAmp, Unisense,
163 Aarhus, Denmark). Oxygen and temperature were measured on three consecutive days, with
164 a mean air temperature fluctuating between 9–12 °C. The gravimetric water contents [%] of
165 the soils were measured by drying 1–2 g of the samples over night at 100 °C and reweighing
166 them. Soil pH was measured in the watery phase of a 10:1 v/w water:soil solution using a
167 portable field pH meter (Multi 350i, WTH, Weilheim, Germany).

168 **(d) Soil C, N, and P**

169 Total soil C (C_{tot}) and N (N_{tot}) [mg g^{-1} dry weight (DW) soil] were measured using an elemental
170 analyzer (EA 1110, CE Instruments, Centro Ricerche Trisaia, Matera, Italy) coupled to a
171 continuous-flow isotopic ratio mass spectrometer (IRMS, DeltaPlus, Finnigan MAT, Waltham,
172 MA, USA). Total soil P (P_{tot}) [µg g^{-1} DW soil] was photometrically determined in 0.5 M H_2SO_4
173 extracts using the malachite-green method (D'Angelo et al. 2001) after the conversion of all
174 organic P sources to inorganic P via the ignition method modified by Kuo (1996). Total
175 dissolved organic C (DOC) and total dissolved N (TDN) [mg g^{-1} DW soil] were quantified in 1 M
176 KCl extracts (soil:solution ratio of 1:15 (w/v)) via a TOC/TN- Analyzer (TOC-VCPH/CPNTNM-1
177 analyzer, Shimadzu, Korneuburg, Austria). Soil nitrate (NO_3^-), ammonium (NH_4^+) and total free
178 amino acids (TFAA) [µg N g^{-1} DW soil] were measured in 1 M KCl extracts using photometric
179 assays following Hood-Nowotny et al. 2010 and a modified version of the fluorometric OPAME
180 method (Prommer et al. 2014). We calculated dissolved organic N (DON) concentrations [mg

g^{-1} DW soil] by subtracting the sum of ammonium and nitrate concentrations from the respective TDN concentrations (for more details see Supplementary Materials and Methods).

(e) Fingerprinting of soil organic matter (SOM) chemical composition

For characterizing the chemical composition of SOM [mg C g^{-1} DW soil] using Pyrolysis-Gas Chromatography/Mass Spectromety (CDS Pyroprobe 6200, CDS Analytical coupled to Pegasus BT, LECO with a Supelcowax 10 polar column, Sigma- Aldrich, St. Louis, MO, USA), we applied a semi-automated high-throughput fingerprinting approach (for more details see Supplementary Materials and Methods).

(f) Soil microbial parameters and characteristics

(i) Soil microbial biomass C (C_{mic}) and N (N_{mic})

Soil microbial biomass C (C_{mic}) and N (N_{mic}) [mg g^{-1} DW soil] were obtained by the chloroform fumigation extraction method (Vance et al. 1987). Following 48 h of incubation in a chloroform saturated atmosphere, soils were extracted with 1 M KCl (soil:solution ratio of 1:15 (w/v)). C_{mic} and N_{mic} concentrations were calculated as the difference between DOC and TDN concentrations of fumigated soils and non-fumigated controls. All respective extracts were measured on a Shimadzu TOC-VCPH/CPNTNM-1 analyzer (for more details see section (d) and Supplementary Materials and Methods).

(ii) Microbial gross- & biomass specific growth

We measured gross- [mg C g^{-1} DW soil h^{-1}] and microbial biomass specific [mg C g^{-1} C_{mic} h^{-1}] growth rates of the peat soil microbial communities using a stable isotope method which is based on the substrate-independent incorporation of the stable oxygen isotope ^{18}O from ^{18}O-labelled water (^{18}O-H_2O) into newly formed microbial DNA (Sphon et al. 2016; Walker et al. 2018). We used a relatively short incubation time and incubated in the dark to avoid labelling via cross-feeding and phototrophic growth.

Subsamples of 200–300 mg fresh weight (FW) peat soil were amended with 90–150 µl of 98 at % (atom percent) ^{18}O-H_2O, achieving an overall enrichment of approximately 30 at % in each sample. A duplicate of each sample was amended with the same amount of molecular grade non-labeled water, serving as natural abundance control. All samples were incubated in gas-tight headspace vials for 38 h at 8.0 °C, which resembled the mean *in-situ* temperature

(8.6 °C) of the peat soils at 2 cm depth on the day of sampling. The incubation and activity of the microbial communities were terminated by shock-freezing samples in liquid N_2. DNA was extracted from the frozen samples using the DNA™ SPIN kit for Soil (MP Biomedicals, Santa Ana, CA, USA) following the manufacturer's instructions. DNA concentrations [ng g^{-1} DW soil] were quantified via qubit DNA assay (Qubit dsDNA HS Assay Kit; Thermo Fischer, Waltham, MA, USA). DNA extracts of labelled samples and natural abundance controls were analyzed for their ^{18}O abundance and total oxygen content using a thermochemical elemental analyzer (EA) coupled to a Delta V Advantage isotope ratio mass spectrometer (IRMS) via a Conflo III (Thermo Fisher, Waltham, MA, USA) (for more details see Supplementary Materials and Methods).

(iii) CO_2 emissions

Aliquots (5 g FW) of the 55 peat soil samples were incubated for 5 days at 8 °C (the mean *in-situ* temperature of the peat soils at 2 cm depth on the day of sampling) in 120 mL bottles. The CO_2 concentrations (ppm) in the headspace of the bottles were measured on day 1, 2, 3, and 5 of the incubation period using gas chromatography (GC) (SRI 8610C gas chromatograph, SRI Instrument, CA, USA with 8600-PKDC 3 cm 9'Haysep D Column 80/100 mesh, Samsi). Gas samples of 0.5 mL were manually injected into the GC with a gastight syringe (Pressure-Lok®, Precision Analytical Syringe, A-2 series, VICI Precision Sampling, Schenkon, Switzerland with Luer Needels A-2, VICI Precision Sampling). H_2 was used as carrier gas and the oven temperature was set to 40 °C. The CO_2 was detected with a flame-ionization detector (FID) detector, set to 380 °C, preceded by a hydrogenating reactor converting the CO_2 into CH_4. CO_2 concentrations were quantified with a standard curve based on gases with known CO_2 concentrations, using the ideal gas law. The obtained CO_2 concentrations were used to determine soil microbial respiration rates [µmol CO_2 g^{-1} DW soil day^{-1}] and to calculate the cumulative respiration (net CO_2 emission) of the respective peat soils.

(iv) Microbial nucleic acids

Total nucleic acids were isolated with a phenol-chloroform extraction using CTAB as buffer, as previously described (Urich et al. 2008; Tveit et al. 2013). Prior to the extraction, the soil samples were ground in liquid N_2. Each sample was extracted twice, using approximately 200 mg of peat soil per extraction. The two extracts per sample were pooled to increase the

yield of total nucleic acids. The extracted DNA and RNA was quantified via qubit DNA and RNA assays (Qubit dsDNA HS Assay Kit and Qubit RNA HS Assay Kit; Thermo Fischer, Waltham, USA). The Turbo™ DNase [2 U/µl] (Thermo Fisher, MA, USA) kit was used to digest DNA in the samples and purify total RNA. RNA quality was assessed prior to sequencing (mean RIN number: 4.6, std. deviation: 1.3).

(g) Bioinformatics

(i) Sequencing

Sequencing and library preparation were performed at IMGM Laboratories GmbH, Martinsried, Germany. The 55 total RNA samples were prepared for sequencing with the NEBNext® UltraTM II Directional RNA Library Prep Kit (New England Biolabs, Ipswich, MA/USA) with an input mass of 20–100 ng RNA. Overlapping, paired-end 2 × 250 bp reads were generated using the Illumina NovaSeq® 6000 next generation sequencing system (Illumina, San Diego, CA/USA). The 55 sequence libraries were pooled according to their sampling sector (1–5) and treatment (Hr, Ex-4, Ex-14) (Figure 1D), resulting in 15 samples with 12–74 million raw reads per sample (Supplementary Table S1).

(ii) Sequence processing

(1) Prokaryotes

Raw sequences were submitted to the phyloFlash v3.4 pipeline using default settings (Gruber-Vodicka et al. 2020). Briefly, SSU sequences were identified using the BBmap mapping algorithm against the phyloFlash modified SILVA v138 (NR99) database. All hits with a minimum identity of 70 % (default) were taxonomically annotated according to the Lowest Common Ancestor (LCA) method and using default parameters. All sequences assigned to bacteria and archaea were directly used for further analysis.

(2) Eukaryotes

Eukaryotic sequences identified with phyloFlash were extracted from the raw sequences, merged using PEAR v0.9.11 (Paired-End reAd mergeR, default settings) (Zhang et al. 2014), and filtered to a minimum length of 250 bp with prinseq-lite v0.20.4 (Schmieder and Edwards 2011). The remaining sequences were reclassified using CREST4 v4.2.6 (Lanzén et al. 2012) with a modified SILVA v138 (NR99) database file which also included a highly curated protist

database PR2 v4.14.1 and the blastn algorithm (default settings). Sequences with a minimum bit-score value of 155 and that score within 2 % of the best hit were assigned a taxonomy based on LCA. The reason for using CREST4 with an advanced protist database was to increase the annotation accuracy to allow for high resolution taxonomic annotation of 18S rRNA (Geisen et al. 2023).

(3) Viruses

For the viral part of the sequence analysis raw paired-end total RNA sequence files were merged with PEAR v0.9.11 (Zhang et al. 2014) and quality filtered (-min_qual_mean 30 -ns_max_n 5 -trim_tail_right 15 -trim_tail_left 15) using prinseq-lite v0.20.4 (Schmieder and Edwards 2011). SortMeRNA v4.3.4 (Kopylova et al. 2012) was used to obtain the non-rRNA reads from the total RNA reads. Taxonomic annotation of all non-rRNA reads was achieved by aligning sequences to the National Center for Biotechnology Information (NCBI) nr database (as of November 2022) (NCBI Resource Coordinators 2018) with a DIAMOND blastx v2.0.13 (Buchfink et al. 2021) search (parameters: -k 50 -e 0.01). The MEtaGenomeANalyzer (MEGAN) v6.24.5 (Huson et al. 2016) tool daa-meganizer was used to obtain one taxonomic annotation per read by applying the MEGAN LCA assignment algorithm (parameters: -ms 50 -me 0.01 -top 10 -mpi 0.0; mapping file: megan-map-Feb2022.db).

We used the web application https://www.ncbi.nlm.nih.gov/genome/viruses/ to screen for the hosts of all annotated viruses. The hosts are assigned to the viruses by a model that gathers virus host information and manually curates a ‘viral host’ property for each new RefSeq record that then is assigned to the respective species within the NCBI database (Brister et al. 2015) (Supplementary Table S2).

(iv) Taxonomic analysis

All eukaryotic annotations and all annotations including *Chloroplast* within *Cyanobacteria* were removed from the phyloFlash annotations. In a similar manner, all annotations of prokaryotes, *Chloroplastida* and *Mitochondria* were removed from the data frame carrying annotations from CREST4. Furthermore, small subunit rRNA reads annotated to plants ranged between 0.4–4.8 % of the total reads and were removed from the data prior to further. The two resulting data frames, representing the prokaryotic and eukaryotic annotations, respectively, were merged and collapsed at family level, and the individual taxonomic

annotations from domain to family level were merged into one taxon string including all taxonomic information between those levels. Next, we rarefied the combined data frame to 2 million reads per sample with the R function *rarefy* (settings: depth = 2000000, seed = 123456) implemented in the package rbiom v1.0.3 (cmmr.github.io/rbiom/index.html). A final filtering step was applied to the data, keeping all taxonomic annotations that were present in at least three of five samples in at least one of the three treatments (Hr, Ex-4, Ex-14).

Predatory taxa

Members of the prokaryotic phyla *Myxococcota* (Petters et al. 2021) and *Bdellovibrionota* (Li et al. 2021) were considered as predatory. Potential predators among eukaryotes included the groups *Ciliophora*, with the exception of the genus *Mesodinium* (Lynn 2016), *Lobosa* within *Amoebozoa* (Dahl et al. 2023), *Apusozoa* (Cavalier-Smith 1995), *Choanoflagellida* (Dayel and King 2014), *Euglenida,* with the exception of the class *Euglenophyceae* (Leander et al. 2017)*,* and *Bodonidae* within *Discoba* (Mitchell et al. 1988), the orders *Araeolaimida, Chromadorida, Desmodorida, Enoplida, Monhysterida, Rhabditida*, and *Triplonchida* within *Nematoda* (Dahl et al. 2023), and *Cercozoa* and *Foraminifera* within *Rhizaria* (Dahl et al. 2023).

Mycorrhizal fungi

We checked for mycorrhiza among fungal families on the FungalRoot database (Soudzilovskaia et al. 2020), by screening the titles and keywords of the publications for each fungal family for the word mycorrhiza (Supplementary Table S3).

Responding prokaryotic and eukaryotic families

Reads not classified on family level were separated from those classified on family level. When further analyzing the classified families, we transformed the data frame to relative abundance in percent [%], normalizing to the sum of counts of all classified families, not including unclassified families. A Venn diagram was used to identify common families and treatment specific ones. Of the 1333 families identified, 1226 families were present in all three treatments. The Venn diagram was created with the function *vennCounts* (default settings) implemented in the R package limma v3.52.4 (bioinf.wehi.edu.au/limma) (Supplementary Figure S1). We continued working with those 1226 families, excluding the treatment specific families as they were very low abundant, below 0.3 % of all families, and as the inability to detect these families in all treatments might have been due to varying sequencing depths.

Information about the treatment-specific families can be found in Supplementary Table S4. We applied an linear mixed effects (LME) model on the dataset containing the 1226 families that were present in all treatments to determine which of these families had changed in relative abundance between treatments; see section (h) Statistics and figures for details. The families responding significantly to one or more of the treatments were used further in our analysis of community and food web changes.

(h) Statistics and figures

Linear mixed-effects (LME) models

We used LME models to investigate the effects of herbivory exclosure on obtained environmental and sequence data. The model was chosen to account for differences between the five sampling sectors, by setting the sampling sector as random effect and treatment as the fixed effect. We used the function *lmer* within the R package lme4 v1.1-30 (github.com/lme4/lme4/) to run the model (formula: variable ~ treatment + (1|sector)), the subsequent pairwise comparison of the LME was performed using the function *emmeans* implemented in the R package emmeans v1.8.1-1 (github.com/rvlenth/emmeans).

Sampling sector normalization

To ensure better comparability between the five sampling sectors in our analysis of environmental and sequencing data, we used a sector normalization approach for nonmetric multidimensional scaling (NMDS) and heatmap analyses. Specifically, we calculated the sum of all measurements for a given variable within a sampling sector (i.e., sum of three treatments: Hr, Ex-4, Ex-14), and then divided each individual measurement in that sector by the sum. This normalization approach was necessary because although the five sampling sectors often showed the same trend of change in response to the treatments, the absolute values of the measurements varied between sectors.

NMDS and PERMANOVA

We used nonmetric multidimensional scaling (NMDS) ordination plots to depict (dis)similarities between biological and physiochemical properties (environmental attributes) of the samples and between the microbial community structure on family level (Supplementary Figure S2). The environmental and sequencing data were sector normalized

(as described above). The *metaMDS* (settings: distance = "euclidean", k = 2, trymax = 999) and *envfit* (setting: permutations = 999) functions were used for the ordination and vector plotting. The function *adonis2* (distance matrix ~ Treatment, permutations = 999) was used to perform permutational analysis of variance (PERMANOVA) to identify the effect of treatment on the distribution of the samples. The distance matrix was calculated with the *vegdist* function (method = "euclidean"). All functions were implemented in the R package vegan v2.6-4 (github.com/vegandevs/vegan).

Alpha and beta diversity

The alpha diversity of the prokaryotic and eukaryotic microbial rRNA based community on family level was determined by the Observed Richness, Pielou's Evenness, and the Shannon Index. We used the R package vegan to calculate the Shannon Index using the function *diversity* (default settings), and the Observed Richness with the function *specnumber* (default settings). Pielou's Evenness was calculated as follows: Shannon Index/log(Observed Richness). We calculated the beta diversity with the function *vegdist* (method = "euclidean") and by testing for homogenous dispersal of the groups via the *betadisper* function (group = "Treatment") within the package vegan. The packages ggplot2 v3.4.0 (github.com/tidyverse/ggplot2) and RColorBrewer v1.1-3 (colorbrewer2.org/) were used to plot the alpha and beta diversity as boxplots (Supplementary Figures S3 and S4).

Figures

Map: The map of Svalbard in Figure 1B was created using the packages cowplot v1.1.1 (wilkelab.org/cowplot/), googleway v2.7.7 (github.com/SymbolixAU/googleway/), ggplot2, ggrepel v0.9.2 (github.com/slowkow/ggrepel), ggspatial v1.1.8 (github.com/paleolimbot/ggspatial), sf v1.0-8 (github.com/r-spatial/sf/), rnaturalearth v0.3.2 (github.com/ropensci/rnaturalearth) and rnaturalearthdata v0.1.0 (github.com/ropenscilabs/rnaturalearthdata). The three tutorials "Drawing beautiful maps programmatically with R, sf and ggplot2" published on the 25th of October 2018 on the webpage r-spatial.org were used to write the R-code to create the map.

Box-plots: The box-plots of Figure 2 were created with ggplot2.

Fold-change: The fold-change displayed in Figure 3B was calculated by dividing the measurements of Ex-4 and Ex-14 by Hr and transforming the values on a log2 scale. For the

plotting of the fold-change the packages ggplot2, reshape2 v1.4.4 (github.com/hadley/reshape), RColorBrewer and gridExtra v2.3 (cran.r-project.org/web/packages/gridExtra/index.html) were used.

Donut chart: The donut charts of the prokaryotic and eukaryotic communities on kingdom and phylum level (Figure 4) were plotted with the jupyter-notebook v6.0.3 (Kluyver et al. 2016) using the packages pandas v1.2.0 (McKinney 2010), NumPy v1.18.1 (Harris et al. 2020) and Matplotlib v3.1.3 (Hunter 2007). We used a modified version of the online tutorial "How to Make a Beautiful Donut Chart and Nested Donut Chart in Matplotlib" (Han 2022) to create the plots.

Heatmaps and color coding: Microbial families that changed significantly in relative abundance, were identified using an LME model. We sector normalized those families (as described above). From this data frame we created heatmaps of the significantly responding families (Figure 5 and 6) with the *heatmap* function provided by R. The color-coded indicators next to the heatmaps were created with the ggplot2 and the RColorBrewer packages.

All plots and figures were plotted in R v4.2.2 or with the jupyter-notebook v6.0.3 and adjusted graphically prior to publication, using Adobe Illustrator v26.0.1.

Results

Herbivory, vegetation, soil physiochemical and biological properties

Over time, the exclusion of herbivores had gradually led to a shift in the composition of functional groups in the tundra vegetation. In the herbivory control plots (Hr) mosses constituted over 98 % of the coverage, and 3 % were composed of vascular plants. After 4 years of herbivore exclusion (Ex-4), moss coverage had decreased to 82 % and vascular plant had increased up to 72 %, with *Poa* grasses being the main contributor to this vegetation change. After 14 years of herbivore exclusion (Ex-14), vascular plants had become dominant with a coverage of 92 %, due to the increase of *Equisetum variegatum* and *Poa* grasses, while the moss coverage had decreased to 73 % (Figure 1E and F and Supplementary Table S5). Along with the increase in vascular plant coverage in the exclosures, we observed significantly higher root biomass in Ex-14 compared to Hr (Hr: 216 g m^{-3}; Ex-4: 1,234 g m^{-3}; Ex-14: 5,225 g m^{-3}) (Supplementary Figure S5 and Table S6). The studied wet tundra soils were characterized

as Histosols and the state of the organic matter of the samples was hemic, but we observed trends towards more fibric peat in Ex-14 plots, and more sapric peat in Hr plots (Figure 1E). The vegetation change corresponded with changes in the SOM composition, with higher content of lignin derivates and N-containing compounds in Ex-14 (Figure 2 and Supplementary Table S7). In line with this, we observed a clear separation of Ex-14 from Ex-4 and Hr in an NMDS plot that was based on 22 obtained soil and microbial parameters (Figure 3A). Vector analysis revealed several variables that were significantly involved in this separation between treatments (Figure 3A). O_2 levels and *in-situ* temperatures (relating to the considered sample depth) did not differ between the treatments, with a mean dissolved oxygen concentration of 233 µmol L^{-1} and a mean temperature of 8.6 °C (Figure 3B). Peat soil pH and gravimetric water contents [%] were significantly lower in Ex-14 compared to Hr and Ex-4 (Hr: pH 7.3, 86.1 H_2O [%]; Ex-4: pH 7.2, 83.4 H_2O [%]; Ex-14: pH 6.3, 72.6 H_2O [%]) (Figure 3B). Concerning the determined C, N, and P compounds, only inorganic P (P_i) content differed significantly, with higher average concentrations measured in Ex-14 than in the other treatments (Hr: 30.7 µg P_i g^{-1} DW; Ex-4: 30.9 µg P_i g^{-1} DW; Ex-14: 47.8 µg P_i g^{-1} DW) (Figure 3B). However, we also observed a trend (p-value: <0.1) of higher total N and total P concentrations in Ex-14 (Supplementary Table S8). Mean DNA and RNA concentrations were significantly lower in Hr than in Ex-14 (Hr: 96.7 µg DNA and 74.0 µg RNA g^{-1} DW soil; Ex-4: 81.4 µg DNA and 62.5 µg RNA g^{-1} DW soil; Ex-14: 58.4 µg DNA and 38.3 µg RNA g^{-1} DW soil) (Figure 3B). Microbial biomass C (C_{mic}) and N (N_{mic}) remained unchanged between the three treatments, with mean concentrations of 26.4 mg C_{mic} g^{-1} DW soil and 3.0 mg N_{mic} g^{-1} DW soil (Figure 3B). C_{mic} to DNA ratios were highest in Ex-14, followed by Ex- 4 and Hr (mean C_{mic} to DNA ratios in Hr: 0.28; Ex-4: 0.31; Ex-14: 0.51). By trend (p-value: <0.1), growth rates per unit of microbial biomass (biomass specific growth) were on average higher after 14 years of herbivory exclusion (Ex-14: 2.7 mg C g^{-1} C_{mic} h^{-1}; Ex-4 and Hr: 1.4 mg C g^{-1} C_{mic} h^{-1}) (Figure 3B). Correspondingly, the mean DNA turnover time of the microbial community was significantly shorter in Ex-14 (23.6 days) compared to Hr (42.6 days), suggesting a faster microbial loop and thus faster death rates (Figure 3B). In contrast, no differences were observed on gross microbial growth [mg C g^{-1} DW soil h^{-1}]. Net CO_2 emission rates (cumulative respiration including microbial respiration and potential root respiration) were significantly higher in Ex-14 compared to Ex-4 and Hr (Hr: 9.5 µmol CO_2 g^{-1} DW soil d^{-1}; Ex-4: 11.0 µmol CO_2 g^{-1} DW soil d^{-1}; Ex-14: 13.6 µmol CO_2 g^{-1} DW soil day(d)$^{-1}$) (Figure 3B).

Prokaryotic and eukaryotic microbial communities

We compared the structures of prokaryotic and eukaryotic communities among the three treatments at kingdom and phylum level, to identify changes in response to the exclusion of herbivores (Figure 4). The relative abundance of total prokaryotes and eukaryotes did not change between the three treatments (Supplementary Figure S9). However, seven of the eleven prokaryotic phyla detected had significantly different relative abundances in Hr compared to Ex-14, while they were not differently abundant in Hr and Ex-4 plots (Figure 4A and B). The two most abundant prokaryotic phyla with significant increases in relative abundance from Hr to Ex-14 were *Actinobacteriota* (Hr:11.3 %; Ex-4: 11.2 %; Ex-14: 17.8 %) and *Proteobacteria* (Hr: 16.3 %; Ex-4: 18.1 %; Ex-14: 20.5 %). The two most abundant phyla that showed significantly lower relative abundance in Ex-14 than in Hr were *Planctomycetota* (Hr: 8.4 %; Ex-4: 7.7 %; Ex-14: 5.9 %) and *Verrucomicrobiota* (Hr: 7.6 %; Ex-4: 7.0 %; Ex-14: 6.3 %). Both bacterial phyla that contained potential predatory taxa decreased in relative abundance in the exclosures, *Bdellovibrionota* significantly (Hr: 1.4 %; Ex-4: 1.2 %; Ex-14: 0.6 %) and *Myxococcota* (Hr: 15.5 %; Ex-4: 15.3 %; Ex-14: 11.4 %) by trend (Figure 4A and B).

Of the eight most abundant eukaryotic kingdoms, four increased in relative abundance and four decreased in relative abundance comparing Hr to Ex-14 (Figure 4C and D). The most abundant kingdom, *Metazoa,* experienced an increase from Hr to Ex-14 (Hr: 4.88 %; Ex-4: 5.99 %; Ex-14: 6.14 %). Responsible for this increase was the phylum *Arthropoda* (including potential predators), being significantly more abundant in Ex-14 than in Hr, and more abundant in Ex-4, but not significantly (Hr: 1.19 %; Ex-4: 2.11 %; Ex-14: 3.45 %). All other phyla belonging to *Metazoa* decreased in relative abundance in Ex-14 compared to Hr. The second most abundant kingdom, *Alveolata*, decreased significantly from in Hr to Ex-14 (Hr: 4.77 %; Ex-4: 4.58 %; Ex-14: 2.35 %). Over 98 % of all classified *Alveolata* reads belonged to the phylum *Ciliophora,* which includes potential predators, and the relative abundance of this phylum decreased significantly from Hr to Ex-14 (Hr: 4.70 %; Ex-4: 4.50 %; Ex-14: 2.29 %). Overall, the relative abundances of eukaryotic phyla that contain potentially predatory members were similar in all three treatments (Hr: 15.14 %; Ex-4: 16.39 %; Ex-14: 14.75 %). The *Fungi* kingdom was the third most abundant kingdom overall and increased significantly from Hr to Ex-14 (Hr: 2.98 %; Ex-4: 2.99 %; Ex-14: 4.93 %) (Figure 4). The increase of *Fungi* in Ex-14 was mainly due to an increase in the relative abundance of the phylum *Ascomycota*, which increased

significantly from Hr to Ex-14 (Hr: 0.33 %; Ex-4: 0.76 %; Ex-14: 1.64 %). *Chytridiomycota,* although not abundant, was the only fungal phylum that decreased significantly in the exclosures (Hr: 0.05 %; Ex-4: 0.06 %; Ex-14: 0.03 %) (Figure 4C and D). Of the 95 classified fungi families, four were considered as mycorrhizal, accounting for 1.88 % in Hr, 5.14 % in Ex-4, and 34.21 % in Ex-14, of the total fungal community (Supplementary Table S3). The two families *Glomeraceae* and *Ceratobasidiaceae*, of which the latter increased significantly in Ex-14 relative to Hr, contributed most to the much higher relative abundance of mycorrhizal fungi in Ex-14 than Hr (Supplementary Table S3).

Changes in prokaryotic and eukaryotic families correlating with the exclusion of herbivores

Of the total 2 603 prokaryotic and eukaryotic taxon strings identified, 1 333 had an annotation on family level, and were used in our subsequent analyses. We observed that richness (number of classified families) decreased from Hr and Ex-4 to Ex-14, albeit not significantly (mean values: Hr: 1 122; Ex-4: 1 130; Ex-14: 1 044) (Supplementary Figure S3). The within-sample distribution (Pielou's Evenness) was similar between treatments (mean values: Hr: 0.62; Ex-4: 0.63; Ex-14: 0.64) (Supplementary Figure S3). Beta diversity was highest in Ex-14, albeit not significantly different to Ex-4 and Hr (mean values: Hr: 56 938; Ex-4: 53 307; Ex-14: 80 708) (Supplementary Figure S4).

We illustrated the overall distribution of the classified families via a Venn diagram (Supplementary Figure S1) and found the majority, namely 1 226 families, present in all three treatments. The remaining 107 families had very low relative abundances (in total making up less than 0.03 % of all reads classified at family level) (Supplementary Table S4). Because we could not distinguish whether the treatment-specific families were truly treatment-specific or could not be detected in the other treatments due to their low relative abundance, we focused our detailed analyses on the shared families. Of those 1 226 families (of which 760 were prokaryotes and 466 were eukaryotes), 335 (27.3 %) (of which 216 were prokaryotes and 119 were eukaryotes) were found to significantly change in relative abundance and are referred to as responding families. Even though only 27.3 % were responding families, these families accounted for 58.9 % of all reads classified at family level.

We found that of all responding prokaryotic families, 63.0 % decreased in relative abundance in Ex-14, these families belonging to five different phyla. Among these were prokaryotic phyla

that contain predatory taxa. *Bdellovibrionota* included four families that significantly decreased in relative abundance in Ex-4 and Ex-14 (mean sum of families: Hr: 1.55 %; Ex-4: 1.32 %; Ex-14: 0.51 %), while *Myxococcota* included seven families that significantly decreased in relative abundance in Ex-4 and Ex-14 (mean sum of families: Hr: 6.80 %; Ex-4: 6.15 %; Ex-14: 3.90 %). Neither of these two phyla included significantly increasing families (Figure 5).

A similar trend was observed among the responding eukaryotic families, where 69.7 % decreased in relative abundance in Ex-14, the decreasing families belonging to nine eukaryotic kingdoms (Figure 6). We identified predatory eukaryotic taxa both among the families that increased and decreased in relative abundance between the herbivory sites and the exclosures (Figure 6). Within the phylum *Ciliophora*, there were five families increasing in Ex-4 and Ex-14 (mean sum of families: Hr: 0.03 %; Ex-4: 0.06 %; Ex-14: 0.13 %) and 32 families decreasing in relative abundance (mean sum of families: Hr: 1.48 %; Ex-4: 1.10 %; Ex-14: 0.32 %). The phylum *Lobosa* had one increasing family and three decreasing families, but these were all very low abundant < 0.05 %. Among the phylum *Choanoflagellida* were four increasing families and five decreasing families, all below an abundance of < 0.05 %. Within the phylum *Cercozoa* was one low abundant (< 0.05 %) increasing family and eleven decreasing families (mean sum of families: Hr: 0.12 %; Ex-4: 0.10 %; Ex-14: 0.02 %). The kingdom *Discoba* had one increasing family within the phylum *Euglenida* and one decreasing family belonging to the group *Kinetoplastida*, both below an abundance of 0.05%. Within the kingdom *Apuszoa*, two low abundant (< 0.05 %) predatory families significantly decreased in Ex-14. Overall, there was a trend of decrease in the relative abundance of potential predatory eukaryotes in the exclosures (Hr: 1.71 %; Ex-4: 1.35 %; Ex-14: 0.55 %).

Despite the rather low relative abundances of significantly changing eukaryotic families, it should be noted that even the most abundant eukaryotic families had a low relative abundance. However, this does not imply that these taxa are relatively less important than the more abundant prokaryotic taxa, as the relationships between cellular RNA content, cell size, biomass, motility, and activity, as well as sequence database coverage can differ substantially both within and between domains (Feijó Delgado et al. 2013; Hausmann et al. 2016). The two most abundant families in Hr were *Sessilida* (Hr: 0.80 %; Ex-4: 0.41 %; Ex-14: 0.13 %) and *Dileptidae* (Hr: 0.15 %; Ex-4: 0.14 %; Ex-14: 0.03 %), both belonging to the phylum *Ciliophora.* The two most abundant families in Ex-14 were the two fungi *Strophariaceae* (Hr:

542 < 0.01 %; Ex-4: 0.01 %; Ex-14: 0.80 %) and *Ceratobasidiaceae* (Hr: < 0.01 %; Ex-4: 0.01 %; Ex-
543 14: 0.75 %).

544 **Viruses**

545 Total relative abundance of viruses based on the mRNA libraries (total viral mRNA reads
546 relative to total mRNA reads) was highest in Ex-14 compared to Ex-4 and Hr (Hr: 2.34 %; Ex-4:
547 2.35 %; Ex-14: 3.96 %). Viruses with prokaryotic hosts had similar abundances in all three
548 treatments (Hr: 1.04 %; Ex-4: 1.13 %; Ex-14: 1.13 %), attributing the increase of total viruses
549 in Ex-14 to viruses with eukaryotic hosts (Hr: 3.14 %; Ex-4: 3.11 %; Ex-14: 4.46 %). The potential
550 eukaryote-infecting viruses were divided into three groups. Those with fungal hosts, increased
551 significantly from Hr to Ex-4 and Ex-14 (Hr: 1.03 %; Ex-4: 1.11 %; Ex-14: 1.79 %), while those
552 with invertebrate hosts (Hr: 1.33 %; Ex-4: 1.22 %; Ex-14: 2.09 %) and protozoan hosts (Hr:
553 0.77 %; Ex-4: 0.78 %; Ex-14: 0.58 %), did not change significantly (Supplementary Table S2).

554

555 ## Discussion

556 **Herbivory, vegetation, roots, and soil chemistry**

557 Herbivore exclusion (breeding Barnacle geese and Svalbard reindeer) had led to a shift from
558 bryophyte-dominated vegetation (Hr), towards increasing ratios of vascular plants (*Poa*
559 grasses) after 4 years of herbivore exclusion (Ex-4), and the dominance of *Equisetum*
560 *variegatum* after 14 years of herbivore exclusion (Ex-14). This corresponds to earlier
561 observations from this area and study sites (Sjörgersten 2011; Bender et al. 2021; Petit Bon et
562 al. 2023). Despite the large vegetation changes, we observed no change in the C, N, and P
563 contents, except for higher concentrations of inorganic P (Pi) in Ex-14. Plants and fungi are
564 taking up Pi through their roots and subsequently store it partly in cell vacuoles, while upon
565 cell death and decay, P is released to the soil (Yang et al. 2017; George et al. 2018; Wang et al.
566 2021). The higher concentrations of Pi in herbivory exclosures might be caused by a deeper
567 reaching root system that is able to access lower pools of P and transport it to the upper soil
568 layers. Despite the similar soil C, N, and P contents, other differences in the SOM composition
569 were observed in Ex-14 relative to Ex-4 and Hr, including higher abundances of N-containing
570 compounds and lignin-derived compounds. This is in line with observations of higher vascular

plant content and altered soil contents of mannan, xyloglucans, galacturonans, and lignin in exclosures at a nearby site (Bender et al. 2021). In an earlier study on the effect of vascular plants on peat decomposition, it was suggested that sedges promote peat decomposition due to a combined influence of altered SOM quality and higher O_2 concentrations (Zeh et al. 2020). While this resembles our observations of higher vascular plant abundance, changed SOM composition, and elevated soil cumulative respiration in Ex-4 and Ex-14, we did not observe differences in O_2 concentration. Roots can directly contribute to respiration rates but can also indirectly promote decomposition through root exudation of easily degradable dissolved organic matter (Canarini et al. 2019). Thus, our observations, in Ex-14, of a faster growing microbial community that also mineralizes the organic C at a faster rate could be driven by exudation from the significantly larger root biomass, but potential root contribution to the cumulative respiration rates complicate our interpretation. Possibly, the observed higher soil respiration rates in the exclosures can be ascribed to a combination of root respiration and faster microbial decomposition supported by an altered SOM composition (polymers and sugars) and increased root exudation.

Growth, turnover time, microbial biomass, DNA and RNA

After 14 years of herbivore exclusion, the microbial community showed trends of faster biomass-specific growth and therefore significantly shorter DNA turnover times (Figure 3B). We postulate that the faster biomass-specific microbial growth rates after 14 years are driven by increased root exudation from a larger root biomass, and an altered composition of plant polymers stemming from the vascular plant cover. This combination of faster biomass-specific growth rates, shorter DNA turnover time, and stable biomass suggested higher microbial death rates in Ex-14. However, the significantly lower DNA and RNA concentrations in the soils in Ex-14 contradict the observations of a stable microbial biomass. Possibly, the large shifts in dominant taxa had led to a reduction in the mean DNA and RNA content per cell, as different microbial taxa have different cell contents. For example, the cellular content of RNA in the model yeast *Saccharomyces cereviscae* has been reported to account for 6–12 % of cell dry matter (Yamada and Sgarbieri 2005; Feijó Delgado et al. 2013), while in the prokaryotic model organism *Escherichia. coli* it was found to be 20 % (Neidhardt et al. 1990; Feijó Delgado et al. 2013). Similar large differences are found in DNA percentage of dry mass, being 3 % in *E. coli* and 0.1–0.6 % in *S. cereviscae* (Feijó Delgado et al. 2013). Considering such differences, the

higher microbial biomass to DNA ratio in Ex-14 could have been caused by the higher fungi content. Other potential factors that could explain the discrepancy between RNA, DNA, and microbial biomass contents are the effect of growth conditions, including temperature and substrate concentrations, on cellular RNA contents (Mairet et al. 2021; Söllinger et al. 2022) or the balance between the release of extracellular RNA and DNA through microbial necromass turnover and consumption of nucleic acids.

Regardless of the explanation for the differences in ratios between microbial biomass and nucleic acids, the observations of faster DNA turnover, stable microbial biomass, and lower nucleic acids concentrations in the exclosures relative to the herbivory sites, both support the same narrative: Higher microbial growth rates do not result in more microbial biomass. Instead, the faster growth rates seem to trigger a faster microbial loop and enhanced respiration.

Microbial death and the soil food web

Microbial death can occur in many ways, like predation by eukaryotes (Richter et al. 2019) or prokaryotes (Thiery and Kaimer 2020; Li et al. 2021; Petters et al. 2021), cell lysis caused by viral infections (Ballaud et al. 2015; Heinrichs et al 2020; Camenzind et al. 2023), antibiotics (Kohanski et al. 2010) and stress events, such as large temperature shifts and freezing, and starvation (Camenzind et al. 2023). In any given ecosystem those potential causes of microbial death are often present simultaneously (Camenzind et al. 2023), which makes it difficult to identify the primary cause of microbial death.

In our study, we observed a lower relative abundance of both eukaryotic and prokaryotic potential predators at the Ex-14 plots compared to the Ex-4 and Hr plots. This was evident from a decrease in both prokaryotic and eukaryotic predatory groups at the phylum and family levels. We also found that while many eukaryotic families containing known predators were decreasing in relative abundance, a few were increasing, such as those belonging to the phyla *Ciliophora*, *Lobosa*, *Choanoflagellida*, *Cercozoa*, and *Euglenida*. This indicates a shift in the microbial food web in Ex-14, to a state where there are fewer predators, possibly resulting in more specialized predatory communities compared to the more diverse and relatively more abundant predatory communities in Hr and Ex-4.

Viral infections are another cause of microbial mortality. We found that viruses with prokaryotic hosts were similarly abundant across all three treatments. This suggests a consistent viral infection pressure on the prokaryotic community, irrespective of treatment. However, viruses infecting eukaryotic hosts were most abundant in the Ex-14 plots. This increase was attributed to a raised abundance of viruses that are known to infect fungi, suggesting a viral response to the concurrent increase in relative abundances of fungi in Ex-14.

Actinobacteriota and fungi were significantly more abundant at the Ex-14 plots and are known to possess antibiotic traits (Broadbent 1966; Clardy et al. 2009; Barka et al. 2016; Hussein et al. 2018; De Simeis and Serra 2021; Dutta et al. 2022). It is possible that antibiotics contribute to microbial death in Ex-14. However, an upregulation of antibiotics excretion over time is likely associated with community selection and increasing antibiotic resistance (Zhu et al. 2019; Ai et al. 2022). While our dataset does not allow for any quantitative estimate of the contribution of antibiotics to community selection and microbial death, we consider it likely that it constitutes a contributing factor to the development of the food web.

The presumed faster microbial loop in Ex-14 could be related to the shift towards a different and relatively smaller, but more potent predatory community, causing higher death rates. By balancing the faster microbial growth rates, these predators may have contributed to maintain similar microbial biomass pools in all treatments. Previous studies have demonstrated hot spots for microbial turnover centered around the roots (rhizosphere) (Kuzyakov 2010). Similarly, a larger proportion of the microbial activity may be concentrated around the more abundant roots in Ex-14, while microbial activity is more evenly distributed throughout the bulk soil in the other treatments. Consequently, in Ex-14, the dynamics of predation and viral infection may have changed due to higher prey concentrations in hotspots where faster microbial growth rates are driven by root exudates. Such spatial restrictions could also help explain our observations that fewer predators and similar relative viral pressure could maintain a faster microbial loop Ex-14. Alternatively, the physical environments in the exclosures, where higher root density led to larger and more abundant pore spaces, could favor motile predators. This would increase the size of the hunting ground and thus the energy requirements from more motile predators (Mitchell and Kogure 2006;

Palma et al. 2022), which in turn could drive a faster rate of microbial biomass turnover despite a lower number of predators.

Summary and Conclusion

The exclusion of herbivores for 4 and 14 years led to the establishment of a vegetation dominated by vascular plants which correlated with a larger root biomass, but despite these shifts, few changes in the soil chemistry were observed. In Ex-14, we observed that the changes in the soil, led to faster microbial growth, but microbial biomass did not increase. This suggested the establishment of a faster microbial loop with enhanced death rates. We propose that this faster microbial loop is driven by a combination of higher microbial growth rates due to increased root exudation and better-quality polymeric substrates and higher microbial death rates driven by more efficient predation and viral lysis.

Climate change is leading to altered population dynamics of Arctic breeding geese and other Arctic herbivores with implications for above and belowground ecosystem functioning. We conclude that vegetation changes caused by removal of herbivory will have a major effect on the soil microbial food web, the soil microbial loop and thereby, soil C cycling. However, several years must pass after the disappearance of herbivores before substantial changes in the vegetation, soil and microbial food web occur.

Figures

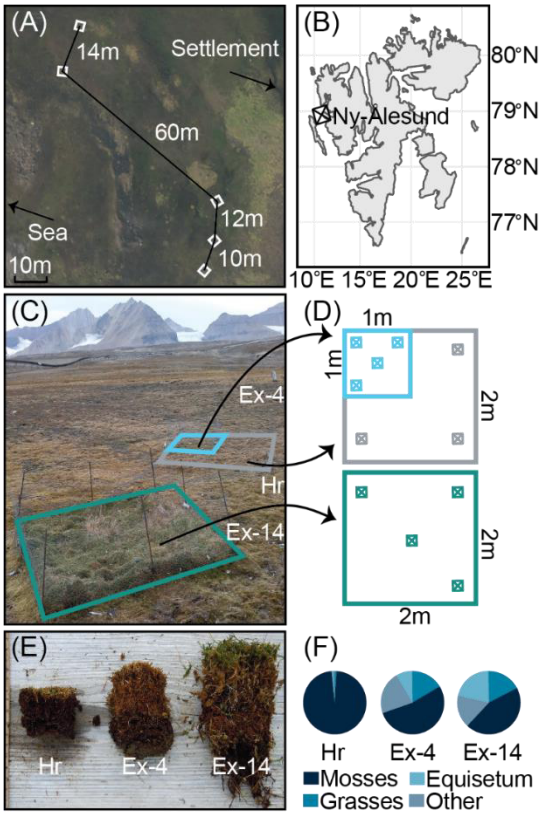

Figure 1. Herbivory exclosure experiments: Location, experimental design, and vegetation. **(A)** Distribution of the five sampling sectors (i.e., biological replicates), across the Thiisbukta peatland, Ny-Ålesund, Svalbard. Starting at sector 1 (bottom right) to sector 5 (top left). The terrain map (A) was retrieved from toposvalbard.npolar.no. **(B)** Location of Ny-Ålesund on Svalbard. **(C)** Picture of one of the five sampling sectors (sector 1). Each sector consisted of three plots representing three treatments: Exclosure – 14 years (Ex-14, in green), Exclosure – 4 years (Ex-4, in blue), and a control plot, Herbivory (Hr, in grey). Ex-14 and Ex-4 have been protected from herbivores with fences around the plots and metal wires across on top. **(D)** Ex-14 and Hr plots were 2 m × 2 m, while Ex-4 plots were 1 m × 1 m and located within the Hr plots. Small squares with a cross inside indicate the within-sector replication. **(E)** Picture for the comparison of vegetation and topsoil layers between the three treatments (Hr, Ex-4, and Ex-14). **(F)** Circle diagrams displaying the vegetation composition in Hr, Ex-4 and Ex-14 (details can be found in Supplementary Table S5).

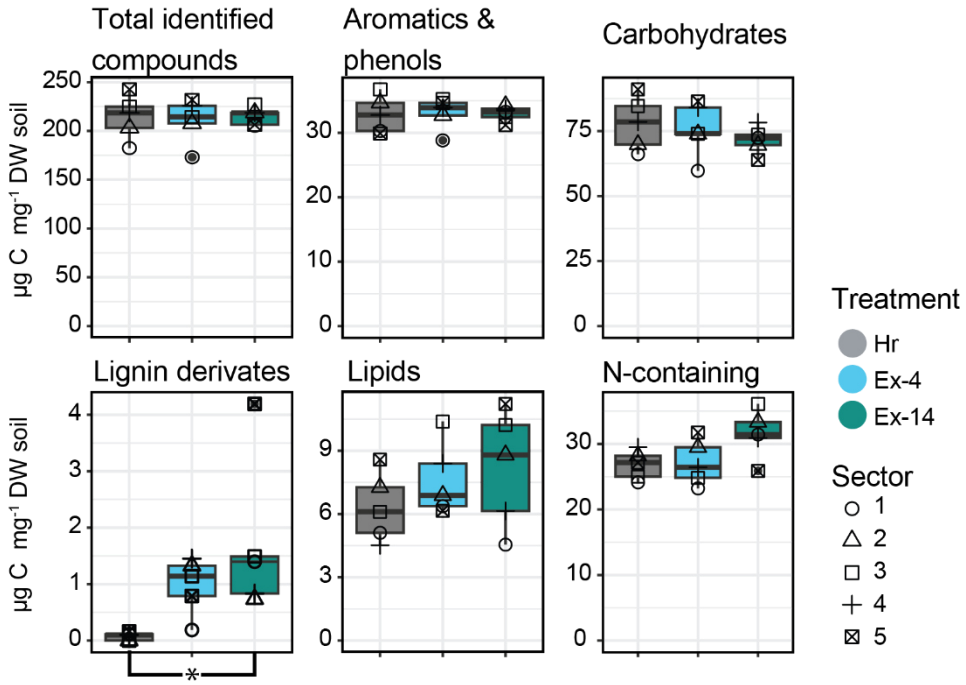

695

696 **Figure 2.** Comparison of different soil organic matter (SOM) compounds, retrieved from
697 pyrolysis GC/MS data. Three treatments were compared: Herbivory (Hr), Exclosure – 4 years
698 (Ex-4), and Exclosure – 14 years (Ex-14). Boxplots show median, 75 percentile and maximum
699 and minimum values, while the data-points from each sector are plotted as symbols 1–5.
700 These five datapoints are the means of the three (Hr) or four (Ex-4 and Ex-14) within-sector
701 replicates of the three treatments as shown in Figure 1. Abbreviations: C, carbon; DW, dry
702 weight. For statistical comparison of the three treatments a linear mixed-effects (LME) model
703 was used (p-value: * = 0.0402; details can be found in Supplementary Table S7).

704

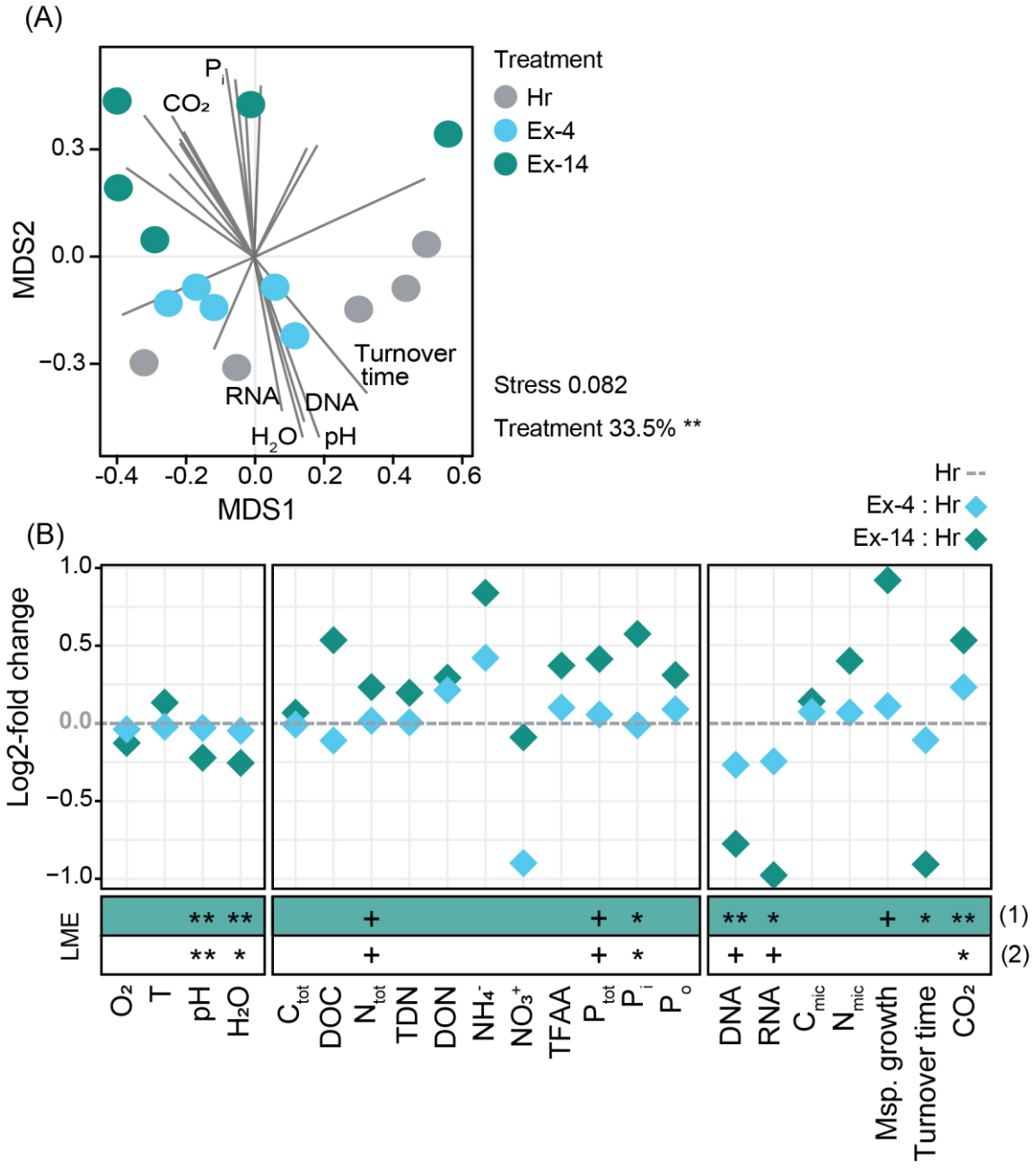

Figure 3. Differences in physicochemical and biological properties between the three treatments: Herbivory (Hr), Exclosure – 4 years (Ex-4), and Exclosure – 14 years (Ex-14). **(A)** NMDS plot showing the difference between Hr (in grey), Ex-4 (in blue), and Ex-14 (in green) in terms of physicochemical and biological properties. Each dot represents the mean of three (Hr) or four (Ex-4 and Ex-14) within-sector replicates as shown in Figure 1. Stress value (2 dimensions) and permutational analysis of variance (PERMANOVA) results are based on n=15 samples. The percentage indicates the variation explained by treatment and the asterisk indicates that the effect is significant (lower right corner). See Supplementary Table S8 for all tested variables that contributed significantly to the separation of the samples. **(B)** A log2-fold

change was used to visualize the change of individual physiochemical and biological soil properties. The same variables as shown in (B) were used for the NMDS in (A). The measurements of Ex-14 (green) and Ex-4 (blue) are shown relative to Hr (grey line). The first and second section show soil physiochemical properties, while the third section shows the soil biological properties related to microbial activities and microbial biomass. A linear mixed-effects (LME) model was used for statistical comparison of the three treatments; results are shown in the lower boxes, comparing in green (1) Hr to Ex-14 and in white (2) Ex-4 to Ex-14 (p-value: ** < 0.01, * < 0.05, + < 0.1; further information: Supplementary Table S8).

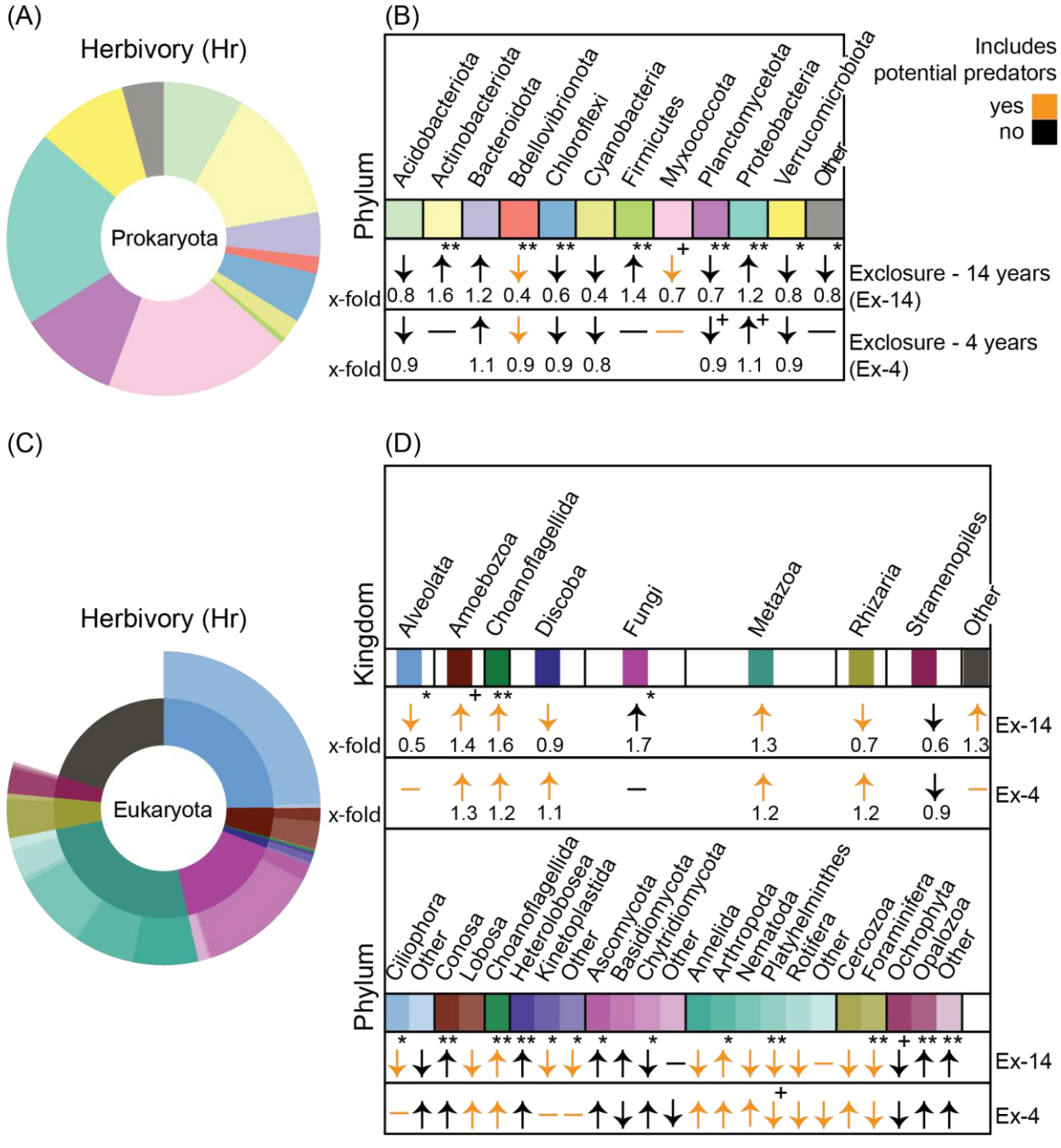

Figure 4. Changes in prokaryotic and eukaryotic communities with changing treatment based on the relative abundances of rRNA. **(A)** Donut plot showing the prokaryotic community composition at Herbivory (Hr) sites (mean of all Hr samples). 'Other' includes all prokaryotic phyla below a mean relative abundance of 0.5 % combined with all prokaryotic reads unclassified on phylum level. **(B)** Changes in the prokaryotic community, on phylum level, after herbivory exclusion. The yellow arrows highlight phyla that include potential predatory taxa, the black arrows correspond to phyla without known predators. The direction of the arrows shows whether a phylum increase (up) or decrease (down) in relative abundance in Exclosure – 14 years (Ex-14) or Exclosure – 4 years (Ex-4) relative to Hr. Below the arrows, the x-fold increase or decrease of each phylum is indicated. A linear mixed-effects (LME)was used for the statistical testing of significantly changing phyla, comparing Ex-14 to Hr and Ex-4 to Hr (p-value: ** < 0.01, * < 0.05, + < 0.1, see Supplementary Table S9). **(C)** Donut plot showing the eukaryotic community composition in Hr plots (mean of all Hr samples). Inner donut represent Kingdom level taxonomy, while the outer donut represent Phylum level taxonomy. 'Other' on kingdom level include all kingdoms below a mean relative abundance of 0.05 % and all eukaryotic reads unclassified on kingdom level. The reason not all kingdoms have an 'Other' group on phylum level is that those were below a mean relative abundance of 0.05 %. **(D)** Similar to (B) this box visualizes if a phylum or kingdom showed an increase or decrease of relative abundance in Ex-14 or Ex-4 relative to Hr, as indicated by the arrows. The x-fold change is shown only for kingdom. The yellow arrows indicate if a kingdom or phyla include potentially predatory taxa. An LME was used for the statistical testing of significantly changing kingdom or phyla, comparing Ex-14 to Hr and Ex-4 to Hr (p-value: ** < 0.01, * < 0.05, + < 0.1, see Supplementary Table S9).

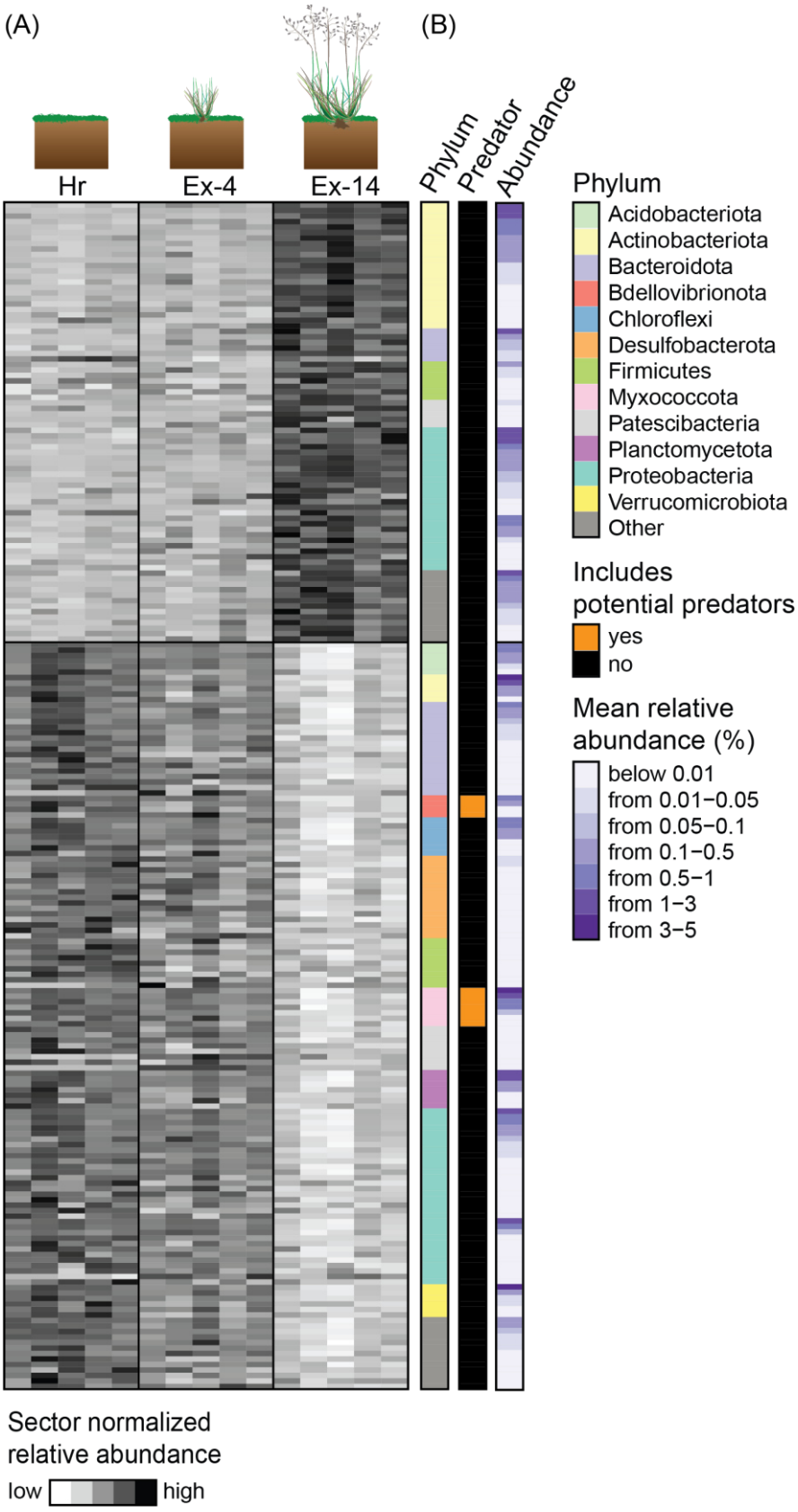

749

750 **Figure 5.** Prokaryotic families responding to the exclusion of herbivores based on the relative
751 abundances of rRNA. **(A)** Heatmap of prokaryotic families that significantly change in relative
752 abundance after the exclusion of herbivores. Each line in the heatmap corresponds to a

753 classified family, comparing its abundance in the three treatments: Herbivory (Hr), Exclosure
754 – 4 years (Ex-4), and Exclosure – 14 years (Ex-14). The two main trends of response are (1) an
755 increase of abundance towards Ex-14 (top third of the heatmap) and (2) a decrease of
756 abundance towards Ex-14 (lower two thirds of the heatmap). The grey scale indicates the
757 sector-normalized relative abundances (see: Materials and Methods section (h) - *Sampling*
758 *sector normalization*) of each family, from black and dark grey (higher relative abundance), to
759 light grey and white (lower relative abundance). **(B)** The column to the right of the heatmap
760 shows which phylum a family belongs to (Phylum). All phyla represented by less than 3 families
761 were combined in 'Other'. The second column shows which families contain known predatory
762 taxa, and the third column shows the mean relative abundance (%) of each family (based on
763 the mean abundance of each row in the heatmap), the darker the purple the higher the
764 relative abundance.
765

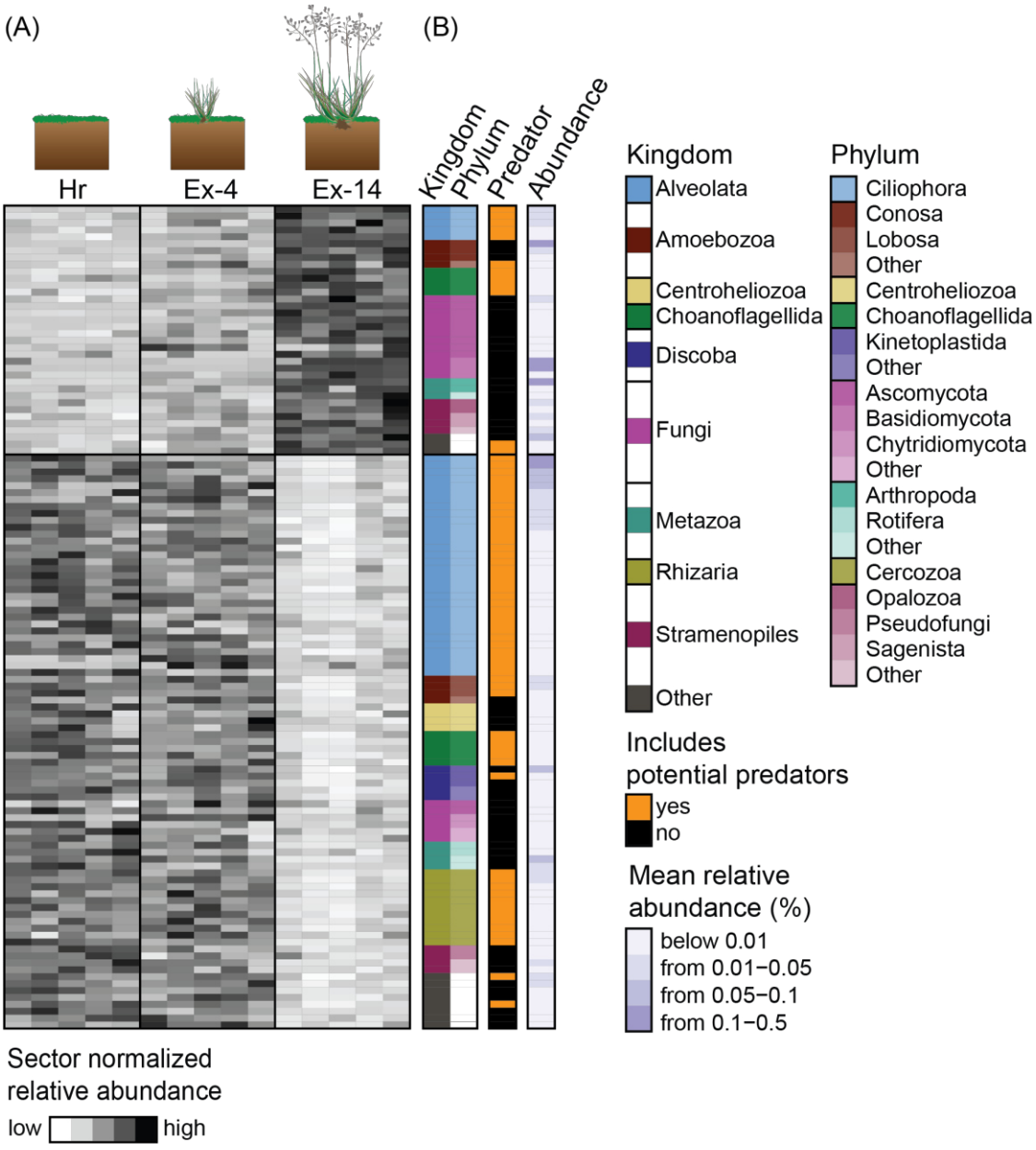

766

767 **Figure 6.** Eukaryotic families responding to the exclusion of herbivores based on the relative
768 abundances of rRNA. **(A)** Heatmap of eukaryotic families that significantly change in relative
769 abundance after the exclusion of herbivores. Each line in the heatmap corresponds to a
770 classified family, comparing its abundance in the three treatments: Herbivory (Hr), Exclosure
771 – 4 years (Ex-4), and Exclosure – 14 years (Ex-14). The two main trends of response are (1) an
772 increase of relative abundance towards Ex-14 (top third of the heatmap) and (2) a decrease of
773 relative abundance towards Ex-14 (lower two thirds of the heatmap). The grey scale indicates
774 the sector normalized relative abundances
775 (see: Materials and Methods section (h) - *Sampling sector normalization*) of each family, from
776 black and dark grey (higher relative abundance), to light grey and white (lower relative

abundance). **(B)** The two columns to the right of the heatmap show which kingdom a certain family belongs to (Kingdom) and which phylum a family belongs to (Phylum). All phyla represented by less than 3 families were combined in 'Other'. The third column shows which or families contain known predatory taxa. The fourth column shows the mean relative abundance (%) of each family (based on the mean abundance of each row in the heatmap), the darker the purple the higher the relative abundance.

References

Ai, J., Li, Y. C., Lv, Y., Zhong, X., Li, J., & Yang, A. J. (2022). Study on microbes and antibiotic resistance genes in karst primitive mountain marshes-A case study of Niangniang Mountain in Guizhou, China. *Ecotoxicology and Environmental Safety, 247*. https://doi.org/10.1016/j.ecoenv.2022.114210

Antala, M., Juszczak, R., van der Tol, C., & Rastogi, A. (2022). Impact of climate change-induced alterations in peatland vegetation phenology and composition on carbon balance. *Science of The Total Environment, 827*, 154294. https://doi.org/10.1016/j.scitotenv.2022.154294

Ballaud, F., Dufresne, A., Francez, A. J., Colombet, J., Sime-Ngando, T., & Quaiser, A. (2015). Dynamics of Viral Abundance and Diversity in a Sphagnum-Dominated Peatland: Temporal Fluctuations Prevail Over Habitat. *Frontiers in Microbiology, 6*, 1494. https://doi.org/10.3389/fmicb.2015.01494

Bao, T., Jia, G., & Xu, X. (2022). Warming enhances dominance of vascular plants over cryptogams across northern wetlands. *Global Change Biology, 28*(13), 4097-4109. https://doi.org/10.1111/gcb.16182

Bardgett, R. D., Wardle, D. A., & Yeates, G. W. (1998). Linking above-ground and below-ground interactions: how plant responses to foliar herbivory influence soil organisms. *Soil Biology and Biochemistry, 30*(14), 1867-1878. https://doi.org/10.1016/S0038-0717(98)00069-8

Bardgett, R. D., & Wardle, D. A. (2003). Herbivore-Mediated Linkages between Aboveground and Belowground Communities. *Ecology, 84*(9), 2258-2268. http://www.jstor.org/stable/3450132

Bardgett, R. D., Freeman, C., & Ostle, N. J. (2008). Microbial contributions to climate change through carbon cycle feedbacks. The *ISME Journal, 2*(8), 805-814. https://doi.org/10.1038/ismej.2008.58

Barka, E. A., Vatsa, P., Sanchez, L., Gaveau-Vaillant, N., Jacquard, C., Meier-Kolthoff, J. P., Klenk, H. P., Clement, C., Ouhdouch, Y., & van Wezel, G. P. (2016). Taxonomy, Physiology, and Natural Products of Actinobacteria. *Microbiology and Molecular Biology Reviews, 80*(1), 1-43. https://doi.org/10.1128/MMBR.00019-15

Bartsch, I., & Moore, T. R. (1985). A preliminary investigation of primary production and decomposition in four peatlands near Schefferville, Québec. *Canadian Journal of Botany, 63*(7), 1241-1248. https://doi.org/10.1139/b85-171

Bender, K. M., Svenning, M. M., Hu, Y., Richter, A., Schückel, J., Jørgensen, B., Liebner, S., & Tveit, A. T. (2021). Microbial responses to herbivory-induced vegetation changes in a high-Arctic peatland. *Polar Biology, 44*(5), 899-911. https://doi.org/10.1007/s00300-021-02846-z

Berner, L. T., Massey, R., Jantz, P., Forbes, B. C., Macias-Fauria, M., Myers-Smith, I., Kumpula, T., Gauthier, G., Andreu-Hayles, L., Gaglioti, B. V., Burns, P., Zetterberg, P., D'Arrigo, R., & Goetz, S. J. (2020). Summer warming explains widespread but not uniform greening in the Arctic tundra biome. *Nature Communications, 11*(1), 4621. https://doi.org/10.1038/s41467-020-18479-5

Berryman, A. A. (1992). The Origins and Evolution of Predator Prey Theory. *Ecology, 73*(5), 1530-1535. https://doi.org/10.2307/1940005

Bjerke, J. W., Tombre, I. M., Hanssen, M., & Olsen, A. K. B. (2021). Springtime grazing by Arctic-breeding geese reduces first- and second-harvest yields on sub-Arctic agricultural grasslands. *Science of the Total Environment, 793*, 148619. https://doi.org/10.1016/j.scitotenv.2021.148619

Brister, J. R., Ako-Adjei, D., Bao, Y., & Blinkova, O. (2015). NCBI viral genomes resource. *Nucleic Acids Research, 43*(D1), D571-577. https://doi.org/10.1093/nar/gku1207

Broadbent, D. (1966). Antibiotics produced by fungi. The *Botanical Review, 32*, 219-242. https://doi.org/10.1007/BF02858660

Buchfink, B., Reuter, K., & Drost, H. G. (2021). Sensitive protein alignments at tree-of-life scale using DIAMOND. *Nature Methods, 18*, 366-368. https://doi.org/10.1038/s41592-021-01101-x

Camenzind, T., Mason-Jones, K., Mansour, I., Rillig, M. C., & Lehmann, J. (2023). Formation of necromass-derived soil organic carbon determined by microbial death pathways. *Nature Geoscience, 16*, 115–122. https://doi.org/10.1038/s41561-022-01100-3

Canarini, A., Kaiser, C., Merchant, A., Richter, A., & Wanek, W. (2019). Root Exudation of Primary Metabolites: Mechanisms and Their Roles in Plant Responses to Environmental Stimuli [Review]. *Frontiers in Plant Science, 10*. https://doi.org/10.3389/fpls.2019.00157

Cavalier-Smith, T. (1995). Zooflagellate phylogeny and classification. *Tsitologiia, 37*(11), 1010-1029. https://www.ncbi.nlm.nih.gov/pubmed/8868448

Clardy, J., Fischbach, M. A., & Currie, C. R. (2009). The natural history of antibiotics. *Current Biology, 19*(11), R437-441. https://doi.org/10.1016/j.cub.2009.04.001

D'Angelo, E., Crutchfield, J., & Vandiviere, M. (2001). Rapid, sensitive, microscale determination of phosphate in water and soil. *Journal of Environmental Quality, 30*(6), 2206-2209. https://doi.org/10.2134/jeq2001.2206

Dahl, M. B., Söllinger, A., Sigurðsson, P., Janssens, I., Peñuelas, J., Sigurdsson, B. D., Richter, A., Tveit, A., & Urich, T. (2023). Long-term warming-induced trophic downgrading in the soil microbial food web. *Soil Biology and Biochemistry, 181*(109044). https://doi.org/10.1016/j.soilbio.2023.109044

855 Davidson, E. A., & Janssens, I. A. (2006). Temperature sensitivity of soil carbon
856 decomposition and feedbacks to climate change. *Nature, 440*(7081), 165-173.
857 https://doi.org/10.1038/nature04514

858 Dayel, M. J., & King, N. (2014). Prey capture and phagocytosis in the choanoflagellate
859 Salpingoeca rosetta. *Plos One, 9*(5), e95577. https://doi.org/10.1371/journal.pone.0095577

860 De Deyn, G. B., Cornelissen, J. H., & Bardgett, R. D. (2008). Plant functional traits and soil
861 carbon sequestration in contrasting biomes. *Ecology Letters, 11*(5), 516-531.
862 https://doi.org/10.1111/j.1461-0248.2008.01164.x

863 De Simeis, D., & Serra, S. (2021). Actinomycetes: A Never-Ending Source of Bioactive
864 Compounds-An Overview on Antibiotics Production. *Antibiotics, 10*(5).
865 https://doi.org/10.3390/antibiotics10050483

866 Drezner, T. D., & Drezner, Z. (2021). Informed cover measurement: Guidelines and error for
867 point-intercept approaches. *Applications in Plant Science, 9*(9-10), e11446.
868 https://doi.org/10.1002/aps3.11446

869 Dutta, B., Lahiri, D., Nag, M., Ghosh, S., Dey, A., & Ray, R. R. (2022). Fungi in Pharmaceuticals
870 and Production of Antibiotics. In A. C. Shukla (Ed.), *Applied Mycology: Entrepreneurship with*
871 *Fungi* (pp. 233-257). Springer International Publishing. https://doi.org/10.1007/978-3-030-
872 90649-8_11

873 Düttmann, H., Kruckenberg, H., Bünte, R., Delingat, J., Emke, D., Garlichs, M., Korner, P.,
874 Kowallik, C., Lauenstein, G., Südbeck, P., & Bairlein, F. (2023). Grazing effects of wintering
875 geese on grassland yield: A long-term study from Northwest Germany. *Journal of Applied*
876 *Ecology, 60*(3), 421-432. https://doi.org/10.1111/1365-2664.14340

877 Erktan, A., Or, D., & Scheu, S. (2020). The physical structure of soil: Determinant and
878 consequence of trophic interactions. *Soil Biology and Biochemistry, 148*, 107876.
879 https://doi.org/10.1016/j.soilbio.2020.107876

880 Feijó Delgado, F., Cermak, N., Hecht, V. C., Son, S., Li, Y., Knudsen, S. M., Olcum, S., Higgins, J.
881 M., Chen, J., Grover, W. H., & Manalis, S. R. (2013). Intracellular water exchange for
882 measuring the dry mass, water mass and changes in chemical composition of living cells. *Plos*
883 *One, 8*(7), e67590. https://doi.org/10.1371/journal.pone.0067590

884 Foley, K. M., Beard, K. H., Atwood, T. B., & Waring, B. G. (2022). Herbivory changes soil
885 microbial communities and greenhouse gas fluxes in a high-latitude wetland. *Microbial*
886 *Ecology, 83*(1), 127-136. https://doi.org/10.1007/s00248-021-01733-8

887 Fox, A. D., Madsen, J., Boyd, H., Kuijken, E., Norriss, D. W., Tombre, I. M., & Stroud, D. A.
888 (2005). Effects of agricultural change on abundance, fitness components and distribution of
889 two arctic-nesting goose populations. *Global Change Biology, 11*(6), 881-893.
890 https://doi.org/10.1111/j.1365-2486.2005.00941.x

Geisen, S., Mitchell, E. A. D., Adl, S., Bonkowski, M., Dunthorn, M., Ekelund, F., Fernández, L. D., Jousset, A., Krashevska, V., Singer, D., Spiegel, F. W., Walochnik, J., & Lara, E. (2018). Soil protists: a fertile frontier in soil biology research. *FEMS Microbiology Reviews, 42*(3), 293-323. https://doi.org/10.1093/femsre/fuy006

Geisen, S., Lara, E., & Mitchell, E. (2023). Contemporary issues, current best practice and ways forward in soil protist ecology. *Molecular Ecology Resources, 00*, 1-11. https://doi.org/https://doi.org/10.1111/1755-0998.13819

George, T. S., Giles, C. D., Menezes-Blackburn, D., Condron, L. M., Gama-Rodrigues, A. C., Jaisi, D., Lang, F., Neal, A. L., Stutter, M. I., Almeida, D. S., Bol, R., Cabugao, K. G., Celi, L., Cotner, J. B., Feng, G., Goll, D. S., Hallama, M., Krueger, J., Plassard, C., . . . Haygarth, P. M. (2018). Organic phosphorus in the terrestrial environment: a perspective on the state of the art and future priorities. *Plant and Soil, 427*(1), 191-208. https://doi.org/10.1007/s11104-017-3391-x

Gruber-Vodicka, H. R., Seah, B. K. B., & Pruesse, E. (2020). phyloFlash: Rapid Small-Subunit rRNA Profiling and Targeted Assembly from Metagenomes. *mSystems, 5*(5). https://doi.org/10.1128/mSystems.00920-20

Han, D. C. (2022). How to Make a Beautiful Donut Chart and Nested Donut Chart in Matplotlib. *Python in Plain English*. Retrieved 08.02.2023 from https://python.plainenglish.io/how-to-make-a-beautiful-donut-chart-and-nested-donut-chart-in-matplotlib-92040c8bbeea

Harris, C. R., Millman, K. J., van der Walt, S. J., Gommers, R., Virtanen, P., Cournapeau, D., Wieser, E., Taylor, J., Berg, S., Smith, N. J., Kern, R., Picus, M., Hoyer, S., van Kerkwijk, M. H., Brett, M., Haldane, A., Del Rio, J. F., Wiebe, M., Peterson, P., . . . Oliphant, T. E. (2020). Array programming with NumPy. *Nature, 585*(7825), 357-362. https://doi.org/10.1038/s41586-020-2649-2

Hatton, I. A., Dobson, A. P., Storch, D., Galbraith, E. D., & Loreau, M. (2019). Linking scaling laws across eukaryotes. *Proceedings of the National Academy of Sciences, 116*(43), 21616-21622. https://doi.org/doi:10.1073/pnas.1900492116

Hausmann, B., Knorr, K.-H., Schreck, K., Tringe, S. G., Glavina del Rio, T., Loy, A., & Pester, M. (2016). Consortia of low-abundance bacteria drive sulfate reduction-dependent degradation of fermentation products in peat soil microcosms. *The ISME Journal, 10*(10), 2365-2375. https://doi.org/10.1038/ismej.2016.42

Heinrichs, M. E., Tebbe, D. A., Wemheuer, B., Niggemann, J., & Engelen, B. (2020). Impact of Viral Lysis on the Composition of Bacterial Communities and Dissolved Organic Matter in Deep-Sea Sediments. *Viruses, 12*(9). https://doi.org/10.3390/v12090922

Heldbjerg, H., Johnson, F., Koffijberg, K., McKenzie, R., Nagy, S., Jensen, G. H., Madsen, J., & Baveco, J. M. (2021). Population status and assessment report 2021. In AEWA EGMP, *AEWA EGMP technical report No. 19.*

Hood-Nowotny, R., Hinko-Najera Umana, N., Inselbacher, E., Oswald-Lachouani, P., & Wanek, W. (2010). Alternative Methods for Measuring Inorganic, Organic, and Total Dissolved Nitrogen in Soil. *Soil Science Society of America Journal, 74*(3), 1018-1027. https://doi.org/10.2136/sssaj2009.0389

Hunter, J. D. (2007). Matplotlib: A 2D Graphics Environment. *Computing in Science & Engineering, 9*(3), 90-95. https://doi.org/10.1109/MCSE.2007.55

Huson, D. H., Beier, S., Flade, I., Gorska, A., El-Hadidi, M., Mitra, S., Ruscheweyh, H. J., & Tappu, R. (2016). MEGAN Community Edition - Interactive Exploration and Analysis of Large-Scale Microbiome Sequencing Data. *PLos Computational Biology, 12*(6), e1004957. https://doi.org/10.1371/journal.pcbi.1004957

Hussein, E. I., Jacob, J. H., Shakhatreh, M. A. K., Al-Razaq, M. A. A., Juhmani, A. F., & Cornelison, C. T. (2018). Detection of antibiotic-producing Actinobacteria in the sediment and water of Ma'in thermal springs (Jordan). *Germs, 8*(4), 191-198. https://doi.org/10.18683/germs.2018.1146

Jefferies, R. L., Jano, A. P., & Abraham, K. F. (2006). A biotic agent promotes large-scale catastrophic change in the coastal marshes of Hudson Bay. *Journal of Ecology, 94*(1), 234-242. https://doi.org/10.1111/j.1365-2745.2005.01086.x

Ji, M., Fan, X., Cornell, C. R., Zhang, Y., Yuan, M. M., Tian, Z., Sun, K., Gao, R., Liu, Y., & Zhou, J. (2023). Tundra Soil Viruses Mediate Responses of Microbial Communities to Climate Warming. *mBio, 14*(2), e0300922. https://doi.org/10.1128/mbio.03009-22

Kluyver, T., Ragan-Kelley, B., Pérez, F., Granger, B. E., Bussonnier, M., Frederic, J., Kelley, K., Hamrick, J. B., Grout, J., Corlay, S., Ivanov, P., Avila, D., Abdalla, S., Willing, C., & Team, J. D. (2016). Jupyter Notebooks - a publishing format for reproducible computational workflows. In F. Loizides & B. Schmidt (Eds.), *Proceedings of the 20th International Conference on Electronic Publishing* (pp. 87 - 90). https://doi.org/10.3233/978-1-61499-649-1-87

Kohanski, M. A., Dwyer, D. J., & Collins, J. J. (2010). How antibiotics kill bacteria: from targets to networks. *Nature Reviews Microbiology, 8*(6), 423-435. https://doi.org/10.1038/nrmicro2333

Kopylova, E., Noe, L., & Touzet, H. (2012). SortMeRNA: fast and accurate filtering of ribosomal RNAs in metatranscriptomic data. *Bioinformatics, 28*(24), 3211-3217. https://doi.org/10.1093/bioinformatics/bts611

960 Kuijper, D. P. J., Bakker, J. P., Cooper, E. J., Ubels, R., Jónsdóttir, I. S., & Loonen, M. J. J. E.
961 (2006). Intensive grazing by Barnacle geese depletes High Arctic seed bank. *Canadian Journal*
962 *of Botany, 84*(6), 995-1004. https://doi.org/10.1139/b06-052

963 Kuijper, D. P. J., Ubels, R., & Loonen, M. J. J. E. (2009). Density-dependent switches in diet: a
964 likely mechanism for negative feedbacks on goose population increase? *Polar Biology, 32*,
965 1789–1803. https://doi.org/10.1007/s00300-009-0678-2

966 Kuiper, J. J., Mooij, W. M., Bragazza, L., & Robroek, B. J. M. (2014). Plant functional types
967 define magnitude of drought response in peatland CO_2 exchange. *Ecology, 95*(1), 123-131.
968 https://doi.org/10.1890/13-0270.1

969 Kuo, S. (1996). Phosphorus. In A. L. P. D.L. Sparks, P.A. Helmke, R.H. Loeppert, P. N.
970 Soltanpour, M. A. Tabatabai, C. T. Johnston, M. E. Sumner (Ed.), *Methods of Soil Analysis:*
971 *Part 3 Chemical Methods* (Vol. 5.3). Soil Science Society of America.
972 https://doi.org/10.2136/sssabookser5.3.c32

973 Kuzyakov, Y. (2010). Priming effects: Interactions between living and dead organic matter.
974 *Soil Biology and Biochemistry, 42*(9), 1363-1371.
975 https://doi.org/10.1016/j.soilbio.2010.04.003

976 Lameris, T. K., Pokrovskaya, O. B., Kondratyev, A. V., Anisimov, Y. A., Buitendijk, N. H.,
977 Glazov, P. M., van der Jeugd, H. P., Kampichler, C., Kruckenberg, H., Litvin, K. E., Loshchagina,
978 J. A., Moonen, S., Muskens, G. J. D., Nolet, B. A., Schreven, K. H. T., Sierdsema, H.,
979 Zaynagutdinova, E. M., & Boom, M. P. (2023). Barnacle geese Branta leucopsis breeding on
980 Novaya Zemlya: current distribution and population size estimated from tracking data. *Polar*
981 *Biology, 46*(1), 67-76. https://doi.org/10.1007/s00300-022-03110-8

982 Lanzén, A., Jorgensen, S. L., Huson, D. H., Gorfer, M., Grindhaug, S. H., Jonassen, I., Ovreas,
983 L., & Urich, T. (2012). CREST - Classification Resources for Environmental Sequence Tags. *Plos*
984 *One, 7*(11). https://doi.org/10.1371/journal.pone.0049334

985 Layton-Matthews, K., Hansen, B. B., Grøtan, V., Fuglei, E., & Loonen, M. J. J. E. (2020).
986 Contrasting consequences of climate change for migratory geese: Predation, density
987 dependence and carryover effects offset benefits of high-arctic warming. *Global Change*
988 *Biology, 26*(2), 642-657. https://doi.org/10.1111/gcb.14773

989 Leander, B. S., Lax, G., Karnkowska, A., & Simpson, A. G. B. (2017). Euglenida. In J. M.
990 Archibald, A. G. B. Simpson, & C. H. Slamovits (Eds.), *Handbook of the Protists* (pp. 1047-
991 1088). Springer International Publishing. https://doi.org/10.1007/978-3-319-28149-0_13

992 Li, Q. M., Zhou, Y. L., Wei, Z. F., & Wang, Y. (2021). Phylogenomic Insights into Distribution
993 and Adaptation of Bdellovibrionota in Marine Waters. *Microorganisms, 9*(4).
994 https://doi.org/10.3390/microorganisms9040757

995 Lucas, J. M., McBride, S. G., & Strickland, M. S. (2020). Trophic level mediates soil microbial
996 community composition and function. *Soil Biology and Biochemistry, 143*, 107756.
997 https://doi.org/10.1016/j.soilbio.2020.107756

998 Lynn, D. H. (2016). Ciliophora. In J. M. Archibald, A. G. B. Simpson, C. H. Slamovits, L.
999 Margulis, M. Melkonian, D. J. Chapman, & J. O. Corliss (Eds.), *Handbook of the Protists* (pp. 1-
1000 52). Springer International Publishing. https://doi.org/10.1007/978-3-319-32669-6_23-1

1001 Lützow, M. v., Kögel-Knabner, I., Ekschmitt, K., Matzner, E., Guggenberger, G., Marschner, B.,
1002 & Flessa, H. (2006). Stabilization of organic matter in temperate soils: mechanisms and their
1003 relevance under different soil conditions – a review. *European Journal of Soil Science, 57*(4),
1004 426-445. https://doi.org/10.1111/j.1365-2389.2006.00809.x

1005 Madsen, J., Schreven, K. H. T., Jensen, G. H., Johnson, F. A., Nilsson, L., Nolet, B. A., & Pessa,
1006 J. (2023). Rapid formation of new migration route and breeding area by Arctic geese. *Current*
1007 *Biology, 33*(6), 1162-1170 e1164. https://doi.org/10.1016/j.cub.2023.01.065

1008 Mairet, F., Gouzé, J.-L., & de Jong, H. (2021). Optimal proteome allocation and the
1009 temperature dependence of microbial growth laws. *npj Systems Biology and Applications,*
1010 *7*(14). https://doi.org/10.1038/s41540-021-00172-y

1011 Maron, J. L., & Crone, E. (2006). Herbivory: effects on plant abundance, distribution and
1012 population growth. *Proceedings of the Royal Society Biology Science, 273*(1601), 2575-2584.
1013 https://doi.org/10.1098/rspb.2006.3587

1014 McKinney, W. (2010). Data Structures for Statistical Computing in Python. In S. van der Walt
1015 & J. Millman (Eds.), *Proceedings of the 9th Python in Science Conference* (pp. 56 - 61).
1016 https://doi.org/10.25080/Majora-92bf1922-00a

1017 Mitchell, G. C., Baker, J. H., & Sleigh, M. A. (1988). Feeding of a Freshwater Flagellate, Bodo
1018 saltans, on Diverse Bacteria. T*he Journal of Protozoology, 35*(2), 219-222.
1019 https://doi.org/10.1111/j.1550-7408.1988.tb04327.x

1020 Mitchell, J. G., & Kogure, K. (2006). Bacterial motility: links to the environment and a driving
1021 force for microbial physics. *FEMS Microbiology Ecology, 55*(1), 3-16.
1022 https://doi.org/10.1111/j.1574-6941.2005.00003.x

1023 NCBI Resource Coordinators (2018). Database resources of the National Center for
1024 Biotechnology Information. *Nucleic Acids Research, 46*(D1), D8-D13.
1025 https://doi.org/10.1093/nar/gkx1095

1026 Neidhardt, F. C., Ingraham, J. L., & Schaechter, M. (1990). Physiology of the Bacterial Cell. A
1027 Molecular Approach:. In C. A. Smith (Ed.), *Biochemical Education* (Vol. 20, pp. 124-125).
1028 https://doi.org/10.1016/0307-4412(92)90139-D

1029 Olefeldt, D., Hovemyr, M., Kuhn, M. A., Bastviken, D., Bohn, T. J., Connolly, J., Crill, P.,
1030 Euskirchen, E. S., Finkelstein, S. A., Genet, H., Grosse, G., Harris, L. I., Heffernan, L., Helbig,

M., Hugelius, G., Hutchins, R., Juutinen, S., Lara, M. J., Malhotra, A., . . . Watts, J. D. (2021). The Boreal-Arctic Wetland and Lake Dataset (BAWLD). *Earth System Science Data, 13*(11), 5127-5149. https://doi.org/10.5194/essd-13-5127-2021

Palma, V., Gutierrez, M. S., Vargas, O., Parthasarathy, R., & Navarrete, P. (2022). Methods to Evaluate Bacterial Motility and Its Role in Bacterial-Host Interactions. *Microorganisms, 10*(3). https://doi.org/10.3390/microorganisms10030563

Petit Bon, M., Hansen, B. B., Loonen, M. J. J. E., Petraglia, A., Bråthen, K. A., Böhner, H., Layton-Matthews, K., Beard, K. H., Moullec, M. L., Jónsdóttir, I. S., & van der Wal, R. (2023). Long-term herbivore removal experiments reveal different impacts of geese and reindeer on vegetation and ecosystem CO_2-fluxes in high-Arctic tundra. *bioRxiv*, 2023.2001.2027.525821. https://doi.org/10.1101/2023.01.27.525821

Petters, S., Groß, V., Söllinger, A., Pichler, M., Reinhard, A., Bengtsson, M. M., & Urich, T. (2021). The soil microbial food web revisited: Predatory myxobacteria as keystone taxa? The *ISME Journal, 15*(9), 2665-2675. https://doi.org/10.1038/s41396-021-00958-2

Prommer, J., Wanek, W., Hofhansl, F., Trojan, D., Offre, P., Urich, T., Schleper, C., Sassmann, S., Kitzler, B., Soja, G., & Hood-Nowotny, R. C. (2014). Biochar decelerates soil organic nitrogen cycling but stimulates soil nitrification in a temperate arable field trial. *Plos One, 9*(1), e86388. https://doi.org/10.1371/journal.pone.0086388

Rantanen, M., Karpechko, A. Y., Lipponen, A., Nordling, K., Hyvärinen, O., Ruosteenoja, K., Vihma, T., & Laaksonen, A. (2022). The Arctic has warmed nearly four times faster than the globe since 1979. *Communications Earth & Environment, 3*(1), 168. https://doi.org/10.1038/s43247-022-00498-3

Richter, A., Kern, T., Sebastian Wolf, Struck, U., & Ruess, L. (2019). Trophic and non-trophic interactions in binary links affect carbon flow in the soil micro-food web. *Soil Biology and Biochemistry, 135,* 239-247. https://doi.org/10.1016/j.soilbio.2019.04.010

Rosqvist, G. C., Inga, N., & Eriksson, P. (2022). Impacts of climate warming on reindeer herding require new land-use strategies. *Ambio, 51*(5), 1247-1262. https://doi.org/10.1007/s13280-021-01655-2

Schmidt, M. W. I., Torn, M. S., Abiven, S., Dittmar, T., Guggenberger, G., Janssens, I. A., Kleber, M., Kögel-Knabner, I., Lehmann, J., Manning, D. A. C., Nannipieri, P., Rasse, D. P., Weiner, S., & Trumbore, S. E. (2011). Persistence of soil organic matter as an ecosystem property. *Nature, 478*(7367), 49-56. https://doi.org/10.1038/nature10386

Schmieder, R., & Edwards, R. (2011). Quality control and preprocessing of metagenomic datasets. *Bioinformatics, 27*(6), 863-864. https://doi.org/10.1093/bioinformatics/btr026

Sjögersten, S., van der Wal, R., Loonen, M. J. J. E., & Woodin, S. J. (2011). Recovery of ecosystem carbon fluxes and storage from herbivory. *Biogeochemistry, 106*(3), 357-370. https://doi.org/10.1007/s10533-010-9516-4

Soudzilovskaia, N. A., Vaessen, S., Barcelo, M., He, J., Rahimlou, S., Abarenkov, K., Brundrett, M. C., Gomes, S. I. F., Merckx, V., & Tedersoo, L. (2020). FungalRoot: global online database of plant mycorrhizal associations. *New Phytologist, 227*(3), 955-966. https://doi.org/10.1111/nph.16569

Spohn, M., Klaus, K., Wanek, W., & Richter, A. (2016). Microbial carbon use efficiency and biomass turnover times depending on soil depth – Implications for carbon cycling. *Soil Biology & Biochemistry, 96*, 74-81. https://doi.org/10.1016/j.soilbio.2016.01.016

Suttle, C. A. (2007). Marine viruses — major players in the global ecosystem. *Nature Reviews Microbiology, 5*(10), 801-812. https://doi.org/10.1038/nrmicro1750

Szumigalski, A. R., & Bayley, S. E. (1996). Decomposition along a bog to rich fen gradient in central Alberta, Canada. *Canadian Journal of Botany, 74*(4), 573-581. https://doi.org/10.1139/b96-073

Söllinger, A., Séneca, J., Borg Dahl, M., Motleleng, L. L., Prommer, J., Verbruggen, E., Sigurdsson, B. D., Janssens, I., Peñuelas, J., Urich, T., Richter, A., & Tveit, A. T. (2022). Down-regulation of the bacterial protein biosynthesis machinery in response to weeks, years, and decades of soil warming. *Science Advances, 8*(12), eabm3230. https://doi.org/doi:10.1126/sciadv.abm3230

Thakur, M. P., & Geisen, S. (2019). Trophic Regulations of the Soil Microbiome. *Trends in Microbiology, 27*(9), 771-780. https://doi.org/10.1016/j.tim.2019.04.008

Thiery, S., & Kaimer, C. (2020). The Predation Strategy of Myxococcus xanthus. *Frontiers in Microbiology, 11*, 2. https://doi.org/10.3389/fmicb.2020.00002

Trap, J., Bonkowski, M., Plassard, C., Villenave, C., & Blanchart, E. (2016). Ecological importance of soil bacterivores for ecosystem functions. *Plant and Soil, 398*(1), 1-24. https://doi.org/10.1007/s11104-015-2671-6

Tveit, A., Schwacke, R., Svenning, M. M., & Urich, T. (2013). Organic carbon transformations in high-Arctic peat soils: key functions and microorganisms. The *ISME Journal, 7*(2), 299-311. https://doi.org/10.1038/ismej.2012.99

Urich, T., Lanzén, A., Qi, J., Huson, D. H., Schleper, C., & Schuster, S. C. (2008). Simultaneous Assessment of Soil Microbial Community Structure and Function through Analysis of the Meta-Transcriptome. *Plos One, 3*(6), e2527. https://doi.org/10.1371/journal.pone.0002527

Vance, E. D., Brookes, P. C., & Jenkinson, D. S. (1987). An extraction method for measuring soil microbial biomass C. *Soil Biology and Biochemistry, 19*(6), 703-707. https://doi.org/10.1016/0038-0717(87)90052-6

1101 Walker, T. W. N., Kaiser, C., Strasser, F., Herbold, C. W., Leblans, N. I. W., Woebken, D.,
1102 Janssens, I. A., Sigurdsson, B. D., & Richter, A. (2018). Microbial temperature sensitivity and
1103 biomass change explain soil carbon loss with warming. *Nature Climate Change, 8*(10), 885-
1104 889. https://doi.org/10.1038/s41558-018-0259-x

1105 Wang, Y., Wang, F., Lu, H., Liu, Y., & Mao, C. (2021). Phosphate Uptake and Transport in
1106 Plants: An Elaborate Regulatory System. *Plant and Cell Physiology, 62*(4), 564-572.
1107 https://doi.org/10.1093/pcp/pcab011

1108 Ward, S. E., Ostle, N. J., Oakley, S., Quirk, H., Henrys, P. A., & Bardgett, R. D. (2013). Warming
1109 effects on greenhouse gas fluxes in peatlands are modulated by vegetation composition.
1110 *Ecology Letters, 16*(10), 1285-1293. https://doi.org/10.1111/ele.12167

1111 Yamada, E. A., & Sgarbieri, V. C. (2005). Yeast (Saccharomyces cerevisiae) protein
1112 concentrate: preparation, chemical composition, and nutritional and functional properties.
1113 *Journal of Agricultural and Food Chemistry, 53*(10), 3931-3936.
1114 https://doi.org/10.1021/jf0400821

1115 Yang, S.-Y., Huang, T.-K., Kuo, H.-F., & Chiou, T.-J. (2017). Role of vacuoles in phosphorus
1116 storage and remobilization. *Journal of Experimental Botany, 68*(12), 3045-3055.
1117 https://doi.org/10.1093/jxb/erw481

1118 Zacheis, A., Hupp, J. W., & Ruess, R. W. (2001). Effects of migratory geese on plant
1119 communities of an Alaskan salt marsh. *Journal of Ecology, 89*(1), 57-71.
1120 https://doi.org/10.1046/j.1365-2745.2001.00515.x

1121 Zeh, L., Igel, M. T., Schellekens, J., Limpens, J., Bragazza, L., & Kalbitz, K. (2020). Vascular
1122 plants affect properties and decomposition of moss-dominated peat, particularly at elevated
1123 temperatures. *Biogeosciences, 17*(19), 4797–4813. https://doi.org/10.5194/bg-17-4797-
1124 2020

1125 Zhang, J., Kobert, K., Flouri, T., & Stamatakis, A. (2014). PEAR: a fast and accurate Illumina
1126 Paired-End reAd mergeR. *Bioinformatics, 30*(5), 614-620.
1127 https://doi.org/10.1093/bioinformatics/btt593

1128 Zhu, Y. G., Zhao, Y., Zhu, D., Gillings, M., Penuelas, J., Ok, Y. S., Capon, A., & Banwart, S.
1129 (2019). Soil biota, antimicrobial resistance and planetary health. *Environment International,*
1130 *131*. https://doi.org/10.1016/j.envint.2019.105059

Supplementary Figures

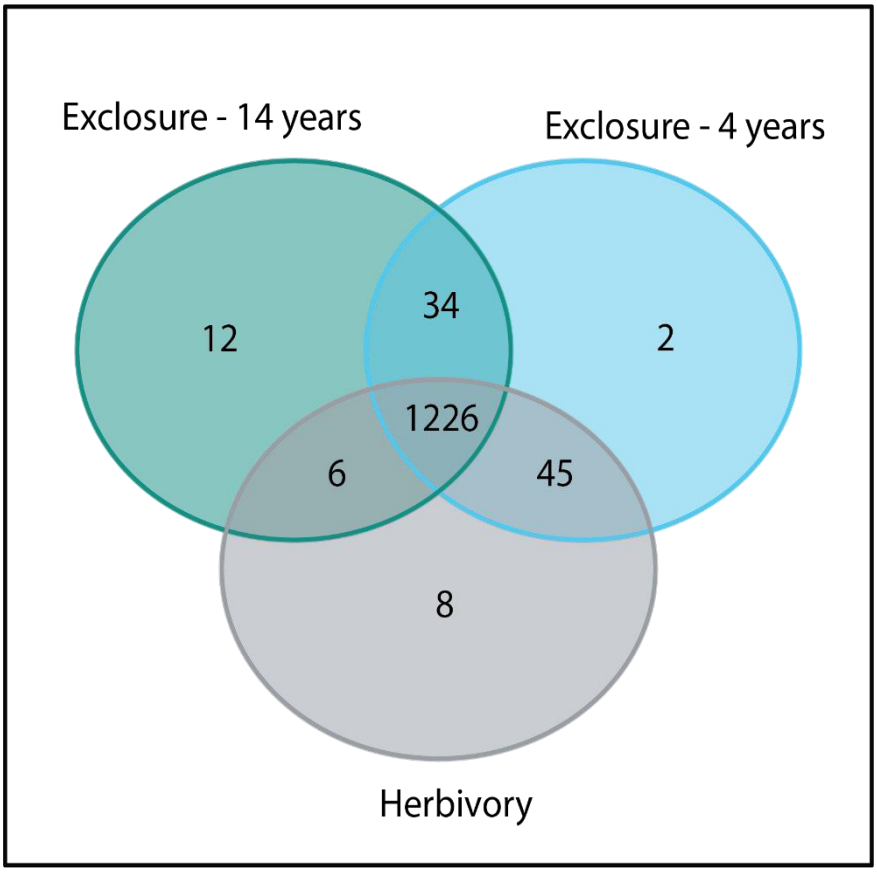

Figure S1. Venn Diagram of family occurrences at the three sites.

Of the total 1333 taxon strings with an annotation on family level, 1226 families were found at all three treatments. 12 families were specific to the Exclosure – 14 years (Ex-14) treatment, 2 families were found only at Exclosure – 4 years (Ex-4), and 8 families were present at Herbivory (Hr) only. Ex-14 and Ex-4 shared 34 families, Ex-4 and Hr had 45 common families and Ex-14 and Hr shared 6 families. Information about the treatment specific families and their abundance can be found in Supplementary Table S4. The 1226 shared families were used for further analysis (Figures 5 and 6).

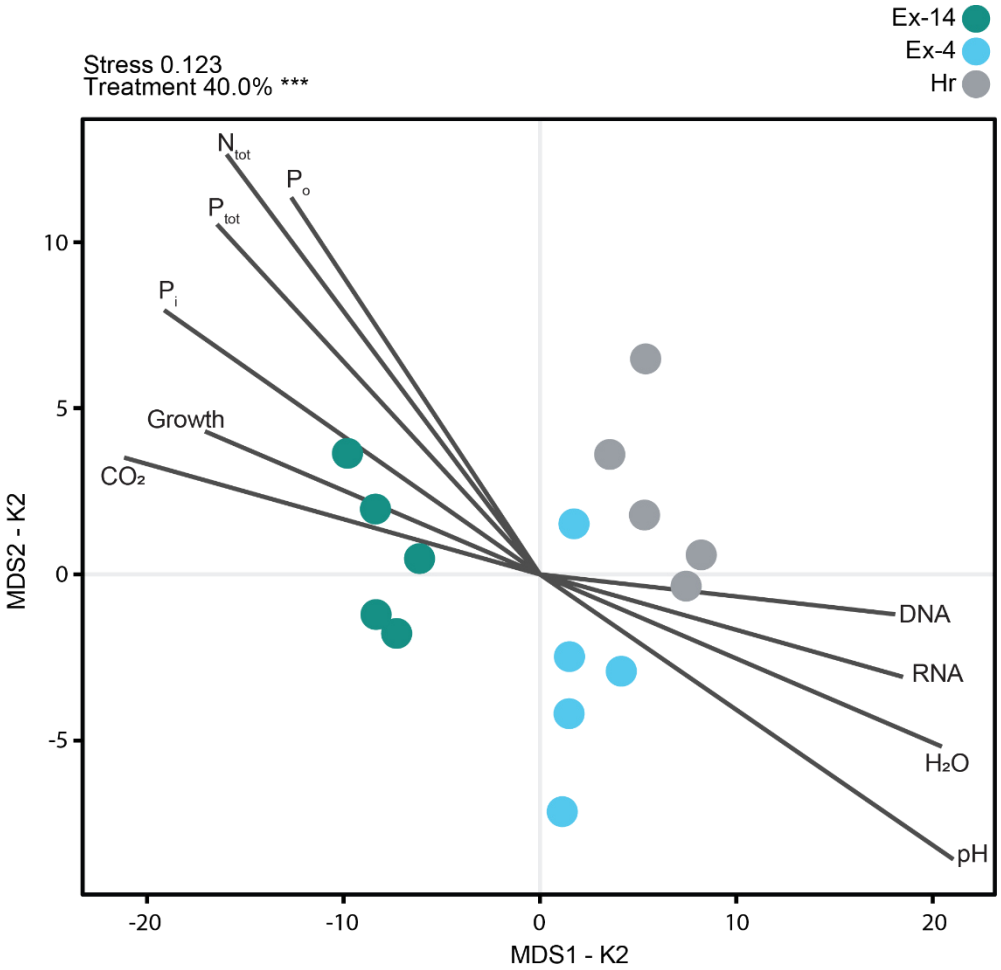

Figure S2. Differences in microbial community structure between the three treatments: Herbivory (Hr), Exclosure – 4 years (Ex-4), and Exclosure – 14 years (Ex-14). The nonmetric multidimensional scaling (NMDS) ordination plot is showing the difference between the three treatments in terms of the microbial community composition on family level, Hr (in grey), Ex-4 (in blue), and Ex-14 (in green). Each dot represents the mean of three (Hr) or four (Ex-4 and Ex-14) within-sector replicates of the three treatments as shown in Figure 1. Stress value (2 dimensions; by adding a 3rd dimension the stress was reduced to 0.074) and permutational analysis of variance (PERMANOVA) results are based on n=15 samples. The percentage indicates the variation explained by treatment and the asterisk indicates that the effect is significant (upper left corner) (p-value: *** < 0.01).

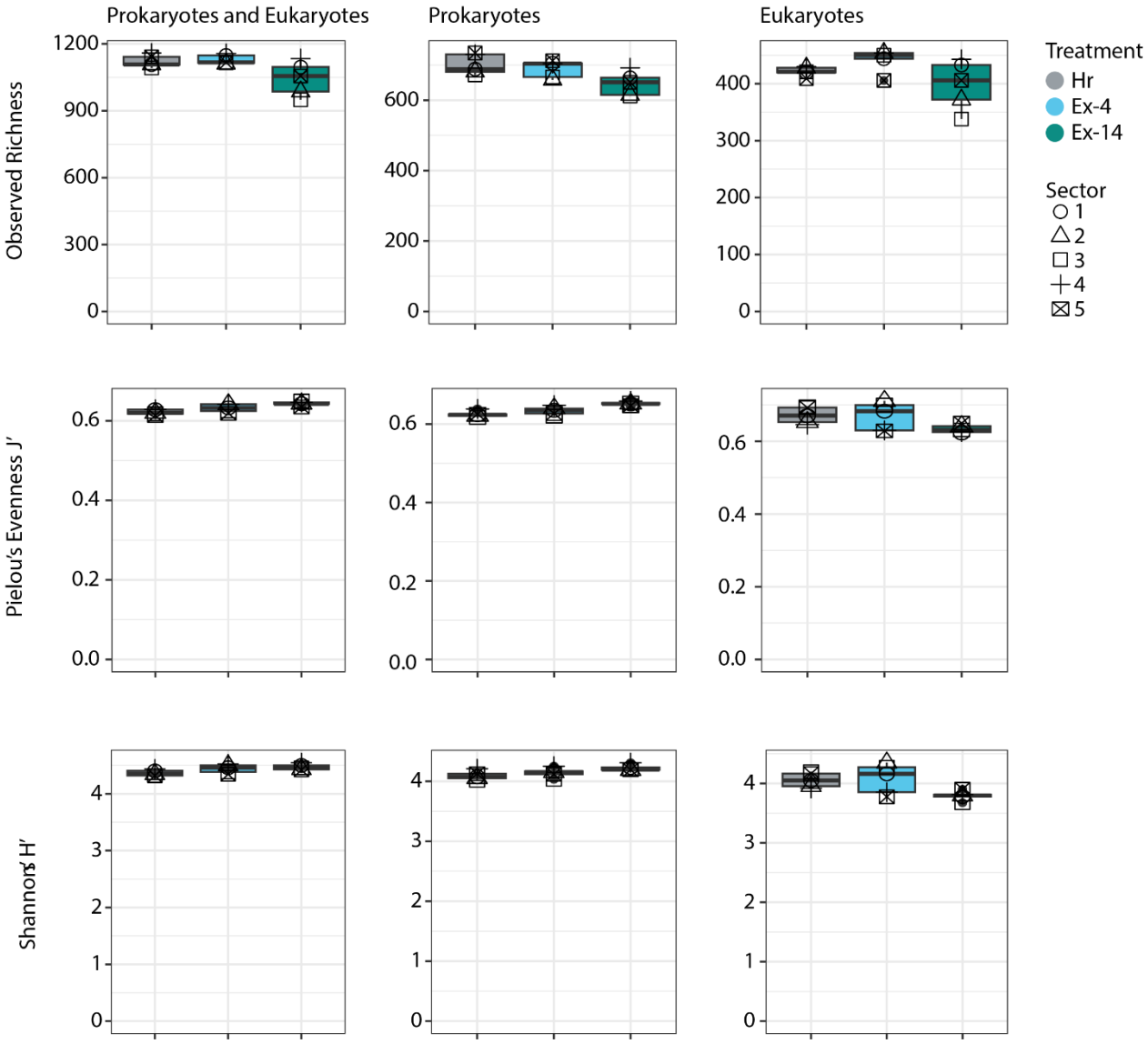

Figure S3. Alpha diversity indexes of the prokaryotic and eukaryotic microbial rRNA-based community on family level. The alpha diversities of the prokaryotic and eukaryotic microbial communities were determined by Shannon's Index H', Observed Richness and Pielou's Evenness J', comparing the three treatments, Herbivory (Hr), Exclosure – 4 years (Ex-4) and Exclosure – 14 years (Ex-14) (see Materials and Methods sections (g) Bioinformatics and (h) Statistics and Figures). Boxplots show median, 75 percentile and maximum or minimum values, while the data-points from each sector are plotted as symbols 1–5. These five datapoints are the means of the three (Hr) or four (Ex-4 and Ex-14) within sector replicates of the three treatments as shown in Figure 1. For statistical comparison of the three treatments a linear mixed-effects (LME) model was used, but no significant differences were observed.

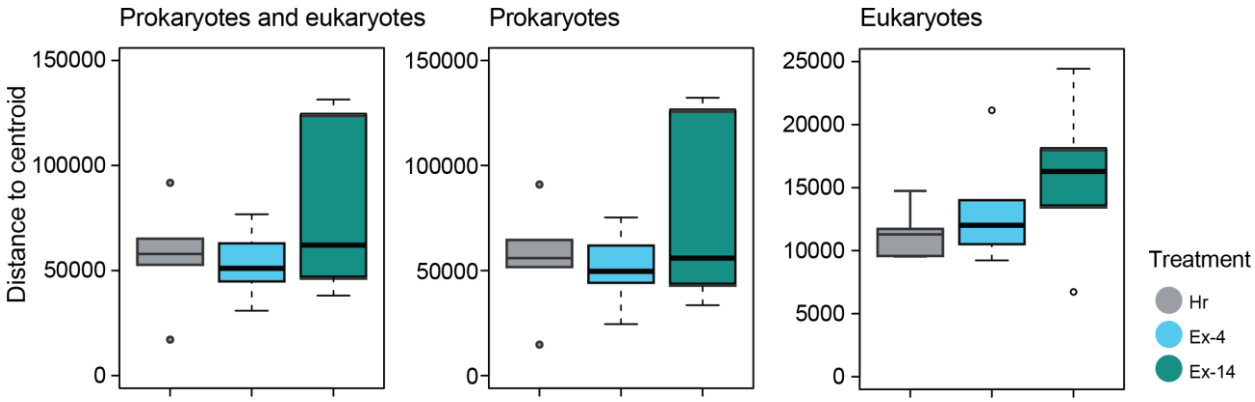

Figure S4. Beta diversity of the prokaryotic and eukaryotic microbial rRNA based community on family level. The beta diversity of the prokaryotic and eukaryotic microbial communities were based on Euclidean distance matrices, comparing the three treatments, Herbivory (Hr), Exclosure – 4 years (Ex-4) and Exclosure – 14 years (Ex-14). Boxplots show median, 75 percentile and maximum or minimum values, while the data-points from each sector are plotted as symbols 1–5. These five datapoints are the means of the three (Hr) or four (Ex-4 and Ex-14) within-sector replicates of the three treatments as shown in Figure 1. For statistical comparison of the three treatments a linear mixed-effects (LME) model was used, but no significant differences were observed.

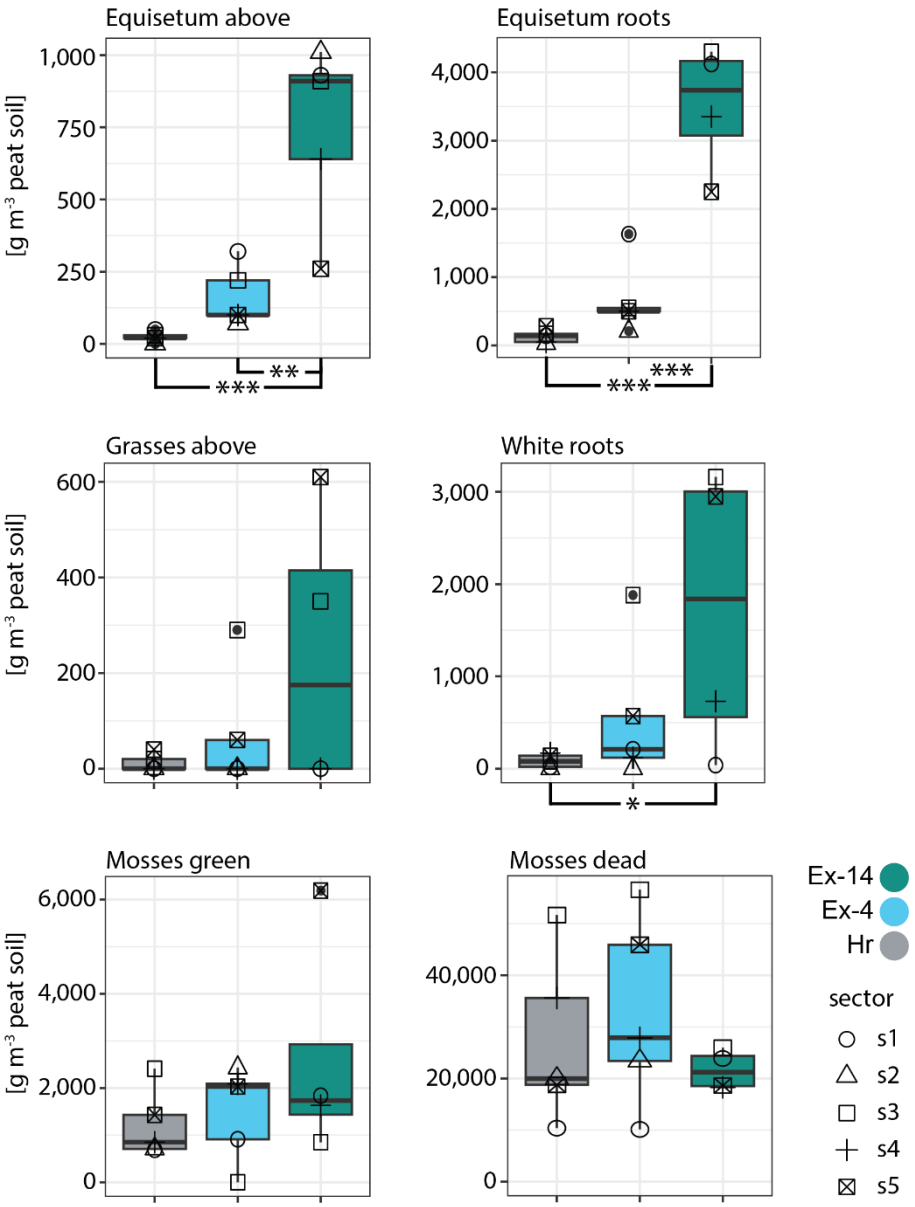

Figure S5. Plant and root biomass of peat blocks from the three treatments., Herbivory (Hr), Exclosure – 4 years (Ex-4) and Exclosure – 14 years (Ex-14) Plant and root biomass were determined by cutting 10 × 10 × 10 cm blocks from the peat soil, separating the roots from decayed and living plant material and then weighing the separated parts, comparing the three treatments, Herbivory (Hr), Exclosure – 4 years (Ex-4) and Exclosure – 14 years (Ex-14). "Above" refers to living plants from the surface of the peat block. White roots include all roots from grasses and other vascular plants, except for Equisetum. Mosses green describes the part of living mosses on top of the peat block. Boxplots show median, 75 percentile and maximum or minimum values, while the data-points from each sector are plotted as symbols 1–5. These five datapoints are the means of the three (Hr) or four (Ex-4 and Ex-14) within sector replicates of the three treatments as shown in Figure 1. For statistical comparison of the three treatments a linear mixed-effects (LME) model was used (p-value: *** < 0.001, ** < 0.01, * < 0.05, see Supplementary Table S6).

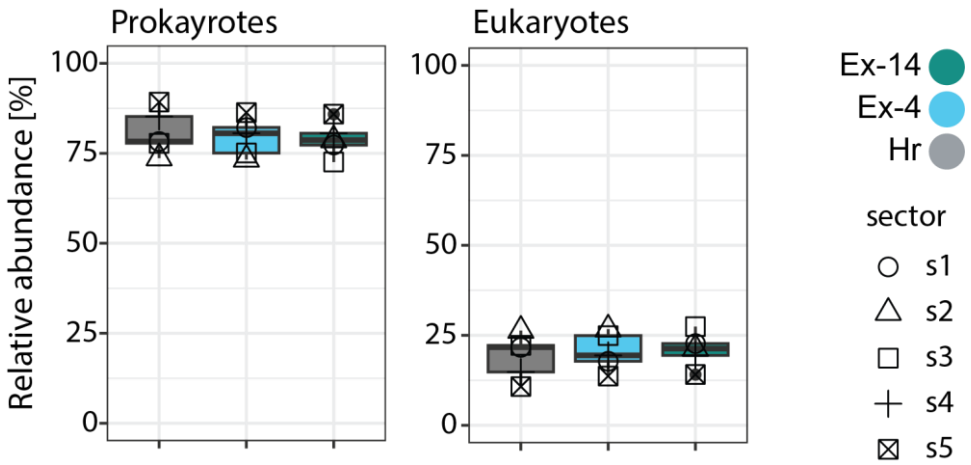

Figure S6. Relative abundance of prokaryotes and eukaryotes on domain level. The relative abundance of prokaryotes and eukaryotes based on annotations of the small subunit rRNA reads, of rarefied and filtered reads (see Materials and methods section (g) Bioinformatics), did not change when comparing the three treatments Herbivory (Hr), Exclosure – 4 years (Ex-4) and Exclosure – 14 years (Ex-14) Boxplots show median, 75 percentile and maximum or minimum values, while the data-points from each sector are plotted as symbols 1–5. These five datapoints are the means of the three (Hr) or four (Ex-4 and Ex-14) within sector replicates of the three treatments as shown in Figure 1. For statistical comparison of the three treatments a linear mixed-effects (LME) model was used, but no significant differences were observed (Supplementary Table S1).

Supplementary Tables

Supplementary Tables S1-S9 (file name: Supplementary_tables_paper2.xlxs)

This file is not included in the print version of the thesis.

Supplementary Materials and Methods

Section (d): Soil C, N, and P

Total soil carbon and nitrogen concentrations: Aliquots of dried (100 °C, 12 h) bulk peat samples were ground to fine powder using a ball-mill (MM-2000, Retsch, Germany) at 200 rpm for 5 min. Subsequently, 1-2 mg of the samples were weighed into tin capsules (IVA Analysetechnik, Germany) for measuring their total carbon (C_{tot}) and Nitrogen (N_{tot}) contents [mg g^{-1} dry weight (DW) soil] using an elemental analyzer (EA 1110, CE Instruments, Italy) that is coupled to a continuous-flow isotopic ratio mass spectrometer (IRMS, DeltaPlus, Finnigan MAT).

Total organic (Po), inorganic (Pi) and total phosphorus (P_{tot}) concentrations: Soil total phosphorus (P_{tot}) concentrations [µg g^{-1} DW soil] were measured with the ignition method modified by Kuo (1996). 50 mg of dry and finely ground samples (see above) were combusted at 450 °C for approximately 5 h (muffle device Heraeus M1100/1) releasing P_{tot} as sum of Pi and Po concentrations. Subsequently, muffled samples were extracted for 16 h with 10 ml 0.5M H_2SO_4 (sulfuric acid) and filtered (Whatman™ quantitative Ashless cellulose filter paper, grade 40). Another duplicate set of samples were directly extracted in the same manner releasing the Pi content. Po concentrations were calculated as the difference between the ignited (P_{tot}) and the non-ignited (Pi) samples. Phosphorus concentrations were analyzed in the fresh extracts by the photometric malachite-green method (D'Angelo and Crutchfield, 2001).

Total dissolved organic carbon (DOC) and total dissolved nitrogen (TDN): Dissolved C and N concentrations [mg g^{-1} DW soil] were determined in 1M KCl (Potassium chloride) extracts (soil: solution ratio of 1:15 (w/v)). Aliquots of fresh peat were extracted for 30 min on a horizontal shaker (IKA KS 501 1digital, IKA Labortechnik), then filtered (Whatman™ quantitative Ashless cellulose filter paper, grade 40) and stored frozen at -20 °C until the quantification of dissolved carbon and nitrogen concentrations via TC/TN- Analyzer (Shimadzu TOC-VCPH with TNM1 and ASI Autosampler, Shimadzu, Korneuburg, Austria).

Soil nitrate (NO_3^-), ammonium (NH_4^+), total free amino acids (TFAA) and dissolved organic nitrogen (DON) concentrations: Soil nitrate (NO_3^-) and ammonium (NH_4^+) concentrations [µg N g^{-1} DW soil] were measured from above mentioned 1M KCl extracts using photometric

assays following the method by Hood-Novotny et al., (2010). Total free amino acids (TFAA) concentrations [µg N g^{-1} DW soil] were determined via a modified version using the fluorometric OPAME method (Prommer et al., 2014). Dissolved organic nitrogen concentrations (DON) [mg g^{-1} DW soil] were calculated by subtracting the sum of ammonium (NH_4^+) and nitrate (NO_3^-) concentrations from the total dissolved N (TDN) concentration.

Section (e): Fingerprinting of soil organic matter (SOM) chemical composition:

We investigated the chemical composition of soil organic matter (SOM) using Pyrolysis-Gas Chromatography/Mass Spectromety (GC/MS). Approximately 0.1 mg of finely ground and dried sample material was weighed into pyrolysis glass tubes (DISC Pyrolysis Sample Tube, CDS Analytical). The ideal sample amounts were determined during pre-tests with the goal to yield chromatograms with the best possible peak height and separation. During pyrolization (CDS Pyroprobe 6200, CDS Analytical), samples were heated to 50 °C for 5 seconds, then the temperature was ramped up to 600 °C with a rate of 20 °C per second, where it was held for 20 seconds. The resulting pyrolysis products were flushed using 1 ml helium per minute into a GC-TOF-MS System (Pegasus BT, LECO) and the pyrolysis chamber was heated to 1000 °C for 15 seconds and flushed to clean it for the next sample. A polar column (Supelcowax 10, Sigma- Aldrich) was used to separate the pyrolysis products via gas chromatography. For this, the column was kept at 50 °C for 2 minutes and then gradually heated to 250 °C with a rate of 7 °C per minute, where the temperature was held for another 5 minutes. The ChromaTOF software (version 5.0, LECO) was used to identify peaks via their mass spectrum.

We developed a high-throughput semi-automated approach for evaluating the obtained chromatograms. We compiled a reference-sample by manually mixing together 5 mg aliquots of dried and finely ground soil powder deriving from three random samples, while each one represents a treatment type and different sampling segments. We visually checked the chromatograms of the measured three technical replicates of this sample to assure the unchanged performance of the pyrolysis over the course of two consecutive runs. Following that, we manually analyzed one of them for its chromatographic fingerprint by identifying and annotating all detectable chemical compounds. Therefore, we manually inspected each individual peak in the chromatogram and compared the mass spectrum to the suggested spectrum from the EI libraries ‘mainlib’ and ‘replib’ contained in the NIST Library of Mass Spectrometry (U.S. Department of Commerce National Institute of Standards and

Technology). To confirm the identity of the individual substances before their final assignment, we additionally considered the fit with in literature reported retention times and the compound's relative position in a sequence of other known identified compounds.

We obtained a list including unambiguously identified substances (e.g., "1-Dodecene") plus unnamed substances which we could not clearly assign to a specific compound from the NIST libraries, but which we still could identify via their unique mass spectrum (e.g., "Peak_1"). This obtained list of compounds from the "mixed reference-sample" which was used to create a project-specific compound-library. This library hence is representative for the SOM pool characteristics of the treatments in the Thiisbukta peatland (see see Supplementary Material Library File). Compounds that were not included in the project specific library were not considered for the following steps.

For the automated analysis of all samples and blanks, we used the library-matching-algorithm of the ChromaTOF software that compares all spectra contained in the project-specific substance library with with every individual peak spectrum that is found within the chromatogram of a sample. A similarity match score provides information on how well the deconvoluted mass spectrum of a certain substance matches the spectrum provided by library (min score of 1 and max score of 1000). After pre-tests and extensive reliability evaluations, the minimum similarity match threshold for automatic compound assignment was set to 800.

To ensure a high quality of this process all automatically matched and assigned (e.g., "1-Dodecene", "Peak_1", etc.) peaks were manually revised and all remaining unidentified (i.e., not matched with library) compounds confirmed. This ensures the inclusion of not-automatically assigned compounds with a similarity < 800 that were missed by the algorithm but still could manually be identified. The laborious manual revision also avoids occasionally occurring wrong assignments due to very similar spectra as e.g., can be found within long-chained-lipids. As result, we retrieved an aligned presence-absence list of all compounds that were matched to our library as well as their corresponding peak areas.

To control for a possible contamination of the pyrolysis system or glass tubes, we performed a blank correction step in which the mean areas of all found substances found in blanks were subtracted from the respective compound areas found in the samples. We then normalized

the peak areas of a sample chromatogram according to the respective amount of pyrolyzed sample and its carbon concentration. Following the assumption that the sum of all compound areas in a sample chromatogram equals its carbon content allowed us to calculate individual compound abundances [µg C mg^{-1} DW soil]. We grouped all normalized and blank corrected compound abundances according to the three treatments.

We employed the "phyloseq" package for further handling the dataset. As final quality insuring step, we transformed the areas of all compounds within the phyloseq object into relative abundances and for each sample excluded those with a lower relative abundance of < 0.1 %. This step assures, that within each sample, only compounds with a significant contribution to the respective overall sample peak area are considered. A strong correlation ($p=2.2\ e^{-16}$, $R^2=0.85$, 95 % confidence interval) confirmed, that this concomitantly resulted in the exclusion of peaks with very low signal to noise ratio (S/N). This filtering step reduced the dataset from a total of 1016 peaks to 348 compounds being considered as most impactful for the chemical SOM fingerprint.

The 348 considered substances were grouped to the compound classes "aromatics & phenols", "carbohydrates", "N-containing compounds", "lignin-derived compounds" and "lipids". This process was supported by extensive literature research or based on the respective molecular structure if no literature classification scheme was available (see Supplementary Material Library file). The additional compound class "compounds of general & unknown origin" allowed the inclusion of substances without biomarker characteristics for the aforementioned groups (e.g., "Methane, bromo-"), or substances matching the unique mass spectra of a nameless compound in our library (e.g., "Peak_1").

For statistical tests and graphical representations, we used the abundance-filtered phyloseq object with the OUT table either representing (a) the abundances of compounds [µg C mg^{-1} DW soil] when investigating differential abundance of compound classes among treatments or (b) the relative abundances of all identified compounds when illustrating the different structure of the SOM pool among treatments in a multivariate manner.

Section (f): Soil microbial parameters and characteristics

(i) Soil microbial biomass carbon (C_{mic}) and nitrogen (N_{mic}) pools

Soil microbial biomass C (C_{mic}) and N (N_{mic}) was obtained by chloroform fumigation extraction method (Brookes et al., 1982). Aliquots of approximately 2 g FW peat per sample were fumigated in a chloroform-saturated atmosphere in the dark for 48 h. Subsequently, the soils were extracted with 30 ml 1M KCl (Potassium Chloride) solution on a horizontal shaker (IKA KS 501 digital, IKA Labortechnik) for 30 min, then filtered (WhatmanTM quantitative Ashless cellulose filter paper, grade 40) and stored frozen at -20 °C until further analyses. Another duplicate set of samples was directly extracted as described above and served as negative control. Dissolved carbon and nitrogen concentrations were quantified with a TC/TN-Analyzer (Shimadzu TOC-VCPH with TNM1 and ASI Autosampler, Shimadzu, Korneuburg, Austria). MBC and MBN concentrations [mg g^{-1} DW soil] were then calculated as the difference between fumigated and non-fumigated samples and by applying an extraction conversion factor of keC/keN = 0.45.

(ii) Microbial gross- & and biomass specific growth

Microbial gross growth rates [µg C g^{-1} DW h^{-1}] on the community level are calculated via the amount of newly produced DNA during the incubation period. Therefore, the ^{18}O at % excess (this is the surplus of ^{18}O abundance relative to the corresponding natural abundance control), the ^{18}O enrichment of the sample and the constant 31.21 (describes the proportional mass of oxygen atoms in an averaged microbial DNA formula) are considered. The sample-specific relation between microbial DNA and MBC is subsequently used to convert gross DNA production into gross microbial biomass carbon production (growth). We calculated microbial mass specific growth rates [µg C g^{-1} C_{mic} h^{-1}] by relating gross growth rates to microbial biomass carbon (C_{mic}) concentrations. The turnover time [d] of the microbial community can be approached and mathematically expressed as reciprocal value of biomass specific growth (1/ mass specific growth) under the assumption of steady state conditions (this is growth rates equaling death rates). For details on calculations see Walker et al., (2018) and Canarini et al., (2021).

References

Brookes, P. C., Powlson, D. S., & Jenkinson, D. S. (1982). Measurement of Microbial Biomass Phosphorus in Soil. *Soil Biology & Biochemistry, 14*(4), 319-329. https://doi.org/10.1016/0038-0717(82)90001-3

Canarini, A., Kaiser, C., Merchant, A., Richter, A., & Wanek, W. (2019). Root Exudation of Primary Metabolites: Mechanisms and Their Roles in Plant Responses to Environmental Stimuli [Review]. *Frontiers in Plant Science, 10*. https://doi.org/10.3389/fpls.2019.00157

D'Angelo, E., Crutchfield, J., & Vandiviere, M. (2001). Rapid, sensitive, microscale determination of phosphate in water and soil. *Journal of Environmental Quality, 30*(6), 2206-2209. https://doi.org/10.2134/jeq2001.2206

Hood-Nowotny, R., Hinko-Najera Umana, N., Inselbacher, E., Oswald-Lachouani, P., & Wanek, W. (2010). Alternative Methods for Measuring Inorganic, Organic, and Total Dissolved Nitrogen in Soil. *Soil Science Society of America Journal, 74*(3), 1018-1027. https://doi.org/10.2136/sssaj2009.0389

Kuo, S. (1996). Phosphorus. In A. L. P. D.L. Sparks, P.A. Helmke, R.H. Loeppert, P. N. Soltanpour, M. A. Tabatabai, C. T. Johnston, M. E. Sumner (Ed.), *Methods of Soil Analysis: Part 3 Chemical Methods* (Vol. 5.3). Soil Science Society of America. https://doi.org/10.2136/sssabookser5.3.c32

Prommer, J., Wanek, W., Hofhansl, F., Trojan, D., Offre, P., Urich, T., Schleper, C., Sassmann, S., Kitzler, B., Soja, G., & Hood-Nowotny, R. C. (2014). Biochar decelerates soil organic nitrogen cycling but stimulates soil nitrification in a temperate arable field trial. *Plos One, 9*(1), e86388. https://doi.org/10.1371/journal.pone.0086388

Walker, T. W. N., Kaiser, C., Strasser, F., Herbold, C. W., Leblans, N. I. W., Woebken, D., Janssens, I. A., Sigurdsson, B. D., & Richter, A. (2018). Microbial temperature sensitivity and biomass change explain soil carbon loss with warming. *Nature Climate Change, 8*(10), 885-889. https://doi.org/10.1038/s41558-018-0259-x

Paper 3

Physiological temperature responses in methanogenic communities control the timing and rates of methanogenesis

Yngvild Bjørdal[1], Kathrin Marina Bender[1], Victoria Sophie Martin[2], Liabo Motleleng[1], Alena Didriksen[1], Oliver Schmidt[1], Torben Røjle Christensen[3], Maria Scheel[4], Tilman Schmider[1], Andreas Richter[2], Andrea Söllinger[1], Alexander Tøsdal Tveit[1]

[1]*Department of Arctic and Marine Biology, UiT, The Arctic University of Norway, Tromsø, Norway.*

[2]*Department of Microbiology and Ecosystem Science, Division of Terrestrial Ecosystems research, University of Vienna, Austria.*

[3] *Department of Ecoscience - Arctic Ecosystem Ecology, Aarhus University, Denmark.*

[4] *Department of Environmental Science - Environmental Microbiology, Aarhus University, Denmark.*

Abstract

Observations of higher wetland methane (CH_4) emissions during autumn cooling relative to spring warming (CH_4 emission hysteresis) have been reported in recent years, potentially conflicting with the idea that CH_4 emissions are controlled by the temperature dependency of methanogenesis. We have investigated the temporal temperature responses of microorganisms involved in CH_4 production, by simulating an Arctic growing season in temperature-ramp time-series laboratory experiments (2 °C – 10 °C – 2 °C), with 2 °C increments per week for nine weeks. Using anoxic wetland soils from high-Arctic Svalbard, we show that net CH_4 production rates are significantly higher in the second half of the temperature experiment, during cooling. This elevated net production of CH_4 corresponded with a drop in the concentrations of propionate and acetate. At the same time, the ratio of soil RNA to DNA increased, indicative of larger microbial investment into ribosomes for protein biosynthesis. The highest microbial growth rates were reached after the initiation of cooling, based on ^{18}O-H_2O incorporation into DNA, which corresponded with increasing abundances of methanogenic Archaea. We propose that the observed CH_4 emission hysteresis resulted from a combination of factors, including the warming-induced increases in methanogenesis, the thermodynamic favorability of aceticlastic methanogenesis, and increased ribosome synthesis in response to cooling to compensate for reduced catalytic activity. We repeated the experiment with wetland soils from high-Arctic Svalbard, Northern Norway, Greenland, Arctic Canada, and Germany, resulting in three out of five tested soils demonstrating sustained net CH_4 production during cooling. Our study highlights how CH_4 emissions depend both directly

on the temperature dependency of enzymatic reactions during warming and indirectly on physiological adjustments to temperature change during cooling. This demonstrates that microbial physiology must be accounted for in predictions of climate change effects on natural greenhouse gas (GHG) emissions.

Keywords

Acetate, microbial growth, protein biosynthesis, hysteresis, methane

Introduction

Methane (CH_4) is responsible for 20 % of the direct radiative forcing since 1750 and constitute a major driver for global warming (1, 2). Methanogenesis is responsible for approximately 70 % of global CH_4 emissions (1, 3). Methanogenic Archaea (methanogens), are widespread globally in anoxic environments (1, 3) such as rice paddies, landfills, lakes, and peatlands and are key microorganisms in the anoxic mineralization of organic material (1, 3). Northern peatlands constitute the largest carbon reservoir (~550 Gt), compared to other soil carbon pools, and are responsible for 11 % of global CH_4 emissions (4-6). At the low temperatures characteristic for northern peatlands, methanogenesis from acetate (aceticlastic methanogenesis) is often the dominating methanogenic pathway (7, 8).

Recently, observations were made of hysteresis in the temperature sensitivity of global wetland CH_4 emissions, including northern peatlands, meaning that emissions during cooling are higher than at the same temperatures during warming (9, 10). Modeling efforts based on a sub-Arctic peatland in northern Sweden suggested that the basis for this CH_4 emission hysteresis is the accumulation of methanogenic substrates and methanogen biomass during spring and summer warming, facilitating the higher CH_4 production rates during autumn (9). High concentrations of acetate and other short-chain fatty acids have been repeatedly observed in wetlands, including peatlands, and wetland soil incubations (8, 11-14), supporting the idea that such pools could fuel CH_4 emission hysteresis (9). Earlier observations of decreasing acetate concentrations during peat cooling (13) were in agreement with this idea. However, available data are insufficient to conclude on the link between field observations of short-chain fatty acid concentrations and CH_4 emissions (15). Thus, more detailed studies are necessary to enhance insights into the mechanisms that control temporal variability in wetland biogeochemistry, thereby enabling more accurate modeling of CH_4 emissions (10). In 2015, we observed indications of a temperature threshold for syntrophic short-chain fatty acid

oxidation and methanogenesis at 7 °C in an Arctic wetland soil from Ny-Ålesund, Svalbard (8). At temperatures below this threshold, acetate and propionate, the key intermediates in anaerobic decomposition and CH_4 production in this system, were present at several-fold higher concentrations than above. This suggested that a microbial metabolic shift due to temperature increase led to the depletion of these short-chain fatty acids, possibly hinting towards a temperature-controlled mechanism that regulate the pools of methanogenesis substrates in peatlands.

Here, based on the above-mentioned insights and three experiments using anoxic soils from the previously studied site in Ny-Ålesund, Svalbard (8) (experiment 1) and other northern and Arctic wetlands (experiments 2 and 3), we have investigated the link between hysteretic temperature sensitivity in CH_4 emissions and short-chain fatty acid consumption. Throughout experiment 1, net CH_4 and (carbon dioxide) CO_2 production rates, nucleic acid concentrations, microbial cell growth, short-chain fatty acids (including common fermentation intermediates such as acetate, propionate, and butyrate), and *mcr*A copy numbers, were monitored. In experiments 2 and 3, we monitored the net CH_4 production rates, using wetland soils from high-Arctic Svalbard, Northern Norway, Arctic Canada, Greenland, and Germany, to compare the observations from experiment 1 to other locations.

CH_4, CO_2 and short-chain fatty acids

Peat soil from Ny-Ålesund, Svalbard (experiment 1), was incubated at 2 °C for 3 months prior to initiation of the main experiment, after thawing under anoxic conditions (see Materials and Methods for further details). The aim of the pre-incubation was to obtain a functionally stable and approximately homogenous ecosystem as the basis for subsequent temperature-ramp experiments. During the last 2 months at 2 °C prior to experiment initiation, the daily net CH_4 production rate was constant at 0.06 μmol g^{-1} DW soil day^{-1} and the concentrations of acetate and propionate were approximately constant, at 2.1 mmol L^{-1} and 1.4 mmol L^{-1}, respectively, while CO_2 fluctuated between net production and net consumption (Fig. S1 and S2, and Tab. S1 and S2). This demonstrated that the microcosms were approximately stable, with a close to steady-state relationship between methanogenesis and the upstream processes supplying substrates for methanogenesis. Thus, the observed system changes during the subsequent

experimentation were interpreted as the effects of temperature change and not variation from system instability induced by sample processing or laboratory conditions.

After the pre-incubation at 2 °C, the peat soil was distributed in incubation bottles for exposure to changing temperature as shown in the experimental design overview in Fig. 1. During the initial five weeks of the experiment, the temperature was increased 2 °C per week, from 2 °C to 10 °C. During that time, the net CH_4 production rate increased 15-fold from a mean of 0.04 µmol g^{-1} DW soil day^{-1} in week 1 to 0.6 µmol g^{-1} DW soil day^{-1} in week 5 (Fig. 2A and Tab. S1). This is a much larger increase than previously observed in samples from the same wetland, where temperature increases from 2 – 10 °C resulted in up to 2.7-fold increase in the net CH_4 production rate (8). In the current manuscript we provided one week of incubation per temperature, in 2 °C increments from 2 – 10 °C (Fig. 1), while the previous experiment (8) provided more than five weeks of incubation at either 2 or 10 °C after a direct sample transfer from the pre-incubation temperature (4 °C). Thus, the observed differences between the two studies indicate a strong effect of incubation time and preceding temperatures on the outcome.

In the following four weeks, during cooling from 10 to 2 °C, we observed significantly higher (p value < 0.01) net CH_4 production rates compared to the same temperatures during warming (Fig. 2A and Tab. S1), resembling patterns of *in-situ* CH_4 emission hysteresis (9, 10). The net CO_2 production rates did not display similar hysteretic patterns as CH_4, being only higher at 2 and 6 °C during cooling than during warming (Fig. 2B and Tab. S1). CO_2 emission hysteresis has, to our knowledge, not been mentioned in literature, possibly due to the influence of plant CO_2 uptake (16, 17) or other processes on *in-situ* emission patterns. The large fluctuations in the net CO_2 production during pre-incubation, suggested that our patterns are heavily influenced by anaerobic microbial CO_2 fixation, complicating the interpretation of net CO_2 production rates.

Propionate and acetate concentrations remained stable with indications for a slight but insignificant (p.value > 0.05) increase during the first three weeks (2 – 6 °C), followed by a decreasing trend starting between week 4 and 5 (8 – 10 °C), and large significant decreases during cooling from 10 – 2 °C in week 6 to week 9 (p. value < 0.05), resulting in the near complete depletion of both fatty acids (Fig. 2C and D, and Tab. S2). The reason for the

corresponding trends of acetate and propionate might be that decreasing concentration of acetate increases the thermodynamic favorability of syntrophic propionate oxidation because acetate is a product of propionate oxidation (8). Other short-chain fatty acids such as butyrate and formate were infrequently detected, and often at concentrations close to the detection limit. This matches observations from earlier experiments using this soil, where acetate and propionate were identified to be key intermediates of anaerobic decomposition (8). Our observations are therefore in line with the many observations of high acetate concentrations in wetlands (8, 9, 11-14). Furthermore, the depletion of acetate and propionate pools during temperature decrease demonstrate that the production of these compounds are slower relative to consumption, during cooling. This could mean that the short-chain fatty acids serve as the sources for the observed hysteretic net CH_4 production rates. If so, our findings agree with recent results based on modeling where the consumption of accumulated substrates for methanogenesis including acetate were suggested as the sources for CH_4 emission hysteresis (9).

Nucleic acids and growth

RNA and DNA concentrations [ng g^{-1} DW soil] were stable in weeks 1 – 3 (2 – 6 °C), followed by a small, but insignificant (p.value > 0.05), increase at 8 and 10 °C in weeks 4 and 5 (Fig. S3 and Tab. S3). During cooling from 10 – 2 °C in weeks 6 – 9, however, DNA concentrations remained constant, while RNA concentrations increased substantially (Fig. S3 and Tab. S3). Thus, the RNA:DNA ratios were stable during warming, but increased significantly during subsequent cooling (Fig. 2E and Tab. S3). This indicated increasing cellular ribosome concentrations during cooling, because ribosomal RNA makes up the largest proportion of microbial total RNA, typically ranging from 82 – 90 % (18). Similar temperature-related changes in cellular ribosome concentrations were recently observed in methanotrophs (19) and in grassland soil communities (20). Earlier observations of temperature-induced alterations in the ribosome content of *Escherichia coli* (21) and *Chlamydomonas reinhardtii* (22) further support our assumption. These observations, across ecosystems and between species, confirm that the adjustment of cellular ribosome concentrations is a key acclimation mechanism to temperature changes in nature, the major role of which is to optimize resource allocation for growth and maintenance (21). Microbial growth, estimated from measurement of ^{18}O incorporation, from $H_2{}^{18}O$ into DNA, suggested stable, yet insignificantly changing,

153 microbial growth rates during the temperature increase from 2 – 6 °C in weeks 1, 2 and 3. This
154 was followed by increasing growth rates in week 4 and 5 (8 – 10 °C), and the highest growth
155 rates in week 6, at the initiation of cooling at 8 °C (Fig. 2F and Tab. S4). Despite the substantial
156 and significant (p.value < 0.0001) increase in growth rate from week 3 to week 6, we did not
157 observe a corresponding increase in DNA g DW soil^{-1}. However, the total amount of DNA
158 increased slightly, but insignificantly (p.value = 0.19), between week 1 and 4. This mismatch
159 between the patterns of the DNA pool size and microbial growth rates during temperature
160 increase, indicates that both the living and dead microbial biomass are likely influenced by
161 other processes than growth; for example predation, viral lysis, and a faster necromass
162 turnover as previously described (8, 23, 24). However, growth rates corresponded with
163 increased abundances of *mcrA* genes (key gene for methanogens, encoding the alpha-subunit
164 of the enzyme that catalyzes the last step of methanogenesis). This suggested that the
165 methanogen population was larger at the initiation of cooling (8 °C, week 6) than at any point
166 during warming (Fig. 2G and Tab. S5). The *mcrA* quantification further showed that the
167 methanogen population continued to increase throughout the experiment to reach its largest
168 size at the end of the cooling phase, at 2 °C, in week 9 (Fig. 2G and Tab. S5), while the overall
169 microbial growth rates (Fig. 2F and Tab. S4) and DNA concentrations (Fig. S3 and Tab. S3)
170 showed no sign of increase during cooling. This suggests that the methanogen growth rate
171 remained relatively higher than the overall community growth during cooling.

172 **Mechanisms behind CH_4 emission hysteresis**

173 A stronger temperature dependence of aceticlastic methanogens compared to other
174 community members could be the basis to our observations of acetate depletion, faster
175 growth of methanogenic Archaea relative to the overall microbial community, increased
176 cellular concentrations of ribosomes and higher net CH_4 production rates during cooling.
177 Methanogenesis has been shown to have a higher apparent activation energy (E_a = 106 kJ mol^{-1}) than other microbial processes have on average, including respiration (49 kJ mol^{-1}) and
179 hydrolysis of organic matter (54 – 125 kJ mol^{-1}) (7). This implies that the rate limiting reactions
180 in methanogenesis are more restricted by the insufficient energy of participating molecules
181 and thus, the corresponding CH_4 production rates responded more strongly to temperature
182 increase. In aceticlastic methanogenesis, acetate activation catalyzed by either acetate kinase
183 or acetyl CoA synthase is likely the rate limiting step (7). This suggests that faster acetate

activation at higher temperatures could be the trigger mechanism for the beginning trend of faster acetate consumption relative to acetate production between 8 and 10 °C (Fig. 2C and Tab. S2). Furthermore, methanogenesis from acetate becomes thermodynamically more favorable when temperatures are increasing (7), allowing for a higher energy yield per acetate consumed.

However, neither of these mechanisms can explain acetate depletion and the faster growth of aceticlastic methanogens during cooling. Thus, we propose the following scenario: The increase in kinetic and energetic potentials during warming triggers faster growth and acetate consumption of aceticlastic methanogens relative to other community members when reaching 8 – 10 °C. This leads to a larger population of methanogens that metabolize acetate faster on a per cell basis, resulting in an overall more rapid acetate consumption than production. While the faster acetate turnover and higher energy yields allow more rapid growth, the onset of cooling triggers a re-allocation of resources into ribosome synthesis to compensate for declining protein biosynthesis rates and overall lower catalytic rates during cooling. We believe that the combination of more methanogen cells and cooling compensation by ribosome synthesis, results in a sustained faster acetate consumption relative to production during cooling, thereby enabling the higher net CH_4 production rates. Our proposition implies that the combination of a sufficiently large acetate pool, thermodynamic and kinetic properties of aceticlastic methanogenesis, and the ability of the methanogens to physiologically acclimate to temperature increase and decrease, forms the basis for CH_4 emission hysteresis. However, while this narrative is logically supported by existing data and theory, specific data on methanogen rRNA transcripts to rRNA gene ratios, and data from several sites, are needed to conclude on this matter.

In 2014, Yvon-Durocher and colleagues showed that the temperature dependency of CH_4 emissions is similar, across a broad range of CH_4 emitting environments, to the temperature dependency of CH_4 production from pure cultures of methanogens. This indicates that methanogenesis often is the rate limiting step of CH_4 emissions (15). Our observations agree that the temperature dependency of methanogenesis is the major control factor for net CH_4 production rates at different temperatures. However, we also show that to predict the timing and rate of methanogenesis at different temperatures, the dynamics of substrate pools for

methanogenesis, the physiological acclimation of methanogens, and the duration of exposure to different temperatures must be considered.

Control experiments

Control experiments corroborate our findings and further improve our understanding of the system response to temperature. The incubation of control samples for four additional weeks at 6 °C and two additional weeks at 10 °C (Fig. 1) show that stronger temperature responses develop over time, as demonstrated by large increases in the net CH_4 and CO_2 production rates during the first four weeks at 6 °C and the first three weeks at 10 °C (Fig. 3A-D and Tab. S1). Also, while acetate concentrations appeared stable in the first two weeks at 6 °C, a slow reduction of the concentrations were seen after three to four weeks at 6 °C (Fig. 3E and Tab. S2), matching the increases in net CH_4 and CO_2 production during the same weeks (Fig. 3A and B), while propionate concentrations remained stable throughout the 6 °C control (Fig. 3F and Tab. S2). The estimation of microbial growth rates after three and five weeks at 6 °C demonstrated that two to four additional weeks at 6 °C is not sufficient to stimulate faster growth, indicating that further temperature increase or even more time at 6 °C would be required for microbial growth rates to increase (Fig. S4 and Tab. S4). Therefore, our observation of increasing growth rates after temperature increases to 8 °C and 10 °C seem to be induced by temperature, and are not a result of incubation time. Increasing copy numbers of *mcrA* genes were observed after three and five weeks at 6 °C (Fig. S5 and Tab. S5), corresponding to the changes in acetate concentrations and net CH_4 production rates after five weeks at 6 °C. Additionally, after three weeks at 10 °C, a substantial increase in *mcrA* was observed (Fig. S5 and Tab. S5), further matching the increase in net CH_4 production rates during the last week at 10 °C. This strongly suggests that the insignificant (p.value > 0.05) indication for increasing *mcrA* during warming from 2 – 10 °C in the main experiment (Fig. 2G) reflects faster methanogen growth, but that the incubation time has been too short to result in a significant increase. RNA and DNA concentrations, and RNA:DNA ratios stayed constant during prolonged incubation at 6 °C, contrary to the main experiment, demonstrating that the RNA increase after reaching 10 °C and the consequential increase in RNA:DNA ratios in the main experiment is a result of the temperature decrease (Fig. 3G and S6, and Tab. S3). Combined with the results from the main experiment, the observations from the control experiments allow us to propose that the observed microbial temperature responses are

results of the temperature at which the response occurs, the time spent on that temperature and the preceding temperatures.

Broader relevance

To identify whether the above-described mechanisms are relevant also in other types of wetlands and in different locations, we performed two follow-up experiments (experiments 2 and 3) with peat soils from wetlands in Canada, Norway, Greenland, Germany, and Svalbard using the same experimental design. Taking all three experiments into account, the soils from Svalbard, Norway and Canada were used in two experiments each, while samples from Greenland and Germany were used in one experiment each. Pre-incubation data from experiments 2 and 3 show that the net CH_4 production rates were overall stable at 2 °C, but with considerable variation in net production in the samples from Canada in experiment 2, and the samples from Norway in experiment 3 (Fig. S7 and S8, and Tab. S6 and S7). We observed averagely higher net CH_4 production rates during cooling compared to warming in the incubations with peat soil from Svalbard, Norway, and Greenland, but not in the incubations from Canada and Germany (Fig. 4 and Tab. S6 and S7). Only the experiments with peat soil from Svalbard and Norway showed consistent (in both experiments) and significantly higher CH_4 production rates during cooling (Fig. 4 and Tab. S1, S6, and S7). However, we would like to point out that the experiment with peat soil from Greenland resulted in higher net CH_4 production rates at all temperatures during cooling relative to the same temperature during warming, although the differences were not significant (Fig. S8 and Tab. S7). Thus, based on our observations, we propose that *in-situ* CH_4 emission hysteresis can originate from responses in anoxic processes, in line with modeling predictions (9). The substantial variation in the strength of hysteretic patterns between sites could be linked to regional variations in climate and thus corresponding differences in microbial temperature adaptation and sensitivity to temperature change (25). The sensitivity of biological processes such as CH_4 oxidation or syntrophic short-chain fatty acid oxidation to small variations in soil chemistry or stochastic variation in microbial interactions could explain differences between and within experiments that result in weaker hysteretic patterns. It is possible that such mechanisms also underlie the large variations in hysteretic CH_4 emission patterns *in-situ* (10), triggered by within-season weather changes that differ every year.

Conclusion

We conclude that CH_4 emission hysteresis (10) can be explained by a combination of the temperature dependency of methanogenesis (7, 15), thermodynamics of aceticlastic methanogenesis (7), and temporal adjustments of microbial physiology. Our study highlights that the consideration of time is fundamental for understanding CH_4 emissions because the effect of temperature on net CH_4 production rates depend on physiological responses to the preceding temperatures and the time granted for acclimation. This has large implications as the timing of CH_4 production further determines the potential influence of CH_4 oxidation, since these two processes are differently constrained by their environment. The connection between temporal physiological acclimation of microorganisms and GHG emissions is important for our understanding of microbial responses to all climate-change driven weather events, including heatwaves, droughts, and floods.

Figures

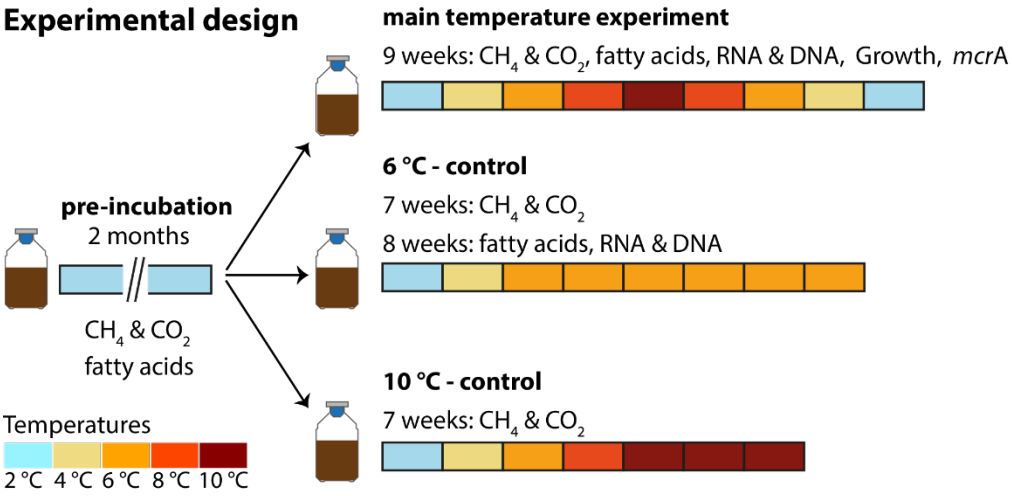

Fig. 1: Experimental design: During the 2-month pre-incubation period at 2 °C net CH_4 and CO_2 production rates, and the concentrations of fatty acids were monitored. Subsequently, the samples were divided into the main temperature experiment, the 6 °C-control, and the 10 °C-control. The main experiment lasted for 9 weeks during which the peat soils were incubated from 2 °C to 10 °C and back to 2 °C. Throughout the main experiment, net CH_4 and CO_2 production rates, the concentrations of fatty acids, RNA, and DNA, microbial growth rates, and *mcr*A copy numbers were monitored. During the 6 °C-control net CH_4 and CO_2 production rates were monitored for 7 weeks, and the concentrations of fatty acids, RNA, and DNA for 8 weeks. The 10 °C-control lasted for 7 weeks during which net CH_4 and CO_2 production rates were monitored. The colors indicate the incubation temperatures ranging from 2 °C (light blue), over 4 °C (light yellow), 6 °C (orange), and 8 °C (tomato red), to 10 °C (dark red).

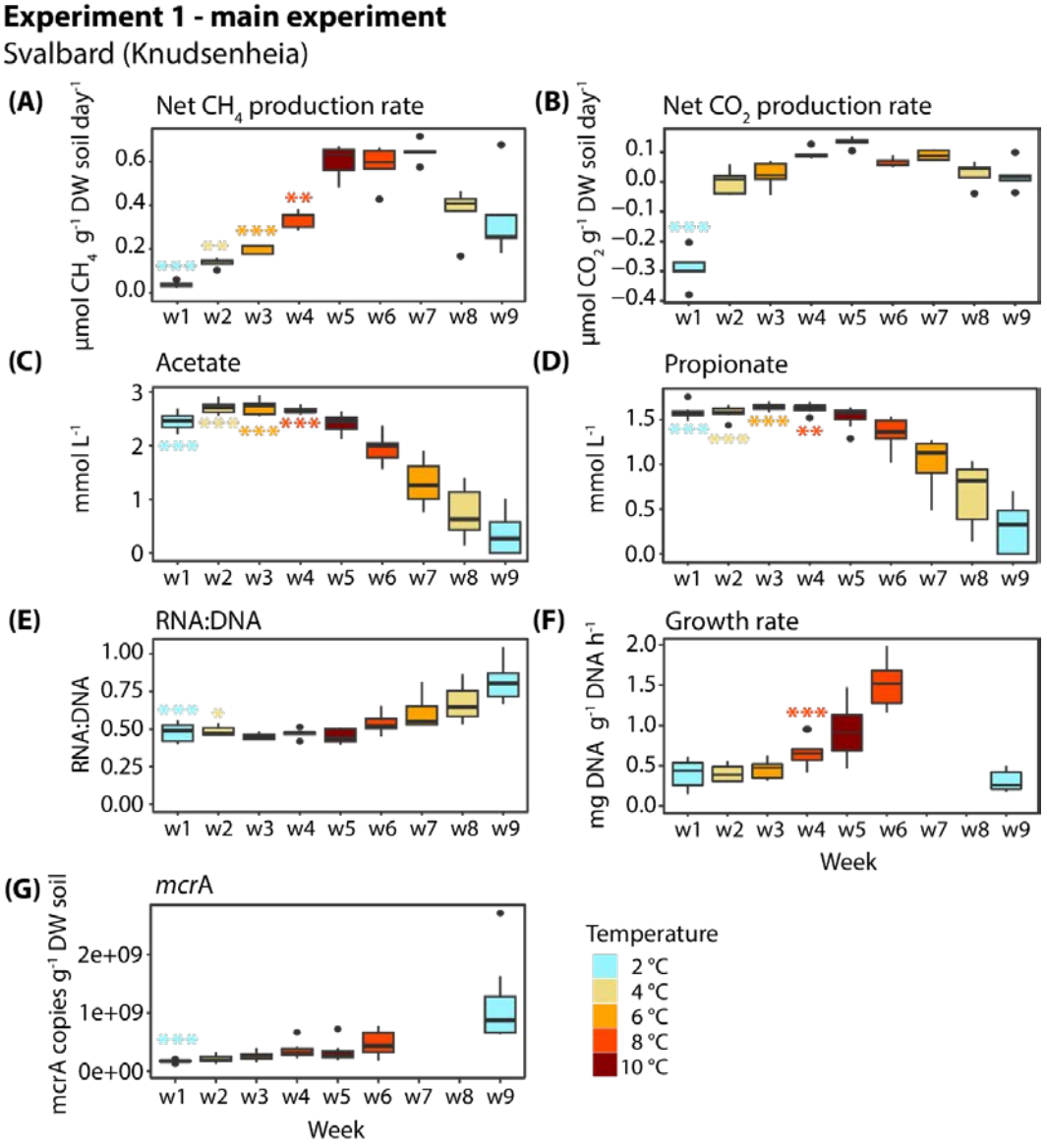

Fig. 2: During the main temperature experiment of Experiment 1 using the Svalbard peat soil weekly measurements of (A) net CH_4 [µmol CH_4 g^{-1} DW soil day^{-1}] and (B) CO_2 production rates [µmol CO_2 g^{-1} DW soil day^{-1}], concentrations [mmol L^{-1}] of the fatty acids (C) acetate and (D) propionate, (E) RNA to DNA ratios [RNA:DNA], (F) microbial growth rates [mg DNA g^{-1} DNA h^{-1}], and (G) *mcr*A gene copy numbers were obtained. Boxplots show median, 75 percentile and maximum or minimum values. The colors indicate the incubation temperatures ranging from 2 °C (light blue), over 4 °C (light yellow), 6 °C (orange), and 8 °C (tomato red), to 10 °C (dark red). A One-way ANOVA was used for the pairwise comparison of the weekly measurements. Significant differences between the same temperatures during temperature increase and temperature decrease (e.g., 2 °C during increase vs. 2 °C during decrease) are indicated by the colored asterisk inside the plots (p.value: *** < 0.001, ** < 0.01, * < 0.05; see supplementary Tab. S1-S5 for all p.values).

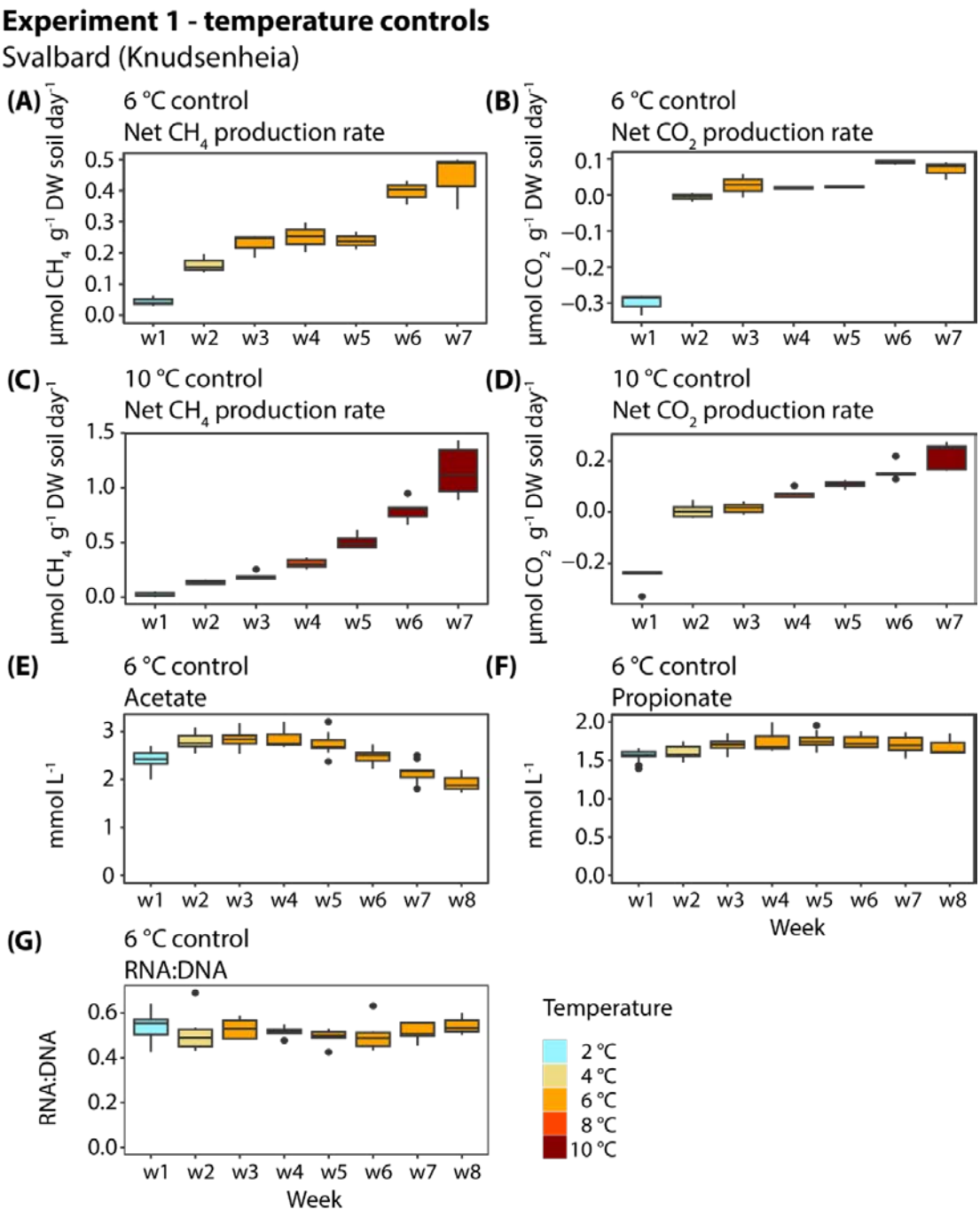

Fig. 3: During the temperature controls of Experiment 1 using the Svalbard peat soil weekly measurements of (A) net CH_4 [µmol CH_4 g^{-1} DW soil day^{-1}] and (B) CO_2 production rates [µmol CO_2 g^{-1} DW soil day^{-1}] of the 6 °C-control, and (C) net CH_4 and (C) CO_2 production of the 10 °C-control, concentrations [mmol L^{-1}] of the fatty acids (E) acetate and (F) propionate of the 6 °C-control, and (G) RNA to DNA ratios [RNA:DNA] of the 6 °C-control were obtained. Boxplots show median, 75 percentile and maximum or minimum values. The colors indicate the incubation temperatures ranging from 2 °C (light blue), over 4 °C (light yellow), 6 °C (orange), and 8 °C (tomato red), to 10 °C (dark red). A One-way ANOVA was used for the pairwise comparison of the weekly measurements (see supplementary Tab. S1, S2, and S3 for all p.values).

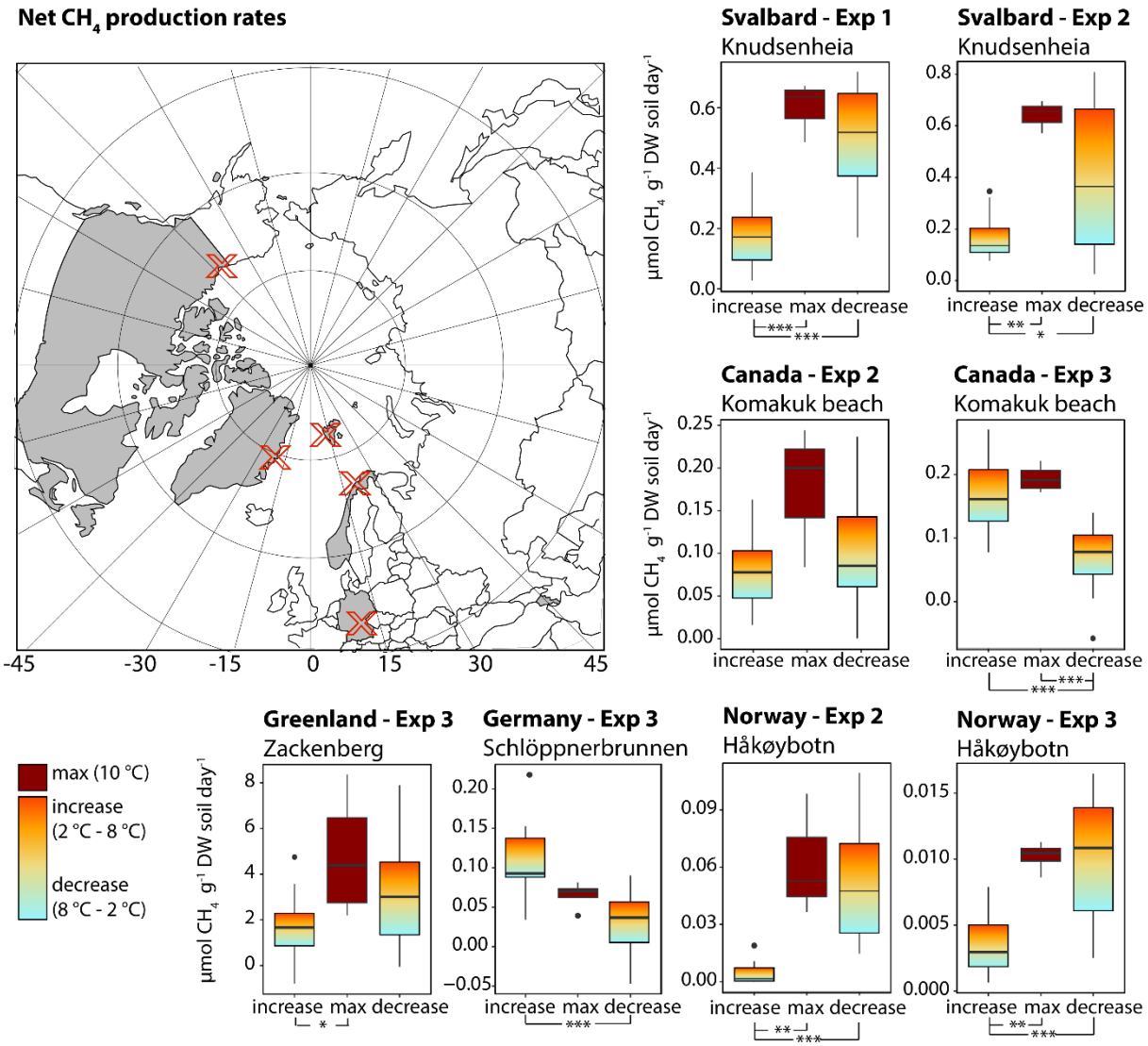

Fig. 4: Net CH_4 production rates [µmol CH_4 g^{-1} DW soil day^{-1}] during the main temperature experiment of Experiments 1, 2, and 3 (Exp 1, 2, and 3), using peat samples from Canda, Germany, Greenland, Svalbard, and Norway. The location of the four wetlands is displayed by the red 'X' on the background map of the northern hemisphere. The colors indicate the temperature phase of the experiment, the temperature increase from 2 °C to 8 °C (light blue to tomato red gradient), the temperature maximum at 10 °C (dark red), and the temperature decrease from 8 °C back to 2 °C (light blue to tomato red gradient). Boxplots show median, 75 percentile and maximum or minimum values. For statistical comparison of the three temperature phases a One-way ANOVA was used, and significant differences between the temperature phases are indicated by the asterisk below the plots (p.value: *** < 0.001, ** < 0.01, * < 0.05; see supplementary Tab. S1, S6, and S7 for all p.values).

Materials and Methods

(a) Study sites and sampling

The peat samples used for this study originated from five different locations around the northern hemisphere: (1) Canada - Komakuk beach (69°35’ north, 140°11’ west), with a pH of 5.2 and an annual mean temperature of -7.12 °C and precipitation of 302 mm; (2) Germany - Schlöppnerbrunnen (50°07’ north, 11°52’ east), with a pH of 5.0 and an annual mean temperature of 9.97 °C and precipitation of 641 mm; (3) Greenland - Zackenberg (74°28’ north, 20°35’ west), with a pH of 6.2 and annual mean temperature of -8.48 °C and precipitation of 339 mm; (4) Norway - Håkøybotn (69°37’ north, 18°47’ east), with a pH of 4.3 and an annual mean temperature of 4.22 °C and precipitation of 942 mm; and (5) Svalbard - Knudsenheia (78°55’ north, 11°56’ east), with a pH of 7.1 and an annual mean temperature of -2.86 °C and precipitation of 544 mm. The sampling was carried out at the end of the respective growing seasons; in late August and early September at the Arctic sites (Canada, Greenland, and Svalbard), in late September at the sub-Arctic site (Norway) and in late October at the temperate site (Germany). From each location, blocks of anoxic peat soil from the below the water table (20 – 40 cm depth) (20 cm × 60 cm × 20 cm) were cut with a knife. The peat blocks were placed in plastic bags, which were filled with peat water to ensure water saturation during transport and storage. The sampled peat was kept cool (4 °C) and then frozen (-20 °C) within 1 – 3 days after sampling.

(b) Sample preparation

Upon thaw, the peat soils were homogenized and mixed with water in a 1:1 ratio under anoxic conditions. This homogenized “peat soil slurry” are for simplification further on referred to as “peat soil”. The homogenization was carried out in an anaerobic glove box (Plas Labs), using a blender (Waring, CT, USA) and in some cases scissors (peat from Norway, Canada and Greenland required use of scissors). The peat soils were prepared before the start of each experiment, stored in 5 L gastight glass bottles, and left at 2 °C to stabilize for one month. The Canadian peat soil was first prepared for Experiment 2 (Exp2) and the leftovers from the same batch was re-used in Experiment 3 (Exp3). All handling of peat soil samples and distribution into bottles was performed under an atmosphere of N_2 with 10 % H_2 at 7 °C (inside an anaerobic glove box). Outside of the anaerobic glove box the headspace of the bottles was flushed with pure N_2 (Instrument Nitrogen 5.0, Linde, München, Germany), and adjusted to

1.2 bar N_2. The prepared peat soils were incubated at 2 °C for 3 months to equilibrate prior to the start of the experiments.

(c) Experiments

(i) General experimental design

A total of three temperature experiments were carried out (Exp1, Exp2, and Exp3) using peat soils obtained from five different locations (Canada, Germany, Greenland, Norway, and Svalbard). The experiments were divided into a pre-incubation phase, followed by a temperature-ramp incubation (main experiment) (Fig 1). During the last two months of the 3-month pre-incubation at 2 °C, sub-samples of the main peat batches, were monitored for net CH_4 and CO_2 production, and concentrations of short-chain fatty acids. The main batches that were later used for the main experiments were incubated together with these samples.

Following the pre-incubation, the samples from the main batches were distributed in smaller bottles which were used for the main experiment. During the main experiment the temperature was increased from the initial 2 °C, in 2 °C increments per week, up to 10 °C, and then reversed back to 2 °C, resulting in a total of nine weeks of incubation. Throughout the nine weeks of the main experiment, net CH_4 and CO_2 production rates, nucleic acid concentrations, microbial cell growth, short-chain fatty acids (including common fermentation intermediates such as acetate, propionate, and butyrate), and *mcr*A copy numbers were monitored.

(ii) Experiment 1 (Exp1)

In Exp1, peat soil from the Svalbard location was used. For the pre-incubation phase five 120 mL glass bottles (small bottles) were filled with 30 mL of peat soil for gas sampling and two 120 mL bottles were filled with 80 mL of peat soils for sampling, from the previously prepared 5 L bottle (main batch). The bottles were closed with gas-tight rubber stoppers (Butyl stoppers, Glasgerätebau Ochs, Bovenden/Lenglern, Germany) and secured with crimp caps (Thermo Fisher, MA, USA). Two times per week, 0.5 mL gas samples for GC measurements (explained in section (d) Gas measurements.) and 0.5 mL of peat water for short-chain fatty acid measurements was sampled. Water was sampled from the aqueous phase of the peat soil after settling in the small bottles by using a hollow sterile disposable syringe needle

(0.80 x 120 mm, Sterican®, B.Braun, Melsungen, Hessen, Germany) to penetrate the rubber stopper.

Following the pre-incubation, a total of 13, 120 mL glass bottles were filled with 30 mL peat soil and used for gas sampling during the main experiment. Five of these 13 bottles were used for the main experiment (2 °C to 10 °C to 2 °C). Another five bottles were used for the 10 °C-control (2 °C to 10 °C, in weekly increments of 2 °C, over 7 weeks), and three bottles were used for the 6 °C-control (2 °C to 6 °C, in weekly increments of 2 °C, over 7 to 8 weeks) (2 °C to 6 °C). Gas samples were taken three times per week. Additionally, six 500 mL tap-bottles (Glasgerätebau Ochs, Bovenden/Lenglern, Germany) were filled with 300 mL slurry, closed with gas-tight rubber stoppers (Bromobutyl Rubber stopper DURAN®, DWK Life Sciences, NJ, USA) and secured with screw caps (Glasgerätebau Ochs, Bovenden/Lenglern, Germany), and used for peat soil sampling. Three of the tap-bottles were used for the main experiment and three tap-bottles were used for the 6 °C-control. Four times per week, peat soil was collected for extraction of nucleic acids and for pore water extraction used for the measurement of short-chain fatty acids. Once per week, until week 6 (8 °C – cooling phase) of the main experiment, peat soil samples were taken for the determination of cell growth and dry weight. Additional, samples were taken in week 5 (at 6 °C) of the 6 °C-control for the same purpose. Due to technical issues, we were not able to determine growth rates from the tap bottles at the temperatures 6, 4 and 2 °C during cooling. Instead, peat soil was sampled from the gas sampling bottles after the end of the experiment in week 9 (2 °C) and used for growth determination. The same was done for the gas sampling control bottles (6 °C and 10 °C) at the end of the control measurements in week 7.

During the main experiment, slurry was sampled from the tap-bottles. Prior to sampling we ensured a slight overpressure in the bottles, using pressurized N_2, before samples were collected by opening the tap of the bottle. Approximately 1.5 mL of peat soil was sampled from each replicate for analysis of short-chain fatty acids and nucleic acids extractions. For dry weight and cell growth estimation, 0.5 mL and 0.3 – 0.35 mL of peat soil were sampled from each replicate, respectively. Samples for the analysis of fermentation intermediates, dry weight and cell growth were prepared for further use immediately after sampling. Peat soil sampled for nucleic acid extractions was immediately frozen in liquid N_2 and stored at -80 °C

426 until further processing. Sampling of peat soils from the gas sampling bottles was done by
427 pipetting after the bottle was opened at the end of the experiment.

428 *(iii) Experiment 2 (Exp2)*

429 In Exp2 peat soils from the locations in Canada, Norway and Svalbard were used. For the pre-
430 incubation, three 120 mL bottles from each location were filled with 30 mL peat soil (total of
431 nine bottles) and sampled for gas once per week. For the main experiment in total nine 120
432 mL bottles were filled with 30 mL of peat soil, hence three per location. The net CH_4
433 production rate) was measured three times per week throughout the main experiment. Gas
434 was sampled as explained in section (d) Gas measurements.

435 *(iv) Experiment 3 (Exp3)*

436 Peat soils from the sampling locations in Canada, Germany, Greenland, and Norway were used
437 for Exp3. For the pre-incubation four 120 mL bottles from each location were filled with 20 –
438 25 mL of peat soil and monitored for net CH_4 production rates two times per week. For the
439 main experiment, four small bottles were prepared with 25 mL peat soil from each location
440 and used for gas sampling two times per week. Gas was sampled as explained in section (d)
441 Gas measurements.

442 **(d) Gas measurements**

443 Gas (0.25 mL in Exp1 and 0.5 mL in Exp2 and Exp3) was sampled from the headspace of the
444 bottles with a gastight syringe (Pressure-Lok® Precision Analytical Syringe, A-2 series, VICI
445 Precision Sampling, Schenkon, Switzerland) and sideport needle (Luer Needles A-2, VICI
446 Precicion Sampling, Schenkon, Switzerland). Gas samples were manually injected into a gas
447 chromatograph (GC) (SRI 8610C gas chromatograph, SRI Instrument, CA, USA) with 8600-PKDC
448 3 cm 9'Haysep D Column 80/100 mesh for measurement of CH_4 and CO_2 concentrations (ppm).
449 We used H_2 (Laboratory Hydrogen 5.5, Linde, München, Germany) as carrier gas and the oven
450 temperature was set to 40 °C. The gases were detected on a flame-ionization detector (FID),
451 set to 380 °C, preceded by a hydrogenating reactor converting the CO_2 into CH_4. The program
452 PeakSimple v 4.88 was used to integrate the peak areas and a standard curve was prepared
453 for quantification of the data. CH_4 and CO_2 concentrations were calculated by comparing the
454 peak area to the standard curve resulting in the gas concentration (ppm) in the headspace of
455 the bottles. The results were adjusted for dissolved gas in the liquid phase using Henry's Law

456 the incubation temperature, the pressure in the bottle, and the volume of removed gas for
457 each measurement, as previously described (8). This allowed the calculation of the total
458 masses of CH_4 and CO_2. Net CH_4 and CO_2 production rates ([µmol CH_4 g^{-1} DW soil day^{-1}] and
459 [µmol CO_2 g^{-1} DW soil day^{-1}]) were estimated by linear regression for each week and
460 temperature.

461 **(e) Short chain fatty acids measurements**

462 *(i) Pore water extraction*

463 After sampling, peat soil samples were transferred to 1.5 mL Eppendorf tubes and
464 centrifugated at 4 °C and 16100 rcf for 7 minutes. The supernatant (pore-water) was
465 transferred into filter tubes and filtered through a 0.2 µm plunge filter (Syringeless filter
466 Devise, Mini-UniPrep™, PVDF filter media with polypropylene housing, Whatman™,
467 Maidstone, UK). The filtrate was stored at -80 °C until further processing.

468 *(ii) Pore-water analyses of the short chain fatty acids acetate and propionate*

469 High pressure liquid chromatography (HPLC) was used to analyse the pore-water for the
470 presence and concentration of short chain fatty acids**.** The measurement was performed on a
471 Waters 2690 separation module HPLC chromatograph (Waters Alliance, Milford, USA) with
472 Aminex Resin-Baced HPX-87H Column, 300 x 7,8 mm (Bio-Rad, Ca, USA) and a 996 Photodiode
473 Array (PDA) detector (Waters Alliance, Milford, USA) (wavelength: 210 λ). The software
474 Empower 2 software Build 2154, feature release 5 (Waters Alliance, Milford, USA) was used
475 to analyse the data. The results were related to standard stock solutions for ion
476 chromatography (Sigma Aldrich, Munich, Germany), milli-Q water was used as blank. The
477 instrument ran with a mobile phase containing 2.5 % Acetonitrile (CH_3CN) (HPLC quality;
478 Merck, Hessen, Germany) and 97.5 % MQ water with 0.005 M H_2SO_4 (VWR, PA, USA). The
479 column had a temperature of 60 °C and the sample a temperature of 10 °C. The flow rate of
480 the mobile phase was at 0.6 mL per minute. Samples were collected and injected to the
481 column automatically using 20 µL sample per injection.

482 The concentrations of the short chain fatty acids were estimated by comparing the peak area
483 given by the program Empower 2 and certified standards for each metabolite. The molecular
484 mass of each compound was used to convert the results into mmol L^{-1}.

(f) DNA and RNA extraction

Total nucleic acids (TNA) were isolated from the peat soils using phenol/chloroform extraction as previously shown (8). Prior to the extractions, the samples were ground to a fine powder in liquid N_2. Approximately 0.2 g of the material was transferred into each lysing tube for extraction (Lysing matrix E tubes, MB biomedicals, CA, USA).

A CTAB buffer, phosphor buffer and phenol:chloroform:isoamylalcohol (25:24:1) (Sigma Aldrich, Munich, Germany) was used to lyse the cells in addition to a mechanical bead beating. The TNA was then extracted with phenol:chloroform:isoamylalcohol (25:24:1) and chloroform:isoamylalcohol (24:1) (Sigma Aldrich, Munich, Germany).

TNA was subsequently precipitated using glycogen (Invitrogen, Thermo Fisher, Waltham, MA, USA) and Polyethylenglycol 6000 (PEG-6000) (Sigma Aldrich, Munich, Germany) as precipitation agents. The final precipitate was washed with ethanol and diluted in nuclease free water (Invitrogen, Thermo Fisher, Waltham, MA, USA). RiboLock RNase Inhibitor (Thermo Fisher, Waltham, MA, USA) was added to the extract. DNA and RNA concentrations were determined using a Qubit 2.0 fluorometer and the Qubit™ dsDNA HS Assay Kit (Thermo Fisher, Waltham, MA, USA). The quality of the TNA was controlled by gel electrophoresis (agarose gel with GelRed)

(h) Microbial cell growth

We measured microbial cell growth rates [ng DNA g^{-1} DW soil h^{-1}] using the substrate-independent incorporation of the stable oxygen isotope ^{18}O from ^{18}O-labelled water (^{18}O-H_2O) (Elementex, Gunnislake, England) into newly formed microbial DNA (26, 27). Peat soil samples of 0.3 – 0.35 mL were supplemented with 0.12 – 0.14 mL of 98 at % (atom percent) ^{18}O-H_2O, resulting in an enrichment of approximately 30 at % in each sample. A second natural abundance control of each sample was prepared using the same amount of molecular grade non-labelled water. The samples were incubated in gas-tight headspace vials for two days at the respective temperatures of the experiment from which the samples were collected. The incubation and microbial cell growth was stopped by shock-freezing the samples in liquid N_2. DNA from the frozen samples was extracted using the Fast DNA™ SPIN kit for Soil (MP Biomedicals, CA, USA) following the manufacturer's instructions. The DNA concentrations [ng g^{-1} DW soil] were measured by Qubit™ dsDNA HS Assay Kit

(Thermo Fischer, Waltham, MA, USA) and used as an estimate for cell number. The quality of the DNA was controlled by running a gel electrophoresis (agarose gel with GelRed). We used a thermochemical elemental analyser (TC/EA, Thermo Fisher, Waltham, MA, USA) coupled via a Conflo III open split system (Thermo Fisher, Waltham, MA, USA) to a Delta V Advantage Isotope Ratio Mass Spectrometer (Thermo Fisher, Waltham, MA, USA) to determine oxygen content and ^{18}O abundance in the DNA extracts. The abundance of ^{18}O in the DNA of the labelled peat soil samples and the natural abundance controls was used to estimate the amount of newly replicated DNA and cell division during the two days of incubation. The equation depicted below was used to calculate the estimated amount of new oxygen incorporated to the DNA (O DNA produced [µg]). The difference of ^{18}O measured in the labelled peat samples and the natural abundance controls (new ^{18}O [at %]), the measured level of oxygen in the samples (DNA O [µg]), and the total ^{18}O enrichment in at % (enrichment [at %]) was used in the calculation. By multiplying O DNA produced with the content of oxygen in DNA ([weight %], 31.1981 %) and correct for sample volume, soil dry weight (DW) [g] and incubation time [h], we obtained an estimate for newly produced DNA per soil dry weight and time [ng DNA g^{-1} DW h^{-1}]. The cellular growth rates were expressed as the level of newly produced DNA per total DNA content (measured on Qubit) in the samples and given as mg DNA g^{-1} DNA h^{-1}.

$$\textbf{\textit{Equation: }} O\ DNA\ produced\ [\mu g] = DNA\ O\ [\mu g] \times \frac{new\ ^{18}\mathrm{O}\ [\mathrm{at\%}]}{\mathrm{enrichment}\ [\mathrm{at\%}]}$$

(g) qPCR

Using the DNA obtained from the growth experiments, copy numbers of mcrA were quantified on a Bio-Rad CFX96 C1000 Touch Real-Time PCR detection system. The primer combination used was Mlas (5´-GTGGTGTMGGDTTCACMCARTA-3´) and mcrA rev (5´-CGTTCATBGCGTAGTTVGGRTAGT-3´) (28). Standard curves were based on pGEM-T plasmids (Promega) with mcrA gene inserts from Methanosarcina barkeri CM1 (10x dilution series from 106 to 101 copies per µL, all standards showing efficiency of 90 – 93 %). Each run included extraction and PCR negative controls. PCR inhibition was checked using a dilution series of extracts from 1:10 to 1:100. All standards, controls, samples, and sample dilutions were run in duplicate or triplicate. Each 20 µL reaction mixture was composed of 10 µL SsoFast EvaGreen 2 x master mix containing SYBR-Green, 0.8 µL of each 10 µM primer solution for a

final concentration of 400 nM, 3 µL DNA template solution, and 5.4 µL molecular-grade H_2O. The qPCR protocol consisted of (1) 95 °C polymerase activation for 5 min, followed by (2) 40 PCR cycles consisting of (a) denaturation for 5 s at 95 °C (b) annealing 57 °C for 30 s (temperatures in Table 3) (c) elongation for 20 s at 72 °C, and (d) fluorescence measurement after 3 s at 80 °C. Each qPCR run was concluded with (3) a stepwise melting curve from 65 °C to 95 °C with 0.5 °C increment and fluorescence measurement after 5 s, which was used to check for primer specificity.

(i) Peat soil pH and gravimetric water content [%]

Peat soil pH were measured in samples taken at the start of the experiments. We used a portable field pH meter (Multi 350i, WTH, Weilheim, Germany) to measure the pH in the peat soil samples after homogenization for pre-incubation. In Exp 1, gravimetric water contents [%] in the peat soil sampling bottles were measured every week until week 6, and once in week 9, by drying 0.5 mL slurry at 60 °C for 24 h and reweighing them. Additionally, for all experiments the gravimetric water content [%] of the peat soils in the bottles used for gas sampling was estimated at the end of the experiments by drying the bottle content at 80 °C for 96 h and reweighing.

(j) Statistics and Figures

We used R v4.3.0 (29) for statistical testing and graphical display of the results. All figures were adjusted graphically using Adobe Illustrator v26.0.1.

One-way ANOVA

We performed a One-way ANOVA for the pairwise comparison of the incubation weeks (formula: variable ~ week) and a second One-way ANOVA for statistical testing of the temperature phases (temperature increase vs decrease) (formula: variable ~ phase). The core R function *aov* was used to perform the testing. The p.values were adjusted with Tukey's Honest Significant Difference (HSD) test post hoc to the ANOVA using the function *emmeans* implemented in the R package emmeans v1.8.7 (github.com/rvlenth/emmeans) (formula: anova results, ~ week or phase), followed by the core R function *pairs* (formula: emmeans results, adjust = "tukey).

Figures

Map: The top-view map of the northern hemisphere in Fig. 4 was created with the R packages ggplot2 v3.4.2 (github.com/tidyverse/ggplot2), sf v1.0-14 (github.com/r-spatial/sf/), and oce v1.8-1 (dankelley.github.io/oce/).

Box-plots: The box-plot figures were created with ggplot2 v3.4.0 (github.com/tidyverse/ggplot2).

References

1. Lyu Z, Shao N, Akinyemi T, Whitman WB. Methanogenesis. Current Biology. 2018;28(13):R727-R32.
2. Mar KA, Unger C, Walderdorff L, Butler T. Beyond CO_2 equivalence: The impacts of methane on climate, ecosystems, and health. Environmental Science & Policy. 2022;134:127-36.
3. Conrad R. The global methane cycle: recent advances in understanding the microbial processes involved. Environmental Microbiology Reports. 2009;1(5):285-92.
4. Abdalla M, Hastings A, Truu J, Espenberg M, Mander Ü, Smith P. Emissions of methane from northern peatlands: a review of management impacts and implications for future management options. Ecology and Evolution. 2016;6(19):7080-102.
5. Harris LI, Richardson K, Bona KA, Davidson SJ, Finkelstein SA, Garneau M, et al. The essential carbon service provided by northern peatlands. Frontiers in Ecology and the Environment. 2022;20(4):222-30.
6. Yu Z, Joos F, Bauska TK, Stocker BD, Fischer H, Loisel J, et al. No support for carbon storage of >1,000 GtC in northern peatlands. Nature Geoscience. 2021;14(7):465-7.
7. Conrad R. Complexity of temperature dependence in methanogenic microbial environments. Frontiers in Microbiology. 2023;14:1232946.
8. Tveit AT, Urich T, Frenzel P, Svenning MM. Metabolic and trophic interactions modulate methane production by Arctic peat microbiota in response to warming. Proceedings of the National Acadamy of Sciences. 2015;112(19):E2507-E16.
9. Chang KY, Riley WJ, Crill PM, Grant RF, Saleska SR. Hysteretic temperature sensitivity of wetland CH_4 fluxes explained by substrate availability and microbial activity. Biogeosciences. 2020;17(22):5849-60.
10. Chang KY, Riley WJ, Knox SH, Jackson RB, McNicol G, Poulter B, et al. Substantial hysteresis in emergent temperature sensitivity of global wetland CH_4 emissions. Nature Communications. 2021;12(2266).
11. Kuzmina DM, Lim AG, Loiko SV, Shefer N, Shirokova LS, Julien F, et al. Dispersed ice of permafrost peatlands represents an important source of labile carboxylic acids, nutrients and metals. Geoderma. 2023;429(116256).
12. Tveit A, Schwacke R, Svenning MM, Urich T. Organic carbon transformations in high-Arctic peat soils: key functions and microorganisms. The ISME Journal. 2013;7(2):299-311.
13. Duddleston KN, Kinney MA, Kiene RP, Hines ME. Anaerobic microbial biogeochemistry in a northern bog: Acetate as a dominant metabolic end product. Global Biogeochemical Cycles. 2002;16(4):1063.
14. Brigham BA, Montero AD, O'Mullan GD, Bird JA. Acetate Additions Stimulate CO_2 and CH_4 Production from Urban Wetland Soils. Soil Science Society of America Journal. 2018;82(5):1147-59.
15. Yvon-Durocher G, Allen AP, Bastviken D, Conrad R, Gudasz C, St-Pierre A, et al. Methane fluxes show consistent temperature dependence across microbial to ecosystem scales. Nature. 2014;507(7493):488-91.

16. Sjögersten S, van der Wal R, Loonen MJ, Woodin SJ. Recovery of ecosystem carbon fluxes and storage from herbivory. Biogeochemistry. 2011;106(3):357-70.
17. Bon MP, Hansen BB, Loonen MJJE, Petraglia A, Bråthen KA, Böhner H, et al. Long-term herbivore removal experiments reveal different impacts of geese and reindeer on vegetation and ecosystem CO_2-fluxes in high-Arctic tundra [Preprint]. bioRxiv. 2023.
18. Blazewicz SJ, Barnard RL, Daly RA, Firestone MK. Evaluating rRNA as an indicator of microbial activity in environmental communities: limitations and uses. The ISME Journal. 2013;7(11):2061-8.
19. Tveit AT, Söllinger A, Rainer EM, Didriksen A, Hestnes AG, Motleleng L, et al. Thermal acclimation of methanotrophs from the genus Methylobacter. The ISME Journal. 2023;17(4):502-13.
20. Söllinger A, Séneca J, Borg DM, Motleleng LL, Prommer J, Verbruggen E, et al. Down-regulation of the bacterial protein biosynthesis machinery in response to weeks, years, and decades of soil warming. Science Advances. 2022;8(12).
21. Mairet F, Gouzé J-L, de Jong H. Optimal proteome allocation and the temperature dependence of microbial growth laws. npj Systems Biology and Applications. 2021;7(1):14.
22. Hessen DO, Hafslund OT, Andersen T, Broch C, Shala NK, Wojewodzic MW. Changes in Stoichiometry, Cellular RNA, and Alkaline Phosphatase Activity of Chlamydomonas in Response to Temperature and Nutrients. Frontiers in Microbiology. 2017;8.
23. Erktan A, Or D, Scheu S. The physical structure of soil: Determinant and consequence of trophic interactions. Soil Biology and Biochemistry. 2020;148.
24. Geisen S, Hu S, dela Cruz TEE, Veen GF. Protists as catalyzers of microbial litter breakdown and carbon cycling at different temperature regimes. The ISME Journal. 2021;15(2):618-21.
25. Marasco R, Fusi M, Coscolín C, Barozzi A, Almendral D, Bargiela R, et al. Enzyme adaptation to habitat thermal legacy shapes the thermal plasticity of marine microbiomes. Nature Communications. 2023;14(1045).
26. Spohn, M., Klaus, K., Wanek, W., & Richter, A. Microbial carbon use efficiency and biomass turnover times depending on soil depth – Implications for carbon cycling. Soil Biology & Biochemistry. 2016, 96, 74-81.
27. Walker, T. W. N., Kaiser, C., Strasser, F., Herbold, C. W., Leblans, N. I. W., Woebken, D., Janssens, I. A., Sigurdsson, B. D., & Richter, A. Microbial temperature sensitivity and biomass change explain soil carbon loss with warming. Nature Climate Change. 2018, 8(10), 885-889.
28. Steinberg, L.M. and J.M. Regan, Phylogenetic Comparison of the Methanogenic Communities from an Acidic, Oligotrophic Fen and an Anaerobic Digester Treating Municipal Wastewater Sludge. Applied and Environmental Microbiology, 2008. 74(21): p. 6663-6671
29. R Core Development Team, R: A Language and Environment for Statistical Computing Vienna, Austria: R Foundation for Statistical Computing.

Figure Supplement:

Experiment 1 - pre-incubation
Svalbard (Knudsenheia)

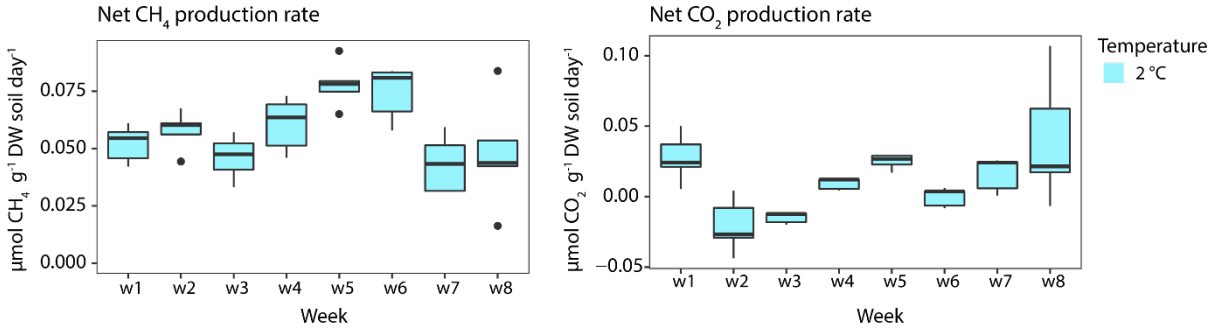

Fig. S1: Weekly net methane (CH_4) [µmol CH_4 g^{-1} DW soil day^{-1}] and net carbon dioxide (CO_2) [µmol CO_2 g^{-1} DW soil day^{-1}] production rates during the pre-incubation of Experiment 1, using the Svalbard peat samples. The color indicates the pre-incubation temperature at 2 °C (light blue). Boxplots show median, 75 percentile and maximum or minimum values. A One-way ANOVA was used for the pairwise comparison of the weekly measurements (see supplementary Tab. S1 for all p.values).

Experiment 1 - pre-incubation
Svalbard (Knudsenheia)

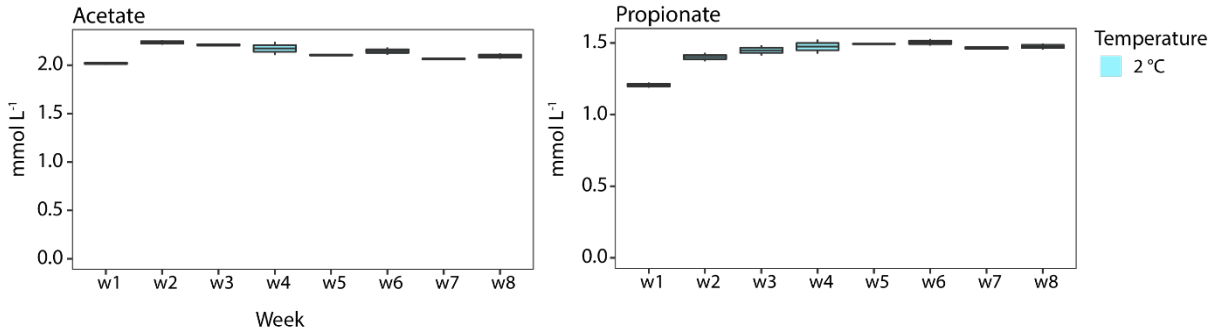

Fig. S2: Weekly concentrations [mmol L^{-1}] of the fermentation intermediates acetate and propionate during the pre-incubation of Experiment 1, using the Svalbard peat samples. The color indicates the pre-incubation temperature at 2 °C (light blue). Boxplots show median, 75 percentile and maximum or minimum values. A One-way ANOVA was used for the pairwise comparison of the weekly measurements (see supplementary Tab. S2 for all p.values).

Experiment 1
Svalbard (Knudsenheia)

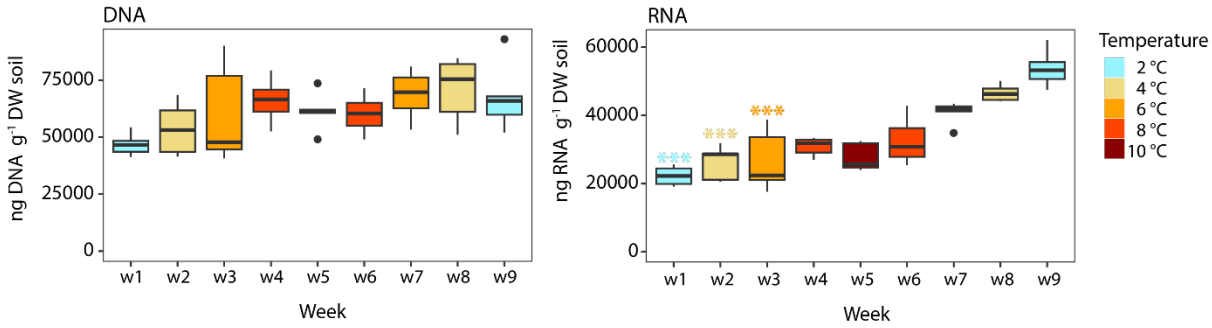

Fig. S3: Weekly concentrations of DNA [ng DNA g^{-1} DW soil] and RNA [ng RNA g^{-1} DW soil] during the main temperature experiment of Experiment 1, using the Svalbard peat samples. The colors indicate the weekly incubation temperatures ranging from 2 °C (light blue), over 4 °C (light yellow), 6 °C (orange), and 8 °C (tomato red), to 10 °C (dark red). Boxplots show median, 75 percentile and maximum or minimum values. A One-way ANOVA was used for the pairwise comparison of the weekly measurements. Significant differences between the same temperatures during temperature increase and temperature decrease (e.g., 2 °C during increase vs. 2 °C during decrease) are indicated by the colored asterisk inside the plots (p.value: *** < 0.001, ** < 0.01, * < 0.05; see supplementary Tab. S3 for all p.values).

Experiment 1
Svalbard (Knudsenheia)

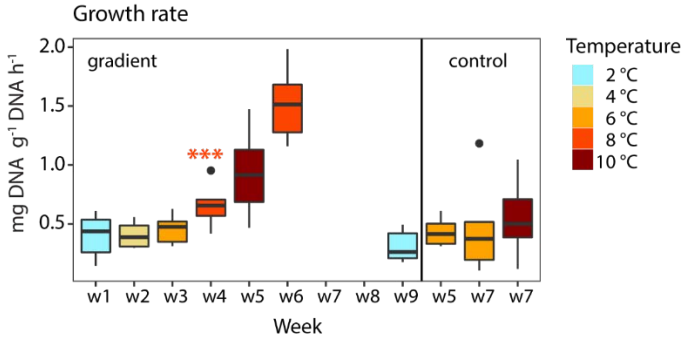

Fig. S4: Weekly microbial growth rates [mg DNA g^{-1} DNA h^{-1}] during the main temperature experiment (gradient) of Experiment 1, using the Svalbard peat samples. Additionally, the 6 °C-control of week 5 and 7, and the 10 °C-control of week 7 are shown. The colors indicate the weekly incubation temperatures ranging from 2 °C (light blue), over 4 °C (light yellow), 6 °C (orange), and 8 °C (tomato red), to 10 °C (dark red). Boxplots show median, 75 percentile and maximum or minimum values. A One-way ANOVA was used for the pairwise comparison of the weekly measurements. Significant differences between the same temperatures during temperature increase and temperature decrease (e.g., 2 °C during increase vs. 2 °C during decrease) are indicated by the colored asterisk inside the plots (p.value: *** < 0.001, ** < 0.01, * < 0.05; see supplementary Tab. S4 for all p.values).

Experiment 1
Svalbard (Knudsenheia)

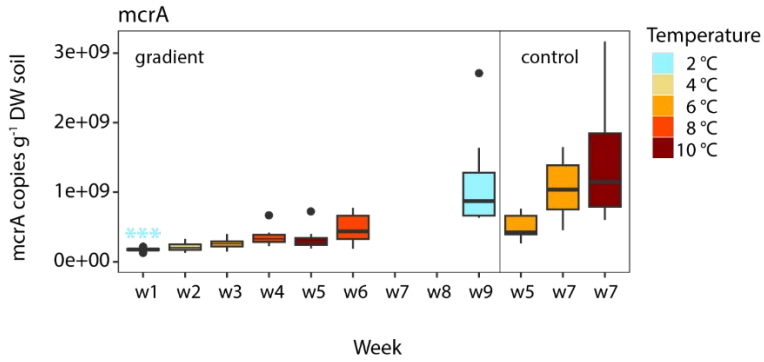

Fig. S5: Weekly number of copies of the gene for anaerobic methane cycling (mcrA) [mcrA copies g^{-1} DW soil] during the main temperature experiment (gradient) of Experiment 1, using the Svalbard peat samples. Additionally, the 6 °C-control of week 5 and 7 (w5 and w7) and the 10 °C-control of week 7 (w7) are shown. The colors indicate the weekly incubation temperatures ranging from 2 °C (light blue), over 4 °C (light yellow), 6 °C (orange), and 8 °C (tomato red), to 10 °C (dark red). Boxplots show median, 75 percentile and maximum or minimum values. A One-way ANOVA was used for the pairwise comparison of the weekly measurements. Significant differences between the same temperatures during temperature increase and temperature decrease (e.g., 2 °C during increase vs. 2 °C during decrease) are indicated by the colored asterisk inside the plots (p.value: *** < 0.001, ** < 0.01, * < 0.05; see supplementary Tab. S5 for all p.values).

Experiment 1
Svalbard (Knudsenheia)
6 °C control

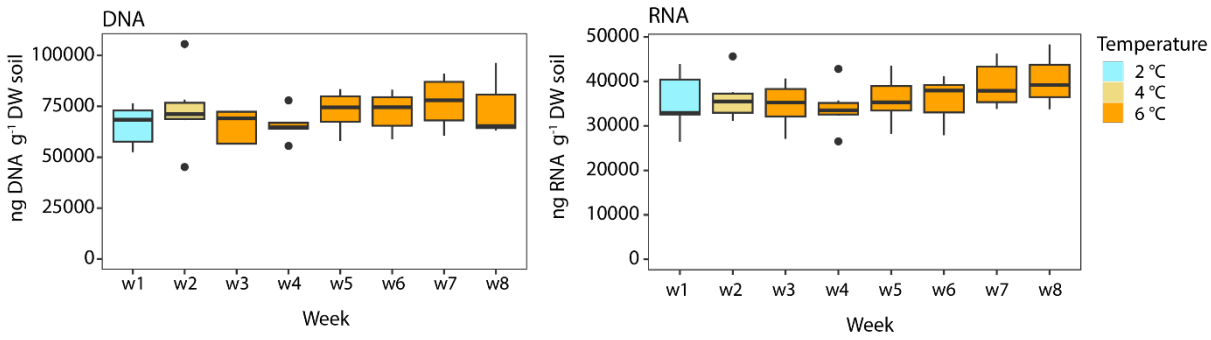

Fig. S6: Weekly concentrations of DNA [ng DNA g^{-1} DW soil] and RNA [ng RNA g^{-1} DW soil] during the 6 °C-control of Experiment 1, using the Svalbard peat samples. The colors indicate the weekly incubation temperatures ranging from 2 °C (light blue), over 4 °C (light yellow), to 6 °C (orange). Boxplots show median, 75 percentile and maximum or minimum values. For the statistical testing a One-way ANOVA was used for the pairwise comparison of the weekly measurements (see supplementary Tab. S3 for all p.values).

Experiment 2
Net CH_4 production rate

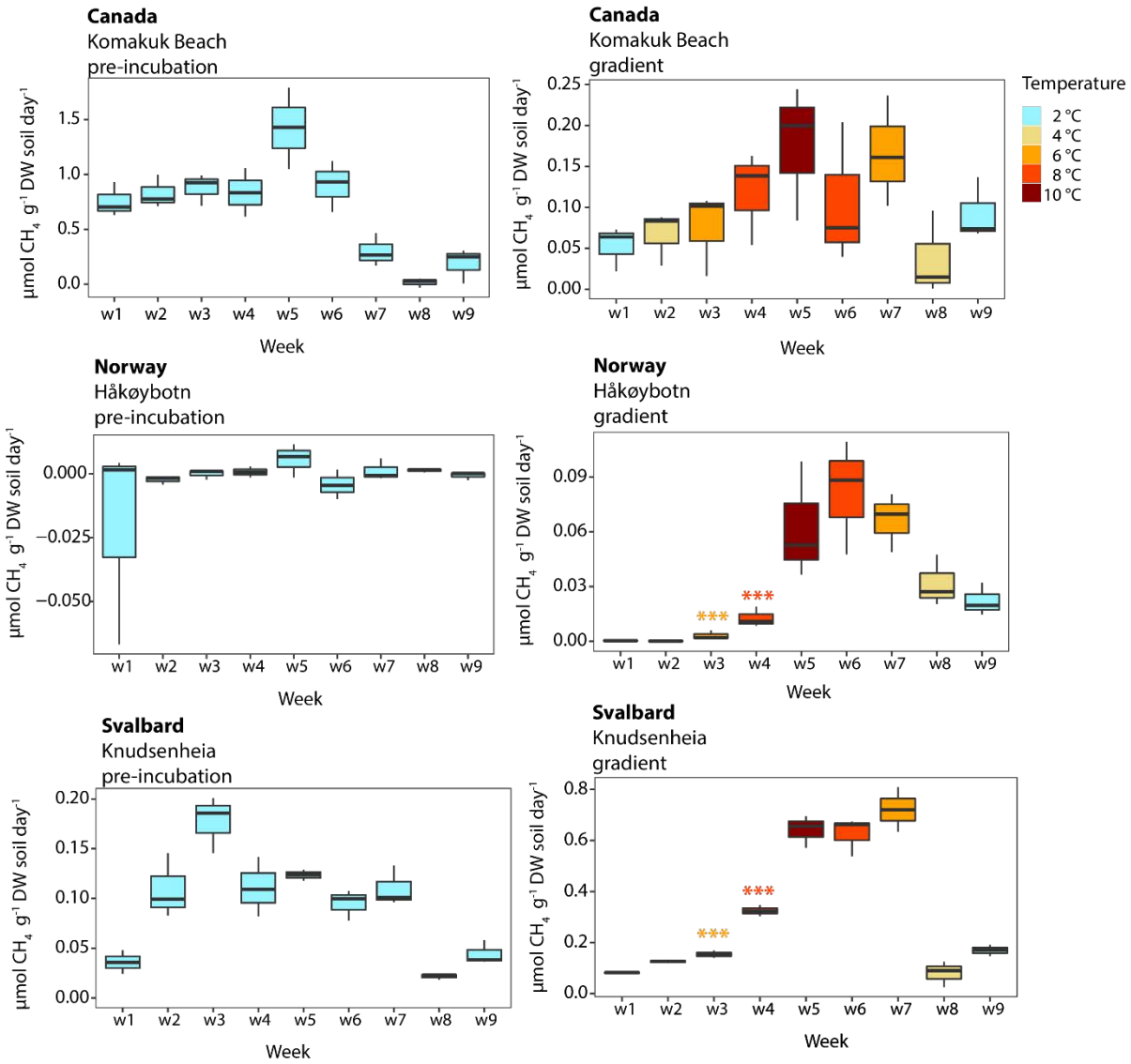

Fig. S7: Weekly net methane (CH_4) [µmol CH_4 g^{-1} DW soil day^{-1}] production rates during the pre-incubation and the main temperature experiment of Experiment 2, using peat samples from Canada, Norway, and Svalbard. The colors indicate the weekly incubation temperatures ranging from 2 °C (light blue), over 4 °C (light yellow), 6 °C (orange), and 8 °C (tomato red), to 10 °C (dark red). Boxplots show median, 75 percentile and maximum or minimum values. A One-way ANOVA was used for the pairwise comparison of the weekly measurements. Significant differences between the same temperatures during temperature increase and temperature decrease (e.g., 2 °C during increase vs. 2 °C during decrease) are indicated by the colored asterisk inside the plots (p.value: *** < 0.001, ** < 0.01, * < 0.05; see supplementary Tab. S6 for all p.values).

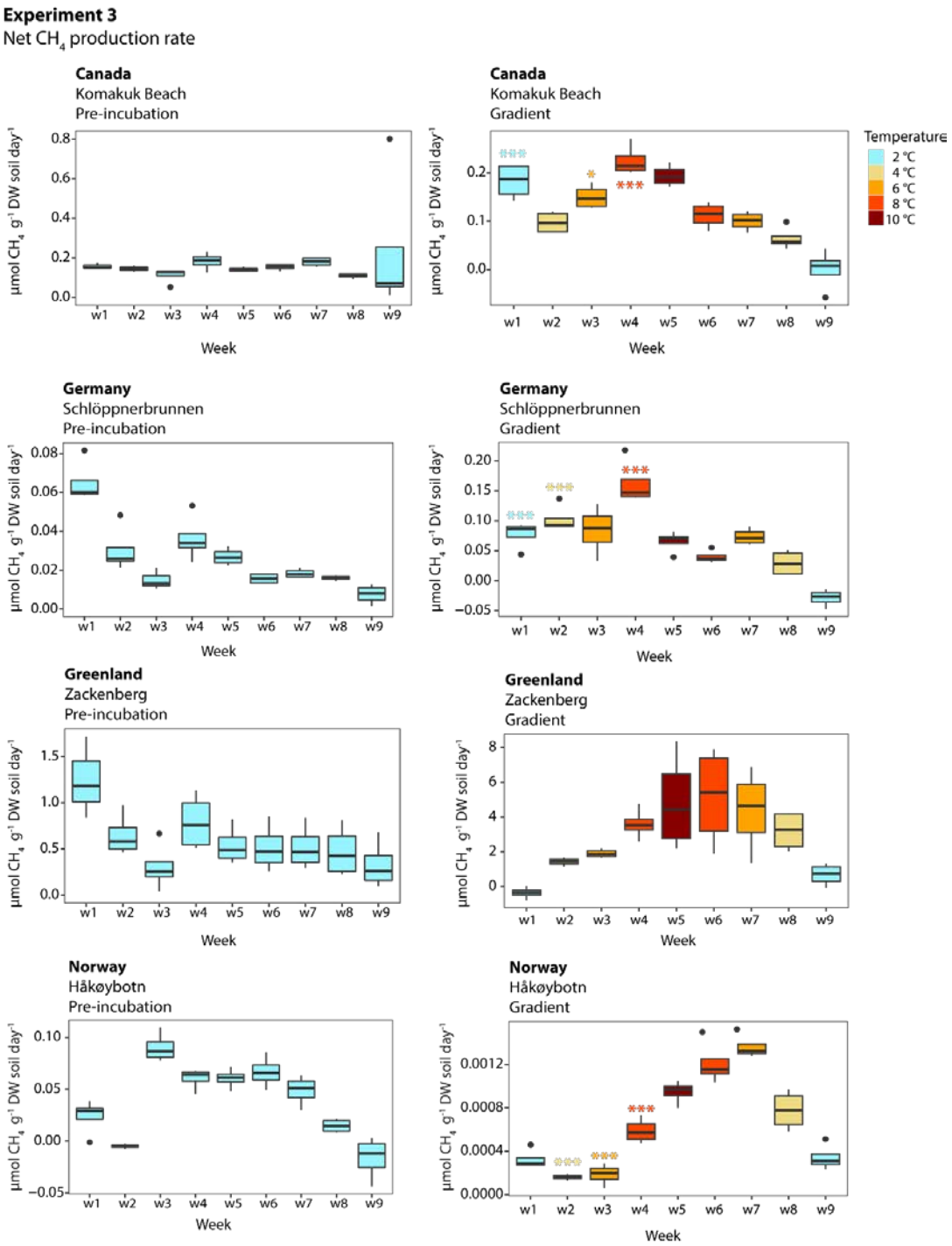

Fig. S8: Weekly net methane (CH_4) [µmol CH_4 g^{-1} DW soil day^{-1}] production rates during the pre-incubation and the main temperature experiment of Experiment 3, using peat samples from Canda, Germany, Greenland, and Norway. The colors indicate the weekly incubation temperatures ranging from 2 °C (light blue), over 4 °C (light yellow), 6 °C (orange), and 8 °C (tomato red), to 10 °C (dark red). Boxplots show median, 75 percentile and maximum or minimum values. A One-way ANOVA was used for the pairwise comparison of the weekly measurements. Significant differences between the same temperatures during temperature increase and temperature decrease (e.g., 2 °C during increase vs. 2 °C during decrease) are indicated by the colored asterisk inside the plots (p.value: *** < 0.001, ** < 0.01, * < 0.05; see supplementary Tab. S7 for all p.values).

Table Supplement:

Supplementary Tab. S1-S7 (file name: Supplementary_tables_paper3.xlxs)

This file is not included in the
print version of the thesis.